รายงานวิจัยฉบับสมบูรณ์

โครงการ การตรวจสอบคุณสมบัติการซึมผ่านผิวหนังของลิโพโซมที่กักเก็บสารที่ละลายน้ำดีหรือสารที่ชอบละลายในไขมันเพื่อระบบนำส่งยาทางผิวหนัง : การหาสูตรตำรับที่เหมาะสมโดยใช้โปรแกรมคอมพิวเตอร์

(Characterization, skin permeation of liposomes incorporated hydrophilic or lipophilic compound for transdermal drug delivery system : optimization by computer program)

โดย รศ.ดร. ธนะเศรษฐ์ ง้าวหิรัญพัฒน์

สิงหาคม ปี พ.ศ. 2559

สัญญาเลขที่ BRG5680016

รายงานวิจัยฉบับสมบูรณ์

โครงการ การตรวจสอบคุณสมบัติการซึมผ่านผิวหนังของลิโพโซมที่กักเก็บสารที่ละลายน้ำดีหรือสารที่ชอบละลายในไขมันเพื่อระบบนำส่งยาทางผิวหนัง : การหาสูตรตำรับที่เหมาะสมโดยใช้โปรแกรมคอมพิวเตอร์

โดย รศ.ดร. ธนะเศรษฐ์ ง้าวหิรัญพัฒน์

คณะเภสัชศาสตร์ มหาวิทยาลัยศิลปากร

สนับสนุนโดยสำนักงานคณะกรรมการอุดมศึกษา

และสำนักงานกองทุนสนับสนุนการวิจัย

กิตติกรรมประกาศ

คณะผู้ทำวิจัยขอขอบคุณสำนักงานคณะกรรมการอุดมศึกษาและสำนักงานกองทุนสนับสนุนการวิจัย ซึ่งให้การสนับสนุนทุนอุดหนุนการวิจัยนี้ คณะเภสัชศาสตร์ มหาวิทยาลัยศิลปากร คณะเภสัชศาสตร์ มหาวิทยาลัยอุบลราชธานี ในความอนุเคราะห์เครื่องมือ อุปกรณ์ และสารเคมีบางส่วน และสวนงูสภากาชาดไทยที่ให้ความอนุเคราะห์คราบงูที่ใช้สำหรับการวิจัย

รหัสโครงการ BRG5680016
ชื่อโครงการ **โครงการ การตรวจสอบคุณสมบัติการซึมผ่านผิวหนังของลิโพโซมที่กักเก็บสาร ที่ละลายน้ำดีหรือสารที่ชอบละลายในไขมัน เพื่อระบบนำส่งยาทางผิวหนัง : การหาสูตรตำรับที่เหมาะสมโดยใช้โปรแกรมคอมพิวเตอร์**
ชื่อนักวิจัย รศ.ดร.ธนะเศรษฐ์ ง้าวหิรัญพัฒน์ คณะเภสัชศาสตร์ มหาวิทยาลัยศิลปากร
E-mail address ngawhirunpat_t@.su.ac.th
ชื่อนักวิจัยร่วม นางสาวสุรีวัลย์ ดวงจิตต์ คณะเภสัชศาสตร์ มหาวิทยาลัยอุบลราชธานี
E-mail address sureewan.d@ubu.ac.th
ระยะเวลาโครงการ สิงหาคม 2556 - สิงหาคม 2559 (3 ปี)

การศึกษานี้มีวัตถุประสงค์เพื่อพัฒนาตำรับลิโพโซมให้เป็นตัวพายาเพื่อช่วยเพิ่มการซึมผ่านยามีล๊อกซิแคม (MX) ทางผิวหนัง และศึกษาอิทธิพลของปัจจัยสูตรตำรับต่อคุณลักษณะทางฟิสิกส์เคมี (ขนาด การกระจายขนาด ประจุ ความยืดหยุ่น ปริมาณยา และประสิทธิภาพในการกักเก็บยา) กายสัณฐานวิทยา คุณสมบัติทางความร้อน ความคงตัวของตำรับ และการซึมผ่านผิวหนัง สูตรตำรับที่เตรียม ได้แก่ ลิโพโซมที่มีประจุของสารลดแรงตึงผิว (ประจุลบ, ไม่มีประจุ และประจุบวก) ความยาวของสายคาร์บอนของสารลดแรงตึงผิว (C4, C12 และC16) และปริมาณของสารลดแรงตึงผิว (10%, 20% และ 29%) และศึกษากลไกที่เป็นไปได้ของลิโพโซมในการเพิ่มการนำส่ง MX ทางผิวหนัง ในการศึกษาก่อนตั้งตำรับลิโพโซมเตรียมโดยใช้ฟอสโฟลิปิด (PC) 10 มิลลิโมลาร์ สารลดแรงตึงผิว (cetylpyridinium, CPC) ร้อยละ 0-90 Chol ร้อยละ 0-90 และ MX ร้อยละ 0-20 พบว่าปริมาณ Chol ร้อยละ 10-40 CPC ร้อยละ 10-40 และ MX ร้อยละ 10 สามารถเตรียมเป็นตำรับลิโพโซมที่กักเก็บ MX ได้ จากนั้นทำการหาค่าเหมาะที่สุดสำหรับตำรับลิโพโซมกักเก็บ MX ใช้โปรแกรม RSM-S โดยกำหนดให้ PC และ MX ปริมาณคงที่คือ 10 มิลลิโมลาร์ และร้อยละ 10 ตามลำดับ ส่วน CPC และ Chol เปลี่ยนแปลงปริมาณในช่วงร้อยละ 10-40 พบว่า เมื่อเพิ่มปริมาณ Chol มีผลเพิ่มขนาดของอนุภาคอย่างมีนัยสำคัญ ส่วนความยืดหยุ่นและประสิทธิภาพในการกักเก็บยา MX ลดลง ในขณะที่เพิ่มปริมาณ CPC มีผลทำให้ขนาดอนุภาคลดลงอย่างมีนัยสำคัญ ส่วนประจุ ความยืดหยุ่น และประสิทธิภาพในการกักเก็บยา MX เพิ่มขึ้น โดยตำรับลิโพโซมกักเก็บ MX ที่เหมาะสมที่สุดประกอบด้วย PC/Chol/CPC ในสัดส่วน100:10.5:29.0 อิทธิพลของปัจจัยสูตรตำรับ พบว่า สูตรลิโพโซมที่ประกอบด้วย Chol ร้อยละ 10 CPC ร้อยละ 29 และมี MX ร้อยละ 10 ช่วยเพิ่มการซึมผ่านผิวหนังของยา MX สูงที่สุด ตำรับลิโพโซมนี้มีขนาด 91±9 นาโนเมตร มีการกระจายขนาดแคบ (0.3±0.06) และมีประจุบวก 48±1 มิลลิโวลต์ มีความยืดหยุ่นในช่วง 89±1 มิลลิกรัมต่อวินาทีต่อตารางเซนติเมตร ประสิทธิภาพในการกักเก็บยาและปริมาณยาในตำรับเท่ากับ ร้อยละ 68±1 และ 526±7 ไมโครกรัมต่อมิลลิลิตร ตามลำดับ กลไกของลิโพโซมในการช่วยเพิ่มการซึมผ่านผิวหนังของ MX ศึกษาจากคุณลักษณะของคราบงูหลังจากการศึกษาการซึมผ่านผิวหนังด้วย FT-IR และ DSC ผล FT-IR สเปกตรัม และ DSC เทอร์โมแกรมแสดงการเปลี่ยนแปลงของพีค ดังนั้นกลไกที่เป็นไปได้คือ กลไกของสารช่วยเพิ่มการซึมผ่านและการหลอมรวมของอนุภาคลิโพโซมกับชั้นสตราตัมคอร์เนียม ผลจากการศึกษานี้จะเป็นข้อมูลพื้นฐานที่เป็นประโยชน์ต่อการพัฒนาตำรับลิโพโซมสำหรับเพิ่มการนำส่งยาชอบไขมันทางผิวหนัง

คำหลัก : ลิโพโซม ทรานสเฟอร์โซม มีล๊อกซิแคม ระบบนำส่งยาทางผิวหนัง สารลดแรงตึงผิว

Project code BRG5680016
Project Title **Characterization, skin permeation of liposomes incorporated hydrophilic or lipophilic compound for transdermal drug delivery system : optimization by computer program**
Investigator Assoc.Prof. Tanasait Ngawhirunpat, Fac.of Pharmacy, Silpakorn U.
E-mail address ngawhirunpat_t@.su.ac.th
Co-investigator Miss sureewan Duangjit Fac.of Pharm.Sci., Ubon Ratchathani U.
E-mail address sureewan.d@ubu.ac.th
Project Period Auguet 2013 – August 2016 (3 years)

The objective of this study was to develop the liposome formulation as carrier for enhancing skin permeation of meloxicam (MX) and to investigate the influences of formulation factors on physicochemical characteristics (vesicle size, size distribution, zeta potential, elasticity, drug content and entrapment efficiency (EE)), morphology, thermal properties, stability of the formulation and *in vitro* skin permeability of liposomes. The vesicle formulations present of charge of surfactants (anionic, neutral and cationic), carbon chain length of surfactants (C4, C12 and C16) and amount of surfactants (10%, 20% and 29%) were formulated. Moreover, the possible mechanisms by which these liposomes could improve the skin delivery of MX were also evaluated. In pre-formulation studies, the liposomes were prepared using 10 mM egg yolk phosphatidylcholine (PC), 0-90 % surfactant (cetylpyridinium, CPC) and 0-90% Chol with 0-20% MX. The results suggested that the 10-40% Chol, 10-40% CPC, and 10% MX were the desirable amount for MX-loaded liposomes. The optimal MX-loaded liposomes were estimated using a nonlinear response-surface method incorporating thin-plate spline interpolation (RSM-S) by fixing the amount of PC and MX, and varying the amount of Chol (10-40%) and CPC (10-40%). The results suggested that an increase of Chol resulted in a significant increase in vesicle size, a decrease in elasticity and a slight increase in EE. While an increase in CPC resulted in a significant decrease in vesicle size, an increase in zeta potential, elasticity and EE. The result revealed that the optimal formulation of PC/Chol/CPC in the molar ratios was 100:10.5:29.0. The influence of formulation factors indicated that the liposomes composed of 10% chol, 29% CPC and 10% MX showed the highest skin permeability. The MX-loaded liposomes vesicle sizes were 91±9 nm with narrow size distribution (0.3±0.06) and zeta potential of 48±1 mV. The elasticity of these MX-loaded liposomes was 89±1 $mg \cdot sec^{-1} \cdot cm^{-2}$. The EE and drug content were 68±1% and 526±7 µg/mL, respectively. The mechanisms of liposomes to enhance skin permeation of MX were determined by characterizing the shed snake skin after skin permeation study with FT-IR and DSC. The FT-IR spectra and DSC thermogram showed that the peak was shifted, indicating that the possible mechanisms were the penetration enhancing mechanism and the vesicle adsorption to and/or fusion with the stratum corneum. This finding provided useful fundamental information to develop the liposome formulation for improving skin delivery of lipophilic drugs.

Keywords: Liposomes, Transfersomes, Meloxicam, Transdermal drug delivery, Surfactant

EXECUTIVE SUMMARY

Since the first paper to report the effectiveness of deformable liposomes which can be used for skin delivery of drug into deep skin region was published and several studies reported that elastic vesicles were more efficient in enhancing the transport of drugs than rigid vesicles. Accordingly, new categories of liposome vesicles with high elasticity, high fluidity or high flexibility have been developed and introduced. The ultra-deformable or deformable liposomes mainly consist of phospholipids and various types of penetration enhancer (e.g., surfactant, non-ionic surfactant, ethanol, terpenes) which only a specially designed of liposome vesicles were shown to be able to allow outstanding transdermal drug delivery carriers. Therefore, recent approaches in vesicular modulating drug delivery through skin at the latest decade have resulted in novel deformable liposome carriers i.e., deformable liposomes (transfersomes), niosomes, ethosomes, invasomes, flexosomes and menthosomes. All special and attractive designed of liposomes and analogues enhanced skin delivery of various hydrophilic and lipophilic drugs.

Meloxicam (MX), a non-steroidal anti-inflammatory drug (NSAID), is used to treat rheumatoid arthritis, osteoarthritis and other joint diseases. It has been reported that MX is an effective NSAID for reducing pain and inflammatory symptoms with no convincing evidence that the risk of the severest adverse GI side effect (e.g., peptic ulceration, perforation, bleeding) is lower with MX than with other NSAIDs. Although, MX preferentially inhibits COX-2 (cyclooxygenease-2) over COX-1 (cyclooxygenease-1), MX still has the incidence of GI side effects (e.g., bellyache, indigestion, ulceration and bleeding) at high doses on long term therapy. If MX could be delivered without incidence of these limitations, MX administration would become safer and more acceptable. Transdermal delivery of NSAIDs offers the advantage of deliver drug to target inflammatory site, in order to maximize local effects and minimize or without systemic side effect. Therefore, it is usefulness for MX, a drug that is often used clinically but has no available option for transdermal delivery which modulates GI side effect and delivers MX to the target site. Although, MX possesses favorable characteristics for transdermal delivery such as low molecular weight, low daily therapeutic dose, the major limitation of MX for transdermal delivery is its very low aqueous solubility (0.012 mg/ml), and the log partition coefficient (log P) is 0.1 in octanol/buffer pH 7.4 that also make them difficult for development as transdermal drug delivery carriers. Numerous TDDS for MX such as microemulsion, gels, patch, nanoemulsion-gel have been developed to improve the skin delivery of MX. However, low drug loading capacity, poor drug controlled and sustained release capacity, and high content of organic solvent in the formulation limited their safe to use as skin

delivery carriers. Therefore, MX is challenging and suitable for development as a transdermal delivery candidate in our study.

Although, recently various kind of novel liposomes and/or deformable liposomes have been developed to enhance the skin permeation of drugs, liposome system and its mechanism have not yet fully understood for transdermal drug delivery carriers. The results have not been consistent; positive and negative results were observed in different type of liposome and analogues. Numerous intensive studies suggested that the permeability of drug in liposome and analogues depends on their intrinsic physicochemical characteristics (i.e., vesicle size, size distribution, zeta potential, elasticity, drug content and entrapment efficiency), and these characteristics was directly affected by vesicle component or formulation factors. However, liposomes can be varied with respect to vesicle component (e.g., phospholipid, cholesterol, surfactant, non-ionic surfactant, ethanol and/or other penetration enhancers) and method of preparation. Furthermore, whether the skin model used, human or animal (e.g., pig, rat, mice, rabbit, snake, etc.), the factor that determines the effectiveness of drug in liposomes and analogues remains a much debated question and must be designed and tested on a case-by-case basis. In this context, the intensive systematic investigation of type and amount of vesicle component are still needed to define the effect of the formulation factors on physicochemical characteristics and skin permeability of drug-loaded liposome formulation. The success will provide the optimal vesicle formulation for transdermal drug delivery carrier for meloxicam and other lipophilic model drug, and also provide the important fundamental information for development other transdermal drug delivery system.

The objective of this study was to develop the liposome formulation as carrier for enhancing skin permeation of meloxicam (MX) and to investigate the influences of formulation factors on physicochemical characteristics (vesicle size, size distribution, zeta potential, elasticity, drug content and entrapment efficiency (EE)), morphology, thermal properties, stability of the formulation and *in vitro* skin permeability of liposomes. The vesicle formulations present of charge of surfactants (anionic, neutral and cationic), carbon chain length of surfactants (C4, C12 and C16) and amount of surfactants (10%, 20% and 29%) were formulated. Moreover, the possible mechanisms by which these liposomes could improve the skin delivery of MX were also evaluated. In pre-formulation studies, the liposomes were prepared using 10 mM egg yolk phosphatidylcholine (PC), 0-90 % surfactant (cetylpyridinium, CPC) and 0-90% Chol with 0-20% MX. The results suggested that the 10-40% Chol, 10-40% CPC, and 10% MX were the desirable amount for MX-loaded liposomes. The optimal MX-loaded liposomes were estimated using a nonlinear response-surface method incorporating thin-plate spline interpolation (RSM-S)

by fixing the amount of PC and MX, and varying the amount of Chol (10-40%) and CPC (10-40%). The results suggested that an increase of Chol resulted in a significant increase in vesicle size, a decrease in elasticity and a slight increase in EE. While an increase in CPC resulted in a significant decrease in vesicle size, an increase in zeta potential, elasticity and EE. The result revealed that the optimal formulation of PC/Chol/CPC in the molar ratios was 100:10.5:29.0. The influence of formulation factors indicated that the liposomes composed of 10% chol, 29% CPC and 10% MX showed the highest skin permeability. MX-loaded liposomes vesicle sizes were 91±9 nm with narrow size distribution (0.3±0.06) and zeta potential of 48±1 mV. The elasticity of these MX-loaded liposomes was 89±1 mg·sec^{-1}·cm^{-2}. The EE and drug content were 68±1% and 526±7 µg/mL, respectively. The mechanisms of liposomes to enhance skin permeation of MX were determined by characterizing the shed snake skin after skin permeation study with FT-IR and DSC. The FT-IR spectra and DSC thermogram showed that the peak was shifted, indicating that the possible mechanisms were the penetration enhancing mechanism and the vesicle adsorption to and/or fusion with the stratum corneum. This finding provided useful fundamental information to develop the liposome formulation for improving skin delivery of lipophilic drugs.

สารบัญเรื่อง (Table of contents)

	หน้า
กิตติกรรมประกาศ	2
บทคัดย่อภาษาไทย	3
บทคัดย่อภาษาอังกฤษ	4
Executive summary	5
สารบัญเรื่อง (Table of contents)	8
สารบัญภาพ (List of tables)	9
สารบัญภาพ (List of figures)	10
คำอธิบายสัญลักษณ์และคำย่อที่ใช้ในการวิจัย (List of abbreviations)	12
บทนำ (Introduction)	15
- ความสำคัญและที่มาของปัญหา (Research problem and its significance)	15
- วัตถุประสงค์ของงานวิจัย (Objectives)	17
- ขอบเขตของการวิจัย (Scope of research)	17
- ประโยชน์ที่คาดว่าจะได้รับ (Expected outcome)	18
วิธีการดำเนินการวิจัย (Research methodology)	19
- สารเคมี (Meterials)	19
- เครื่องมือและอุปกรณ์ (Equipment needed for the project)	20
- ระเบียบวิธีวิจัย (Research methodology)	21
ผลการวิจัยและอภิปรายผล (Results and discussion)	27
สรุปผลการดำเนินงานของโครงการ (Conclusions)	55
เอกสารอ้างอิง	56
OUTPUTS ที่ได้จากโครงการ	64
ภาคผนวก	66

สารบัญภาพ (List of tables)

		หน้า
Table 1	The composition of each liposome carriers	22
Table 2	Classification of investigation studies	32
Table 3	Effect of the surfactant on vesicle size, zeta potential, elasticity and entrapment efficiency of the vesicle formulation	33
Table 4	The predicted and experimental response variables of the optimal formulation	43
Table 5	Bootstrap Optimal Solutions and Bootstrap Standard Deviations by Different Frequencies of Bootstrap Resampling	48
Table 6	Confidence Interval of Simultaneous Optimal Solution Estimated by RSM-S	49
Table 7	The Physicochemical Properties and Characteristics of the Different Formulations	49

สารบัญภาพ (List of figures)

		หน้า
Figure 1	The turbidity of different vesicle component in the formulation.	27
Figure 2	The molar turbidity of the different vesicle component in the liposomes and transfersomes formulation.	28
Figure 3	The entrapment (*white bar*) and loading (*solid circle*) efficiencies of meloxicam-loaded vesicle formulation.	29
Figure 4	The response surface of the model formulation of (A) vesicle size, (B) zeta potential, (C) elasticity and (D) entrapment efficiency.	30
Figure 5	The response surface of the concentration of MX permeated the skin at *t* h of (A) 2 h, (B) 4 h, (C) 8h, (D) 10 h, (E) 12 h and (F) flux.	31
Figure 6	TheTEM image of MX-loaded vesicle formulation; (A) N-CLP (10,000X), (B) N-CLP (30,000X), (C) N-CLP (50,000X), (D) C-TFS (30,000X), (E) C-TFS (30,000X), (F)C-TFS (50,000X), (G) A-TFS (30,000X), (H) A-TFS (30,000X), and (I)A-TFS (50,000X).	36
Figure 7	Freeze-fractured transmission electron microscopy images of the optimized meloxicam-loaded vesicle formulation.	37
Figure 8	The influence of (A) surfactant charge, (B) surfactant carbon chain length, and (C) surfactant content on the remaining MX at different days (n=3).	38
Figure 9	The DSC thermogram of vesicle formulation; conventional liposomes (CLP) and transfersomes (TFS)	39
Figure 10	The influence of (A) surfactant charge, (B) surfactant carbon chain length, and (C) surfactant content on the skin permeation profile and the steady-state flux of the vesicle formulation (n=3).	40
Figure 11	The response surface for the skin permeation flux (A) and the reliability (B) of the model formulation.	42
Figure 12	The skin-permeation profile of MX from the optimal formulation: predicted values; and experimental values.	43

สารบัญภาพ (List of figures) (ต่อ)

		หน้า
Figure 13	The Contribution Index of Effective Causal Factor for Predicting Response Variables (a) Skin permeability (Y_1) and (b) stability of formulation (Y_2).	44
Figure 14	The Response Surface of Skin Permeability (Flux, Y_1) (Left) and Stability of Formulation (Drug Remaining, Y_2) (Right) as Function of X_4 and X_5 (a, d), X4 and X_9 (b, e) and X_5 and X_9 (c, f) at a Constant of Z_2 (0.0689%mol), X_5 (514 µg/mL) and X_4 (74.5 $mg{\cdot}s^{-1}{\cdot}cm^{-2}$).	46
Figure 15	The Leave-One-Out-Cross-Validation (LOOCV) estimated accuracy and reliability of the response surface variables (a) skin permeability (flux) and (b) stability of formulation (drug remaining at 25°C for 30 d) predicted by X_4, X_5, and Z_2.	47
Figure 16	(A) The skin permeation profile 12 h in full-thickness skin after treated with MTS, TFS, CLP and SUS on hair-less mice skin (Laboskin®), (B) flux and (D) MX deposit in the full-thickness skin after skin permeation.	52
Figure 17	The influence of (A) surfactant charge, (B) surfactant carbon chain length, and (C) surfactant content of the shed snake skin after skin permeation	54

คำอธิบายสัญลักษณ์และคำย่อที่ใช้ในการวิจัย (List of abbreviations)

%EE	percent entrapment efficiency
%v/v	percent volume by volume
%w/v	percent weight by volume
%w/w	percent weight by weight
ºC	degree Celsius or degree centigrade
θ	theta
µg	microgram(s)
µL	microliter(s)
µm	micrometer(s)
A12	anionic surfactant with 12 carbon atoms
A16	anionic surfactant with 16 carbon atoms
ABS	acetate buffer solution
ATRA	all-trans-retinoic acids
BPC	butylpyridinium chloride (C4)
C4	cationic surfactant with 4 carbon atoms
C12	cationic surfactant with 12 carbon atoms
C16	cationic surfactant with 16 carbon atoms
CAP	Capsaicin
Chol	cholesterol
C_i	the initial concentration of MX added into the formulation
C_L	the concentration of MX loaded in the formulation
CLP	conventional liposomes
cm^{-1}	wavenumbers
cm^2	square centimeter(s)
CM	Clindamycin
Conc.	concentration
CPC	cetylpyridinium chloride (C16)
CoS	Cosurfactant
DEA	Diethanolamine
DPC	dodecylpyridinium chloride (C12)
D_t	the total amount of MX in the formulation
e.g.	exempli gratia (Latin); for example
Eq.	equation
et al.	and others
etc.	et cetera (Latin); and other things/ and so forth

คำอธิบายสัญลักษณ์และคำย่อที่ใช้ในการวิจัย (List of abbreviations)

g	gram(s)
GI	gastrointestinal
Gly	Glycerin
h	hour(s)
i.d.	inner diameter
i.e.	id est (Latin); that is
IPM	isopropyl myristate
J	the steady-state flux
J_{flux}	the penetration rate through a permeability membrane
k	kilo(s)
kDa	kilodalton
kg	kilogram(s)
K_p	permeability coefficients
kV	kilovolt(s)
L	liter(s)
LE	loading efficiency
log P	log octanol-water partition coefficient
LP	liposomes
Liposomes	liposopmes and their analogues
L_t	the total amount of PC added into the formulation
ME	Microemulsions
MEN	menthol
mg	milligram(s)
min	minute(s)
mL	milliliter(s)
mm	millimeter(s)
mM, mmol	millimolar(s)
MPa	megapascal(s)
MTS	menthosomes
mV	millivolt(s)
MW	molecular weight
MWCO	molecular weight cut off
MX	meloxicam
ng	nanogram(s)
nm	nanometer(s)

คำอธิบายสัญลักษณ์และคำย่อที่ใช้ในการวิจัย (List of abbreviations)

nM	nanomolar(s)
nmol	nanomolar(s)
NE	Nanoemulsions
NLC	Nanostructure lipid carriers
o.d.	outer diameter
PBS	phosphate buffer solution
PC	phosphatidylcholine
PI, PDI, PdI	polydispersity index
pH	potentia hydrogenii (Latin); power of hydrogen
r^2	coefficient of determination
rpm	revolutions per minute orrounds per min
r_p	membrane pore size
RSM-S	nonlinear response surface method incorporating thin-plate spline interpolation
RT	room temperature
r_v	vesicle size after extrusion
S	Surfactant
s	sec(s)
SC	stratum corneum
SDS	sodium dodecyl sulfate (A12)
S.E.	standard error
SHS	sodium hexadecyl sulfate (A16)
SLN	Solid lipid nanoparticles
TFS	transfersomes
T_g	glass transition temperature
V	volt(s)
Vesicles	liposomes and transfersomes
XG	Xyloglucan

บทนำ (Introduction)

ความสำคัญและที่มาของปัญหา (Research problem and its significance)

Transdermal drug delivery systems (TDDS) have become a global priority because the most common route of drug delivery (oral and parenteral) was associated with numerous limitations. Oral drug delivery has poor bioavailability due to hepatic first pass metabolism by gastrointestinal enzymetic system, variable absorption rate and serum concentration which may be unpredictable, acid and food problem in gastrointestinal (GI) tract. While parenteral drug delivery has advantage of avoidance of GI tract problem and regarded as 100% bioavailability, however patients were not typically able to self administer, severe adverse drug reaction in case of allergy, risk of infection and especially pain from injection and patient compliance becomes a major problem of parenteral drug administration [27]. In order to avoid these disadvantages, the transdermal drug delivery administration was widely used as an alternative drug administration route because TDDS can offers many advantages over the previous limitations such as avoid hepatic first pass metabolism and GI irritation, convenient and painless administration, reduce frequency of drug administration, ease of dose termination in case of severe adverse side effects. However, the major limitation of TDDS was the permeability of the skin; it was permeable to small molecules and suitable partition coefficient lipophilic drugs and highly impermeable to macromolecules and hydrophilic drugs. Furthermore, the main barrier and rate-limiting step for diffusion of drugs across the skin was provided by the outermost layer of the skin, the stratum corneum (SC). To overcome the skin's barrier, several strategies have been developed both physical and chemical methods, including the use of ultrasound [28], iontophoresis [29], electroporation [30], microneedles [31], chemical enhancers [32], microemulsion [33] and liposomes [34], which provide an alternative for improved drug delivery through the skin.

Liposomes were one of the potential strategies that utilize for transdermal delivery of hydrophilic drugs [35], lipophilic drugs [24], gene [36], protein [37] and macromolecule [38]. Recent approaches in liposomes modulating drug delivery through the skin have resulted in various types of liposomes carriers e.g., deformable liposomes (transfersomes) [39], niosomes [40], ethosomes [41], invasomes [4], flexosomes [42], transethosomes [43] and menthosomes [6]. Transfersomes were the first generation of elastic vesicles introduced by Cerv et al. (1992) and compose of phospholipids and an edge activator or a single-chain surfactant which having a high radius of curvature that destabilizes and increases deformability of the lipid bilayers [7]. Niosomes were the second generation of elastic liposomes introduced by van den Bergh et al. (1999) and the lipid were predominantly non-ionic surfactant and cholesterol which form bilayer. Ethosomes were another novel liposomal carriers, developed and introduced by Touitou

et al. (2000) and compose of phospholipids, ethanol and water. Invasomes were introduced by Verma (2002) and incorporate phospholipids, ethanol and a mixture of terpenes. Flexible liposomes (Flexosomes) were one type of elastic liposomes introduced by Song and Kim (2006) and incorporate phospholipids, non-ionic surfactant and edge activator. Transethosomes were one of a special carrier which was a combination between transfersomes and ethosomes. And menthosomes, a novel ultradeformable liposomes compose of phospholipids, menthol and edge activator. These special designed liposome carriers enhanced skin delivery of various drugs [39].

Several intensive studies suggested that the permeability of drug in liposomes and their analogs depends on their physicochemical characteristics e.g., particle size, size distribution, zeta potential, elasticity, drug content, entrapment efficiency, stability and thermal properties which these characteristics were directly affected by the formulation factors or their composition. Moreover, liposomes and their analogs can vary with respect to type and amount of the formulation factor (e.g., phospholipid, cholesterol, edge activator, penetration enhancer, etc.). However, the effect of different type of liposomes on TDDS was not fully clarified as there were both positive and negative results. Furthermore, most reports studied under different type of liposomes (conventional liposomes, transfersomes, niosomes, ethosomes, invasomes, flexosomes, transethosomes, menthosomes), different experiment conditions (*in vitro*, *in vivo*, *ex vivo*), different composition (type, amount), different type of drug (hydrophilic, lipophilic) and different skin model (human, animal); therefore, the obtained results cannot be compared. Nowadays, liposomal systems for skin delivery still remains a much debated questions and have to test on a case-by-case basis because did not fully understand the behavior. The most potential liposome carriers for excellent transdermal drug delivery of both hydrophilic and lipophilic drugs were still needed to define. Thus, the finding results will provide important fundamental information for simplifying the development of novel liposomal systems for transdermal drug delivery.

In the research and development of liposomal systems for transdermal drug delivery carriers, it was complicated to design and investigate the optimized liposomal formulations having appropriate skin permeation of both hydrophilic and lipophilic drugs. For this objective, a design of experiment (DOE) processions and a statistical computer programs was employed. For example, using a nonlinear response-surface method incorporating thin-plate spline interpolation (RSM-S), complicated relationships between causal factors (formulation factor) and response variables (physicochemical characteristics) can be easily understood, and a stable and reproducible simultaneous optimal formulation was obtained [44]. A bootstrap (BS) re-sampling method and a Kohonen self-organizing map (SOM) were used to evaluate the reliability of the optimal formulation

estimated by RSM-S. These statistical approaches were helpful in formulating an appropriate transdermal drug delivery system for hydrophilic and lipophilic model drugs. Moreover, a Bayesian network (BN) was applied to gain an understanding of the relationships between formulation factor and physicochemical characteristics.

วัตถุประสงค์ของงานวิจัย (Objectives)

1. To optimize and find the most potential liposomal systems as a transdermal drug delivery carrier for enhancing skin permeation of hydrophilic or lipophilic drugs by computer programs, and investigate the novel optimal formulation by the experiment.
2. To understand the important fundamental information and the relationships between formulation factor and physicochemical characteristics for simplifying the development of novel liposomal systems for transdermal drug delivery.
3. To compete and overcome the the commercial products with the novel liposomal formulation for transdermal drug delivery of both hydrophilic and lipophilic drugs.

ขอบเขตของงานวิจัย (Scope of research)

1. The liposomal system formulations in this study were formulated and performed based on 2 studies:

    1.1 The computer program study: to optimize the optimal formulation of each liposomal carrires, the design of experiments (DOE) were used for designing and developing the model formulations for computer program.

    1.2 The experimental study: to confirm and compare the potential use of the optimal formulation estimated using computer programs, the optimal formulation of each liposomal carriers were performed by the experiment.

2. The physicochemical characteristics e.g., particle size, size distribution, zeta potential, elasticity, drug content, entrapment efficiency, stability and thermal properties and the skin permeability parameters e.g., lag time, skin permeation at *t* h and flux of model formulations were investigated.
3. The optimal formulation of each liposomal carriers estimated using computer programs was formulated and characterized by the experiment. The comparative study was performed to choose the most potential liposomal systems for transdermal drug delivery carriers for hydrophilic and lipophilic drugs.
4. The most potential liposomal systems of both hydrophilic or lipophilic drugs were incorporated in topical base formulation and compare to the commercial products.

ประโยชน์ที่คาดว่าจะได้รับ (Expected outcome)

1. To optimize and find the most potential liposomal systems as a transdermal drug delivery carrier for enhancing skin permeation of hydrophilic or lipophilic drugs.
2. To understand the important fundamental information and the relationships between formulation factor and physicochemical characteristics for simplifying the development of novel liposomal systems for transdermal drug delivery.
3. To compete and overcome the the commercial products with the novel liposomal formulation for transdermal drug delivery of both hydrophilic or lipophilic drugs.

ระเบียบวิธีวิจัย (Research methodology)

สารเคมี (Materials)

1. All other chemicals were commercially available and analyticalgrade.
   - Acetronitrile (Fisher Scientific UK, Loughborough, Leicester, UK)
   - Acetronitrile (Wako Pure Chemical Industries, Osaka, Japan)
   - Cetylpyridinium chloride; CPC (Sigma Aldrich®, St. Louis, MO, USA)
   - Chloroform; $CHCl_3$ (Wako Pure Chemical Industries, Osaka, Japan)
   - Chloroform; $CHCl_3$ (RCI Labscan, Bangkok, Thailand)
   - Cholesterol; Chol (Carlo Erba Reagenti, Strada Rivoltana, Rodano, Italy)
   - Disodium hydrogenphosphate dodecahydrate; $Na_2HPO_4{\cdot}12H_2O$ (Ajax Finechem, Australia)
   - Methanol; MeOH (Fisher Scientific UK, Loughborough, Leicester, UK)
   - Methanol; MeOH (Wako Pure Chemical Industries, Osaka, Japan)
   - Potassium chloride; KCl (Ajax Finechem, Australia)
   - Potassium dihydrogenphosphate; KH_2PO_4 (Ajax Finechem, Australia)
   - Sodium acetate trihydrate; $C_2H_3O_2Na{\cdot}3H_2O$ (Ajax Finechem, Australia)
   - Sodium chloride; NaCl(Ajax Finechem, Australia)
   - Triton® X-100 (Amresco®, Solon, Ohio, USA)
2. all-trans-retinoic acids; ATRA (Sigma, St. Louis, MO, U.S.A.)
3. Butylcetylpyridinium chloride; BCP (Tokyo Chemical Industry, Tokyo, Japan)
4. Laurylpyridinium chloride; LCP (Tokyo Chemical Industry, Tokyo, Japan)
5. Cetylpyridinium chloride; CPC (MP Biomedicals, Illkirch, France)
6. Cholesterol; Chol (Wako Pure Chemical Industries, Osaka, Japan)
7. Capsaicin; CAP (Hunan Huacheng Biotech, Inc., Changsha, China)
8. Clindamycin phosphate; CM (Bangkoklab and Cosmetics Co., Ltd., Ratchaburi, Thailand).
9. Meloxicam; MX (Fluka, Buchs, Switzerland)
10. Methyl 4-Hydroxybenzoate (Tokyo Chemical Industry, Tokyo, Japan)
11. Phosphatidylcholine; PC (LIPOID GmbH, Cologne, Germany)
12. Sodium hexadecyl sulfate; SHS (Tokyo Chemical Industry, Tokyo, Japan)
13. Shed snake skin of *Naja kaouthia* (The Queen Saovabha Memorial Institute, Thai Red Cross Society, Bangkok, Thailand)

เครื่องมือและอุปกรณ์ (Equipment needed for the project)

1. Desiccator
2. N_2 gas in larminar hood
3. Sonicator bath
4. Probe sonicator (Sonics Vibra Cell™)
5. Ice bath
6. Centrifugation and Ultracentrifugation
7. Thermo-regulated water bath
8. Shaking incubator
9. Diffusion cell (sidy-by-side or franz cell)
10. Micropipette (2-20 μl, 20-200 μl, 100-1000 μl, 1-5 ml) and micropipette tip
11. Microcentrifuge tube 1.5 ml (Eppendorf ® tubes)
12. Filter set and filter membrane 0.45 μm
13. Zetasizer Nano ZS (Malvern Instruments, Malvern, UK)
14. Transmission Electron Microscope (TEM)
15. High performance liquid chromatography (HPLC)
16. Confocal laser scanning microscopy (CLSM)
17. Differential scanning calorimetry (DSC)
18. Aluminum seal pan and cap
19. Refrigerator, Freezer -20°C, Freezer 4°C
20. Magnetic stirrer and Magnetic bar
21. Analytical balance
22. Aluminium foil
23. Vortex mixer
24. Thermometer
25. pH meter
26. Parafilm

ระเบียบวิธีวิจัย (Methods)

1. Review literatures

2. Preparation of formulation

The pre-formulation containing a controlled amount of phosphatidylcholine (PC) and various amounts of other composition e.g., surfactants (Surf), non-ionic surfactant (Non-Surf), cholesterol (Chol), ethanol (EtOH), terpenes (Terp) and menthol (MEN) were formulated. The composition concentration was varied from minimize to maximize composition in liposomes, and the drugs (hydrophilic and lipophilic drugs) concentration was varied to maximize drugs in liposomes in percentages molar ratio of PC, respectively. The sonication method was used to prepare different model formulations. The entrapment efficiency, loading efficiency, molar turbidity, stability and skin irritation of pre-formulation were investigated for choosing the optimum composition ratio for formulating each model liposomal formulation. The high entrapment efficiency, high loading efficiency, high molar turbidity, high stability and low skin irritation model formulations were selected.

2.1 Hydrophilic and lipophilic drugs-loaded model liposomal preparation

Each model formulations of liposomes, transfersomes, niosomes, ethosomes, invasomes, flexosomes, transethosomes and menthosomes were prepared according to formulations obtained from a experimental design. As shown in Table 1, the numerous formulations of hydrophilic and lipophilic drugs-loaded model liposomal system composed of a controlled amount of PC and model drug, and various amounts of surfactant, cholesterol, ethanol, terpene and menthol as chemical enhancer were prepared. The concentration of each composition was selected as causal factors (X_1,X_2, ... and X_n). The concentration of PC was fixed at 0.773% (w/v). The model liposomal formulations were prepared by the sonication method. Briefly, the composition mixtures of PC, surfactant, cholesterol, ethanol, terpene and menthol were dissolved in chloroform/methanol (2:1 v/v ratio). The solvent was evaporated under nitrogen gas stream. The lipid film was placed in a desiccator for 6 h to remove the remaining solvent. The dried lipid film was hydrated with acetate buffer solution (pH 5.5). The hydrophilic drug ($Drug_H$) was incorporated during the hydrated process while the lipophilic drug ($Drug_L$) was incorporated during the lipid mix process. The model formulations were subsequently sonicated for two cycles of 15 min using a bath-type sonicator (5510J-DTH Branson Ultrasonics, Danbury, USA). The liposomal formulations were freshly prepared or stored in airtight containers at 4 °C prior to use.

Tablel 1 The composition of each liposome carriers

Liposome carriers	PC	Chol	Surf	Non-Surf	EtOH	Terp	MEN	$Drug_H$	$Drug_L$
Liposomes	✓	✓	-	-	-	-	-	✓	✓
Transfersomes	✓	✓	✓	-	-	-	-	✓	✓
PEGylated liposomes	✓	✓	-	-	✓	✓	-	✓	✓
Menthosomes	✓	✓	✓	-	-	-	✓	✓	✓

3. Characterization of model liposomal formulations and other model formulations

3.1 Particle size, size distribution and zeta potential

The particle size, size distribution and zeta potential of the model formulations were determined by a Zetasizer Nano ZS (Malvern Instruments, Malvern, UK) at room temperature. One hundred µL of the liposome and transfersome suspensions were diluted with 1400 µL deionized water. At least three independent samples were taken, each of which was measured at least three times.

3.2 Morphology study

The morphology of the lipid assembly was observed by transmission electron microscopy (TEM) and freeze-fractured transmission electron microscopy (FF-TEM). A small drop of sample solution placed on a small copper block was rapidly frozen in nitrogen slash, which was freshly prepared just before its use by decompression in a vacuum chamber [45]. The quenched sample was fractured in a freese-fractured apparatus JFD-9010 (JEOL, Tokyo, Japan). The fractured surface was rotary-shadowed with platinum-carbon at an angle of 10° and the shadowed surface was coated with carbon. The freeze-fractured replica obtained was washed with chloroform/methanol (4:1 v/v ratio) and observed with a transmission electron microscope JEM1400 (JEOL, Tokyo, Japan) equipped with a digital CCD camera (ES500W Erlangshen, Gatan, USA).

3.3 Elasticity evaluation

The elasticity value of the vesicle bilayer was directly proportional to equation (1) following:

$$\text{Elasticity} = J_{flux} \times (r_v/r_p)^2 \qquad (1)$$

Where J_{flux} was the penetration rate through a permeability membrane, r_v was the vesicle size after extrusion and r_p was the membrane pore size. To measure J_{flux}, the liposomes were extruded through a polycarbonate membrane with a pore size diameter of 50 nm (r_p), at a pressure of 0.5 MPa. After 5 min of extrusion, the extrudate was weighed (J), and the average vesicle diameter after extrusion (r_v) was measured by particle size analyzer.

3.4 Drug content, entrapment efficiency (%EE) and loading efficiency (LE)

The concentration of drug in the formulation was determined by HPLC analysis after disruption of the vesicles with Triton® X-100 (0.1% w/v) at a 1:1 volume ratio and appropriate dilution with phosphate buffer solution pH 7.4 (PBS). The liposomal/Triton® X-100 solution was centrifuged at 10,000 rpm at 4°C for 10 min. The supernatant was filtered with a 0.45 μm nylon syringe filter. The entrapment efficiencies and the loading efficiencies of the drug-loaded formulation were calculated by equations (2) and (3), respectively.

$$\% \text{ entrapment efficiency} = 100-(C_L/C_i) \times 100 \quad (2)$$

$$\% \text{ entrapment efficiency} = (C_L/C_i) \times 100 \quad (3)$$

Where C_L was the concentration of drug loaded in the formulation as described in the above methods and C_i was the initial concentration of drug added into the formulation. The equations (1) were chosen for hydrophilic drug-loaded formulation calculation and the equations (2) were chosen for lipophilic drug-loaded formulation calculation.

$$\text{Loading efficiency} = D_t/L_t \quad (4)$$

Where D_t was the total amount of drug in the formulation and L_t was the total amount of PC added into the formulation.

3.5 Stability evaluation

The model liposomal formulations were stored at 4±1 °C and 25±1 °C (room temperature, RT) for 30 days. Both the physical and the chemical stability of the model formulation were evaluated and the optimal formulation. The physical stability was assessed by visual observation for sedimentation. The chemical stability was determined by measuring the drug remaining in the formulation by HPLC on day 1 and 30 for the model formulation evaluation and on day 1, 15, 30, 60, and 90 for the optimal formulation, respectively.

3.6 Thermal properties measurement

Differential scanning calorimetry (DSC) measurements were performed using a Thermo plus DSC-8230 instrument (Rigaku Co., Tokyo, Japan), heated from -20 to 80°C with heating scan at the rate of 1°C/min. The empty vesicles and vehicle or continues phase were separated by ultracentrifugation, the sediment was used as sample for DCS measurement. The sample (10 mg) was weighed and placed in an aluminum pan (Rigaku Co., Tokyo, Japan). The transition temperature was determined as the peak of the endothermic transition peaks.

3.7 HPLC analysis

The drug concentration was analyzed by HPLC. All samples were stored at 4 °C until analysis.

4. *In vitro* skin permeation study

Human skin obtained by abdominalplasty surgeries supported by Yanhee Hospital, Bangkok, Thailand was used as a model membrane for the skin permeation study. The study was carried out with the approval of the committee on human rights related to human experimentation, Silpakorn University, Thailand. The excess adipose layer was sectioned off from the received skin by dissecting with the surgical scissors. The epidermis was separated from the dermis using the heat separation technique. The skin was immersed into hot water for controlling the temperature at 60°C for 1 min. Then, the epidermal layer was carefully separated from the dermis using blunt forceps to produce intact sheets ready for mounting on diffusion cells. The obtained epidermis were wrapped with aluminum foil and stored at -20°C until used. The stored epidermis were allowed to thaw, cut into 4.5 cm×4.5 cm pieces and hydrated by placing in isotonic phosphate buffer in a refrigerator (at about 4°C) overnight before used. The skin samples were mounted between the diffusion chambers with a 32±1 °C water jacket to control the temperature. The dorsal surface of the skin was placed in contact with the donor chamber, which was filled with the model liposomal formulation. The receptor chamber was filled with PBS and stirred with a Teflon magnetic bar driven by a synchronous motor. At time intervals, one mL aliquot of receptor was withdrawn, and the same volume of fresh medium was added back into the chamber. The concentration of permeants in the samples was analyzed by HPLC, and the cumulative skin permeation profile was plotted against time. The steady-state flux was determined as the slope of linear portion of the plot. Lag time was also obtained by extrapolating the linear portion of the penetration profile to the abscissa. The skin permeation of model drug was analyzed using the mathematical model based on the Fick's law of diffusion. The permeability coefficients (K_p) were calculated from the cumulative skin permeation profile using the steady-state flux (J), and the donor concentration (C_d) of the formulations by equations (5)

$$K_p = J/C_d \qquad (5)$$

5. Determination of optimal formulation

5.1 Optimization by RSM-S The optimization study of each liposomal carriers formulation based on RSM-S was performed with the data set obtained for the model liposomal formulations [46]. Details of the simultaneous optimization methods with RSM-

S have been fully given previously [47-49]. The optimal formulation was defined as a sufficient cumulative drug-permeated skin at 2, 4, 6, 8, 10 and 12 h, the flux and the skin permeability coefficient. The best liposomal formulation should have the maximum value of permeability coefficient value, flux and cumulative drug-permeated skin at 2–12 h, and minimum lag time. Once the RSM-S-estimated optimal formulation was obtained, its reliability was evaluated using BS resampling, which has been fully described previously [50].

5.2 Latent structure analysis To elucidate the latent structure underlying the menthosomes, a BN analysis was applied. BN was used to construct a probabilistic graphical model of the latent structure and elucidate the relationships within the latent structure by estimating conditional probability distributions that could clarify the relationships between formulation factors (causal factors), the physicochemical characteristics (latent variables) and skin-permeability response variables, as a path diagram for simplifying to understand the important foundation information.

6. The comparative study

The optimal formulation of each liposomal carriers (liposomes, transfersomes and menthosomes) estimated using computer programs was formulated by the experiment. Particle size, size distribution, zeta potential, elasticity, drug content, entrapment efficiency, morphology, stability and thermal properties of each optimal liposomal formulation were characterized and compared. The skin irritation and skin permeation study were performed using human skin as a skin model membrane. Then, the skin samples were observed under the light microscope and the confocal laser scanning microscopy (CLSM), respectively. The best novel liposomal carriers formulation for transdermal drug delivery of hydrophilic and lipophilic drugs was chosen. The most potential liposomal systems of both hydrophilic and lipophilic drugs were incorporated in topical formulation cream or gel base and compared to the potential commercial products.

7. Computer programs

dataNESIA, Version 3.2 (Yamatake Corp., Fujisawa, Japan) was used for drawing the response surfaces for each variable and predicting the latent variables and response variables (skin permeation) for the various formulations. SOM clustering was performed using Viscovery SOMine, (Version 5.0, Eudaptics Software GmbH, Vienna, Austria). BayoNet (Version 5.0, Mathematical Systems Inc., Tokyo, Japan), was used to construct the probabilistic graphical model among the formulation factors, the latent variables and the response variables, and to estimate conditional independencies.

8. Ethics in the animal study

This human skin study was performed at Silpakorn University and complied with the regulations of the committee on ethics in the human rights related to human experimentation, Silpakorn University, Thailand.

9. Data analysis

Data were expressed as the means $\pm$ standard error (SE) of the mean and statistical significance of differences between formulations employing the one-way analysis of variance (ANOVA). The value of $p<0.05$ was considered statistically significant.

ผลการวิจัยและอภิปรายผล (Results and discussion)

1. Formulation of meloxicam-loaded liposomes

1.1 Pre-formulation study

To obtain the optimal molar ratio of the vesicle component in the vesicle formulation with high entrapment efficiency (EE), high loading efficiency (LE) and high molar turbidity, the pre-formulation of liposome and/or transfersome was prepared and investigated. The concentration of MX and lipid composition (i.e., cholesterol and surfactant) was varied from 0 to 20% w/w and 0 to 90% molar ratio of PC, respectively. The molar turbidity was used as the major parameter to identify the vesicle formulation such as the liposome (CLP) or transfersome (TFS) formulation in our study. The optimal molar ratio of Chol and CPC used was in the same range between 10 and 40% molar ratio of PC.

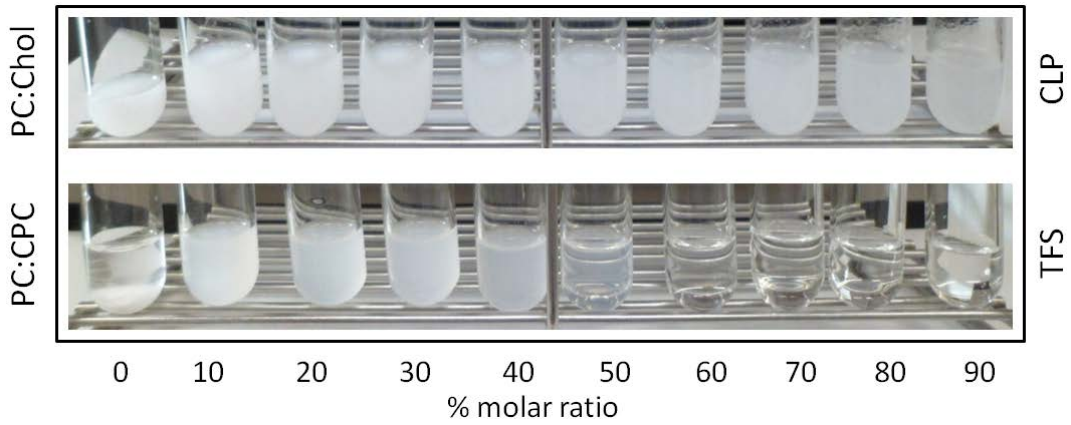

Figure 1 The turbidity of different vesicle component in the formulation.

The turbidity of different vesicle component of Chol and CPC is shown in Figure 1. In liposome formulation (PC:Chol), Chol was uneffect on the turbidity due to no significantly difference in manner of the formular which using Chol in the range of 0-90% molar ratio. However, in transfersome formulation (PC:CPC), the turbidity was markedly decreased at 40% CPC, and the higher CPC (more than 60%), the transparent dispersion was observed.

The molar turbidity of liposome and transfersome formulation detected by the spectroscopy is shown in Figure 2. The molar turbidity of liposome and transfersome formulation corresponded well with the results of the turbidity by visual observation (Figure 1). The molar turbidity of liposome was unsignificantly difference in the range of Chol from 0-90% molar ratio. It is reported that the incorporation of Chol affects liposome interaction and bilayer stability [51] e.g., (i) the physical stability of liposome can

be enhanced by cholesterol incorporation [52], (ii) 11 mol% Chol can reduce the van der Waals attraction force and increase the net repulsion forces between bilayers [53], (iii) the lower fluidity and more rigidity of phosphatidylcholine vesicle are obtained after Chol addition [54], (iv) 50 mol% is the maximum amount of Chol that can incorporate into reconstituted bilayers, although the solubility limit for cholesterol in lipid shows a subtle dependence on lipid molecular structure [55], and furthermore, Chol in the range of 10-40 mol% affects membrane elasticity making the bilayer membrane more rigidity [56]. Therefore, the 10-40% molar ratio of Chol was chosen in our studies.

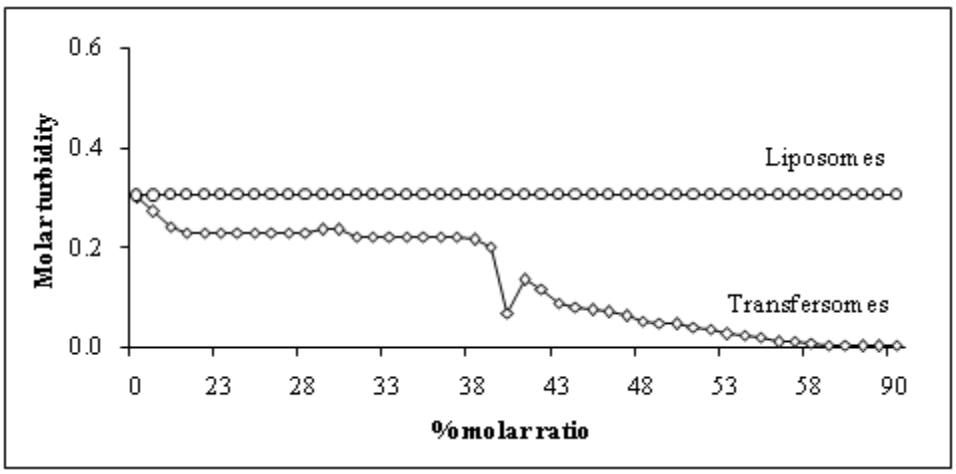

Figure 2 The molar turbidity of the different vesicle component in the liposomes (◯; PC:Chol) and transfersomes (◇; PC:CPC) formulation.

Conversely, the molar turbidity of transfersome decreased markedly at 40% of CPC, and subsequently decreased in the range of 41-90% molar ratio. The change in turbidity indicated that transfersomes possibly reformed to mixed micelle structure. Transfersomes and mixed micelle structure had the different intrinsic characteristics resulting in different effect on skin permeation as transdermal drug delivery. Therefore, the 10-40% CPC was chosen to differentiate the pure transfersome structure to the mixed micelle.

The EE and LE of meloxicam-loaded vesicle formulation were determined by HPLC. The data of EE, LE and drug content in the formulation of 20% MX was not detected (N.D.) because MX powder was not completely dissolved in chloroform/methanol (2:1 v/v ratio), therefore 20% MX-loaded vesicle formulation could not be prepared and determined. The maximum concentration of MX dissolved in chloroform/methanol (2:1 v/v ratio) was up to 10% w/w of PC.

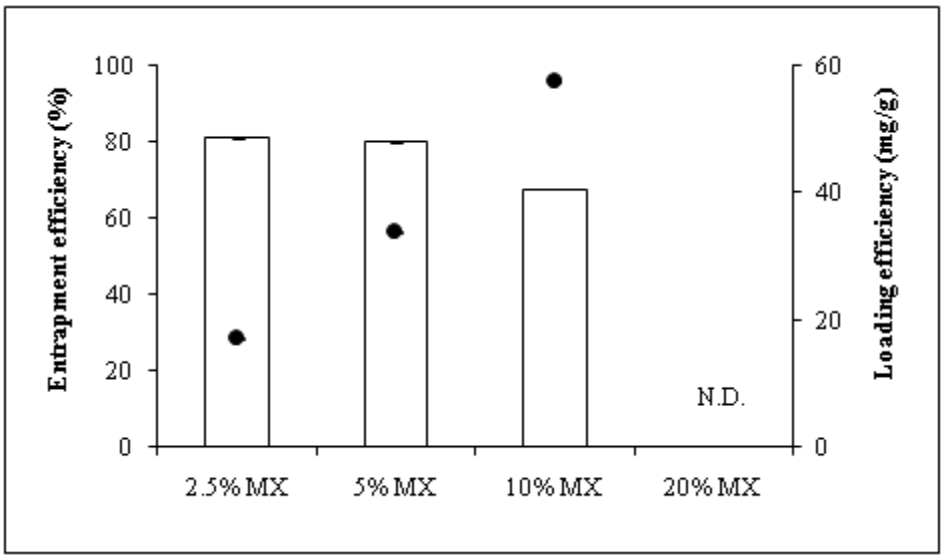

Figure 3 The entrapment (*white bar*) and loading (*solid circle*) efficiencies of meloxicam-loaded vesicle formulation.

Figure 3 shows the entrapment and loading efficiencies of meloxicam-loaded vesicle formulation. The 2.5% MX-loaded vesicle formulation had the highest EE but the lowest LE, while the 10% MX-loaded vesicle formulation had the lowest EE but the highest LE and drug content in the formulation. The drug content in the formulation of the 2.5, 5 and 10% MX-loaded vesicle formulation was 156.83, 309.53 and 524.21 mg/mL, respectively. Therefore, 10% MX-loaded vesicle formulation was the optimal ratio of MX for this investigation, as it provided high EE, high LE and high drug content in the formulation.

Based on the turbidity studies, EE, LE and drug content in the formulation of all investigated MX-loaded vesicle formulations, it can be suggested that the 10-40% Chol, CPC, and the 10% MX-loaded vesicle formulation were desirable for further investigation to formulate model liposomes and/or transfersomes for transdermal drug delivery carriers.

1.2 Optimization of liposomes

To obtain the optimal molar ratio of model MX-loaded transfersome formulation to improve in skin permeation of MX, 10 formulations of MX-loaded transfersomes according to the formulations obtained from a two-factor spherical second-order composite experimental design were prepared. The concentration of PC and MX were fixed at 0.773 and 0.077% (w/w), respectively. The concentration of Chol and CPC selected as causal factors was varied from 10-40% molar ratio (from the pre-formulation study). The physicochemical characteristics (e.g., vesicle size, zeta potential, elasticity and entrapment efficiency) selected as basic characteristics (latent variables), an *in vitro* skin-

permeation study of MX-loaded transfersomes at 2–12 h, and the steady-state flux value selected as response variables were also investigated. The optimal MX-loaded transfersome formulation was estimated using a nonlinear response-surface method incorporating thin-plate spline interpolation (RSM-S) and confirmed by the experiment. Moreover, the response surfaces estimated by RSM-S show the relationship between causal factors and latent variables, and the relationship between causal factors and response variables.

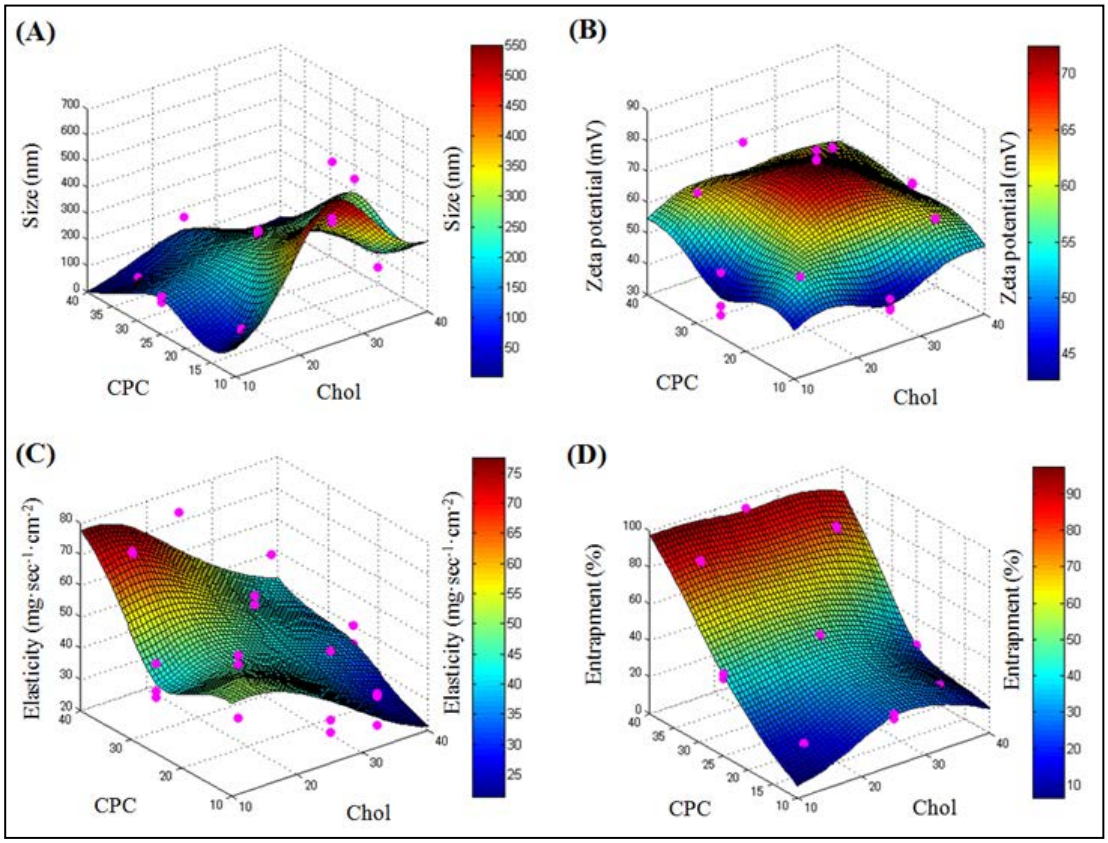

Figure 4 The response surface of the model formulation of (A) vesicle size, (B) zeta potential, (C) elasticity and (D) entrapment efficiency.

Figure 4 shows the response surfaces of vesicle size, zeta potential, elasticity and entrapment efficiency determined by RSM-S. The response surface represented the effect of Chol and CPC in MX-loaded transfersomes on their physicochemical characteristics (e.g., vesicle size, zeta potential, elasticity and entrapment efficiency). The results suggested that an increasing of Chol content resulted in a significant increase in vesicle size, a decrease in elasticity and a slightly increase in entrapment efficiency. While an increasing of CPC resulted in a significant decrease in vesicle size, but increase in zeta potential, elasticity and entrapment efficiency.

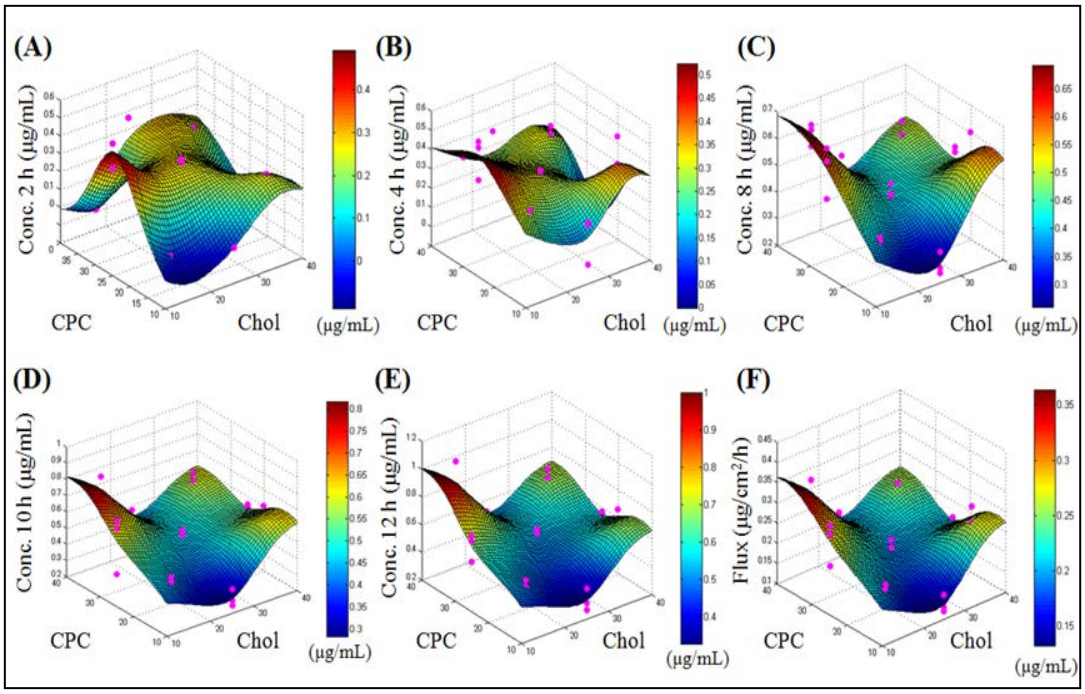

Figure 5 The response surface of the concentration of MX permeated the skin at *t* h of (A) 2 h, (B) 4 h, (C) 8h, (D) 10 h, (E) 12 h and (F) flux.

Figure 5 shows the response surfaces of the concentration of MX-permeated skin at 2, 4, 8, 10 and 12 h and the steady-state flux value determined by RSM-S. The response surface represented the effect of Chol and CPC on skin permeation of MX-loaded transfersomes. The results suggested that the concentration of MX-permeated skin at *t* h and steady-state flux value increased as the concentrations of Chol and CPC increased. Although in the early phase of skin permeation (conc. 2 h), a slight difference in the response surfaces was observed, for the most part of all investigated, response surfaces also showed a similar pattern. This result suggested that RSM-S successfully estimated the relationship between the causal factors and response variables attributed to the MX-loaded transfersomes.

The 10 model formulations of MX-loaded transfersomes were optimized based on the original data set using RSM-S. The search directions for the response variables were set to produce a high permeability and also a high steady-state flux value. X_1 = 10.5% and X_2 = 29.0% molar ratio were estimated as the optimal MX-loaded transfersome formulation.

1.3 Meloxicam-loaded liposomes

The optimal formulation of PC/Chol/CPC; 100:10.5:29.0 molar ratios estimated using RSM-S was chosen to be a model formulation of various liposome and transfersome formulations in our further investigation. As shown in Table 2, various transfersome

formulations were formulated in order to investigate the influence of the formulation factors i.e., surfactant's charge, surfactant's carbon chain length and surfactant's amount.

Table 2 Classification of investigation studies

Surfactant factor	Code	Lipid component (%w/v)							Acetate buffer (mL)
		MX	PC	Chol	C4	C12	C16	A16	
Charge	N-CLP	0.07	0.77	0.04	–	–	–	–	100
	C-TFS	0.07	0.77	0.04	–	–	0.10	–	100
	A-TFS	0.07	0.77	0.04	–	–	–	0.10	100
Carbon chain length	C4	0.07	0.77	0.04	0.05	–	–	–	100
	C12	0.07	0.77	0.04	–	0.08	–	–	100
	C16	0.07	0.77	0.04	–	–	0.10	–	100
Content	0% CPC	0.07	0.77	0.04	–	–	–	–	100
	10% CPC	0.07	0.77	0.04	–	–	0.04	–	100
	20% CPC	0.07	0.77	0.04	–	–	0.07	–	100
	29% CPC	0.07	0.77	0.04	–	–	0.10	–	100

Note: The concentration of PC in the formulation was fixed at 10 mM. C4, cationic surfactant with 4 carbons; C12, cationic surfactant with 12 carbons; C16, cationic surfactant with 16 carbons; A16, anionic surfactant with 16 carbons.
Abbreviations: A-TFS, anionic transfersomes; Chol, cholesterol; CPC, cetylpyridinium chloride; C-TFS, cationic transfersomes; MX, meloxicam; N-CLP, neutral conventional liposome; PC, phosphatidylcholine.

2. The influence of formulation factors

To investigate the influence of formulation factors i.e., surfactant's charge, surfactant's carbon chain length and surfactant's amount, on physicochemical characteristics (e.g., vesicle size, size distribution, zeta potential, elasticity, drug content in the formulation and entrapment efficiency), morphology, thermal properties, *in vitro* drug release and *in vitro* skin permeation were characterized.

2.1 Physicochemical characteristics

2.1.1 Effect of surfactant charge

The physicochemical characteristics of the anionic transfersomes (A-TFS), neutral conventional liposomes (N-CLP) and cationic transfersomes (C-TFS) outlined in Table 4 reveal that the addition of anionic surfactant, i.e. sodium hexadecyl sulfate (SHS) in A-TFS, and cationic surfactant, i.e. cetylpyridinium chloride (CPC) in C-TFS, produced significant differences in vesicle size (nm), zeta potential (mV), elasticity ($mg \cdot sec^{-1} \cdot cm^{-2}$) and EE (%) compared with N-CLP. A-TFS displayed a large vesicle size (~164 nm) with a negative charge (~-60.8 mV). In contrast, C-TFS exhibited a small vesicle size (~90 nm) with a positive charge (~+48.3 mV). Moreover, the elasticity and EE of both types of TFS were higher than that of N-CLP. The neutralization of the anionic drug (MX) and cationic vesicles (C-TFS) may have resulted in smaller vesicle sizes due to a reduction in the repulsive forces in the C-TFS bilayer. In contrast, the synergistic effects of the anionic drug (MX) and anionic vesicles (A-TFS) may have resulted in large vesicle sizes due to the induction of repulsive forces in the A-TFS bilayer [57]. The vesicle formulations were composed of neutral material, i.e. Chol, and positively and negatively charged surfactants,

i.e. CPC and SHS, respectively. Under the experimental condition of pH 5.5, the isoelectric point (PI) of PC (PI = 6) was higher than the pH. However, the PI of MX (PI = 2.6) was lower than the pH. Therefore, PC and MX displayed a net positive charge and a net negative charge, respectively. Thus, the net charges of A-TFS, N-CLP and C-TFS were negative, neutral and positive, respectively, as a result of the intrinsic properties of their surfactants and the total net charge of the liposome composition. SHS and CPC exhibit a high radius of curvature, which could destabilize and increase the deformability of the vesicle bilayer, thus increasing its fluidity or elasticity [58]. The carbon chain lengths of CPC and SHS were the same, but C-TFS exhibited a stronger interaction with the bilayer than SHS due to its significantly higher elasticity. This result suggests that the hydrophilic head group of the surfactant directly affects the elasticity of the vesicle bilayer. The beneficial roles of SHS and CPC within TFS were readily apparent, as the intrinsic properties of the surfactants led to the increased solubility of MX in the vesicle bilayer and therefore EE values for A-TFS and C-TFS that were significantly higher than that of N-CLP. Our results were consistent with a previous study that demonstrated that the EE of a drug in phosphatidyl-ethanolamine vesicles is significantly increased when sodium stearate (anionic surfactant) is incorporated into the vesicles [59].

Table 3 Effect of the surfactant on vesicle size, zeta potential, elasticity and entrapment efficiency of the vesicle formulation (mean ± standard error)

	Vesicle size (nm)	Zeta potential (mV)	Elasticity ($mg \cdot sec^{-1} \cdot cm^{-2}$)	Entrapment efficiency (%)
Effect of surfactant charge				
A-TFS	164.3±3.2	−60.8±0.51	19.2±1.68	54.11±0.33
N-CLP	108.8±10.6	1.3±1.01	11.6±1.64	26.36±0.26
C-TFS	90.6±9.2	48.3±0.67	88.7±0.98	68.06±0.84
Effect of surfactant carbon chain length				
C4	113.3±3.5	10.9±3.21	120.1±2.87	9.92±0.41
C12	94.5±2.0	26.9±2.63	108.7±1.74	46.11±0.29
C16	90.6±9.2	48.3±0.67	88.7±0.98	68.06±0.84
Effect of surfactant content				
0% CPC	108.8±10.6	1.3±1.01	11.6±1.64	26.36±0.26
10% CPC	78.8±9.2	36.6±1.37	23.6±2.40	29.51±0.98
20% CPC	81.6±1.0	39.7±3.98	52.6±1.32	47.25±0.67
29% CPC	90.6±9.2	48.3±0.67	88.7±0.98	68.06±0.84

Abbreviations: A-TFS, anionic transfersomes; CPC, cetylpyridinium chloride; C-TFS, cationic transfersomes; N-CLP, neutral conventional liposomes.

2.1.2 Effect of surfactant carbon chain length

The physicochemical characteristics of MX-loaded vesicle formulations containing short chain (butylpyridinium chloride; BPC (C4)), medium chain (laurylpyridinium chloride; LPC (C12)) and long chain (cetylpyridinium chloride; CPC (C16)) carbons are shown in Table 3. The vesicle size and elasticity decreased slightly with increasing carbon chain length in the order of C4, C12 and C16. The vesicle size and elasticity decreased approximately 20% and 26%, respectively, as C4 was substituted by C16. Surfactants with

longer carbon chains may increase vesicle rigidity by inserting deeper into the bilayer; thus, increasing the carbon chain length led to decreased vesicle size. Meanwhile, the vesicle size and zeta potential of liposomes containing 1,2-dimyristoyl-sn-glycero-3-phosphocholine (DMPC, C14), 1,2-dipal- mitoyl-sn-glycero-3-phosphocholine (DPPC, C16) and 1,2-diste -aroyl-sn-glycero- 3-phosphocholine (DSPC, C18) and loaded with midazolam or propofol were not significantly influenced by the lipids having the same head group [60]. The insertion of C8 (short chain carbon) resulted in decreased vesicle sizes in the order of poly (asparagines) grafted with C8, C12, C18 and C22 [61]. These results suggest that varying trends in vesicle size may be influenced by the hydrophilic head group of the surfactant and the method of preparation. The zeta potential increased significantly with increasing carbon chain length in the order of C4, C12 and C16, with an increase of approximately 77% when C4 was substituted with C16. These results could be due to the intrinsic properties of each surfactant. The hydrophobicity of long chain carbons is greater than that of short chain carbons, and long chain carbons can led to the increased solubility of the surfactant molecule in the PC bilayer. The amount of long chain carbons in the PC bilayer was greater than the amount of short chain carbons, and long chain carbons might therefore exhibit stronger electrostatic interactions and zeta potentials than short chain carbons. The elasticity of the vesicle increased in the order of C16, C12 and C4. These results are consistent with the findings of Park *et al.*, in which the elasticity was observed to increase with decreasing carbon chain length (increased in the order of C22, C18, C12 and C8).[61] Because long-chain carbons exhibit strong hydrophobic interactions with PC, the PC bilayer of the vesicles becomes tighter. Long chain carbons decrease the elasticity of the vesicle through their deep insertion into the PC bilayer. Furthermore, short-chain carbons increase the elasticity of the vesicle through their shallow insertion into the PC bilayer. Therefore, the EE significantly increased with increasing carbon chain length in the order of C4, C12 and C16, with ~85% increase when C4 was substituted with C16. These results are consistent with Ali *et al.*, who demonstrated that an increase in carbon chain length led to an increase in the encapsulation of hydrophobic drugs, such as propofol and midazolam, into vesicles [60]. Increasing the carbon chain length was also found to increase the encapsulation of water-insoluble drugs, such as ibuprofen, into vesicles in the order of dimyristoyl phosphatidyl-choline, DMPC (C14); distearoyl phosphatidylcholine, DSPC (C18); and dilignoceroyl phosphatidylcholine, DGPC (C24) [62]. The increase in the EE values of long-chain carbons could be attributed to the increased hydrophobic area within the PC bilayer [62, 63].

2.1.3 Effect of surfactant content

The physicochemical characteristics of MX-loaded vesicles composed of varying contents of surfactant, including the control (0% CPC), low (10% CPC), medium (20% CPC) and high (29% CPC) surfactant contents, are shown in Table 3. The vesicle size and zeta potential tended to increase slightly, while the elasticity and EE significantly increased in the order of 10% CPC, 20% CPC and 29% CPC. The vesicle size, zeta potential, elasticity and EE increased by approximately 13%, 23%, 73% and 56%, respectively, when 10% CPC was substituted with 29% CPC. The trends in increasing vesicle size, zeta potential, elasticity and EE were recognized as intrinsic properties of the surfactant. Liu *et al.*, demonstrated that an increase in the biosurfactant produced by some *Bacillus subtilis* strains from 0.05-0.24 mg/mL resulted in a decrease in the vesicle size of soy PC liposomes [64]. However, Mohammed *et al.*, demonstrated that an increase in stearylamine (cationic surfactant) from 1-6 μM resulted in an increase in the vesicle size of egg PC liposome.[62] The insertion of surfactant into the vesicle bilayer could increase its curvature and resulted in decreased vesicle size [61]. However, the net effect on vesicle size was influenced by other factors. In addition to the method of preparation, the drug loading in the vesicle bilayer may result in increased vesicle size, as confirmed by the study of Mohammed *et al* [62].

2.2 Morphology and thermal properties of liposomes

2.2.1 Transmission Electron Microscopy (TEM)

The morphology of the two-dimensional (2D) of liposome and analogues was further observed using TEM, justifying the vesicular characteristics. A small size and spherical shape of vesicle was observed from MX-loaded N-CLP, C-TFS and A-TFS as seen in Figure 6.

2.2.2 *Freeze-Fractured Transmission Electron Microscopy (FF-TEM)*

The morphology of the three-dimensional optimal model formulation was further observed using freeze-fractured transmission electron microscopy to determine the details of the vesicular morphology. Nano-sized, smooth surfaces and spherical vesicles were observed, as depicted in Figure 7.

2.3 Stability evaluation

The physicochemical stabilities of MX-loaded vesicle formulations from day 1 to day 120 at 4°C and 25°C were evaluated for recommended storage conditions. After storage at 4°C for 30 days, the MX content had slightly decreased but remained at 90% of the initial formulation. After storage at 25°C for 30 days, the MX remaining in nearly all of the formulations had decreased slightly but remained at 90% and 80% of the initial formulation at day 15 and day 30, respectively. However, after storage at 4 and 25°C for

120 days, the MX remaining in nearly all of the formulations decreased approximately 70-80% and 80-90% from the initial formulation, respectively (Figure 8).

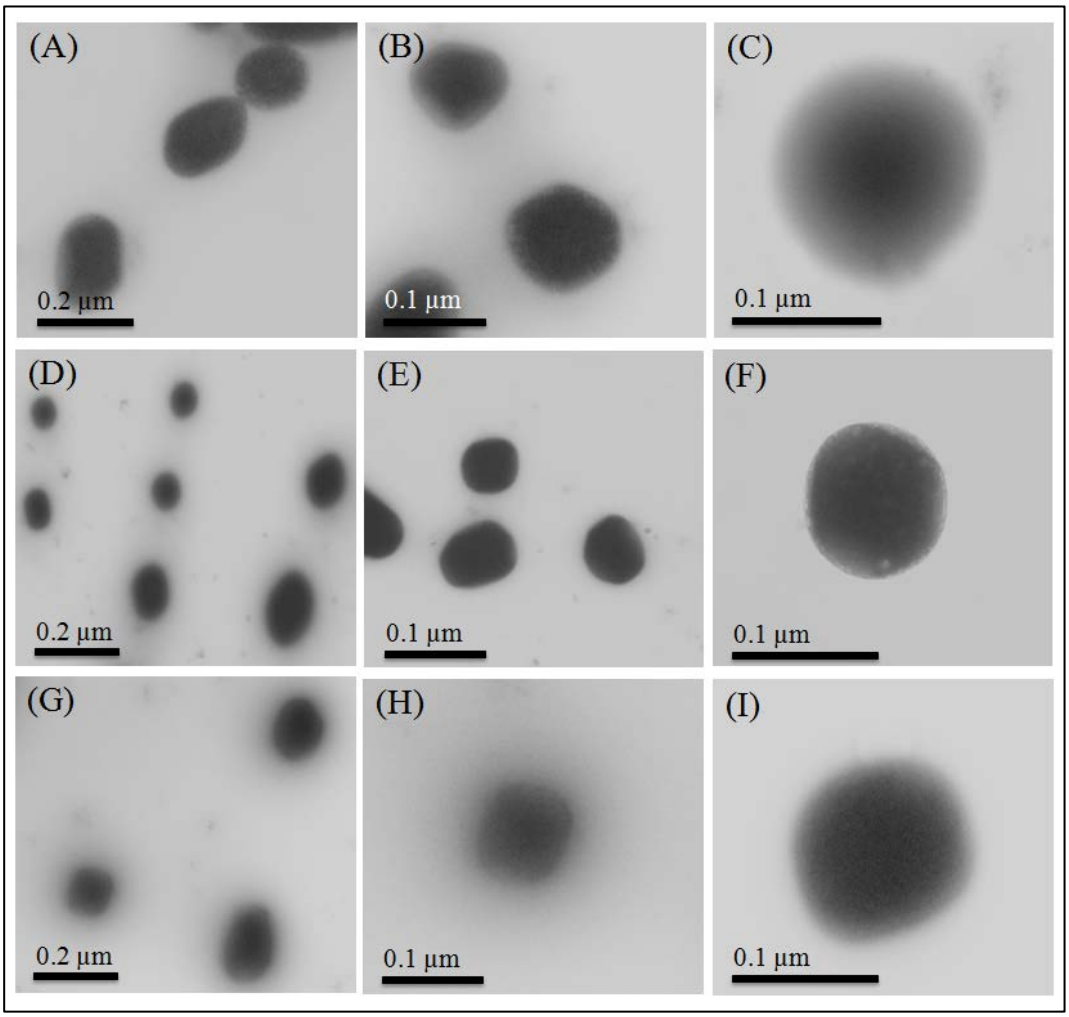

Figure 6 TheTEM image of MX-loaded vesicle formulation; (A) N-CLP (10,000X), (B) N-CLP (30,000X), (C) N-CLP (50,000X), (D) C-TFS (30,000X), (E) C-TFS (30,000X), (F)C-TFS (50,000X), (G) A-TFS (30,000X), (H) A-TFS (30,000X), and (I)A-TFS (50,000X)

The physicochemical stabilities (i.e. vesicle size and zeta potential) of the vesicle formulations were not significantly different between the experimental temperatures of 4°C and 25°C over a period of 30 days. The physicochemical stabilities of nearly all of the vesicle formulations exhibited similar trends to the MX remaining results, indicating the good physicochemical stability of our vesicle formulations at 4°C for 30 days as well as at 25°C for 15 days. In our study, the addition of Chol was essential to the vesicle formulation, which can be attributed to its stabilizing effects.[65, 66] The physicochemical stability of the vesicle formulation was not significantly different between the

experimental temperatures of 4°C and 25°C over 30 days, while the physicochemical stability of the vesicle formulation at the two experimental temperatures (i.e. 4°C and 25°C) was significantly different between day 1 and day 120 of storage. Therefore, the storage age was the primary factor affecting the physicochemical stability of the vesicle formulation in this study. The recommended storage conditions for the vesicle formulation are therefore 4°C for 30 days and/or 25°C for 15 days.

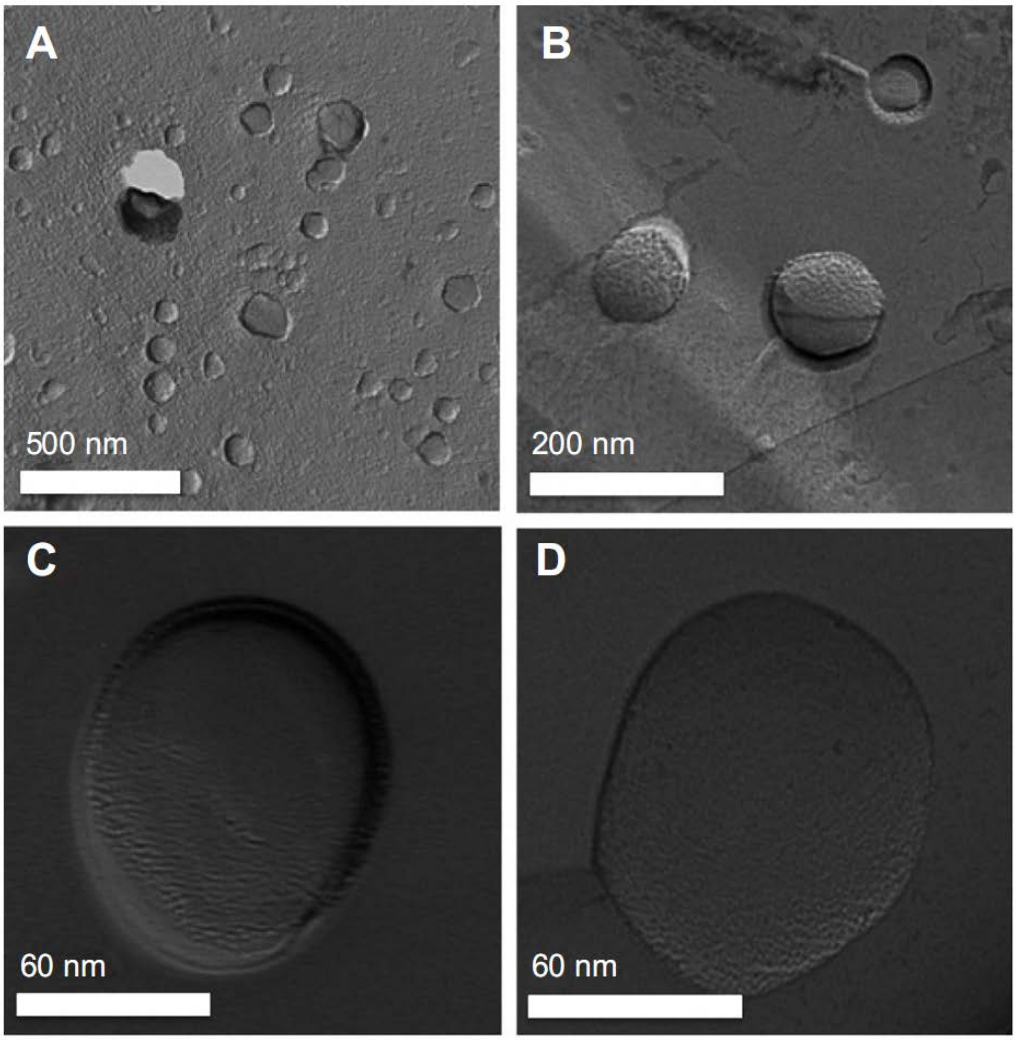

Figure 7 Freeze-fractured transmission electron microscopy images of the optimized meloxicam-loaded vesicle formulation. Notes: (A) 5,000×; (B) 30,000×; (C) 100,000×; (D) 100,000×.

2. 4 Thermal properties measurement

The differential scanning calorimetry *(DSC)* thermograms of the CLP and TFS in the different basic components were shown in Figure 25. The increase in Chol and CPC in TFS resulted in the transition temperature (T_g) shifted to high T_g and low T_g, respectively,

however the net result indicated that the transition temperature of TFS shifted to a lower temperature than CLP as shown in Figure 9. CLP and TFS underwent a single endothermic transition temperature of lipid bilayer at 2.08 and 1.72 °C, respectively. The transition temperature of TFS system was shifted to a lower temperature than CLP, by the addition of CPC.

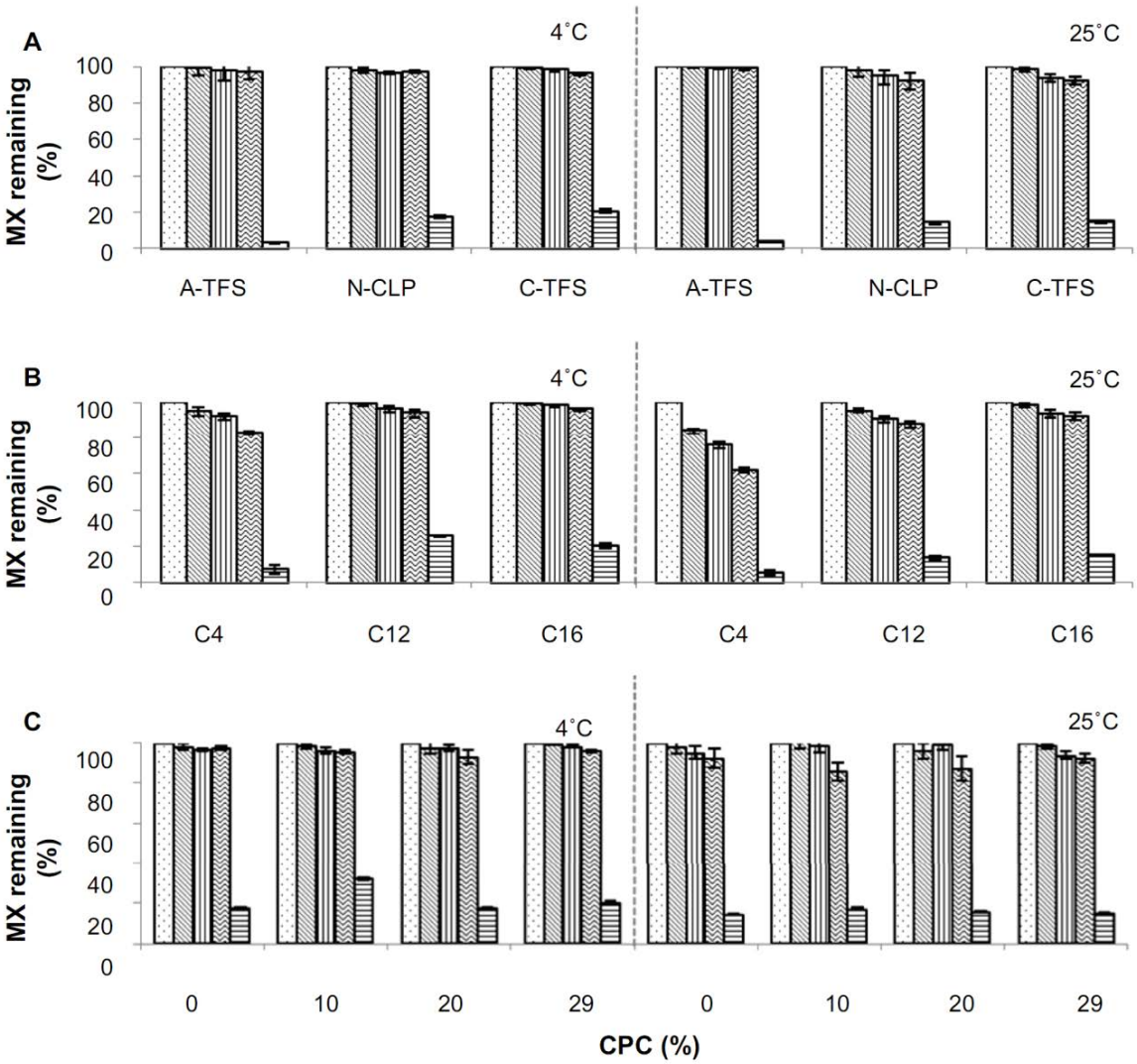

Figure 8 The influence of (A) surfactant charge, (B) surfactant carbon chain length, and (C) surfactant content on the remaining MX at different days (n=3). Notes: ⚀ Day 1; ⚁ day 7; ⚂ day 15; ⚃ day 30; ⚄ day 120. Abbreviations: a-TFs, anionic transfersomes; c-TFs, cationic transfersomes; MX, meloxicam; N-clP, neutral conventional liposomes; cPc, cetylpyridinium chloride

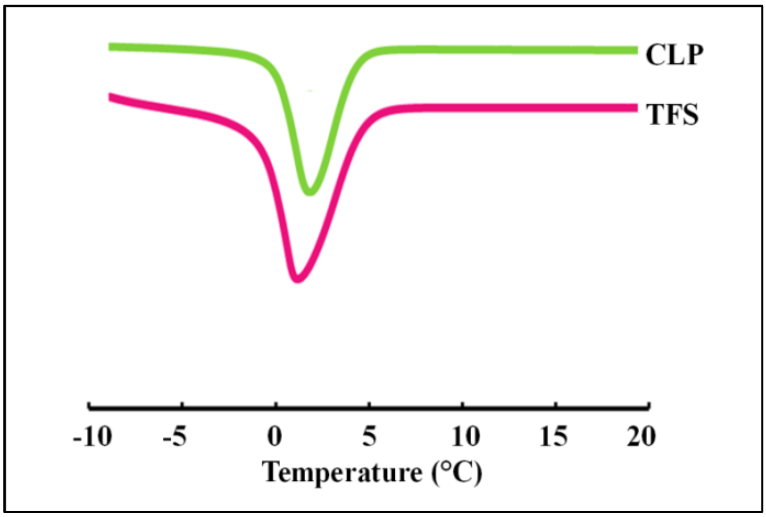

Figure 9 The DSC thermogram of vesicle formulation; (■) conventional liposomes (CLP) and (■) transfersomes (TFS)

3. *In vitro* skin permeation study

Figure 10 shows the graphic plot of the cumulative skin permeation per unit area and the steady-state flux of various MX-loaded vesicle formulations over an incubation period of 2 to 12 h. The skin permeabilities (skin permeation profile and steady-state flux) of A-TFS and C-TFS were not significantly different, while the skin permeabilities of the charged transfersomes were significantly greater than those of the non-charged liposomes (N-CLP). The steady state flux of A-TFS and C-TFS were significantly higher than N-CLP, at approximately 58% and 63%, respectively. The surfactants SHS and CPC in A-TFS and C-TFS can open the dense keratin structures in corneocytes, and both anionic and cationic surfactants swell the SC and interact with the intercellular keratin, thus increasing the skin permeation of various drugs (e.g. hydrocortisone, lidocaine) [67]. Surfactants can interact with skin constituents in many ways. For example, surfactants are widely known to interact with proteins, and thus can inactivate enzymes and bind strongly within the SC. They can swell the SC (most likely by uncoiling the keratin fiber and altering the α-helices to a β-sheet conformation) and are able to modify the binding of water to the SC. Anionic surfactant-treated SC is somewhat brittle, possibly due to the extraction of natural moisturizing factor (NMF). Cationic surfactants are also able to extract lipids from the SC and can disrupt the lipid bilayer packing within the tissue [68]. Clearly, cationic surfactants cause a greater increase in the steady-state flux of MX than anionic surfactants, which, in turn, cause a greater increase in the flux than neutral CLP. Ashton *et al.*,[69] compared the effects of dodecyltrimethylammonium bromide (DTAB), sodium lauryl sulfate (SLS) and polyoxyethylene fatty ether (Brij 36T) on the *in vitro* flux of methyl nicotinamide across excised human skin and reported that permeation enhancement occurred in the following order: cationic, anionic and neutral. However, Brij

36T exhibited a small charge as non-ionic surfactants but a more immediate effect on skin permeation [67].

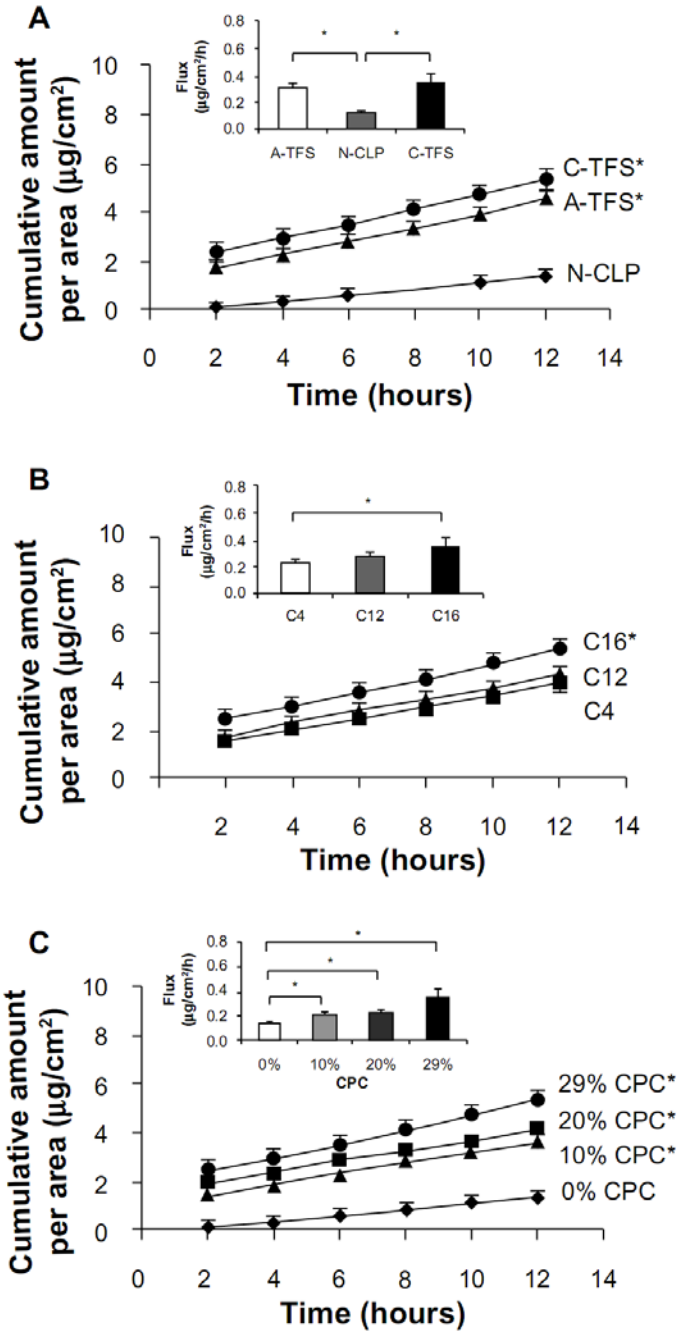

Figure 10 The influence of (A) surfactant charge, (B) surfactant carbon chain length, and (C) surfactant content on the skin permeation profile and the steady-state flux of the vesicle formulation (n=3). *is statistical significance (P-value > 0.05). Abbreviations: a-TFS, anionic transfersomes; CPC, cetylpyridinium chloride; c-TFS, cationic transfersomes; h, hour; N-CLP, neutral conventional liposomes

This result revealed that the anionic and/or cationic surfactants significantly affected the skin permeation of MX across the skin by swelling the SC and interacting with intercellular keratin. However, the crossing of TFS across the skin was attributed to the high deformability of these specialized vesicles due to the accumulation of these "single-chain surfactants" at sites of high stress as a result of their increased propensity to form high-curvature structures. This rearrangement was claimed to reduce the energy required for deformation; the stress was reportedly produced upon drying of the vesicles, which, being flexible, were able to follow the transdermal hydration gradient [70] .

In our study, the skin permeability of the transfersomes increased when the carbon chain length of the surfactant increased. The skin permeability of the vesicle formulation increased with increasing chain length in the order C4, C12 and C16. The_skin permeability of C16 was significantly greater than C4, with an approximately 17% increase when C4 was substituted with C16. These results are consistent with a previous study [71] demonstrating that, as the carbon chain length in the vesicle increased from C7 to C12, the permeation of naloxone increased. Ogiso and Shintani revealed that C12-C14 were the most effective carbon chain lengths used in increasing the permeation of propranolol [72]. Duangjit *et al.*, reported that C18-C24 were more effective than C32 in the permeation of meloxicam [73]. Short-chain carbons may suffer from insufficient lipophilicity for skin permeation, whereas longer chain fatty acids might have much higher affinities for lipids in the SC, thereby hindering their permeation. Our studies suggest that C16 possesses an optimal balance between partition coefficient and affinity to the skin. These results revealed that skin permeability is also affected by the carbon chain length of the surfactant.

The surfactant content affected skin permeability, with the skin permeability of the transfersomes increasing with increasing surfactant content. The skin permeability of the vesicle formulation increased in the order 0% CPC, 10% CPC, 20% CPC and 29% CPC. The skin permeabilities of the 29% CPC, 20% CPC and 10% CPC formulations were significantly higher than that of 0% CPC, by approximately 63%, 41% and 35%, respectively. This result reveals that the surfactant content significantly affected the skin permeability of the vesicle formulation due to the intrinsic properties of the surfactant (CPC), as reported above.

These skin permeability studies demonstrated that the surfactant factor (i.e. charge, carbon chain length and content of surfactant) directly affected the skin permeability of MX.

4. Determination of optimal formulation

4.1 Optimization by RSM-S

Based on its maximum drug loading capacity and molar turbidity, the vesicle formulation composed of over 40% Chol and surfactant, likely re-assembled to a mixed micelle structure. Liposomes and mixed micelle structures display different intrinsic characteristics, resulting in significantly different influences on skin delivery. A content of 10% MX was determined to be the maximum loading capacity in the vesicle formulation. Thus, it was concluded that 0-40 mol% Chol and surfactant and 10 mol% MX-loaded vesicle formulations were desirable for further optimization to develop model vesicle formulations. The twelve model formulations obtained from the two-factor spherical second-order composite experimental design were formulated and evaluated based on the original data set using RSM-S. A response surface and its reliability for the flux variable of the model formulation are illustrated in Figure 2. The search direction for the response variables was set to produce a high flux value. Moreover, to confirm the accuracy and reliability of the optimal formulation estimated using RSM-S, the optimal formulation was confirmed by experiment. It was found that the skin permeation flux value predicted by the RSM-S (predicted flux = 0.31 μg/cm^2/h) was very close to the experimental value (0.31±0.6 μg/cm^2/h). This high reliability suggested that the vesicle composition ratio of the optimal formulation (PC/Chol/surfactant/MX; 0.77: 0.04: 0.10: 0.07% w/v ratio) could be used as the model formulation ratio in further experiments. Moreover, the morphology of the three-dimensional (3D) optimal model formulation was further observed using FF-TEM to determine the details of the vesicular morphology. Nano-sized, smooth surface and spherical vesicles were observed, as depicted in Figure 11.

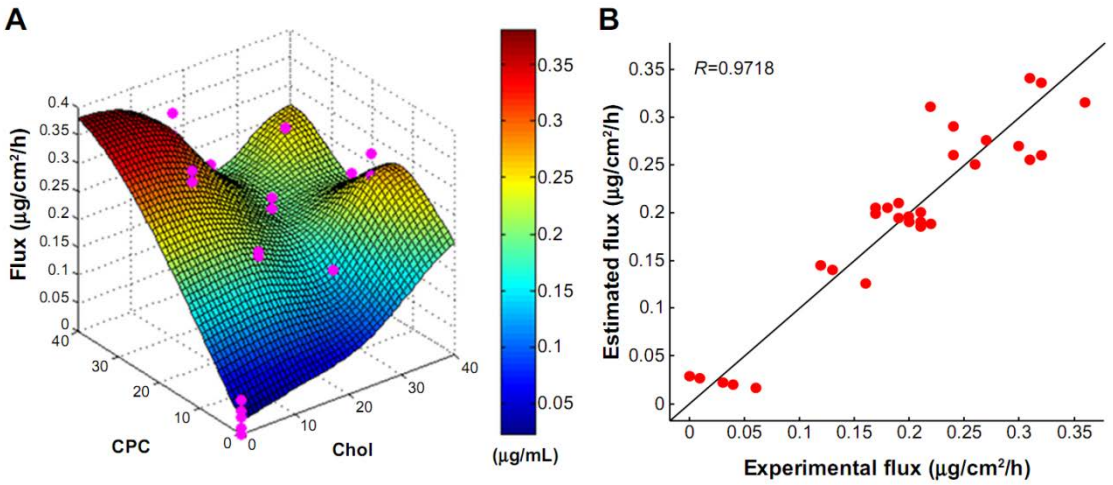

Figure 11 The response surface for the skin permeation flux (A) and the reliability (B) of the model formulation. Abbreviations: chol, cholesterol; cPc, cetylpyridinium chloride; h, hour.

To confirm the accuracy and reliability of the optimal formulation estimated using RSM-S, the optimal formulation was confirmed by the experiment. The studies of the physicochemical characteristics and *in vitro* skin permeation were also performed with the optimal formulation experiment. The composition of the optimal formulation was PC/Chol/CPC; 100: 10.5: 29.0 molar ratios.

Table 4 The predicted and experimental response variables of the optimal formulation

Response	Concentration of MX permeated the skin at *t* h (μg/mL)					*Flux* (μg/cm^2/h)
	2 h	4 h	8 h	10 h	12 h	
Predicted	0.36	0.50	0.64	0.68	0.79	0.31
Experimental	0.40±0.13	0.50±0.14	0.68±0.15	0.73±0.11	0.82±0.11	0.31±0.06

Table 4 shows the predicted and experimental response variables of the optimal formulation and Figure 12 illustrates the skin-permeation profile of MX from the optimal formulation. It was found that the concentration of MX-permeated skin at 2–12 h and the steady-state flux values predicted by the RSM-S were very close to the experimental values. The sufficiently high reliability suggested that RSM-S successfully estimated the optimal formulation of MX-loaded transfersomes.

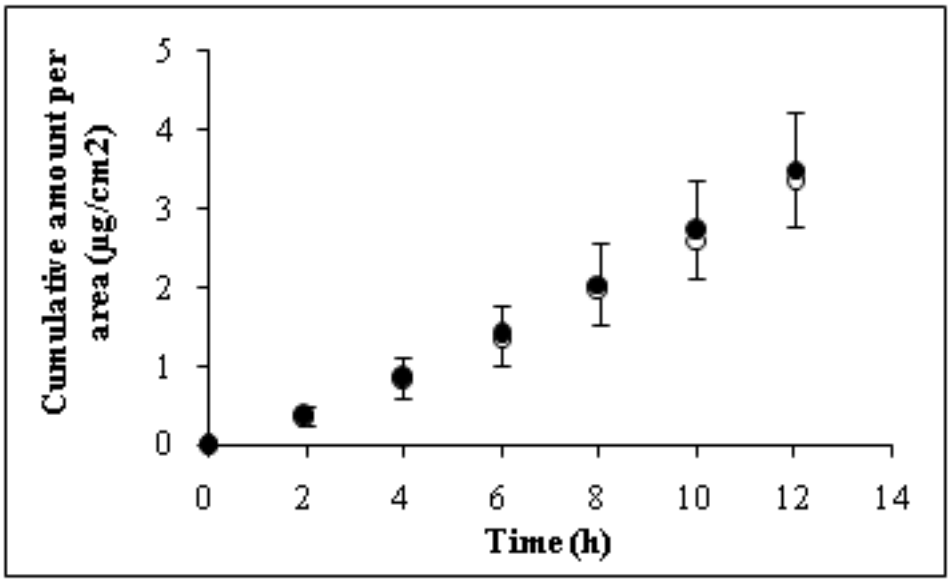

Figure 12 The skin-permeation profile of MX from the optimal formulation: predicted values; (○) and experimental values; (●). Each experimental value is a mean ± S.D. (*n* = 3-4)

4.2 Latent structure analysis

4.2.1 Prediction of response variables and simultaneous optimization

In this study, the formulation characteristics (e.g., vesicle size (X_1), size distribution (X_2), zeta potential (X_3), elasticity (X_4), drug content (X_5), entrapment efficiency (X_6), release rate (X_7)) and formulation factors (e.g., type of PE (Z_1) and content of PE (Z_2)) were used as the causal factors of the response variables. The selection of significant causal factors as the original dataset for the dataNESIA analysis was key to generating an accurate optimal formulation because the evaluation of the precise optimal formulation depended significantly on the integrity and the correctness of the original dataset. The result indicated that the elasticity (X_4), drug content (X_5) and content of PE (Z_2) were selected as effective causal factors for RSM-S by MRA, incorporating a stepwise way of factor selection. The correlation coefficients for the skin permeability (Y_1) and the stability of formulation (Y_2) were sufficiently high (0.7601 and 0.9700, respectively), suggesting that X_5 and Z_2 and X_4, X_5 and Z_2 were important to Y_1 and Y_2, respectively. The contribution index of the effective causal factor for predicting Y_1 and Y_2 is shown in Figure 13.

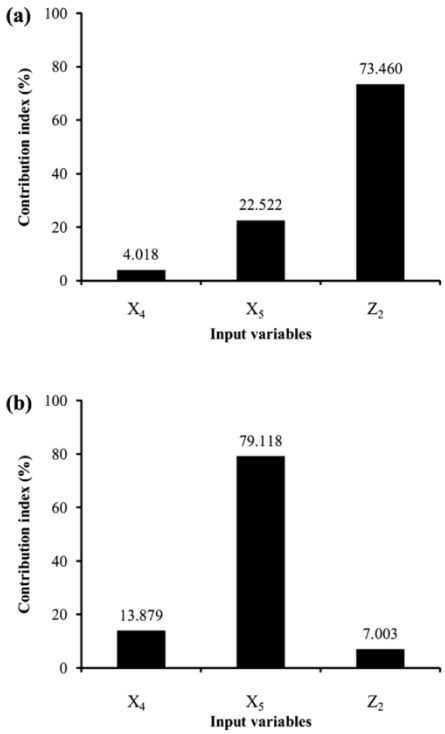

Figure 13 The Contribution Index of Effective Causal Factor for Predicting Response Variables (a) Skin permeability (Y_1) and (b) stability of formulation (Y_2).

The liposome formulation was optimized based on the original dataset using RSM-S. X_4 = 74.5 (mg·sec^{-1}·cm^{-2}), X_5 = 514 (μg/mL) and Z_2 = 0.0689 (%mol) were estimated as optimal formulation characteristics and formulation factors variables. The following were

predicted to be the optimal response variables: Y_1 = 0.269 (μg/cm^2/h) and Y_2 = 375 (μg/mL). The results indicated that the original optimal formulation, which was considered ideal, had a relatively high elasticity (X_4), high drug content (X_5) and high content of PE (Z_2). The formulation characteristics and formulation factors could directly affect the effectiveness of liposome formulation for improving skin permeability, as reported in a previous study [74]. The stability of liposome formulation could be modified by altering aspects of the composition of the liposome, such as the presence of cholesterol [62]. Thus, these effective causal factors might be factors affecting both the efficacy and stability of liposome formulation. The approximate actual relationship between causal factors (formulation characteristics and formulation factors) on response variables (skin permeability and stability of formulation) is shown in Figure 14.

Figure 14a, 14b and 14c show the response surfaces of the skin permeability estimated by RSM-S. Each response surface exhibited relationships among three effective causal factors (X_4, X_5, Z_2) and response variables (Y_1, Y_2) by fixing one effective causal factor at an optimal constant value and then generating the response surface of two remain causal factors to one response variable. The results indicated that as the elasticity (X_4) was held constant (74.5 mg·sec^{-1}·cm^{-2}), the increase in the drug content (X_5) and the content of PE (Z_2) to high values (over 350 μg/mL and 0.06 %mol, respectively) resulted in higher skin permeability, as shown in Fig. 3a and 3c, respectively. When the drug content (X_5) was constant, as shown in Fig. 13b, the content of PE (Z_2) was demonstrated to be a major factor inducing higher skin permeability. Zucker *et al*. noted that the capability to entrap sufficient drug content in the formulation was necessary in pharmaceutical liposome formulation to achieve therapeutic efficacy [75]. These results indicated that the skin permeability of the liposome formulation in our study was influenced by the drug content (X_5) and the content of PE (Z_2); thus, these responses were confirmed by the contribution index shown in Figure 13a.

Figure 14d, 14e and 14f show the response surfaces of the stability of formulation predicted by RSM-S. The results revealed that as the content of PE (Z_2) was kept steady, the increase in elasticity (X_4) and drug content (X_5) to high values (over 60 mg·sec^{-1}·cm^{-2} and 350 μg/mL, respectively) tended to increase both the drug content remaining in the formulation and the stability of the formulation, as shown in Figure 14d. Good stability of formulation was exhibited when the elasticity (X_4) and the content of PE (Y_2) was higher than 60 mg·sec^{-1}·cm^{-2} and 0.06 %mol, respectively, as shown in Fig. 3e. Elsayed *et al*. revealed that a single-chain surfactant (as PE) with a high radius of curvature could destabilize or increase the deformability of the vesicle [58]. The present results suggested that our liposome formulation still displayed good stability; The present results suggested that our liposome formulation had high elasticity characteristics but still displayed good

stability because all of the model liposome formulations used in this study contained an optimal amount of cholesterol as a membrane stabilizer [62, 76]. Liposome formulations with high elasticity values could improve the *in vitro* and *in vivo* skin permeability of various drugs [77-79]. Moreover, the level of high drug content remaining in the formulation after storage at 25°C for 30 days was obtained (Fig. 3f) as the content of PE (Y_2) decreased and the drug content (X_5) increased. These results could be summarized as follows: the stability of liposome formulation in our study was affected by the elasticity (X_4), the drug content (X_5) and the content of PE (Z_2). These responses were also confirmed by the contribution index shown in Figure 13b.

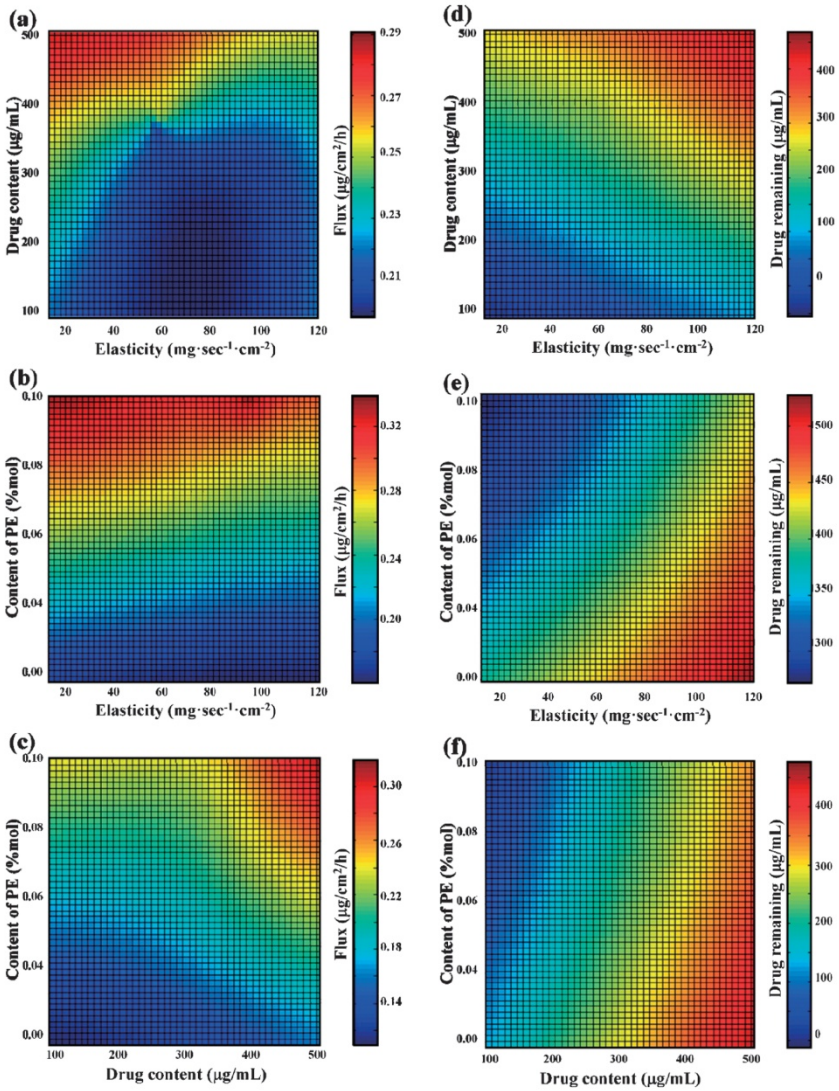

Figure 14 The Response Surface of Skin Permeability (Flux, Y_1) (Left) and Stability of Formulation (Drug Remaining, Y_2) (Right) as Function of X_4 and X_5 (a, d), X4 and X_9 (b, e) and X_5 and X_9 (c, f) at a Constant of Z_2 (0.0689%mol), X_5 (514 μg/mL) and X_4 (74.5 mg·s^{-1}·cm^{-2}).

The approximate relationships obtained from our study were consistent with the results of a previous study: the formulation characteristics and formulation factors directly affected the skin permeability effectiveness of the liposome formulation. Furthermore, the present findings could provide beneficial basic knowledge and help determine the essential causal factor information for the further development of liposome in transdermal drug delivery. An effective liposome formulation should contain both acceptable skin permeability and good stability in one liposome formulation. The elasticity (X_4), drug content (X_5) and content of PE (Z_2) were significant factors that should be considered in liposome optimization. Therefore, the chosen liposome composition should extremely affect these significant factors, and this technique can be applied for selecting the liposome composition. To date, it has been difficult to interpret all of the influences on the confounded relationships between formulation characteristics (as latent variables) and formulation factors [80], although several recent pharmaceutical studies have been successful in formulation optimization. However, our study was successful in achieving this purpose by using both formulation characteristics and formulation factors as causal factors for RSM-S analysis, to understand the relationships of formulation characteristics (as latent variables), formulation factors and pharmaceutical response variables.

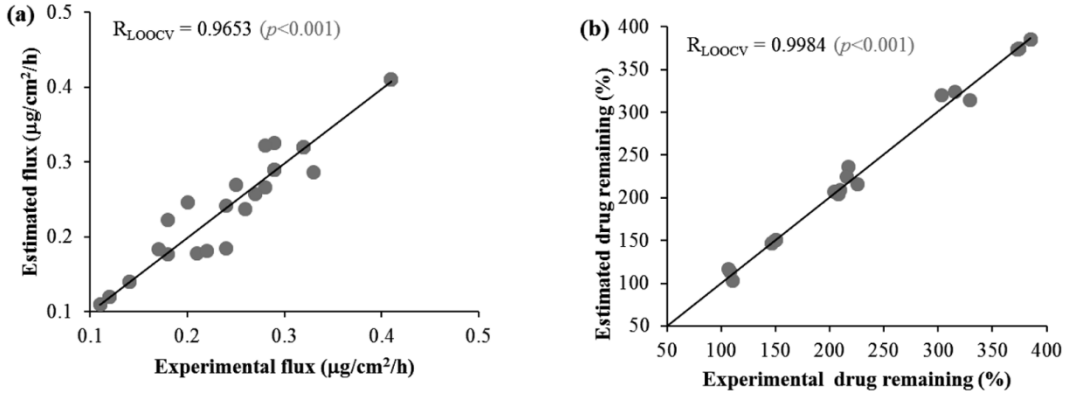

Figure 15 The Leave-One-Out-Cross-Validation (LOOCV) estimated accuracy and reliability of the response surface variables (a) skin permeability (flux) and (b) stability of formulation (drug remaining at 25°C for 30 d) predicted by X_4, X_5, and Z_2.

The accuracy and reliability of the response surface of original optimal formulation were determined by LOOCV, as shown in Figure 15. The correlation coefficients of the estimated and experimental values for the skin permeability (Y_1) and the stability of formulation (Y_2) were extremely high (R_{LOOCV}=0.9653 and 0.9984, respectively). These

results suggested that RSM-S successfully predicted the relationship between the causal factors (formulation characteristic and formulation factors) and pharmaceutical response variables [81, 82]. These results indicated that an original optimal formulation with acceptable characteristics (e.g., high skin permeability and good stability formulation) could be estimated with RSM-S.

4.2.2 Evaluation of the reliability of the optimal formulation using BS resampling

In evaluating the reliability of the optimal formulation, the LOOCV method efficiently provided a versatile assessment of the response surfaces [83]. The correlation coefficients are values that indicate the stability of the response surface. Thus, the reliability of the original optimal formulation cannot be quantitatively evaluated using these values. Therefore, BS resampling was needed to evaluate the reliability of the optimal formulation [84-86] estimated by RSM-S. The BS datasets were generated from the original datasets through BS resampling at a frequency of 250, 500, 750 and 1000. The BS optimal formulation and predicted responses are shown in Table 5. The BS optimal formulations and their standard deviation were stable, regardless of altering the frequency of resampling, indicating that a resampling frequency of more than 250 was adequate to determine the stability of the optimal formulations. Consistent with a previous study [87], a small frequency size of more than 50 resamplings was also sufficient to evaluate the stability of the optimal pharmaceutical formulation.

Table 5 Bootstrap Optimal Solutions and Bootstrap Standard Deviations by Different Frequencies of Bootstrap Resampling

BS resampling frequency	Optimized formulations			Predicted responses	
	X_4[c] ($mg \cdot s^{-1} \cdot cm^{-2}$)	X_5[d] ($\mu g/mL$)	Z_2[e] (%mol)	Y_1[f] ($\mu g/cm^2/h$)	Y_2[g] ($\mu g/mL$)
$N=0$[a]	74.5	514	0.0689	0.2692	375
$N=250$[b]	74.4 (0.194)	514 (0.202)	0.0690 (0.0001)	0.2690 (0.0000)	375 (0.266)
$N=500$[b]	74.3 (0.189)	514 (0.219)	0.0689 (0.0001)	0.2690 (0.0001)	375 (0.210)
$N=750$[b]	74.3 (0.185)	514 (0.217)	0.0689 (0.0001)	0.2690 (0.0001)	375 (0.215)
$N=100$[b]	74.4 (0.187)	514 (0.200)	0.0689 (0.0001)	0.2690 (0.0001)	375 (0.213)

a) Original optimal solution. *b*) BS optimal solution. *c*) Elasticity. *d*) Drug content. *e*) Content of penetration enhancer. *f*) Skin permeation flux. *g*) Drug remaining at 25°C, 30 d. ( ) bootstrap standard deviation.

The confidence intervals of the original optimal formulation are shown in Table 6. The ranges of confidence intervals of most of the factors (X_4, X_5 and Z_2) were quite narrow for practical studies of liposome formulations. While further study is required to confirm the potential of the optimal formulation predicted by RSM-S compared with the optimal formulation found in the experiment, a previous study [80] suggested that the characteristic values predicted by RSM-S were quite similar to the experimental values. Therefore, these results support the hypothesis that the RSM-S method can be employed to estimate simultaneous optimal formulations. The reliability of the optimal formulation improved with an increase in the size of the experimental original dataset, although the

precision of the optimal formulations was ensured, even with a small size of original dataset.

Table 6 Confidence Interval of Simultaneous Optimal Solution Estimated by RSM-S

Causal factor	Original optimal solution	250[a]		500[b]		750[c]		1000[d]	
		Lower	Upper	Lower	Upper	Lower	Upper	Lower	Upper
X_4 ($mg \cdot s^{-1} \cdot cm^{-2}$)	74.5	74.2	75.0	73.8	74.8	73.9	74.9	73.8	74.9
X_5 ($\mu g/mL$)	514	513	514	513	515	513	515	513	514
Z_2 (%mol)	0.0689	0.0688	0.0691	0.0687	0.0691	0.0688	0.0692	0.0688	0.0691
Y_1 ($\mu g/cm^2/h$)	0.269	0.2689	0.2690	0.2688	0.2692	0.2689	0.2692	0.2689	0.2691
Y_2 ($\mu g/mL$)	375	374	376	374	375	374	376	374	375

a) BS resampling frequency at 250. *b*) BS resampling frequency at 500. *c*) BS resampling frequency at 750. *d*) BS resampling frequency at 1000.

5. The comparative study

5.1 Physicochemical characteristics

The physicochemical characteristics of MTS, TFS and CLP are shown in Table 7. The incorporation of different component (Chol, CPC and/or MEN) in the liposome systems affected the size, zeta potential, elasticity, drug content, entrapment efficiency and transition temperature of the vesicle formulation. The physicochemical characteristics of the liposomes and their analogues are an important factor that differentiates the liposomes system from the other lipid dispersed systems, especially the bilayer and their elasticity.

Table 7 The Physicochemical Properties and Characteristics of the Different Formulations

Formulation	Size (nm)	PDI	Zeta potential (mV)	Elasticity ($mg \cdot s^{-1} \cdot cm^{-2}$)	Content drug ($\mu g/mL$)	EE (%)	T_g (C°)
MTS	65±2.7	0.3±0.02	49.7±2.1	150.2±7.3	634.8±14.8	65.2±1.5	0.41
TFS	83±4.4	0.4±0.02	43.8±1.6	82.4±2.3	860.8±14.1	88.5±1.4	1.72
CLP	98±5.1	0.3±0.02	4.4±1.7	23.8±1.1	230.4±31.3	23.7±3.2	2.08

The vesicle size were in the nano-size range of 60-100 nm with the size distribution (polydispersity index; PDI) of 0.3-0.4 suggesting that sonication method can prepare a nano-size vesicle. While, MX-SUS were in the micro-size range of 20-30 μm. Deformable liposomes (MTS and TFS) had smaller vesicle sizes compared to conventional liposomes (CLP) ranked as follows: MTS<TFS<CLP. The vesicle size decreased as the liposome component such as Chol and CPC was incorporated in the vesicles. The previous study [88] showed that incorporation of 10-15% Chol increase the vesicle size as Chol can increase the net repulsion force and reduce the van der Waals attraction force between the lipid bilayer of liposomal systems. The incorporation of CPC can achieve

higher curvature, thus deformable liposomes resulting in decrease in vesicle size compared to conventional liposomes.

The zeta potential of MTS, TFS and CLP were in positive charge range of 4-50 mV (Table 7). Deformable liposomes (MTS and TFS) also had higher positive zeta potential compared to CLP ranked as follows: MTS > TFS > CLP. On the other hand, the charge of MX-SUS was -20 mV. Under experimental condition of pH 5.5 which is lower than the isoelectric point (PI) of PC around 6, and higher than the PI of MX was 2.6, PC carries the net positive charge and MX is the negatively charge form, respectively. Moreover, the incorporation of CPC, a cationic surfactant also affected the net positive charge of the formulation. Although, the vesicle formulation were composed of neutral charge material e.g., Chol, positive charge material e.g., PC and CPC, and negative charge material e.g., MX, the net charge was positive zeta potential vesicles. Therefore, the net charge of the vesicle was affected by the total net charge of the vesicle component.

The elasticity was ranked as follows: MTS > TFS > CLP, penetration enhancers such as MEN and CPC may a factor that affected the elasticity of vesicles by insertion into the bilayer. The incorporation of Chol, CPC and/or MEN affected the elasticity of vesicle bilayers. Chol can increase rigidity and packing density of PC molecules, thus to decrease elasticity of vesicle bilayers [89, 90]. In contrast, the incorporation of edge activator e.g., CPC which have a high radius of curvature can increase deformability of the vesicle bilayers. MEN can decrease the orderly lipid microstructure by insertion and thus increase the fluidity or elasticity of vesicle bilayer [91, 92].

The content drug in the formulation and entrapment efficiency of MTS, TFS and CLP were determined by analysis of total drugs presented in the formulation. The entrapment efficiency of MX in the vesicles varied in the range of 20-80% with the content drug in the formulation varied in the range of 230-860 µg/mL (Table 7). The solubility of MX in acetate buffer solution (pH 5.5) is 8 µg/mL, indicating that MX solubility was quite small in acetate buffer solution compared to MX in vesicle formulation. The results indicated that the entrapment efficiencies for deformable liposomes incorporating the mixture of CPC and/or MEN, were higher than that incorporating PC alone. The beneficial role of edge activators within vesicle bilayers are well recognized as the intrinsic properties of CPC led to increase solubility of MX in vesicle bilayers. Consistency with the previous study [93], as sodium stearate (edge activator) was incorporated into the phosphatidylethanolamine vesicles, the entrapment efficiency of the drug was significantly increased. However, incorporating MEN decreased the entrapment efficiencies of MX in MTS compared to TFS, as MEN may compete with MX and/or CPC to solubilize in the vesicle bilayers. Although, some vesicle component might form micelle and MX could be entrapped in micelle, however our pre-formulation study indicated that the

vesicle component under this experiment was chosen to differentiate the liposome from micelle or mixed micelle, using turbidity evaluation.

5.2 Skin permeation study

Figure 16 shows (A) skin permeation profile, (B) steady-state flux and (C) MX deposit in the skin after skin permeation study. The cumulative amount per area of MX in each vesicle formulation increased linearly with lag time before 2 h. This linear accumulation was also observed for other formulations (Figure 16A).

The steady-state flux of MX through hairless mice skin from each formulation was determined as the slope of the linear portion of the plot and could be ranked as follows: MTS > TFS > CLP > SUS. The steady-state flux of MX in MTS, TFS and CLP was significantly higher than in SUS ($p<0.05$). Moreover, the steady-state flux of MX in deformable vesicles such as MTS and TFS was also significantly higher than in rigid vesicles such as CLP ($p<0.05$) (Figure 16B).

The MX deposit in the skin was determined after skin permeation study. MX suspension (SUS) was used as a control for MX deposit in the skin. MTS and TFS gave a slightly higher MX deposit in the skin than SUS. On the other hand, CLP gave a significantly higher MX deposit in the skin than control. The MX deposit in the skin was ranked as follows: CLP > MTS > TFS > SUS (Figure 16C).

The skin permeation results indicated that MX in high elasticity value vesicles (MTS and TFS) had a significantly higher MX flux than low elasticity value vesicles (CLP). In contrast, CLP had a significantly higher MX deposited in the skin than MTS and TFS. These results may be explained by the effect of intrinsic characteristics of each liposome systems. The present study was consistent with the previous study [94] that conventional liposomes are of little or no value as transdermal drug delivery carriers compared to deformable liposomes because they remain confined to upper layers of the stratum corneum. The thermodynamic activity of MX in formulation may be a factor affecting the skin permeation. An increase in content of MX in the formulation resulted in further increase MX permeated the skin. The content of MX in MTS and TFS were significantly higher than CLP, indicating that the thermodynamic activity of MX in MTS and TFS formulation was important for its promotion of MX permeation flux through the skin. The positive charge of elastic vesicles (MTS and TFS) might affect the skin permeability and skin deposit [95] as positive charge of vesicle interacted with negative charge of skin, thus MTS showed higher skin deposit than TFS because MTS has a greater positive charge than TFS. Table 7 shows the significant difference of elasticity between MTS and TFS formulation. However, no significant difference between MTS and TFS formulation was observed in the cumulative amount per area and skin permeation flux. Elasticity is a

factor influencing skin permeability, however the skin permeability is still depended on total effect of all physicochemical characteristics of vesicle formulation. The elastic vesicles were smaller size, higher zeta potential, higher elasticity, higher entrapment efficiencies and lower transition temperature, providing that MTS and TFS could penetrate through the skin easier than CLP.

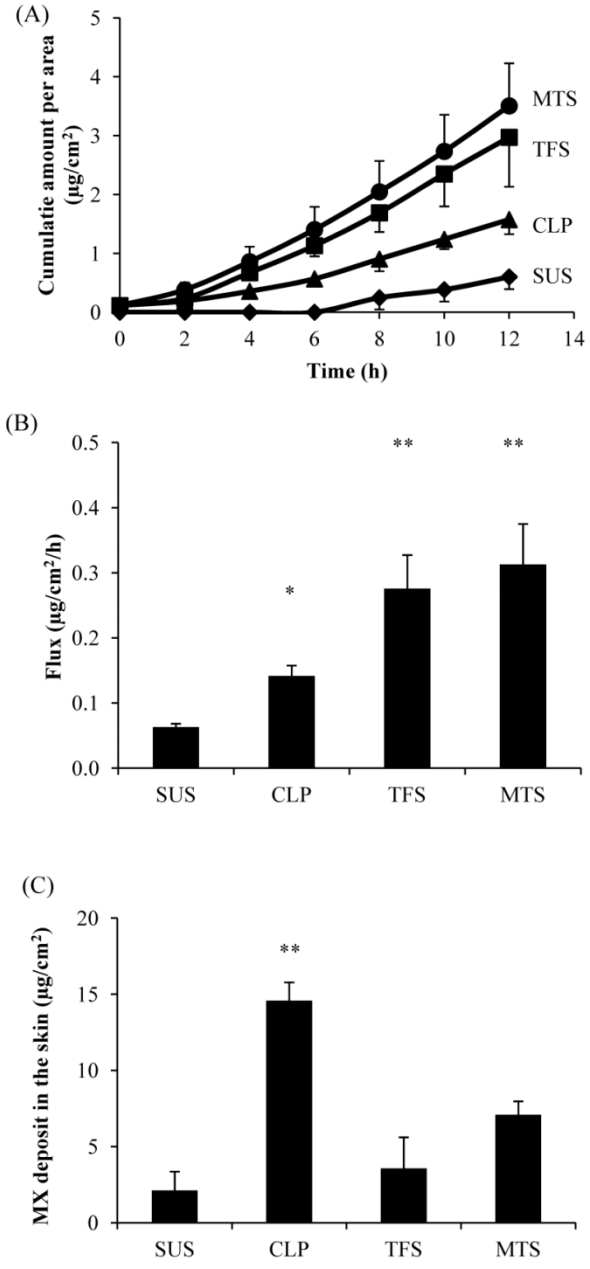

Figure 16 (A) The skin permeation profile 12 h in full-thickness skin after treated with (●) MTS, (■) TFS, (▲) CLP and (◆) SUS on hair-less mice skin (Laboskin®), (B) flux and (D) MX deposit in the full-thickness skin after skin permeation. Each value represents the mean±S.D. (n=3), * $p<0.05$, ** $p<0.01$ compare to SUS

6. The mechanisms of liposomes on skin permeation

Changes in the ultra-structures of the intercellular lipids occurred following the treatment of skin with the vesicle formulation, as shown in the FT-IR spectra and DSC thermogram (Figure 17). The FT-IR peaks from the absorption-broadened C-H (CH_2) symmetric and asymmetric stretches are near 2850 cm^{-1} and 2920 cm^{-1}, respectively. These peaks in the FT-IR spectra of the skin treated with the vesicle formulation shifted from 2850 cm^{-1} to 2850.7-2851.3 cm^{-1} and from 2920 cm^{-1} to 2920.3-2920.9 cm^{-1}, respectively. Meanwhile, the DSC thermogram also displayed peak shifts, from 231.72°C for the skin sample treated with the MX suspension (control) to a lower transition temperature for the skin sample treated with the vesicle formulations. The SC lipid of the skin sample existed in the liquid state at the peak shifted range of 230.53-229.18°C, depending on vesicle formulation. These results are consistent with previous studies [96-99], which demonstrated that liposome vesicles do not penetrate into the SC but rather that the lipid components of the vesicles can penetrate and change the enthalpy of the SC lipid-related transitions of the skin. These results suggest that the SC lipid arrangement of the skin sample treated with the vesicle formulation was disrupted by altering the fluidity or flexibility of the SC lipids. The interruption of the SC lipids by vesicle formulation or by the vesicle components caused an increase in the skin permeability of MX; the FT-IR spectra and DSC thermograms also support the conclusions of this *in vitro* skin permeation study.

The vesicles may adsorb to the SC surface with subsequent transfer of the drug directly from the vesicles to the skin, or the vesicles may fuse and mix with the SC lipid matrix, increasing drug partitioning into the skin. Our results indicate that the vesicles can be taken into the skin but cannot penetrate through the intact, healthy SC; instead, they dissolve and form a unit membrane structure with the skin sample, as evidenced by the alteration and rearrangement of the lipid structures of the skin sample treated with the vesicles as revealed by FT-IR and DSC characterization (Figure 17).

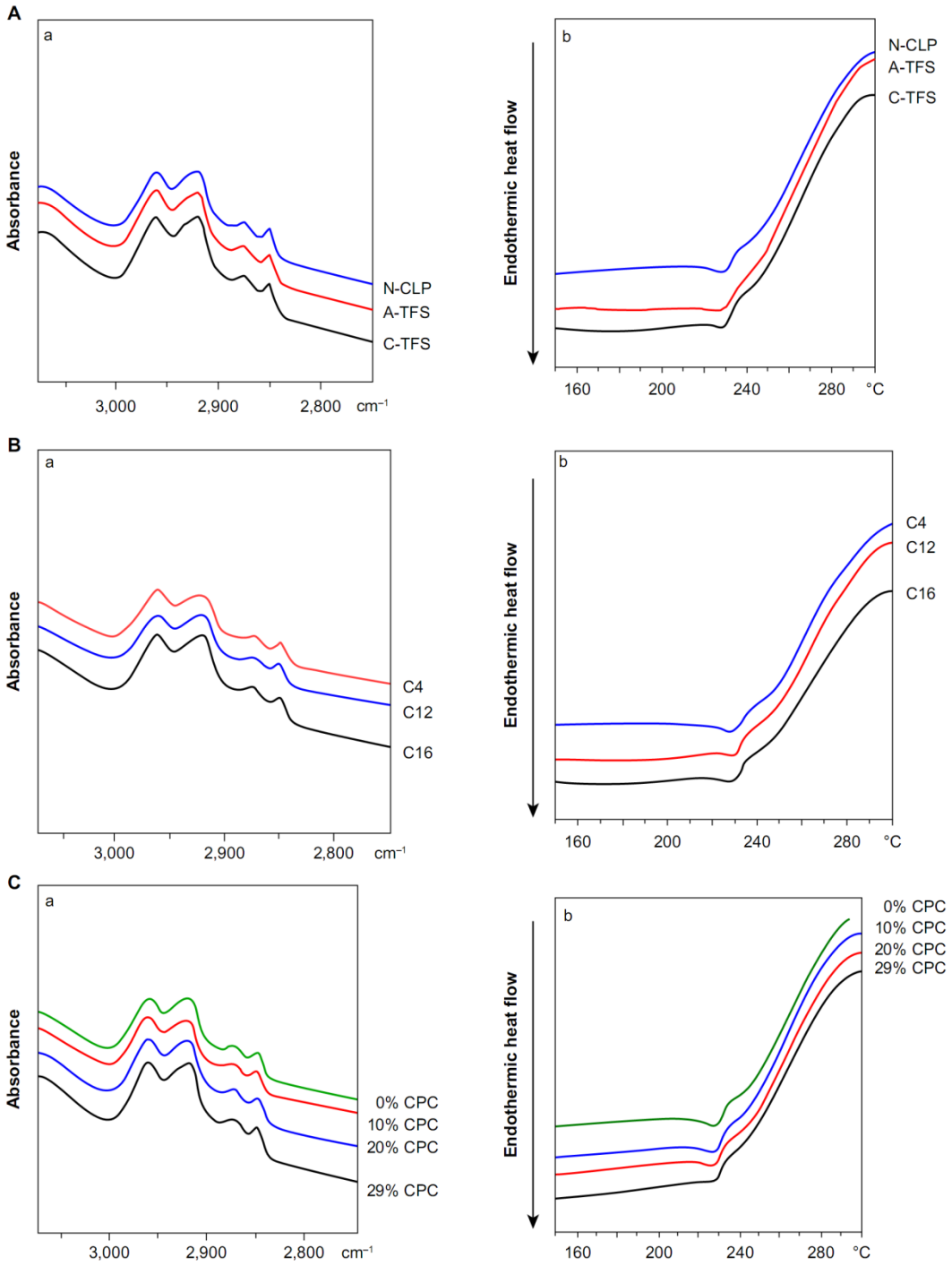

Figure 17 The influence of (A) surfactant charge, (B) surfactant carbon chain length, and (C) surfactant content of the shed snake skin after skin permeation Notes: (a) Fourier transform infrared spectra; (b) differential scanning calorimetry thermograms. Abbreviations: a-TFs, anionic transfersomes; cPc, cetylpyridinium chloride; c-TFs, cationic transfersomes; N-clP, neutral conventional liposomes.

สรุปผลการดำเนินงานของโครงการ (Conclusions)

In this study, the liposome formulations as skin delivery carrier for meloxicam (MX) was formulated and optimized. Various formulation factors such as charge of surfactants, carbon chain length of surfactants and amount of surfactants on physicochemical characteristics, morphology, thermal properties, stability of the formulation and *in vitro* skin permeability were evaluated. The possible mechanisms by which these liposomes could improve the skin delivery of MX were also clarified. It can be concluded as follows,

The desirable amount for MX-loaded liposome formulations were 10-40% Chol, 10-40% CPC and 10% MX. An increase of Chol resulted in a significant increase in vesicle size, a decrease in elasticity and a slight increase in entrapment efficiency. While an increase in CPC resulted in a significant decrease in vesicle size, an increase in zeta potential, elasticity and entrapment efficiency. The optimal formulation was PC/Chol/CPC in the molar ratios of 100:10.5:29.0 with 10 % MX.

The liposome formulation composed of 10% chol, 29% CPC (cationic surfactant) with 16 carbons chain length and 10% MX showed the highest skin permeation flux through the skin. The vesicle sizes of these MX-loaded liposomes were nanosize (91±9 nm) with narrow size distribution (PDI; 0.3±0.06) and zeta potential of 48±1 mV. The elasticity of these MX-loaded liposomes was 89±1 mg·sec-1·cm-2. The EE and drug content were 68±1% and 526±7 µg/mL, respectively. The formulation factors significantly affected the physicochemical characteristics and skin permeability of MX-loaded liposomes.

In our study, the possible mechanisms for enhancing the skin permeation of MX by liposomes can be explained by the penetration enhancing mechanism and the vesicle adsorption to and/or fusion with the stratum corneum.

Our finding provided useful fundamental information for developing novel designing of liposome formulation for enhancing skin delivery of lipophilic drugs, especially liposomes containing surfactant systems.

เอกสารอ้างอิง (References)

1. Cevc, G. and G. Blume, *Lipid vesicles penetrate into intact skin owing to the transdermal osmotic gradients and hydration force* Biochimica et Biophysica Acta, 1992. **1104**: p. 226-232
2. van den Bergh, B.A., et al., *Elasticity of vesicles affects hairless mouse skin structure and permeability.* Journal of Controlled Release, 1999. **62**: p. 367-379.
3. Touitou, E., et al., *Ethosomes — novel vesicular carriers for enhanced delivery: characterization and skin penetration properties.* Journal of Controlled Release, 2000. **65**: p. 403–418.
4. Verma, D.D., *Invasomes-novel topical carriers for enhanced topical delivery: characterization and skin penetration properties*, 2002, Marburg/Lahn.
5. Song, Y.-K. and C.-K. Kim, *Topical delivery of low-molecular-weight heparin with surface-charged flexible liposomes.* Biomaterials, 2006. **27**: p. 271–280.
6. Duangjit, S., et al., *Menthosomes, novel ultradeformable vesicles for transdermal drug delivery: Optimization and characterization.* Biological & Pharmaceutical Bulletin, 2012. **35**(10): p. 1-9.
7. Elsayed, M.M.A., et al., *Deformable liposomes and ethosomes: Mechanism of enhanced skin delivery.* International Journal of Pharmaceutics, 2006. **322**: p. 60-66.
8. Luger, P., et al., *Structure and physicochemical properties of meloxicam, a new NSAID.* European Journal of Pharmaceutical Sciences, 1996. **4**: p. 175-187
9. Engelhardt, G., et al., *Anti-inflammatory, analgesic, antipyretic and related properties of meloxicam, a new non-steroidal anti-inflammatory agent with favourable gastrointestinal tolerance.* Inflammation Research, 1995(44): p. 423–433.
10. Degner, F., R. Sigmund, and H. Zeidler, *Efficacy and tolerability of meloxicam in an observational, controlled cohort study in patients with rheumatic disease.* Clinical Therapeutics, 2000(22): p. 400–410.
11. Distel, M., et al., *Safety of meloxicam: a global analysis of clinical trials.* British Journal of Rheumatology 1996. **35**: p. 68-77.
12. Lanes, S.F., L.A. Rodriguez, and G.E. Hwang, *Baseline risk of gastrointestinal disorders among new users of meloxicam, ibuprofen, diclofenac, naproxen and indomethacin.* Pharmacoepidemiology and Drug Safety, 2000. **9**: p. 113–117.
13. Yuan, Y., et al., *Investigation of microemulsion system for transdermal delivery of meloxicam.* International Journal of Pharmaceutics, 2006. **321**: p. 117-123.

14. Villegas, I., et al., *Effects of food intake and oxidative stress on intestinal lesions caused by meloxicam and piroxicam in rats.* European Journal of Pharmacology, 2001. **414**: p. 79-86.
15. Gupta, S.K., et al., *Comparison of analgesic and anti-inflammatory activity of meloxicam gel with dichlofenac and piroxicam gel in animal models: pharmacokinetic parameters after topical application.* Skin Pharmacology and Applied Skin Physiology, 2002(15): p. 105–111.
16. Jantharaprapap, R. and G. Stagni, *Effects of penetration enhancers on in vitro permeability of meloxicam gels.* International Journal of Pharmaceutics, 2007. **343**: p. 26-33.
17. Young-Chang, A., et al., *A novel transdermal patch incorporating meloxicam: In vitro and in vivo characterization.* International Journal of Pharmaceutics, 2010. **385**: p. 12-19.
18. Khurana, S., N.K. Jain, and P.M.S. Bedi, *Nanoemulsion based gel for transdermal delivery of meloxicam: Physicochemical, mechanistic investigation.* Life Sciences, 2013. **doi:10.1016/j.lfs.2013.01.005**.
19. Haigh, J.M., et al., *In vitro permeation of progesterone from a gel through the shed skin of three different snake species.* International Journal of Pharmaceutics, 1998(170): p. 151 – 156.
20. Ngawhirunpat, T., et al., *Comparison of the percutaneous absorption of hydrophilic and lipophilic compounds in shed snake skin and human skin.* Pharmazie, 2006. **61**: p. 331-336.
21. Montenegro, L., et al., *In vitro retinoic acid release and skin permeation from different liposome formulations.* International Journal of Pharmaceutics, 1996(133): p. 89-96.
22. Mohammed, A.R., et al., *Liposome formulation of poorly water soluble drugs: optimisation of drug loading and ESEM analysis of stability.* International Journal of Pharmaceutics, 2004. **285**: p. 23-34.
23. Katahira, N., et al., *Enhancement of topical delivery of a lipophilic drug from charged multilamellar liposomes.* Journal of Drug Targeting, 1999. **6**: p. 404-414
24. Sinico, C., et al., *Liposomes as carriers for dermal delivery of tretinoin: in vitro evaluation of drug permeation and vesicle–skin interaction.* Journal of Controlled Release, 2005(103): p. 123 – 136.
25. Manosroi, A., et al., *Transdermal absorption enhancement through rat skin of gallidermin loaded in niosomes.* International Journal of Pharmaceutics, 2010. **392**: p. 304-310.

26. Gillet, A., et al., *Liposome surface charge influence on skin penetration behaviour.* International Journal of Pharmaceutics, 2011. **411**: p. 223-231.
27. Jain, K.K., *Methods in molecular biology: Drug Delivery Systems*. Drug Delivery Systems - An Overview, ed. K.K. Jain. 2008, Hatfield, Herts, UK: Humana Press.
28. Polat, B.E., et al., *Ultrasound-mediated transdermal drug delivery: Mechanisms, scope, and emerging trends.* Journal of Controlled Release, 2011. **152**: p. 330–348.
29. Hashima, I.I.A., et al., *Potential use of iontophoresis for transdermal delivery of NF-kB decoy oligonucleotides.* International Journal of Pharmaceutics 2010(393): p. 127–134.
30. Hu, Q., et al., *Enhanced transdermal delivery of tetracaine by electroporation.* International Journal of Pharmaceutics, 2000. **202**: p. 121-124.
31. Park, J.-H., et al., *A microneedle roller for transdermal drug delivery.* European Journal of Pharmaceutics and Biopharmaceutics, 2010(76): p. 282–289.
32. Lee, P.J., et al., *Evaluation of chemical enhancers in the transdermal delivery of lidocaine.* International Journal of Pharmaceutics, 2006(308): p. 33–39.
33. Liu, C.H., F.Y. Chang, and D.K. Hung, *Terpene microemulsion for transdermal curcumin delivery: Effects of terpenes and cosurfactants.* Colloids and Surfaces B: Biointerfaces, 2011. **82**: p. 63-70.
34. El Maghraby, G.M., B.W. Barry, and A.C. Williams, *Liposomes and skin: From drug delivery to model membranes.* European Journal of Pharmaceutical Sciences, 2008(34): p. 203-222.
35. Verma, D.D., et al., *Liposomes increase skin penetration of entrapped and non-entrapped hydrophilic substances into human skin: a skin penetration and confocal laser scanning microscopy study.* European Journal of Pharmaceutics and Biopharmaceutics, 2003. **55**: p. 271–277.
36. Geusens, B., et al., *Lipid-mediated gene delivery to the skin.* European Journal of Pharmaceutical Sciences, 2011. **43**: p. 199–211.
37. Gupta, P.N., et al., *Non-invasive vaccine delivery in transfersomes, niosomes and liposomes: a comparative study.* International Journal of Pharmaceutics, 2005(293): p. 73-82.
38. Betz, G., et al., *Heparin penetration into and permeation through human skin from aqueous and liposomal formulations in vitro.* International Journal of Pharmaceutics, 2001(228): p. 147-159.
39. Cevc, G. and G. Blume, *Lipid vesicles penetrate into intact skin owing to the transdermal osmotic gradients and hydration force.* Biochimica et Biophysica Acta, 1992. **1104**(1): p. 226–232.

40. Van den Bergh, B.A., et al., *Elas-ticity of vesicles affects hairless mouse skin structure and permeability.* Journal of Controlled Release, 1999(62): p. 367–379.
41. Touitou, E., et al., *Ethosomes — novel vesicular carriers for enhanced delivery: characterization and skin penetration properties.* Journal of Controlled Release, 2000(65): p. 403–418.
42. Song, Y.-K. and C.-K. Kim, *Topical delivery of low-molecular-weight heparin with surface-charged flexible liposomes.* Biomaterials, 2006. **27**: p. 271-280.
43. Song, C.K., et al., *A novel vesicular carrier, transethosome, for enhanced skin delivery of voriconazole: characterization and in vitro/in vivo evaluation.* Colloids Surf B Biointerface, 2012. **92**(1): p. 299-304.
44. Takayama, K., et al., *Multivariate spline interpolation as a novel method to optimize pharmaceutical formulations.* Pharmazie, 2004. **59**: p. 392-395.
45. Shotton, D.M. and N.J. Servers, eds. *An introduction to freeze fracture and deep etching. In: Shotton, D.M., Servers N.J. (Eds.), Rapid freezing, freeze fracture, and deep etching.* 1995, Wiley: New York. 1-31.
46. Takayama, K., et al., *Neural network based optimization of drug formulations.* Advanced Drug Delivery Reviews, 2003. **55**: p. 1217-1231.
47. Kikuchi, S., et al., *Latent Structure Analysis in Pharmaceutical Formulations Using Kohonen's Self-Organizing Map and a Bayesian Network.* Journal of Pharmaceutical Sciences, 2011. **100**: p. 964-975.
48. Kikuchi, S. and K. Takayama, *Reliability assessment for the optimal formulations of pharmaceutical products predicted by a nonlinear response surface method.* International Journal of Pharmaceutics, 2009. **374**(1-2): p. 5-11.
49. Kikuchi, S. and K. Takayama, *Multivariate statistical approach to optimizing sustained-release tablet formulations containing diltiazem hydrochloride as a model highly water-soluble drug.* International Journal of Pharmaceutics, 2010. **386**: p. 149-155.
50. Dupret, G. and M. Koda, *Bootstrep re-sampling for unbalanced data in superised learning.* European Journal of Operational Research, 2001. **134**: p. 141-156.
51. Liang, X., G. Mao, and K.Y.S. Ng, *Mechanical properties and stability measurement of cholesterol-containing liposome on mica by atomic force microscopy.* Journal of Colloid and Interface Science, 2004. **278**: p. 53-62.
52. Liu, D., et al., *Effects of cholesterol on the release of free lipids and the physical stability of lecithin liposomes.* Journal of the Chinese Institute of Chemical Engineers, 2000. **31**: p. 269.

53. Rand, R.P., et al., *The effect of cholesterol on measured interaction and compressibility of dipalmitoylphosphatidylcholine bilayers.* Canadian Journal of Biochemistry, 1980. **58**: p. 959-968.
54. Liu, D., et al., *Microcalorimetric studies of the effects of cholesterol on the physical stability of liposome.* Colloids and surfaces B: Biointerfaces, 2000. **172**: p. 57-67.
55. Needham, D. and R.S. Nunn, *Elastic deformation and failure of lipid bilayer membranes containing cholesterol.* Biophysical Journal, 1990. **58**: p. 997-1009.
56. Nasseri, B., *Effect of cholesterol and temperature on the elastic properties of niosomal membranes.* International Journal of Pharmaceutics, 2005. **300** p. 95-101.
57. Manosroi, A., et al., *Transdermal absorption enhancement through rat skin of gallidermin loaded in niosomes.* International Journal of Pharmaceutics, 2010. **392**: p. 304-310.
58. Elsayed, M.M.A., et al., *Lipid vesicles for skin delivery of drugs: Reviewing three decades of research.* International Journal of Pharmaceutics, 2007. **332**: p. 1-16.
59. Fang, Y.-P., et al., *Comparison of 5-aminolevulinic acid-encapsulated liposome versus ethosome for skin delivery for photodynamic therapy.* International Journal of Pharmaceutics, 2008(356): p. 144–152.
60. Ali, M.H., et al., *The role of lipid geometry in designing liposomes for the solubilisation of poorly water soluble drugs.* International Journal of Pharmaceutics, 2013. **453**(1): p. 225-232.
61. Park, S.-I., et al., *Polymer-hybridized liposomes anchored with alkyl grafted poly(asparagine).* Journal of Colloid and Interface Science, 2011. **364**: p. 31–38.
62. Mohammed, A.R., et al., *Liposome formulation of poorly water soluble drugs: optimisation of drug loading and ESEM analysis of stability.* International Journal of Pharmaceutics, 2004. **285**: p. 23-34.
63. Dan, N., *Lipid tail chain asymmetry and the strength of membrane-induced interactions between membrane proteins.* Biochimica et Biophysica Acta, 2007. **1768**: p. 2393–2399.
64. Liu, J., A. Zou, and B. Mu, *Surfactin effect on the physicochemical property of PC liposome.* Colloid and Surface A, 2010. **361**: p. 90–95.
65. Liu, D., et al., *Microcalorimetric studies of the effects of cholesterol on the physical stability of liposome.* Colloids and Surfaces B: Biointerfaces, 2000. **172**: p. 57-67.

66. Nasseri, B., *Effect of cholesterol and temperature on the elastic properties of niosomal membranes.* International Journal of Pharmaceutics, 2005. **300** p. 95-101.
67. Barry, B.W., *Penetration Enhancer Classification*, in *Percutaneous Penetration Enhancers*, W.S. Eric and I.M. Howard, Editors. 2006, CRC Press: New York. p. 1-15.
68. Williams, A.C., *Transdermal and Topical Drug Delivery; from Theory to Clinical Practice*. 2003, London: Pharmaceutical Press.
69. Ashton, P., et al., *Surfactant effects in percutaneous absorption. I. Effects on the transdermal flux of methyl nicotinate.* International Journal of Pharmaceutics, 1992. **87**: p. 261.
70. Cevc, G., A. Schatzlein, and G. Blume, *Transdermal drug carriers: basic properties, optimization and transfer efficiency in the case of epicutaneously applied peptides.* Journal of Controlled Release, 1995. **36**: p. 3-16.
71. Aungst, B.J., R. N.J., and E. Shefter, *Enhancement of naloxone penetration through human skin in vitro using fatty acids, fatty alcohols, surfactants, sulfoxides and aminds.* International Journal of Pharmaceutics, 1986. **33**: p. 225.
72. Ogiso, T. and M. Shintani, *Mechanism for the enhancement effect of fatty acids on the percutaneous absorption of propranolol.* J Pharm Sci, 1990. **79**: p. 1065.
73. Duangjit, S., et al., *Characterization and in vitro skin permeation of meloxicam-loaded liposomes versus transfersomre.* Journal of Drug Delivery, 2010. **2012, Article ID 418316, 9 pages, doi:10.1155/2011/418316**.
74. Duangjit, S., et al., *Evaluation of meloxicam-loaded cationic transfersomes as transdermal drug delivery carriers.* AAPS PharmSciTech 2012. **doi: 10.1208/s12249-012-9904-2**.
75. Zucker, D., et al., *Liposome drugs' loagind efficiency: A working model based on loaded conditions and drugs' physicochemical properties.* Journal of Controlled Release, 2009. **139**: p. 73-80.
76. Chen, L.-Y., et al., *Exploring the effect of cholesterol in lipid bilayer membrane on the melittin penetration mechanism.* Anal Biochem, 2007. **367**: p. 49–55.
77. Gupta, P.N., et al., *Non-invasive vaccine delivery in transfersomes, niosomes and liposomes: a comparative study.* International Journal of Pharmaceutics, 2005(293): p. 73-82.
78. Ahad, A., et al., *Formulation and optimization of nanotransfersomes using experimental design technique for accentuated transdermal delivery of valsartan.* Nanomedicine, 2012. **8**: p. 237–249.
79. Uchino, T., et al., *Physicochemical characterization of drug-loaded rigid and elastic vesicles.* International Journal of Pharmaceutics, 2011. **412**: p. 142-147.

80. Duangjit, S., et al., *Menthosomes, novel ultradeformable vesicles for transdermal drug delivery: Optimization and characterization.* Biological & Pharmaceutical Bulletin, 2012. **35**(10): p. 1-9.
81. Onuki, Y., et al., *Formulation optimization of photocrosslinked polyacrylic acid modified with 2-hydroxyethyl methacrylate hydrogel as an adhesive for a dermatological patch.* Journal of Controlled Release, 2005. **108**: p. 331-340.
82. Surini, S., et al., *Release phenomena of insulin from an implantable device composed of a polyion complex of chitosan and sodium hyaluronate.* Journal of Controlled Release, 2003. **90**: p. 291-301.
83. Bourquin, J., et al., *Comparison of artificial neural networks (ANN) with classical modelling techniques using different experimental designs and data from a galenical study on a solid dosage form.* European Journal of Pharmaceutical Sciences., 1998. **6**(4): p. 287-301.
84. Ueda, N. and R. Nakano, *Estimating expected error rates of neural network clasifiers insmall sample size situations: a comparison of cross-validation and bootstrep*, in *IEEE International Conference Neural Networks Proceeding*1995, IEEE: Perth, WA. p. 101-104.
85. Dupret, G. and M. Koda, *Bootstrep re-sampling for unbalanced data in superised learning.* European Journal of Operational Research, 2001. **134**: p. 141-156.
86. Zhang, J., *Inferential estimation of polymer quality using bootstrep aggregated neural networks.* Neural Network, 1999. **12**: p. 927-938.
87. Arai, H., et al., *Bootstrap Re-sampling Technique to Evaluate the Optimal Formulation of Theophylline Tablets Predicted by Non-linear Response Surface Method Incorporating Multivariate Spline Interpolation.* Chemical & Pharmaceutical Bulletin, 2007. **55**(4): p. 586-593.
88. Liang, X., G. Mao, and K.Y.S. Ng, *Mechanical properties and stability measurement of cholesterol-containing liposome o n mica by atomic force microscopy.* Journal of Colloid and Interface Science, 2004. **278**: p. 53-62.
89. Elsayed, M.M.A., et al., *Lipid vesicles for skin delivery of drugs: Reviewing three decades of research.* International Journal of Pharmaceutics, 2007. **332**: p. 1-16.
90. Gracià, R.S., et al., *Effect of cholesterol on the rigidity of saturated and unsaturated membranes: fluctuation and electrodeformation analysis of giant vesicles.* Soft Matter, 2010. **6**: p. 1472-1482.
91. Watanabe, H., et al., *Effect of l-menthol on the thermotropic behavior of ceramide 2/cholesterol mixtures as a model for the intercellular lipids in stratum corneum.* Colloids and Surfaces B: Biointerfaces, 2009. **73**: p. 116-121.

92. Patel, T., Y. Ishiuji, and G. Yosipovitch, *Menthol: a refreshing look at this ancient compound.* Journal of the American Academy of Dermatology, 2007. **57**: p. 873-878.
93. Fang, Y.-P., et al., *Comparison of 5-aminolevulinic acid-encapsulated liposome versus ethosome for skin delivery for photodynamic therapy.* International Journal of Pharmaceutics, 2008(356): p. 144–152.
94. O. Braun-Falco and H.C. Kortung, *Liposome Dermatics*, in *Griesbach Conference: ,* , H.I. Maibach, Editor 1992, Springer-Verlag: Berlin, Heidelberg, .
95. Sinico, C., et al., *Liposomes as carriers for dermal delivery of tretinoin: in vitro evaluatio n of drug permeation and vesicle–skin interaction.* Journal of Controlled Release, 2005. **103**: p. 123 - 136.
96. Kato, A., Y. Ishibashi, and Y. Miyake, *Effect of egg yolk lecithin on transdermal delivery of bunazosin hydrochloride.* Journal of Pharmacy and Pharmacology, 1987. **39**: p. 399–400.
97. Zellmer, S., W. Pfeil, and J. Lasch, *Interaction of phosphatidylcholine liposomes with the human stratum corneum.* Biochimica et Biophysica Acta, 1995. **1237**: p. 176-182.
98. Kirjavainen, M., et al., *Interaction of liposomes with human skin in vitro—the influence of lipid composition and structure.* Biochimica et Biophysica Acta, 1996a. **1304**: p. 179-189.
99. Obata, Y., et al., *Infrared spectroscopic study of lipid interation in stratum corneum treated with transdermal absorption enhancers.* International Journal of Pharmaceutics, 2010. **389**: p. 18-23.

OUTPUTS ที่ได้จากโครงการ

1. ผลงานที่ตีพิมพ์ในวารสารระดับนานาชาติ จำนวน 11 ฉบับ

1) Duangjit, S., Pamornpathomkul, B., Opanasopit, P., Rojanarata, T., Obata, Y., Takayama, K., **Ngawhirunpat, T**., 2014a. Role of the charge, carbon chain length, and content of surfactant on the skin penetration of meloxicam-loaded liposomes. *International Journal of Nanomedicine* 9, 2005-2017.
2) Subongkot, T., Pamornpathomkul, B., Rojanarata, T., Opanasopit, P., **Ngawhirunpat, T**., 2014. Investigation of the mechanism of enhanced skin penetration by ultradeformable liposomes. *International Journal of Nanomedicine* 9, 3539-3550.
3) Duangjit, S., Opanasopit, P., Rojanarata, T., Takayama, J., Takayama, K., **Ngawhirunpat, T**., 2014b. Bootstrap resampling technique to evaluate the reliability of the optimal liposome formulation: skin permeability and stability response variables. *Biological & Pharmaceutical Bulletin* 37, 1543-1549.
4) Charoenputtakun, P., Pamornpathomkul, B., Opanasopit, P., Rojanarata, T., **Ngawhirunpat, T**., 2014. Terpene composited lipid nanoparticles for enhanced dermal delivery of all-trans-retinoic acids. *Biological & Pharmaceutical Bulletin* 37, 1139-1148.
5) Rangsimawong, W., Opanasopit, P., Rojanarata, T., Ngawhirunpat, T., 2014. Terpene-containing PEGylated liposomes as transdermal carriers of a hydrophilic compound. *Biological & Pharmaceutical Bulletin* 37, 1936-1943
6) Duangjit, S., Buacheen, P., Priebprom, P., Limpanichkul, S., Asavapichayont, P., Chaimanee, P., **Ngawhirunpat, T.**: Development and Evaluation of Tamarind Seed Xyloglucan for Transdermal Patch of Clindamycin. *Advance Material Research,* **1060**, 21-24 (2015).
7) Rangsimawong, W., Opanasopit, P., Rojanarata, T., **Ngawhirunpat, T**., 2015. Mechanistic study of decreased skin penetration using a combination of sonophoresis with sodium fluorescein-loaded PEGylated liposomes with d-limonene. *International Journal of Nanomedicine* 10, 7413-7423.
8) Subongkot, T., **Ngawhirunpat, T**., 2015. Effect of liposomal fluidity on skin permeation of sodium fluorescein entrapped in liposomes. International Journal of Nanomedicine 10, 4581-4592.
9) Duangjit, S., Chairat, W., Opanasopit, P., Rojanarata, T., **Ngawhirunpat, T**., 2016a. Application of Design Expert for the investigation of capsaicin-loaded microemulsions for transdermal delivery. *Pharmaceutical Development and Technology* 21, 698-705.
10) Duangjit, S., Chairat, W., Opanasopit, P., Rojanarata, T., Panomsuk, S.,

Ngawhirunpat, T., 2016b. Development, Characterization and Skin Interaction of Capsaicin-Loaded Microemulsion-Based Nonionic Surfactant. *Biological & Pharmaceutical Bulletin* 39, 601-610.

11) Rangsimawong, W., Opanasopit, P., Rojanarata, T., Duangjit, S., **Ngawhirunpat, T.**, 2016. Skin Transport of Hydrophilic Compound-Loaded PEGylated Lipid Nanocarriers: Comparative Study of Liposomes, Niosomes, and Solid Lipid Nanoparticles. Biological & Pharmaceutical Bulletin 39, 1254-1262.
12) Rangsimawong, W., Opanasopit, P., Rojanarata, T., Panomsuk, S. and Ngawhirunpat, T. 2016. Influence of sonophoresis on transdermal drug delivery of hydrophilic compound-loaded lipid nanocarriers. *Pharmaceutical Development and Technology* ***(IN PRESS)***

2. ผลงานที่เสนอในที่ประชุมวิชาการระดับนานาชาติ จำนวน 4 เรื่อง

1) Duangjit S., Obata Y., Sano H., Kikuchi S., Onuki Y., Rojanarata T., Opanasopit P., Takayama K., Maitani, Y., **Ngawhirunpat, T.**, 2014. Multivariate Statistical Approach to Optimize Menthosomes Incorporating l-menthol as Novel Ultradeformable Vesicles for Transdermal Drug Delivery, in: Wungsintaweekul, J. (Ed.), The 3rd Current Drug Development International Conference (CDD 2014). Prince of Songkla University, Ao Nang Beach, Krabi, Thailand, pp. 126-129.
2) Duangjit, S., Buacheen, P., Priebprom, P., Limpanichkul, S., Asavapichayont, P., Chaimanee, P., **Ngawhirunpat, T.**: Development and Evaluation of Tamarind Seed Xyloglucan for Transdermal Patch of Clindamycin. *Pharmaceutical Technology 2015 (PharmaTech 2015),* **1060**, 21-24 (2015).
3) Duangjit, S., Nimcharoenwan, T., Chomya, N., Locharoenrat, N., **Ngawhirunpat, T.,** 2016. Design and development of optimal invasomes for transdermal drug delivery using computer program. Asian Federation for Pharmaceutical Sciences Conference 2015 (AFPS2015) Bangkok, Thailamd. Asian Journal of Pharmaceutical Sciences 11, 52-53.

รอเพิ่มงานวิจัยของน้องๆ ค่ะ

3. การนำวิจัยไปใช้ประโยชน์

เชิงวิชาการ นำไปใช้ในการเรียนการสอนระดับปริญญาเอกที่คณะเภสัชศาสตร์ ม.ศิลปากรและเป็นหัวข้อสร้างนักวิจัยปริญญาเอก ชื่อ น.ส. สุรีวัลย์ ดวงจิตต์ นายถิรพิทย์ สุบงกช และ น.ส.วรนันท์ รังสิมวงศ์ โครงการปริญญาเอกกาญจนาภิเษก

ภาคผนวก

The cover of output paper; 12 papers

1

International Journal of Nanomedicine

Dovepress
open access to scientific and medical research

Open Access Full Text Article

ORIGINAL RESEARCH

Role of the charge, carbon chain length, and content of surfactant on the skin penetration of meloxicam-loaded liposomes

Sureewan Duangjit[1,2]
Boonnada Pamornpathomkul[1]
Praneet Opanasopit[1]
Theerasak Rojanarata[1]
Yasuko Obata[2]
Kozo Takayama[2]
Tanasait Ngawhirunpat[1]

[1]Faculty of Pharmacy, Silpakorn University, Nakhon Pathom, Thailand; [2]Department of Pharmaceutics, Hoshi University, Shinagawa-ku, Tokyo, Japan

Video abstract

Point your SmartPhone at the code above. If you have a QR code reader the video abstract will appear. Or visit: http://dvpr.es/1MpYDq

Correspondence: Tanasait Ngawhirunpat
Faculty of Pharmacy, Silpakorn University, Sanamchandra Palace Campus, 6 Ratchamankanai Road, Muang, Nakhon Pathom 73000, Thailand
Tel +66 34 255 800
Email tanasait@su.ac.th

Abstract: The objective of this study was to investigate the influence of surfactant charge, surfactant carbon chain length, and surfactant content on the physicochemical characteristics (ie, vesicle size, zeta potential, elasticity, and entrapment efficiency), morphology, stability, and in vitro skin permeability of meloxicam (MX)-loaded liposome. Moreover, the mechanism for the liposome-enhanced skin permeation of MX was determined by Fourier transform infrared spectroscopy and differential scanning calorimetry. The model formulation used in this study was obtained using a response surface method incorporating multivariate spline interpolation (RSM-S). Liposome formulations with varying surfactant charge (anionic, neutral, and cationic), surfactant carbon chain length (C4, C12, and C16), and surfactant content (10%, 20%, and 29%) were prepared. The formulation comprising 29% cationic surfactant with a C16 chain length was found to be the optimal liposome for the transdermal delivery of MX. The skin permeation flux of the optimal formulation was 2.69-fold higher than that of a conventional liposome formulation. Our study revealed that surfactants affected the physicochemical characteristics, stability, and skin permeability of MX-loaded liposomes. These findings provide important fundamental information for the development of liposomes as transdermal drug delivery systems.

Keywords: optimal liposome, optimization, transdermal drug delivery, surfactant charge, surfactant carbon chain length, surfactant content

Introduction

Meloxicam (MX) is an effective nonsteroidal anti-inflammatory drug for reducing pain and inflammatory symptoms.[1–3] Long-term therapy with high doses of MX can lead to gastrointestinal side effects such as upset stomach, indigestion, ulceration, and bleeding.[4] Moreover, the high content of organic solvent in the MX formulation[5,6] limits its safety for skin delivery. Therefore, the development of MX as a transdermal drug delivery (TDD) candidate presents many challenges.

Since the first report that lipid vesicles incorporating sodium cholate as a surfactant could penetrate deep into intact skin to deliver drugs,[7] the use of surfactants in liposome formulations as penetration enhancers for the TDD of various drugs has attracted considerable interest. Numerous formulations have incorporated various types of surfactants in liposome bilayers. Although the use of cationic surfactants in liposomes has been reported to enhance the skin delivery of several drugs,[8–11] anionic surfactants in liposomes are also effective in improving skin delivery.[12–14] The influence of surfactants on the effectiveness of liposomes for skin delivery remains a much-debated question. Herein, liposome delivery systems must be designed and evaluated on a case-by-case basis because surfactants exhibit a diverse variety of hydrophilic head groups and

2

International Journal of Nanomedicine

Dovepress

open access to scientific and medical research

Open Access Full Text Article

ORIGINAL RESEARCH

Investigation of the mechanism of enhanced skin penetration by ultradeformable liposomes

Thirapit Subongkot
Boonnada Pamornpathomkul
Theerasak Rojanarata
Praneet Opanasopit
Tanasait Ngawhirunpat

Faculty of Pharmacy, Silpakorn University, Nakhon Pathom, Thailand

Abstract: This study aimed to determine the mechanism by which ultradeformable liposomes (ULs) with terpenes enhance skin penetration for transdermal drug delivery of fluorescein sodium, using transmission electron microscopy (TEM) and confocal laser scanning microscopy (CLSM). Skin treated with ULs containing d-limonene, obtained from in vitro skin penetration studies, was examined via TEM to investigate the effect of ULs on ultrastructural changes of the skin, and to evaluate the mechanism by which ULs enhance skin penetration. The receiver medium collected was analyzed by TEM and CLSM to evaluate the mechanism of the drug carrier system. Our findings revealed that ULs could enhance penetration by denaturing intracellular keratin, degrading corneodesmosomes, and disrupting the intercellular lipid arrangement in the stratum corneum. As inferred from the presence of intact vesicles in the receiver medium, ULs are also able to act as a drug carrier system. CLSM images showed that intact vesicles of ULs might penetrate the skin via a transappendageal pathway, potentially a major route of skin penetration.

Keywords: ultradeformable liposomes, mechanism of enhanced skin penetration, transmission electron microscopy, confocal laser scanning microscopy

Introduction

A transdermal drug delivery system utilizes skin to deliver drug into the circulation system. The main obstacle in this system is poor percutaneous absorption, because the uppermost layer of the skin (the stratum corneum) acts as a barrier. To improve percutaneous absorption of drug, many techniques have been applied, such as iontophoresis,[1] sonophoresis,[2] microneedles,[3] and lipid vesicle carriers.[4,5] Among the group of lipid vesicle carriers, ultradeformable liposomes (ULs) have received considerable attention in transdermal drug delivery research. Introduced by Cevc and Blume,[6] ULs are a type of elastic liposome, created by incorporating edge activators into liposomes. ULs have been shown to be effective for transdermal delivery of macromolecules, which are difficult to permeate through the skin.[7–11]

Two possible mechanisms proposed for the enhancement of skin penetration by ULs are a penetration-enhancing effect and a drug carrier system. The first mechanism suggests that ULs increase drug penetration into the skin by acting as a penetration enhancer.[12,13] The second mechanism proposes that ULs act as a drug carrier system.[6,14–18] To investigate the penetration-enhancing effect, various techniques have been used, such as infrared spectroscopy, differential scanning calorimetry, and skin penetration study. Although these techniques proved to be convenient and simple, they could not reveal the ultrastructural changes in skin caused by penetration enhancers. To assess the drug carrier system mechanism, drug-loaded vesicles must be able to pass through the skin into systemic circulation as intact vesicles. Cevc et al[15] reported the presence of drug-loaded vesicles in the blood of mice after fluorescently-labeled

Correspondence: Tanasait Ngawhirunpat
Department of Pharmaceutical Technology, Faculty of Pharmacy, Silpakorn University, 6 Racchamakkanai Road, Muang, Nakhon Pathom 73000, Thailand
Tel +66 34 255 800
Fax +66 34 255 801
Email tanasait@su.ac.th

September 2014 Regular Article *Biol. Pharm. Bull.* 37(9) 1543–1549 (2014) 1543

Bootstrap Resampling Technique to Evaluate the Reliability of the Optimal Liposome Formulation: Skin Permeability and Stability Response Variables

Sureewan Duangjit,[a,c] Praneet Opanasopit,[a] Theerasak Rojanarata,[a] Jun Takayama,[b] Kozo Takayama,[c] and Tanasait Ngawhirunpat*[,a]

[a] *Faculty of Pharmacy, Silpakorn University; Sanamchandra Palace Campus, Nakhon Pathom 73000, Thailand:* [b] *Research Fellow of Japan Society for the Promotion of Science; 5–3–1 Kojimachi, Chiyoda-ku, Tokyo 102–0083, Japan: and* [c] *Department of Pharmaceutics, Hoshi University; 2–4–41 Ebara, Shinagawa-ku, Tokyo 142–8501, Japan.*
Received May 9, 2014; accepted June 22, 2014; advance publication released online July 9, 2014

A nonlinear response surface method incorporating multivariate spline interpolation (RSM-S) is a useful technique for the optimization of pharmaceutical formulations, although the direct reliability of the optimal formulation must be evaluated. In this study, we demonstrated the feasibility of using the bootstrap (BS) resampling technique to evaluate the direct reliability of the optimal liposome formulation predicted by RSM-S. The formulation characteristics (X_n), including vesicle size (X_1), size distribution (X_2), zeta potential (X_3), elasticity (X_4), drug content (X_5), entrapment efficiency (X_6), release rate (X_7), and the penetration enhancer (PE) factors as formulation factors (Z_n), with the type of PE (Z_1) and content of PE (Z_2) were used as causal factors of the response surface analysis. The intended responses were high skin permeability (flux, Y_1) and high stability formulation (drug remaining, Y_2). Based on the dataset obtained, the simultaneous optimal solutions were estimated using RSM-S. Leave-one-out-cross-validation showed satisfying reliability of the optimal solution. Concurrently, similar BS optimal solutions were estimated from the BS dataset that was generated from the original dataset through BS resampling at frequencies of 250, 500, 750, and 1000. The analysis and simulation indicated that X_6, X_7, and Z_2 were the prime factors affecting Y_1 and Y_2. These findings suggest that this approach could also be useful for evaluating the reliability of an optimal liposome formulation predicted by RSM-S and would be beneficial for the pharmaceutical development of liposomes for transdermal drug delivery.

Key words bootstrap; response surface; simultaneous optimal solution; transdermal drug delivery

Optimization techniques using computer-based rationales to research and develop pharmaceutical formulations have recently become attractive and interesting. A non-linear response surface method incorporating multivariate spline interpolation (RSM-S) is a powerful method for pharmaceutical optimization.[1)] RSM-S has shown that the complex relationships between causal factors and response variables could be simply comprehended and that the simultaneous optimal solutions obtained would be stable and reproducible.[2)] Several intensive studies successfully developed novel pharmaceutical formulations using RSM-S (*e.g.*, water-in-oil-water multiple emulsion of insulin for intestinal delivery,[3)] sustained release of diltiazem tablets for oral delivery[4)] and ultra-deformable liposome of meloxicam for transdermal delivery[5)]). RSM-S was determined to be a promising technique for formulation optimization.[3–7)] Simultaneously, it is considerable to evaluate the accuracy and reliability of each optimal formulation estimated by RSM-S. The leave-one-out-cross-validation (LOOCV) method was also employed. The LOOCV method can evaluate the generalization error of a given response surface.[8)] Moreover, the reliability of optimal formulation estimated by certain response surface can be directly evaluated using bootstrap (BS) resampling methods. The BS method is a simulation technique based on the empirical distribution of the experimental data that introduced by Efron.[9)] BS resampling is generally used to estimate confidence intervals and the bias and variance of an estimator. The basic idea of BS resampling is randomly sampling from original dataset (experimental data). A BS samples ($X^*=X_1^*,X_2^*,\cdots,X_n^*$) is randomly sampled that replacement from the original data ($X=X_1,X_2,\cdots,X_n$) by reproducing the BS resampling procedure.

When designing and developing liposome for transdermal drug delivery, the safety, stability and efficacy of formulation must be simultaneously optimized. Generally, the liposome formulation is composed of various formulation characteristics and several formulation factors. The formulation characteristics and formulation factors are the major parameters directly affecting the skin permeability of a liposome formulation.[10)] The development of liposomes has previously been based primarily on trial and error to obtain an appropriate formulation for satisfying multiple characteristics of the formulation. Designing and testing on a case-by-case basis (or by trial and error techniques) was considered a wasteful method for designing each liposome formulation. The acceptable liposome formulation for one characteristic was often not satisfactory for other characteristics. Thus, these restrictions incurred difficulties in the design and development of liposome formulations. The optimal liposome formulation is generally influenced by a mixture of acceptable formulation characteristics and formulation factors. Therefore, an understanding of the actual relationships between causal factors (*e.g.*, formulation characteristics and formulation factors) and pharmaceutical responses (*e.g.*, skin permeability and stability of formulation) is required to develop satisfying liposome for transdermal drug delivery.

In this study, the original dataset used was obtained from the experiment. The formulation characteristics (X_n) and formulation factors (Z_n) of 30 model liposome formulations

The authors declare no conflict of interest.

* To whom correspondence should be addressed. e-mail: tanasait@su.ac.th

July 2014 Regular Article *Biol. Pharm. Bull.* 37(7) 1139–1148 (2014) 1139

Terpene Composited Lipid Nanoparticles for Enhanced Dermal Delivery of All-*trans*-Retinoic Acids

Ponwanit Charoenputtakun, Boonnada Pamornpathomkul, Praneet Opanasopit, Theerasak Rojanarata, and Tanasait Ngawhirunpat*

Faculty of Pharmacy, Silpakorn University; Nakhon Pathom 73000, Thailand.
Received January 8, 2014; accepted April 23, 2014; advance publication released online May 3, 2014

In the present study, terpene composited lipid nanoparticles and lipid nanoparticles were developed and evaluated for dermal delivery of all-*trans*-retinoic acids (ATRA). Terpene composited lipid nanoparticles and lipid nanoparticles were investigated for size, size distribution, zeta potential, entrapment efficiency, photostability, and cytotoxicity. *In vitro* skin permeation of ATRA lipid formulations were also evaluated. To explore the ability of lipid nanocarriers to target the skin, the distribution of rhodamine B base in the skin was investigated using confocal laser scanning microscopy (CLSM). The results indicated that the physicochemical characteristics of terpene composited lipid nanoparticles influenced skin permeability. All lipid nanocarriers significantly protected ATRA from photodegradation and were non-toxic to normal human foreskin fibroblast cells *in vitro*. Solid lipid nanoparticles containing 10% limonene (10% L-SLN) had the highest ATRA skin permeability. Terpene composited SLN and nanostructured lipid carriers (NLC) showed higher epidermal permeation of rhodamine B across the skin based on CLSM image analysis. Our study suggests that terpene composited SLN and NLC can be potentially used as dermal drug delivery carriers for ATRA.

Key words lipid nanoparticle; terpene; dermal delivery; all-*trans*-retinoic acid

Transdermal drug delivery has been chosen as a feasible alternative route of drug delivery due to its various advantages over conventional oral and intravenous routes such as reduction of drug metabolism *via* first pass effect, minimization of pain, and possible controlled drug release.[1,2] However, the effectiveness of transdermal drug delivery depends on the capability of drugs to penetrate across the skin in sufficient amounts to reach therapeutic levels.[3] The stratum corneum is an important barrier of the skin for drug absorption.[4,5] To facilitate drug delivery through the skin, penetration enhancers, which ideally cause a temporary reversible reduction in the barrier function of the stratum corneum, are extensively used to increase percutaneous absorption.[6]

Terpenes are a series of naturally occurring compounds consisting of isoprene (C_5H_8) units. They have been used in transdermal research since 1960s as skin permeation enhancers. They are reported to be a very safe and are an effective class of penetration enhancers that has been classified by the Food and Drug Administration (FDA) as generally regarded as safe (GRAS).[7] Limonene is a hydrocarbon lipophilic terpene obtained from the lemon peel of citrus lemon.[8] Previous studies have demonstrated that permeability enhancement by limonene can occur through multiple possible mechanisms, which may have contributed to the enhanced permeability of ketoprofen.[9] 1,8-Cineole, a terpene, has also been used to promote percutaneous absorption of several lipophilic drugs through hairless mouse skin[10,11] and was recently reported to have an enhancing effect on percutaneous Zidovudine (AZT) absorption across rat skin.[12] The mechanism of percutaneous permeation enhancement involves increasing the solubility of drugs in skin lipids, disruption of lipid/protein organization, and/or extraction of skin micro-constituents that are responsible for maintenance of barrier status. Hence, terpenes appear to offer great promise for use in transdermal formulations.[13]

Solid lipid nanoparticles (SLN) and nanostructured lipid carriers (NLC), which are the first and the second generation of lipid nanoparticles, respectively, are improved compared to nanoemulsions (NE). Lipid nanoparticles (SLN, NLC and NE) were chosen as the transdermal dosage form because of their promising novel dosage form and suitability for efficient delivery of active ingredients through the skin. The large surface area of these lipid nanoparticle systems allows rapid penetration of active molecules.[14,15] The lipid matrices of SLN are composed of solid lipids only, whereas NLC are composed of both solid and liquid lipids. In contrast with NE, both NLC and SLN are in the solid state at room and body temperatures. Moreover, the degradation of ascorbyl palmitate loaded in SLN and NLC showed lower degradation than NE.[16] A number of drugs can be used as a model drug for transdermal drug delivery; however, liphophilic drugs typically pose stability problems and thus, lipophilic drugs are good model drugs, which represent poor water solubility and/or photo instable drugs.

When applied topically, all-*trans*-retinoic acids (ATRA) have demonstrated efficacy in keratinization disorders and in the treatment of other cutaneous lesions.[17] Nevertheless, ATRA is sensitive to decomposition by light or high temperature and possesses poor aqueous solubility.[18] Accordingly, a desirable drug delivery system, such as lipid nanoparticles (SLN, NLC and NE), should be used to solve these problems. Moreover, little knowledge is available regarding the incorporation of terpenes in various lipid nanoparticles and the comparison for their effectiveness to other lipid nanoparticles as skin delivery carriers.

The objective of this study was to enhance the skin permeability of ATRA using lipid nanoparticles incorporated with terpenes as a permeation enhancer and to compare their effectiveness with other lipid nanoparticles as skin delivery carriers. Particle size, size distribution, zeta potential, entrapment efficiency, photo-stability, cytotoxicity, and *in vitro* skin permeability of these formulations were evaluated.

The authors declare no conflict of interest.

* To whom correspondence should be addressed. e-mail: tanasait@su.ac.th

1936 Regular Article *Biol. Pharm. Bull.* 37(12) 1936–1943 (2014) Vol. 37, No. 12

Terpene-Containing PEGylated Liposomes as Transdermal Carriers of a Hydrophilic Compound

Worranan Rangsimawong, Praneet Opanasopit, Theerasak Rojanarata, and Tanasait Ngawhirunpat*

Faculty of Pharmacy, Silpakorn University; Nakhon Pathom 73000, Thailand.

Received July 24, 2014; accepted September 29, 2014; advance publication released online October 8, 2014

We investigated the effect of PEGylated liposomes (PLs) containing a terpene on the penetration of a hydrophilic compound through porcine skin. PLs composed of *N*-(carbonyl-methoxypolyethyleneglycol-2000)-1,2-distearoyl-*sn*-glycero-3-phosphoethanolamine (PEG_{2000}–DSPE), the sodium salt of PEG_{2000}–DSPE, phosphatidylcholine (PC), cholesterol (Chol), Tween 20, and *d*-limonene were prepared as carriers for fluorescein sodium (NaFI). The physicochemical characteristics of PLs and their effects on *in vitro* skin penetration were evaluated. Tape stripping was used to evaluate NaFI deposition in skin layers, and confocal laser scanning microscopy (CLSM) was used to investigate the depth of skin penetration and the pathways used by NaFI-loaded vesicles. PLs containing *d*-limonene were smaller and conferred higher entrapment efficiency and skin penetration on NaFI than did PLs and conventional liposomes (CLs). The deposition of NaFI from PLs with *d*-limonene was greater in epidermis and dermis (6.10±1.74 μg) than stratum corneum (2.06±0.47 μg). CLSM images revealed that NaFI penetrated into the deepest skin layer with maximum fluorescence intensity. NaFI penetrated deeper (180 μm) in follicular than nonfollicular regions (145 μm), suggesting a transfollicular pathway predominates in skin penetration by NaFI-loaded PLs. In conclusion, grafting PEG onto ultra-deformable liposomes may enhance transdermal NaFI delivery and may be used as a carrier to prolong liposome circulation time.

Key words polyethylene glycol (PEG)ylated liposome; hydrophilic compound; skin permeation; confocal laser scanning microscopy

Liposomes have been used for dermal and transdermal drug delivery. Lipids, usually phospholipids arranged in one or more concentric bilayers enclosing an equal number of aqueous compartments, can entrap hydrophilic agents within the inner aqueous sphere. Lipophilic agents can intercalate into the lipid bilayer.[1] However, traditional liposomes are of little or no value for transdermal drug delivery because they do not deeply penetrate skin, remaining confined to the upper layers of the stratum corneum.[2] Cevc *et al.* have reported deformable liposomes (Transfersomes®), the first generation of elastic vesicles that can increase skin permeability, but only when applied under non-occluded conditions.[3] They consist of phospholipids and an edge activator. An edge activator is often a single-chain surfactant that destabilizes the lipid bilayer of the vesicles and increases deformability.[4]

Terpenes have been widely used as skin penetration enhancers for both hydrophilic and hydrophobic drugs. Monoterpenes such as *d*-limonene ($C_{10}H_{16}$) were generally more efficacious due to their small molecular sizes. *d*-Limonene fluidizes or perturbs the integrity of the barrier function of stratum corneum for enhanced the transport of drugs through skin.[5] Ultra-deformable liposomes containing Tween20 as an edge activator and terpenes as skin penetration enhancers have been reported to enhance skin penetration of NaFI by a synergistic effect of penetration enhancer, using mainly a transfollicular pathway, with smaller contributions from intercellular and transcellular pathways.[6]

A stealth liposome strategy can be achieved by modifying the surface of liposomal membranes with hydrophilic polymer conjugates, such as poly(ethylene glycol) (PEG). PEG is the most widely used polymer conjugate and reduces systemic uptake of mononuclear phagocytes. PEGylated liposomes (PLs) were developed to improve the blood circulation time of liposomes after intravenous administration. PEG has been widely used as a polymeric stabilizer that can be incorporated into the liposome surface in difference ways. The most widely used method at present is to anchor the polymer in the liposome membrane *via* a cross-linked lipid (*i.e.*, PEG–distearoylphosphatidylethanolamine (PEG–DSPE)).[6] In addition, it is possible to improve the colloidal stability of liposomes by changing the physicochemical properties of the particles *via* the polymer coating. Shielding the liposomes with a hydrophilic polymer coating (PEG) causes repulsion between bilayers, and thereby reduces the interactions between liposomes in the dispersion.[7]

Few reports are available on dermal application of PLs. Jain *et al.* reported the topical application of PEGylated surfactant-containing liposomes: PEGylation of surfactant-containing liposomes can increase the skin permeation of the low molecular weight drug, Zidovudine, by binding to water molecules, which could increase the hydration of the stratum corneum resulting in enhanced permeation of the stratum corneum barrier.[8] In addition, calcipotriol-loaded liposomes with 1 mol% PEG significantly increased the accumulation of calcipotriol in skin and hair follicles compared to non-PEGylated liposomes. The size of the liposomes affected the penetration of calcipotriol into the stratum corneum: small unilamellar vesicles enhanced calcipotriol penetration more than large ones.[9] The use of PLs as carriers for transdermal drug delivery requires further study. Liposomes with long circulation times containing skin penetration enhancers may yield a transdermal drug delivery system that can affect the blood circulation time of liposomes.

Fluorescein sodium (NaFI) is a low molecular hydrophilic

The authors declare no conflict of interest.

* To whom correspondence should be addressed. e-mail: tanasait@su.ac.th

6

Advanced Materials Research Vol. 1060 (2015) pp 21-24
© (2015) Trans Tech Publications, Switzerland
doi:10.4028/www.scientific.net/AMR.1060.21

Submitted: 15.07.2014
Revised: 22.08.2014
Accepted: 12.09.2014

Development and Evaluation of Tamarind Seed Xyloglucan for Transdermal Patch of Clindamycin

Sureewan Duangjit,[1,a] Parin Buacheen,[1,b]
Pongsakorn Priebprom,[1,c] Sittikun Limpanichkul,[1,d]
Panida Asavapichayont,[1,e] Porntip Chaimanee,[2,f]
and Tanasait Ngawhirunpat,[1,g]

[1]Faculty of Pharmacy, Silpakorn University, Nakhon Pathom 73000 Thailand

[2]Faculty of Science, Silpakorn University, Nakhon Pathom 73000 Thailand

[a]dsureewan@hotmail.com, [b]parin.docu@gmail.com, [c]prieprom802@hotmail.com,
[d]sittikun.t@hotmail.com, [e]apanida@su.ac.th, [f]porntip@su.c.th, [g]tanasait@su.ac.th

Keywords: Tamarind seed extract, Xyloglucan, Clindamycin, Transdermal patch, Acne vulgaris, Staphyllococus aureus

Abstract. The object of this study was to develop the clindamycin transdermal patch using extracts of tamarind seeds as novel gelling agent for transdermal delivery. The patch was composed of tamarind seed extracts having xyloglucan as a main composition, 1% clindamycin, and various ratios of glycerin and propylene glycol i.e. 10:0, 8:2, 6:4, 5:5, 4:6, 2:8 and 0:10, as plasticizer and penetration enhancer, respectively. The clindamycin patch was prepared by casting method. The content of clindamycin in the patch, the tensile strength and the drug release from the patch were evaluated. Moreover, the cup and plate method was used to determine the antimicrobial activity of clindamycin patch compared with commercial available clindamycin gel in the market, and *Staphyllococcus aureus* was used as test organism in this study. The results showed that the good physical stability of clindamycin patches were successfully prepared. The ratio of composition in the formulation affected the tensile strength and the drug release. As the ratio of propylene glycol to glycerin in the formulation was increased, the tensile strength and the drug release increased. The formulation composed of the ratio of glycerin and propylene glycol (4:6) showed the highest drug release and the best efficiency in antibiotic test. Our results indicated that the extracts of tamarind seeds could be a potential biopolymer and also applied as controlled release in transdermal delivery system.

Introduction

Natural polymers have been extensively used as biopolymers in pharmaceutics because of their naturalness and non-toxicity materials. Xyloglucan (XG) is a natural glucosaminoglycan polysaccharide derived from the tamarind seed (*Tamarindus indica*). Thus, tamarind seed XG was used as binder, stabilizer, plasticizers, thickening agent and gelling agent in various drugs delivery system such as oral [1], buccal [2] or rectal [3] drug delivery, because of its biodegradability and biocompatibility properties. Acne vulgaris is a common chronic inflammatory disease of the pilosebaceous units. Standard therapies were available for acne vulgaris e.g. oral and topical antibiotics. Clindamycin phosphate is the most common topical antibiotic used in the treatment of acne vulgaris for over 20 years [4]. However, poor patient compliance was a major cause of treatment failure because of low efficacy, slow onset of action, adverse effects [5]. The new formulation of topical acne treatment to improve patient adherence with medication, which is ease of use, prolong release, reduce lesion counts and conceal redness is extremely interested. In this study, novel transdermal patch of clindamycin was developed using extracts from tamarind seed to overcome acne treatment failures. Moreover, the content of clindamycin in the patch, the tensile strength, the drug release from the patch and the antimicrobial activity were evaluated.

International Journal of Nanomedicine

Dovepress
open access to scientific and medical research

Open Access Full Text Article

ORIGINAL RESEARCH

Mechanistic study of decreased skin penetration using a combination of sonophoresis with sodium fluorescein-loaded PEGylated liposomes with D-limonene

Worranan Rangsimawong
Praneet Opanasopit
Theerasak Rojanarata
Tanasait Ngawhirunpat

Faculty of Pharmacy, Silpakorn University, Nakhon Pathom, Thailand

Abstract: The effect of low frequency sonophoresis (SN, 20 kHz) on the skin transport of sodium fluorescein (NaFl)-loaded liposomes was investigated. An in vitro skin penetration study in open and blocked hair follicles was performed, and confocal laser scanning microscopy and scanning electron microscopy were used to visualize the penetration pathways. The results showed that SN significantly increased the flux of NaFl solution, whereas it significantly decreased the flux of NaFl-loaded polyethylene glycol-coated (PEGylated) liposomes with D-limonene (PL-LI). SN did not significantly affect the flux of NaFl-loaded conventional liposomes and PEGylated liposomes. In the blocked follicles, the flux of NaFl-loaded PL-LI both with and without SN decreased, indicating that NaFl-loaded PL-LI penetrated the skin via the transfollicular pathway. A confocal laser scanning microscopy image showed that in the skin without SN, the fluorescence intensity of NaFl-loaded PL-LI was observed in the skin and along the length of hair inside the skin, whereas in the skin with applied SN, the fluorescence intensity was detected only on the top of hair outside the skin. From scanning electron microscopy images, SN dislocated the corneocytes and reduced the deposition of PL-LI around hair follicles. These results revealed that SN may partially plug hair follicle orifices and reduce percutaneous absorption through the follicular pathway.

Keywords: sonophoresis, PEGylated liposomes, hydrophilic compound, follicular pathway

Introduction

Sonophoresis (SN) is a non-invasive technique for increasing the skin permeability of various medications, including hydrophilic and large molecular weight compounds such as caffeine,[1,2] hydrocortisone,[3] calcein, and FITC-labeled dextrans. The transdermal delivery of hydrophilic solutes with low-frequency ultrasound is likely to occur as non-specific transport across the stratum corneum (ie, both the intracellular lipid regions and the corneocytes).[4] Several possible mechanisms for SN as a transport pathway have been suggested, such as thermal effects by absorption of ultrasound energy and cavitation effects caused by collapse and oscillation of cavitation bubbles in the ultrasound field.[5,6] Cavitation has been found to be the main factor in creating aqueous pathways across the stratum corneum by distorting the lipid bilayer, which can lead to enhancing the transport of hydrophilic drugs across the skin.[7]

Low-frequency SN typically enhances the transport of hydrophilic molecules in solution across the skin. It can easily be coupled with other transdermal drug delivery techniques such as tape stripping,[8] microneedle,[9] electroporation,[10] iontophoresis,[11] and chemical enhancement to produce a synergistic effect on transdermal

Correspondence: Tanasait Ngawhirunpat
Faculty of Pharmacy, Silpakorn University,
6 Racchamakka Nai Road, Nakhon Pathom 73000, Thailand
Fax +66 3 425 5801
Email ngawhirunpat_t@su.ac.th

International Journal of Nanomedicine

Dovepress
open access to scientific and medical research

Open Access Full Text Article

ORIGINAL RESEARCH

Effect of liposomal fluidity on skin permeation of sodium fluorescein entrapped in liposomes

Thirapit Subongkot[1]
Tanasait Ngawhirunpat[2]

[1]Department of Pharmaceutical Technology, Faculty of Pharmaceutical Sciences, Burapha University, Chonburi, Thailand; [2]Department of Pharmaceutical Technology, Faculty of Pharmacy, Silpakorn University, Nakhon Pathom, Thailand

Abstract: The purpose of this study was to investigate the effect of ultradeformable liposome components, Tween 20 and terpenes, on vesicle fluidity. The fluidity was evaluated by electron spin resonance spectroscopy using 5-doxyl stearic acid and 16-doxyl stearic acid as spin labels for phospholipid bilayer fluidity at the C5 atom of the acyl chain near the polar head group (hydrophilic region) and the C16 atom of the acyl chain (lipophilic region), respectively. The electron spin resonance study revealed that Tween 20 increased the fluidity at the C5 atom of the acyl chain, whereas terpenes increased the fluidity at the C16 atom of the acyl chain of the phospholipid bilayer. The increase in liposomal fluidity resulted in the increased skin penetration of sodium fluorescein. Confocal laser scanning microscopy showed that ultradeformable liposomes with terpenes increase the skin penetration of sodium fluorescein by enhancing hair follicle penetration.

Keywords: ultradeformable liposomes, terpenes, fluidity, electron spin resonance spectroscopy, confocal laser scanning microscopy

Introduction

Transdermal drug delivery systems utilize skin as a transportation route and offer many advantages, including avoidance of first-pass hepatic metabolism, sustained and controlled drug release, and improved patient compliance. However, the stratum corneum, the outermost skin layer, exhibits a rate-limiting step in regulating drug absorption into the skin. Various strategies have been used to increase drug absorption across the skin, such as microneedles,[1] iontophoresis,[2] sonophoresis,[3] electroporation,[4] microdermabrasion,[5] microemulsion,[6] niosomes,[7] and liposomes.[8–10] Ultradeformable liposomes (ULs), also called transfersomes, are a type of elastic vesicle, introduced by Cevc and Blume.[11] ULs generally consist of phospholipids and surfactant as a membrane softening agent. Due to their flexibility, ULs fit through narrow pores approximately one-tenth of their diameter. ULs also penetrate as intact vesicles through the skin into the blood circulation without permanent disintegration.[12] ULs effectively increase the skin penetration of drugs both in vitro and in vivo.[13–15]

Terpenes, a class of penetration enhancers obtained from natural sources, have successfully been used as skin penetration enhancers for percutaneous absorption enhancement in various types of liposomes, specifically invasomes,[16,17] and ULs.[18,19] Electron spin resonance (ESR), also known as electron paramagnetic resonance, is a spectroscopy technique used to study molecular mobility by characterizing the unpaired electron of free radicals, also called spin probes, in an extreme applied magnetic field. This technique has been used to study membrane fluidity,[20,21] the skin penetration enhancement mechanism of penetration enhancers and nanocarriers,[22,23] and antioxidant properties.[24]

Correspondence: Tanasait Ngawhirunpat
Department of Pharmaceutical Technology, Faculty of Pharmacy, Silpakorn University, 6 Rajamankha Nai Road, Muang, Nakhon Pathom 73000, Thailand
Tel +66 34 255 800
Fax +66 34 255 801
Email ngawhirunpat_t@su.ac.th

submit your manuscript | www.dovepress.com
Dovepress
http://dx.doi.org/10.2147/IJN.S86424

Pharmaceutical Development and Technology

http://informahealthcare.com/phd
ISSN: 1083-7450 (print), 1097-9867 (electronic)

Pharm Dev Technol, Early Online: 1–8
© 2015 Informa Healthcare USA, Inc. DOI: 10.3109/10837450.2015.1048552

informa healthcare

RESEARCH ARTICLE

Application of Design Expert for the investigation of capsaicin-loaded microemulsions for transdermal delivery

Sureewan Duangjit[1,2], Wisuta Chairat[1], Praneet Opanasopit[1], Theerasak Rojanarata[1], and Tanasait Ngawhirunpat[1]

[1]Faculty of Pharmacy, Silpakorn University, Nakhon Pathom, Thailand and [2]Faculty of Pharmaceutical Sciences, Ubon Ratchathani University, Ubon Ratchathani, Thailand

Abstract

Our previous study reported that the Design Expert® Software showed a beneficial role in the development of microemulsions (ME) for transdermal drug delivery. To fully confirm the reproducibility and the reliability of simultaneous optimal ME formulations, the optimal ME formulations predicted by the Design Expert® Software were experimentally formulated and verified for their skin permeability. Ternary phase diagrams were used to predict the optimal ME area, and the ME formulations selected from outside this area were considered as candidate ME systems. Our ME systems were formulated with isopropyl myristate (IPM) as the oil phase, cocamide diethanolamine (DEA) as the surfactant, ethanol as a co-surfactant and water as the aqueous phase. The droplet size, size distribution, electrical conductivity, pH, drug content and skin permeability of the candidate ME systems were monitored. Our findings indicated that the skin permeability of the optimal ME and all of the candidate ME formulations was significantly greater than that of the commercial capsaicin (CAP) product. Our study succeeded in predicting and developing the ME systems for the transdermal delivery of CAP. The simplex lattice design used in this study is experimentally useful for the development of pharmaceutical formulations.

Keywords

Capsaicin, cocamide diethanolamine, Design Expert, microemulsions, simplex lattice design

History

Received 29 January 2015
Revised 16 April 2015
Accepted 28 April 2015
Published online 21 May 2015

Introduction

In the development of pharmaceutical formulations, a complicated relationship exists between the formulation factors and the pharmaceutical responses. Therefore, design of experiment (DoE) was used to clarify the relationship between the formulation factors or causal factors (X_n) and the pharmaceutical responses or response variables (Y_n). Currently, DoE is an acceptable and well-organized technique for determining the critical attributes that may affect pharmaceutical products and processes[1]. DoE analysis utilizes a response surface method (RSM) to resolve optimization troubles, and several pharmaceutical research studies have successfully utilized RSM[2–4]. Our previous study has also suggested that a simplex lattice design is beneficial for the development of microemulsions (ME) used in transdermal drug delivery[5].

Microemulsions (ME) are transparent colloidal systems composed of two immiscible phases that are stabilized by a surfactant system. ME have long been used in several drug delivery systems, including oral, parenteral, nasal and topical applications[6–10]. ME have also been extensively studied for transdermal delivery because they offer several advantages, such as high-loading capacities for hydrophilic and lipophilic drugs, ease of preparation and thermodynamic stability[11,12]. However, the ME that provides relatively high-skin permeability also contains high concentrations of surfactant systems[13]. Therefore, skin irritation and the safety of the surfactant system used may restrict the utilization of these ME. In the development of suitable ME for transdermal delivery, it is important to prepare optimal ME formulations that have the proper skin permeability without inducing skin irritation. Moreover, ME containing at least three components (oil, water and a surfactant) could simultaneously affect the physicochemical characteristics and the skin permeability of the ME. Therefore, it was appropriate to apply DoE in clarifying the relationships between the causal factors and the response variables to optimize the ME formulation.

Capsaicin (CAP) is a potent, pungent taste compound from chili peppers that is applied for reducing pain associated with various diseases, such as lumbago, sciatica, rheumatism, post-hepatic neuralgia or musculoskeletal inflammation. The hot, pungent taste of CAP reliably relieves pain due to its ability to cause a burning sensation in mammalian tissues[14]. However, high concentrations of CAP (0.75% w/w) may cause local skin irritation[15]. The chemical structure of CAP is shown in Figure 1.

The aims of this study were to develop ME systems based on computer design and to optimize these ME systems for the transdermal delivery of CAP. The challenge in achieving our aims was to discover a potential ME that incorporated a low dose of CAP (0.15% w/w) and a low concentration of the surfactant system. The model ME formulations were obtained from a pseudo-ternary phase diagram. A CAP-loaded ME composed of isopropyl myristate (IPM) as the oil phase, cocamide

Address for correspondence: Tanasait Ngawhirunpat, Faculty of Pharmacy, Silpakorn University, Sanamchan Palace Campus, Nakhon Pathom 73000, Thailand. Tel: +66-34-255800. Fax: +66-34-255801. E-mail: ngawhirunpat_t@su.ac.th

Vol. 39, No. 4 *Biol. Pharm. Bull.* **39**, 601–610 (2016) 601

Regular Article

Development, Characterization and Skin Interaction of Capsaicin-Loaded Microemulsion-Based Nonionic Surfactant

Sureewan Duangjit,[a,b] Wisuta Chairat,[b,c] Praneet Opanasopit,[b,c] Theerasak Rojanarata,[b,c] Suwannee Panomsuk,[b,c] and Tanasait Ngawhirunpat*[,b,c]

[a] *Faculty of Pharmaceutical Sciences, Ubon Ratchathani University; Ubon Ratchathani 34190, Thailand:* [b] *Pharmaceutical Development of Green Innovation Group (PDGIG), Faculty of Pharmacy, Silpakorn University; Sanamchan Palace Campus, Nakhon Pathom 73000, Thailand: and* [c] *Faculty of Pharmacy, Silpakorn University; Sanamchan Palace Campus, Nakhon Pathom 73000, Thailand.*

Received November 30, 2015; accepted January 5, 2016

The aim of this study was to develop novel microemulsions (MEs) for the transdermal delivery of capsaicin. Microemulsion-based nonionic surfactants consisting of isopropyl myristate as the oil phase, various nonionic surfactants as the surfactant (S), various glycols or alcohol as the co-surfactant (CoS), and reverse osmosis water as the aqueous phase were formulated. Based on the optimal ME obtained from Design Expert®, MEs containing a fixed concentration of oil, water or surfactant were prepared while varying the amounts of the other two fractions. The results indicated that the skin permeation flux of low dose capsaicin (0.15% (w/w)) was significantly higher for the selected ME than the commercial product and capsaicin in ethanol (control) by approximately two- and four-fold, respectively. We successfully demonstrated the feasibility of the transdermal delivery of capsaicin-loaded ME using a low concentration of nonionic surfactant and ethanol. Moreover, the optimization using computer program helped to simplify the development of a pharmaceutical product.

Key words capsaicin; microemulsion-based nonionic surfactant; decyl glucoside; polyethylene glycol (PEG)-7 glyceryl cocoate; cocamide diethanolamine; Design Expert

Microemulsions (MEs) are transparent systems consisting of two immiscible phases that are stabilized by a surfactant or surfactant systems (a mixture of surfactant (S) and co-surfactant (CoS)). MEs are widely used in transdermal drug delivery because they offer several advantages, including simple preparation, a high loading capacity for hydrophilic and lipophilic drugs, thermodynamic stability and a high potential for enhanced skin permeation.[1)] Numerous studies have shown that MEs are more effective than other topical formulations, such as solutions, suspensions, gels, creams, hydrogels, micelles, liquid crystalline and liposomes.[2–9)] Several mechanisms have been proposed to explain how MEs enhance drug penetration into the skin.[10,11)] In recent years, MEs have continued to be designed and developed as transdermal delivery carriers for various poorly soluble drugs because they can improve the solubilization and bioavailability of lipophilic drugs and provide a large region per concentration ratio for mass transfer. A high ratio of ionic surfactants (which serve as the S phase) to ethanol (which serves as the CoS phase) is generally used to improve the potential for skin delivery by MEs. However, the high S/CoS ratio in the surfactant system used to generate MEs to ensure high skin permeability may also concurrently cause severe skin irritation. Consequently, ME-based nonionic surfactants with low S/CoS ratios need to be developed to avoid safety concerns related to the skin irritation. Software (Design Expert®) is a powerful tool to simplify the complex relationship between the concentration of surfactant systems and ME characteristics (both skin permeability and skin irritation).[12)]

Capsaicin (8-methyl *N*-vanillyl-6-nonenamide) is a natural alkaloid (capsaicinoid) and the major active spicy ingredient extracted from chili peppers. Capsaicin is a fat-soluble, odorless, spicy, off-white solid with a melting point between 62–65°C and a molecular weight of 305.4 kDa. Capsaicin is notable because of its spiciness and ability to cause a burning sensation in mammalian tissues. Because capsaicin is not soluble in water, alcohol and other organic solvents are used to solubilize capsaicin in conventional topical preparations and sprays. Capsaicin is topically applied to treat various diseases, including musculoskeletal inflammation, rheumatism, posthepatic neuralgia, lumbago and sciatica.[13)] The mechanisms of action of capsaicin have been extensively studied over the past several decades. Capsaicin can release substance P from the afferent nociceptive neurons, and the resulting depletion of substance P desensitizes small afferent sensory neurons.[14)] However, orally administered capsaicin undergoes significant first-pass metabolism in rats and mice,[15)] and the spiciness of capsaicin limits its clinical applications. Several current studies have reported the topical and transdermal delivery of capsaicin using novel carriers, *e.g.*, niosomes or ME, but these formulations remain limited by their high concentration of capsaicin (0.75% (w/w))[9)] and the use of high levels of ethanol or benzyl alcohol.[13,16)] Therefore, MEs featuring improved co-surfactant systems may be useful for the transdermal delivery of low-dose capsaicin (0.15% (w/w)) using a low concentration of surfactants.

The aim of the present study was to develop ME systems consisting of novel surfactant systems for the transdermal delivery of capsaicin. Various surfactant systems were screened to be incorporated with capsaicin. The ME systems consisted of isopropyl myristate (IPM) as the oil phase; decyl glucoside (Plantacare® 2000), polyethylene glycol (PEG)-7 glyceryl cocoate (Cetiol® HE) or cocamide diethanolamine (Comperlan® KD) as the surfactant; propylene glycol (PG), ethanol, PEG

* To whom correspondence should be addressed. e-mail: ngawgirunpat_t@su.ac.th

1254 *Biol. Pharm. Bull.* **39**, 1254–1262 (2016) Vol. 39, No. 8

Regular Article

Skin Transport of Hydrophilic Compound-Loaded PEGylated Lipid Nanocarriers: Comparative Study of Liposomes, Niosomes, and Solid Lipid Nanoparticles

Worranan Rangsimawong,[a] Praneet Opanasopit,[a] Theerasak Rojanarata,[a] Sureewan Duangjit,[b] and Tanasait Ngawhirunpat*,[a]

[a] *Faculty of Pharmacy, Silpakorn University; Nakhon Pathom 73000, Thailand: and* [b] *Faculty of Pharmaceutical Sciences, Ubon Ratchathani University; Ubon Ratchathani 34190, Thailand.*

Received December 2, 2015; accepted April 1, 2016

The effect of surface grafting with *N*-(carbonyl-methoxypolyethylene glycol-2000)-1,2-distearoyl-*sn*-glycero-3-phosphoethanolamine (PEG2000-DSPE) onto three types of lipid nanocarriers, liposomes, niosomes and solid lipid nanoparticles (SLNs) on the skin penetration of sodium fluorescein (NaFI) was investigated. Confocal laser scanning microscopy (CLSM) was used to visualize the penetration pathways. Fourier transform infrared spectroscopy (FT-IR) was used to determine the skin hydration. The results showed that the physicochemical properties of each nanocarrier were modified after PEG grafting. In the skin penetration study, PEG grafting increased the flux of NaFI-loaded PEGylated liposomes and significantly decreased the flux of NaFI-loaded PEGylated niosomes and NaFI-loaded PEGylated SLNs. The skin deposition study and CLSM images showed that the intact liposome vesicles permeated into the skin. The niosomes and SLNs had little or no vesicles in the skin, suggesting that NaFI may have been released from these nanocarriers before permeation. Additionally, the fluorescent CLSM images of the SLNs showed that NaFI deposited along the length of hair follicles inside the skin, indicating that the skin penetration route may be through the transfollicular pathway. For the PEGylated nanocarriers, the PEGylated liposomes had higher fluorescence intensities than the non-PEGylated liposomes, indicating higher NaFI concentrations. The PEGylated niosomes and PEGylated SLNs had lower fluorescence intensities than those of the non-PEG modified niosomes and SLNs. For FT-IR results, PEGylated liposomes increased the skin hydration, while the grafting PEG onto niosomes and SLN surfaces decreased the skin hydration. This study showed that the surface grafting of PEG onto various nanocarriers affected the skin transport of NaFI.

Key words PEGylated nanocarrier; liposome; niosome; solid lipid nanoparticle; hydrophilic compound; skin penetration

Transdermal routes provide a controlled and non-invasive method of drug delivery. The outermost layer of skin, the stratum corneum, is a major protective barrier against the ingress of xenobiotics and controls the rate of water loss from the body. Therefore, drug transports *via* simple vehicles are unable to achieve therapeutic drug concentrations. Many strategies for enhancing skin penetration have been developed, such as chemical penetration, supersaturated systems, vesicles or physical mechanisms. A few examples of these strategies include the use of prodrugs, iontophoresis, electroporation, and ultrasound.[1)]

Lipid-based nanocarriers are the most sought after devices for topical and transdermal delivery applications. These nanocarriers include liposomes, niosomes, ethosomes, transferosomes, solid lipid nanoparticles (SLNs) and nanostructure lipid carriers (NLCs) have been extensively studied for the transdermal delivery of drugs. Liposomes have the potential to be drug-carrier systems for transdermal delivery. They contain amphipathic phospholipids arranged in one or more concentric bilayers enclosing an equal number of aqueous compartments. Hydrophilic agents can be entrapped within the inner aqueous sphere and lipophilic agents can intercalate in the lipid bilayers. Liposomes have been extensively studied for transdermal applications due to their similarity to biological membranes, ability to interact with similar lipids in skin, and decreased systemic absorption.[2,3)]

Niosomes, another lipid vesicle formulation, are similarly prepared and have the same functional and physicochemical properties as liposomes, such as the bilayer structure. However, niosomes differ from liposomes in their chemical structure. Niosomes are made of cholesterol and hydrated non-ionic surfactants and as such, have greater stability and lack many of the disadvantages associated with liposomes, *i.e.*, high cost, low availability, and various purity issues commonly associated with phospholipids. Vesicular nanocarriers have been used as potential transdermal drug delivery systems due to their enhanced penetration capabilities, localized depots for sustained drug release, and rate-limiting membranes for the modulation of systemic absorption of drugs *via* the skin.[4)]

SLNs have been reported as alternatives to emulsions, liposomes, microparticles, and their polymeric counterparts for various application routes due to various advantages, such as the ability to incorporate lipophilic and hydrophilic drugs, improved physical stability, low costs relative to liposomes and easy scale-up and manufacturing potential.[5,6)] SLNs are colloidal nanocarriers system consisting of surfactant-coated, high melting point lipid nanoparticles (including high melting point glycerides or waxes).[7)] The small particle sizes of SLNs enable their close contact with the stratum corneum and thereby enhances the amount of encapsulated agent penetrating into the skin.[8)] Moreover, SLNs form occlusive films and have enhanced drug permeation.[9)]

* To whom correspondence should be addressed. e-mail: ngawhirunpat_t@su.ac.th

PHARMACEUTICAL DEVELOPMENT AND TECHNOLOGY, 2016
http://dx.doi.org/10.1080/10837450.2016.1221428

Taylor & Francis

RESEARCH ARTICLE

Influence of sonophoresis on transdermal drug delivery of hydrophilic compound-loaded lipid nanocarriers

Worranan Rangsimawong, Praneet Opanasopit, Theerasak Rojanarata, Suwannee Panomsuk and Tanasait Ngawhirunpat

Faculty of Pharmacy, Silpakorn University, Bangkok, Thailand

ABSTRACT

The effect of sonophoresis on the transdermal drug delivery of sodium fluorescein (NaFl)-loaded lipid nanocarriers such as liposomes (LI), niosomes (NI) and solid lipid nanoparticles (SLN) was investigated by confocal laser scanning microscopy (CLSM), Fourier transform infrared spectroscopy (FTIR) and scanning electron microscopy (SEM). The results showed that SN decreased the skin penetration of NaFl-loaded SLN (6.32-fold) and NI (1.79-fold), while it increased the penetration of NaFl-loaded LI (5.36-fold). CLSM images showed the red fluorescence of the LI and NI bilayer on the superficial layer of the stratum corneum. However, the red fluorescent probe of the SLN was not visualized in the skin. FTIR results of the LI and NI with SN showed no effect on lipid stratum corneum ordering, suggesting that the fragment of bilayer vesicles might repair the damaged skin. For SLN, the strengthening of stratum corneum by covering the disrupted skin with solid lipids was shown. SEM images show disrupted carriers of all the formulations adsorbed onto the damaged skin. In conclusion, the SN changed the properties of both the skin surface and lipid nanocarrier, demonstrating that disrupted skin might be repaired by a disrupted nanocarrier.

ARTICLE HISTORY
Received 6 May 2016
Revised 26 June 2016
Accepted 28 June 2016
Published online ▮▮▮

KEYWORDS
Liposomes; niosomes; solid lipid nanoparticles; hydrophilic compound; sonophoresis; skin penetration

Introduction

Sonophoresis (SN) has been proposed as a noninvasive technique for increasing the skin permeability to various drugs by using several mechanisms, such as thermal effects by absorption of ultrasound energy and cavitation effects caused by the collapse and oscillation of cavitation bubbles in an ultrasound field[1,2]. The main effect of cavitation has been found to create aqueous pathways across the stratum corneum by distorting the lipid bilayer, which can lead to enhancement of skin transport of hydrophilic molecules[3].

A simultaneous application of ultrasound to the skin is performed by applying ultrasound energy through a coupling medium containing the drug onto the skin surface, which causes enhancement of drug transport in two ways: (i) by changing the skin structures, leading to increase in skin permeability and (ii) through convection-related mechanisms that occur only when an ultrasound is applied. However, the action of ultrasound on drugs or other active ingredients can cause molecular degradation or other chemical reactions, which can result in a loss of activity or effectiveness of the therapeutic compound and may also cause undesired reactions[1,4,5].

Lipid-based nanocarriers, including liposomes (LI), niosomes (NI), ethosomes, transferosomes, solid lipid nanoparticles (SLN) and nanostructure lipid carriers (NLC), were extensively studied for transdermal delivery of drug by using several permeation mechanisms, such as intact drug-loading vesicle penetration into the different layers of the skin; lipid vesicles acting as penetration enhancers via their skin lipid-fluidizing property; the drug released from carrier and intercalated in the lipid bilayer of the stratum corneum; or lipid vesicle-mediated enhanced transdermal drug delivery via appendageal pathways (e.g. hair follicles and sweat ducts)[6]. A few studies have investigated a combination of SN and a lipid nanocarrier system. Vyas et al. showed that the application of ultrasound and ointment containing LI enhanced diclofenac-entrapped LI permeation across the skin[7], while Dahlan et al. reported that LI application to sonicated skin prior to the application of bovine serum albumin (BSA) solution reduced BSA penetration and transepidermal water loss due to the repair of sonication-induced skin disruption[8]. Moreover, no mechanistic study for the skin penetration of NI and SLN combined with SN has been reported.

Therefore, the aim of this study was to investigate the effect of low frequency SN (20 kHz) on the permeation pathway for the transport of sodium fluorescein (NaFl)-loaded lipid nanocarriers into porcine skin. Lipid nanocarriers, such as LI, NI and SLN, have been used as carriers to enhance the transdermal delivery of NaFl. LI and NI formulations were prepared using a sonication method. SLN was prepared using a *de novo* emulsification method. Particle size, surface charge, entrapment efficiency, loading efficiency and *in vitro* skin penetration were investigated. Confocal laser scanning microscopy (CLSM) was used to visualize the skin penetration pathways of the vesicles. Fourier transform infrared spectroscopy (FTIR) was used to evaluate the stratum corneum change after applying a lipid nanocarrier and SN. Scanning electron microscopy (SEM) was also used to observe the skin surface after applying ultrasound energy.

Materials and methods

Materials

Egg phosphatidylcholine (PC) was a gift from Lipoid GmbH, Ludwigshafen, Germany. Cholesterol (Chol) was obtained from

CONTACT Tanasait Ngawhirunpat ngawhirunpat_t@su.ac.th Department of Pharmaceutical Technology, Silpakorn University, Bangkok 73000, Thailand

The cover of output oral presentation; 2 proceedings

1

ASIAN JOURNAL OF PHARMACEUTICAL SCIENCES 11 (2016) 52–53

HOSTED BY

Available online at www.sciencedirect.com

ScienceDirect

journal homepage: www.elsevier.com/locate/ajps

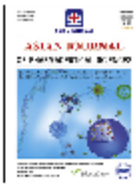

Design and development of optimal invasomes for transdermal drug delivery using computer program

Sureewan Duangjit [a,c,*], *Tassanan Nimcharoenwan* [b], *Nutcha Chomya* [b], *Natthporn Locharoenrat* [b], *Tanasait Ngawhirunpat* [b,c]

[a] *Division of Pharmaceutical Chemistry and Technology, Faculty of Pharmaceutical sciences, Ubon Ratchathani University, Ubon Ratchathani 34190, Thailand*

[b] *Department of Pharmaceutical Technology, Faculty of Pharmacy, Silpakorn University, Nakhon Pathom 73000, Thailand*

[c] *Pharmaceutical Development of Green Innovations Group (PDGIG), Faculty of Pharmacy, Silpakorn University, Nakhon Pathom 73000, Thailand*

ARTICLE INFO

Article history:
Available online 25 November 2015

Keywords:
Design expert
Invasomes
Liposomes
Capsaicin

Capsaicin (CAP) is a major pungent component that has been widely studied in medical and pharmaceutical fields. CAP was used both orally and topically for pain relief. However, the extreme pungency and the water insolubility of CAP lead to its restriction in the development of CAP as drug delivery system [1]. Our previous study suggested that the computer software exhibited a beneficial role in the development of menthosomes for transdermal drug delivery [2]. To confirm the reliability and reproducibility of simultaneous optimal formulations, the optimal ultraflexible liposomes (invasomes) estimated by the computer software (Design Expert®) were experimentally formulated and investigated. To achieve this purpose, invasomes with Comperlan® KD and *d*-limonene as potential penetration enhancer were developed. Using a two-factor factorial design with centroid replication as a model experimental design, the invasomes were demonstrated. The model invasome formulations containing a constant composition of 10 mM phosphatidylcholine, 1 mM cholesterol and 0.15% capsaicin, and various percentages of *d*-limonene and Comperlan® KD were prepared. The physicochemical characteristics e.g., vesicle size, size distribution, zeta potential, entrapment efficiency and skin permeability of the model invasome formulations were evaluated. The compositions and the physicochemical characteristics of invasomes were defined as formulation factor (X_n) and response variables (Y_n), respectively. The relationship between formulation factor and response variables was predicted, and the optimal invasome formulation was also optimized using Design Expert®. The response surfaces estimated by Design Expert® illustrated obvious relationship between formulation factor and response variables. The formulation factor directly

* E-mail address: sureewan.d@ubu.ac.th.

Peer review under responsibility of Shenyang Pharmaceutical University.
http://dx.doi.org/10.1016/j.ajps.2015.10.039

Multivariate Statistical Approach to Optimize Menthosomes Incorporating l-menthol as Novel Ultradeformable Vesicles for Transdermal Drug Delivery

Sureewan Duangjit[1,2], Yosuke Obata[2], Hiromu Sano[2], Shingo Kikuchi[2], Yoshinori Onuki[2], Theerasak Rojanarata[1], Prasert Opanasopit[1], Kozo Takayama[3], Yoshie Maitani[3], Tanasit Ngawhirunpat[1]
[1]Faculty of Pharmacy, Silpakorn University, Nakhon Pathom, Thailand.
[2]Department of Pharmaceutics, Hoshi University, Tokyo, Japan
[3]*Department of Drug Delivery Research, Hoshi University, Tokyo, Japan*
E-mail address: tanasit@su.ac.th

Abstract The multivariate statistical techniques were utilized for optimizing novel carrier for transdermal drug delivery of meloxicam, a model water-insoluble drug. Menthosomes (MTS), a novel ultradeformable vesicle composed of phosphatidylcholine (PC), cholesterol (Chol), hexadecyl pyridinium chloride (HPC) and l-menthol (MEN) were formulated. A two-factor spherical and second-order composite experimental design was employed to prepare the model of vesicle formulations. The model formulations were optimized using a nonlinear-response surface method incorporating thin-plate spline interpolation (RSM-S). Moreover, the confidence intervals and the reliability of the optimal MTS formulation predicted by RSM-S were estimated using a bootstrap (BS) resampling method and a Kohonen self-organizing map (SOM), respectively. The various amounts of HPC and Chol were selected as formulation factors. The physicochemical characteristics (e.g. vesicle size, charge, elasticity and drug content) and *in vitro* skin permeability (e.g. flux value) were selected as response variables. The response surface results clearly indicated nonlinear relationships between the formulation factors and the response variables. The experimental values of optimal MTS formulation coincided well with the values predicted by the computer programs. The confocal laser scanning microscopy (CLSM) image displayed the vesicle mechanism for delivery meloxicam across the hairless mice skin. The result indicated that the optimal MTS formulation exhibited higher skin permeability than conventional liposomes. Our study suggested the optimal MTS formulation was successfully optimized using RSM-S and had a potential to use as novel carrier incorporating MEN for transdermal drug delivery of meloxicam. These statistical approaches were helpful in formulating an appropriate transdermal delivery system.

Introduction

Since the first publication reported that the effectiveness of surfactant in deformable liposomes can be used for transdermal delivery of drug into deep skin was distributed, the novel deformable vesicles with various penetration enhancers have been developed (e.g. transfersomes, ethosomes, flexosomes and invasomes).[1] These innovative deformable vesicles mainly were composed of phospholipids and penetration enhancer (e.g. surfactant, ethanol, terpenes etc.) in which only a specially designed vesicle was shown to be able to allow through the deep skin region. Hence, several researchers previously used various penetration enhancers to promote skin delivery of drugs. Menthosomes (MTS), novel ultradeformable liposomes consisting of phospholipids, surfactant and l-menthol were also introduced in this study. L-menthol is well-known as a competent permeation enhancer, and has been reported to improve the skin permeation of various drugs by increasing drug partition and diffusion.[2] In the development of a novel transdermal drug delivery carrier, it is important to determine the optimized vesicle formulations having appropriate skin permeation. A nonlinear response-surface method incorporating thin-plate spline interpolation (RSM-S) was performed in our study. Using RSM-S, the complicated relationships between formulation factors and response variables can be easily understood, and a stable and reproducible simultaneous optimal formulation is obtained. A bootstrap (BS) resampling method and a Kohonen self-organizing map (SOM) were used to evaluate the reliability of the optimal formulation estimated by RSM-S. These statistical approaches are helpful in formulating an appropriate transdermal delivery system. In this study, meloxicam (MX), a nonsteroidal anti-inflammatory drug (NSAID) as a preferential COX-1 inhibitor, was used as the model drug.[3] Because oral and injectable administrations of MX are not appropriate for peptic ulcers and patient compliance, MX is suitable for development as a transdermal delivery candidate. Moreover, MX is a potent drug and safe drug for reducing pain and inflammatory symptoms with low toxicity and low skin irritate less than other NSAID drugs.

Materials and Methods

1) *Materials*: Phosphatidylcholine (PC) was purchased from LIPOID GmbH. Cholesterol (Chol) was purchased from Wako Pure Chemical Industries. Meloxicam (MX) was supplied from Fluka. Hexadecyl pyridinium chloride (HPC) and l-Menthol (MEN) was purchased from Tokyo Chemical Industry. All other chemicals used were of reagent grade and purchased from Wako Pure Chemical Industries (Osaka, Japan).

2) Preparation of menthosomes: The MX-loaded MTS composed of MX, PC, MEN, HPC and Chol were prepared. MTS were prepared by the sonication method.[1] Briefly, all compositions were separately dissolved in chloroform/methanol (2:1 v/v). The lipid mixtures were evaporated under nitrogen gas stream. The lipid film was

International Journal of Nanomedicine

Dovepress
open access to scientific and medical research

Open Access Full Text Article

ORIGINAL RESEARCH

Role of the charge, carbon chain length, and content of surfactant on the skin penetration of meloxicam-loaded liposomes

This article was published in the following Dove Press journal:
International Journal of Nanomedicine
29 April 2014
Number of times this article has been viewed

Sureewan Duangjit[1,2]
Boonnada Pamornpathomkul[1]
Praneet Opanasopit[1]
Theerasak Rojanarata[1]
Yasuko Obata[2]
Kozo Takayama[2]
Tanasait Ngawhirunpat[1]

[1]Faculty of Pharmacy, Silpakorn University, Nakhon Pathom, Thailand; [2]Department of Pharmaceutics, Hoshi University, Shinagawa-ku, Tokyo, Japan

Video abstract

Point your SmartPhone at the code above. If you have a QR code reader the video abstract will appear. Or use: http://dvpr.es/1fApH3g

Correspondence: Tanasait Ngawhirunpat
Faculty of Pharmacy, Silpakorn University, Sanamchandra Palace Campus, 6 Ratchamankanai Road, Muang, Nakhon Pathom 73000, Thailand
Tel +66 34 255 800
Email tanasait@su.ac.th

Abstract: The objective of this study was to investigate the influence of surfactant charge, surfactant carbon chain length, and surfactant content on the physicochemical characteristics (ie, vesicle size, zeta potential, elasticity, and entrapment efficiency), morphology, stability, and in vitro skin permeability of meloxicam (MX)-loaded liposome. Moreover, the mechanism for the liposome-enhanced skin permeation of MX was determined by Fourier transform infrared spectroscopy and differential scanning calorimetry. The model formulation used in this study was obtained using a response surface method incorporating multivariate spline interpolation (RSM-S). Liposome formulations with varying surfactant charge (anionic, neutral, and cationic), surfactant carbon chain length (C4, C12, and C16), and surfactant content (10%, 20%, and 29%) were prepared. The formulation comprising 29% cationic surfactant with a C16 chain length was found to be the optimal liposome for the transdermal delivery of MX. The skin permeation flux of the optimal formulation was 2.69-fold higher than that of a conventional liposome formulation. Our study revealed that surfactants affected the physicochemical characteristics, stability, and skin permeability of MX-loaded liposomes. These findings provide important fundamental information for the development of liposomes as transdermal drug delivery systems.

Keywords: optimal liposome, optimization, transdermal drug delivery, surfactant charge, surfactant carbon chain length, surfactant content

Introduction

Meloxicam (MX) is an effective nonsteroidal anti-inflammatory drug for reducing pain and inflammatory symptoms.[1–3] Long-term therapy with high doses of MX can lead to gastrointestinal side effects such as upset stomach, indigestion, ulceration, and bleeding.[4] Moreover, the high content of organic solvent in the MX formulation[5,6] limits its safety for skin delivery. Therefore, the development of MX as a transdermal drug delivery (TDD) candidate presents many challenges.

Since the first report that lipid vesicles incorporating sodium cholate as a surfactant could penetrate deep into intact skin to deliver drugs,[7] the use of surfactants in liposome formulations as penetration enhancers for the TDD of various drugs has attracted considerable interest. Numerous formulations have incorporated various types of surfactants in liposome bilayers. Although the use of cationic surfactants in liposomes has been reported to enhance the skin delivery of several drugs,[8–11] anionic surfactants in liposomes are also effective in improving skin delivery.[12–14] The influence of surfactants on the effectiveness of liposomes for skin delivery remains a much-debated question. Herein, liposome delivery systems must be designed and evaluated on a case-by-case basis because surfactants exhibit a diverse variety of hydrophilic head groups and

lipophilic carbon chain lengths. Thus, comparisons of previous research on liposome formulations composed of various surfactant types are difficult to make. Furthermore, the skin models and conditions used to evaluate the surfactants also vary widely. To date, no proper method for estimating the effects of individual surfactant factor (eg, charge, carbon chain length, and content) on the intrinsic properties of liposomes has yet been established. As a result, a rational approach for designing liposome formulations containing surfactants for skin delivery has not yet been fully described.

In this study, three types of liposome carriers neutral conventional liposomes (N-CLP), anionic transfersomes (A-TFS), and cationic transfersomes (C-TFS) were prepared as skin delivery carriers of MX. The vesicle composition ratio was obtained from a two-factor spherical second-order composite experimental design. The influences of the charge, carbon chain length, and content of surfactant on the physicochemical characteristics (ie, vesicle size, zeta potential, elasticity, and entrapment efficiency [EE]), morphology, in vitro skin permeation, and stability of the liposome formulation were evaluated. The possible mechanisms for the surfactant-enhanced skin permeability of MX-loaded liposomes were also investigated.

Materials and methods

Materials

Phosphatidylcholine (PC) from soybean (90%) was generously supplied by Lipoid GmbH (Ludwigshafen, Germany). Cholesterol (Chol) was purchased from Wako Pure Chemical Industries (Osaka, Japan). Butylpyridinium chloride, laurylpyridinium chloride, and cetylpyridinium chloride (CPC) were purchased from MP Biomedicals (Santa Ana, California, USA). Sodium hexadecyl sulfate (SHS) was purchased from Tokyo Chemical Industry Co., Ltd (Tokyo, Japan). MX was supplied by Sigma-Aldrich Production GmbH, (Buchs, Switzerland). All other chemicals used were of reagent grade and were purchased from Wako Pure Chemical Industries.

Optimization of liposome formulation

The liposome formulation was composed of a constant concentration of PC (10 mM) as the vesicle-forming bilayer, and varying concentrations of Chol and surfactant as a membrane stabilizer and penetration enhancer, respectively. The concentrations of Chol and surfactant varied from 0%–90% molar ratios of PC to determine the optimal Chol and surfactant concentrations in the liposome formulation. Moreover, the MX concentration varied from 0%–20% weight/weight (w/w) of PC to maximize the drug loading in the liposome formulation. The maximum drug-loading capacity and molar turbidity of the liposome formulations were the selection criteria used to determine the optimal vesicle composition of the liposome formulation. Liposomes and transfersomes were prepared according to formulations obtained from a two-factor spherical-order composite experimental design.[15] The optimal formulation was defined as the maximum flux value of MX permeating the skin for 12 hours. The dataNESIA program (v 3.2; Azbil Corporation, Tokyo, Japan) was used to draw the response surfaces for each variable and predict the response variables (skin permeation flux) of the optimal formulations. Once the optimal formulation estimated with response surface method incorporating multivariate spline interpolation (RSM-S) was obtained, its reliability was evaluated using bootstrap resampling, which has been fully described previously.[16,17] The vesicle composition ratio of the optimal formulation was used as the model composition ratio for further formulations.

Preparation of MX-loaded liposomes and MX suspensions

Three types of liposome carriers (N-CLP, A-TFS, and C-TFS) were prepared according to the vesicle composition ratio obtained from our optimization study. The chemical structures of the vesicle compositions are displayed in Figure 1. As shown in Table 1, vesicle formulations were prepared by the sonication method.[18] Briefly, lipid mixtures of PC, Chol, surfactant, and MX were dissolved in chloroform/methanol (2:1 volume/volume [v/v] ratio), and the solvent was evaporated under a nitrogen gas stream. The lipid film was dried in a desiccator for 6 hours to remove the remaining solvent. The dried lipid film was hydrated with acetate buffer solution (pH 5.5). Vesicles were subsequently sonicated for 30 minutes using a bath-type sonicator (5510J-DTH; Branson Ultrasonics, Danbury, CT, USA), then sonicated a second time in an ice bath using a probe sonicator (Vibra-Cell™; Sonics and Materials, Inc., Newtown, CT, USA) for 30 minutes. The excess lipid composition was removed by centrifugation at 4°C and 15,000 rpm for 15 minutes, and the supernatant was collected. All formulations were freshly prepared or stored in air-tight containers at 4°C prior to further studies.

The MX suspension was prepared by adding MX to acetate buffer solution (pH 5.5) at a concentration ten times higher than the solubility of MX and stirring for 48 hours to ensure constant thermodynamic activity throughout the course of the permeation experiment. The concentration of MX in the suspension was determined, and the MX suspension was used as a control in the skin permeation experiment.

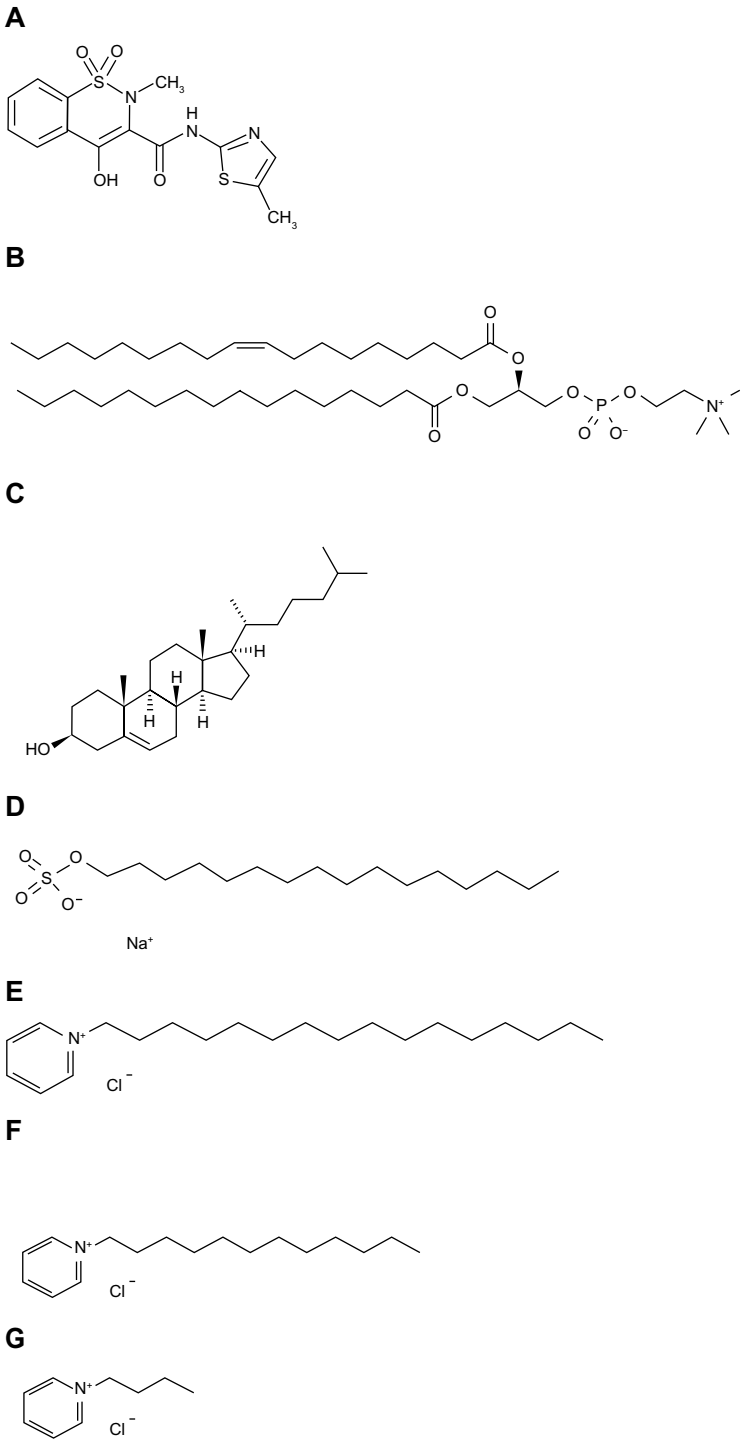

Figure 1 The chemical structures of the vesicle compositions.
Notes: (**A**) Meloxicam; (**B**) phosphatidylcholine; (**C**) cholesterol; (**D**) sodium hexadecyl sulfate; (**E**) cetylpyridinium chloride; (**F**) laurylpyridinium chloride; (**G**) butylpyridinium chloride.

Vesicle size and zeta potential investigation

The average vesicle size (nm) and zeta potential (mV) of the vesicle formulations were measured by photon correlation spectroscopy (PCS) (Zetasizer Nano series; Malvern Instruments, Malvern, UK). Twenty microliters of each vesicle formulation were diluted with 1,480 µL of deionized water. All measurements were performed at room temperature, at least three independent samples were collected, and the vesicle size and zeta potential were measured in triplicate.

Table 1 Liposome and transfersome formulation

Surfactant factor	Code	Lipid component (%w/v)							Acetate buffer (mL)
		MX	PC	Chol	C4	C12	C16	A16	
Charge	N-CLP	0.07	0.77	0.04	–	–	–	–	100
	C-TFS	0.07	0.77	0.04	–	–	0.10	–	100
	A-TFS	0.07	0.77	0.04	–	–	–	0.10	100
Carbon chain length	C4	0.07	0.77	0.04	0.05	–	–	–	100
	C12	0.07	0.77	0.04	–	0.08	–	–	100
	C16	0.07	0.77	0.04	–	–	0.10	–	100
Content	0% CPC	0.07	0.77	0.04	–	–	–	–	100
	10% CPC	0.07	0.77	0.04	–	–	0.04	–	100
	20% CPC	0.07	0.77	0.04	–	–	0.07	–	100
	29% CPC	0.07	0.77	0.04	–	–	0.10	–	100

Note: The concentration of PC in the formulation was fixed at 10 mM. C4, cationic surfactant with 4 carbons; C12, cationic surfactant with 12 carbons; C16, cationic surfactant with 16 carbons; A16, anionic surfactant with 16 carbons.

Abbreviations: A-TFS, anionic transfersomes; Chol, cholesterol; CPC, cetylpyridinium chloride; C-TFS, cationic transfersomes; MX, meloxicam; N-CLP, neutral conventional liposome; PC, phosphatidylcholine.

The morphology of the liposomes was characterized using freeze-fractured transmission electron microscopy. A drop of sample solution placed on a small copper block was rapidly frozen in nitrogen slush, which was freshly prepared immediately prior to use by decompression in a vacuum chamber.[19] The quenched sample was fractured in a freeze-fracture apparatus (JFD-9010; JEOL, Tokyo, Japan). The fractured surface was rotary-shadowed with platinum-carbon at an angle of 10°, and the shadowed surface was coated with carbon. The freeze-fractured replica obtained was washed with chloroform/methanol (4:1 v/v ratio) and observed with a JEM-1400 transmission electron microscope (JEOL) equipped with a digital charge-coupled device camera (ES500W Erlangshen; Gatan, Inc., Pleasanton, CA, USA).

Elasticity evaluation

The elasticity value of the lipid bilayer of the vesicles was directly proportional to $J_{Flux} \times (r_v/r_p)^2$:

$$\text{Elasticity value } (\text{mg} \cdot \text{sec}^{-1} \cdot \text{cm}^{-2}) = J_{Flux} \times \left(\frac{r_v}{r_p}\right)^2, \quad (1)$$

where J_{Flux} is the rate of penetration through a permeable barrier ($\text{mg} \cdot \text{sec}^{-1} \cdot \text{cm}^{-2}$); r_v is the size of the vesicles after extrusion (nm); and r_p is the pore size of the barrier (nm).[20] To measure J_{Flux}, the vesicles were extruded through a polycarbonate membrane (Nuclepore; GE Healthcare Life Sciences, Buckinghamshire, UK) with a pore diameter of 50 nm (r_p) at a pressure of 0.5 MPa. Five minutes after extrusion, the extrudate was weighed (J_{Flux}) and the average vesicle diameter (r_v) was measured by PCS.

Drug EE (%EE)

The excess lipid composition was removed from the MX-loaded liposome formulation by centrifugation. The concentration of MX in the formulation was determined by high-performance liquid chromatography (HPLC) analysis after disruption of the vesicles with Triton® X-100 (Amresco; Solon, Ohio, USA) (0.1% w/v) at a 1:1 volume ratio and diluted with phosphate-buffered saline (pH 7.4). The vesicle/Triton® X-100 solution was centrifuged at 10,000 rpm at 4°C for 10 minutes. The supernatant was filtered with a 0.45 µm nylon syringe filter. The EEs of the MX loaded in the formulations were calculated according to the following equation:

$$\%EE = \left(\frac{C_L}{C_i}\right) \times 100, \quad (2)$$

where C_L is the concentration of MX loaded in the formulation, as described above, and C_i is the initial concentration of MX added to the formulation.

In vitro skin permeation studies

The shed skin of *Naja kaouthia* was used as a permeation model membrane because a previous study reported that it exhibits similar permeability to human skin.[21] It was donated by the Queen Saovabha Memorial Institute, Thai Red Cross Society, Bangkok, Thailand. Whole snake skins were obtained immediately after shedding from five to seven different snakes. Each snake skin was divided into 10–12 pieces. The thickness of the shed snake skins was approximately 0.02–0.03 mm. They were stored at −10°C

prior to use. After thawing, the skin was cut and then immediately placed on a side-by-side diffusion cell with an available diffusion area of 0.95 cm^2. The shed snake skin was mounted between the diffusion cells connected with a 32°C ±1°C control temperature jacket. The stratum corneum (SC) side of the skin faced the donor chamber, which was filled with 3 mL of MX-loaded vesicle formulation and/or MX suspension. The receiving chamber was also filled with 3 mL of 0.1 M phosphate-buffered solution (pH 7.4) and stirred with a star-head magnetic stir bar driven by a synchronous motor. The sink condition in the receiving medium was determined in this study. At appropriate intervals of 2, 4, 6, 8, 10, and 12 hours, 0.5 mL aliquots of the receiving medium were withdrawn and immediately replaced with an equal volume of fresh buffer solution. The concentration of drug in the receiving medium was analyzed by HPLC, and the cumulative amount (μg/cm^2) was plotted against time. The steady-state flux value was determined as the slope of the linear portion of the plot.

Stability evaluation

The MX-loaded vesicle formulations were prepared (at least 400 samples) and kept in the glass bottles at 4°C for 200 bottles and 25°C for 200 bottles. The physicochemical stability of the MX-loaded vesicle formulations, such as vesicle size and zeta potential, were evaluated by PCS. The MX remaining in the formulation was determined by HPLC at days 1, 7, 15, 30, and 120. The results of the physicochemical characterization immediately after preparation (at day 1) were used as a control, and the MX entrapped in the formulation at day 1 was also normalized to 100%.

HPLC analysis

The MX concentration was analyzed by HPLC. All samples were stored at 4°C until analysis. The HPLC system comprised a SIL-20A autosampler, an LC-20AT liquid chromatograph, and an SPD-20AUV detector (Shimadzu Corporation, Kyoto, Japan). The analytical column was a YMC-Pack ODS-A (150×4.6 mm inner diameter, S-5; YMC Co., Ltd, Kyoto, Japan), and the mobile phase was composed of acetate buffer solution (pH 4.6)/methanol (50:50, v/v). The flow rate was set at 0.8 mL/minute, and the wavelength used was 272 nm. The calibration curve for MX was in the range of 1–50 μg/mL with a correlation coefficient of 0.999. The percent recovery ranged from 99.85%–100.30%, and the relative standard deviations for both the intraday and inter-day measurements were less than 2%.

The mechanisms of liposomes on skin permeation

Following the skin permeation experiment, the shed snake skin was washed with water, blotted dry, and stored in a desiccator. The spectrum of the skin sample was recorded in the range of 500–4,000 cm^{-1} using Fourier transform infrared spectroscopy (FTIR) (Nicolet 4700 spectrophotometer; Thermo Fisher Scientific, Waltham, MA, USA). The FTIR spectra of the skin treated with the MX suspension was also recorded and used as a control. Thermal analysis of the shed snake skin following the permeation experiment, prepared using the same method used for the FTIR analysis, was performed with differential scanning calorimetry ([DSC] Pyris Sapphire DSC; PerkinElmer, Waltham, MA, USA). The skin sample (2 mg) was weighed into an aluminum seal pan and was heated from 0°C to 300°C at a heating rate of 10°C/minute. All DSC measurements were collected under a nitrogen atmosphere with a flow rate of 30 mL/minute. The DSC thermograms of the skin treated with the MX suspension was also recorded and used as a control.

The existence of intact vesicles in the release medium after the in vitro skin permeation study was characterized by PCS. Moreover, the release medium following the in vitro skin permeation study was also characterized for PC using a Phosphatidylcholine Assay Kit (Cat No.83377; Abcam®, Cambridge, UK), and the compositions of the intact liposomes or non-intact vesicles in the release medium were determined.

Data analysis

The data are reported as the means ± standard error (n=3–6), and statistical analysis of the data was carried out using one-way analysis of variance followed by the Student's *t*-test. A *P*-value of less than 0.05 was considered to be statistically significant.

Results and discussion

Optimal liposome formulation

Based on its maximum drug-loading capacity and molar turbidity, the vesicle formulation composed of over 40% Chol and surfactant likely reassembled to a mixed micelle structure. Liposomes and mixed micelle structures display different intrinsic characteristics, resulting in significantly different influences on skin delivery. A concentration of 10% MX was determined to be the maximum loading capacity in the vesicle formulation. Thus, it was concluded that 0–40%mol Chol and surfactant and 10%mol MX-loaded vesicle formulations were desirable for further optimization to develop model vesicle

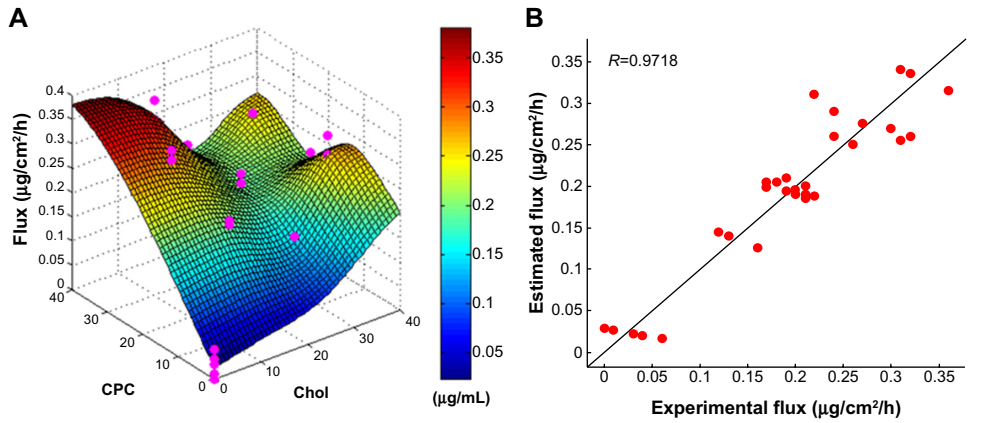

Figure 2 The response surface for the skin permeation flux (**A**) and the reliability (**B**) of the model formulation.
Abbreviations: Chol, cholesterol; CPC, cetylpyridinium chloride; h, hour.

formulations. The 12 model formulations obtained from the two-factor spherical second-order composite experimental design were formulated and evaluated based on the original data set using RSM-S. A response surface and its reliability for the flux variable of the model formulation are illustrated in Figure 2. The search direction for the response variables was set to produce a high flux value. Moreover, to confirm the accuracy and reliability of the optimal formulation estimated using RSM-S, the optimal formulation was confirmed by experiment. It was found that the skin permeation flux value predicted by the RSM-S (predicted flux =0.31 μg/cm²/hour) was very close to the experimental value (0.31±0.6 μg/cm²/hour). This high reliability suggested that the vesicle composition ratio of the optimal formulation (PC/Chol/surfactant/MX 0.77%:0.04%:0.10%:0.07% w/v ratio) could be used as the model formulation ratio in further experiments. Moreover, the morphology of the three-dimensional optimal model formulation was further observed using freeze-fractured transmission electron microscopy to determine the details of the vesicular morphology. Nano-sized, smooth surfaces and spherical vesicles were observed, as depicted in Figure 3.

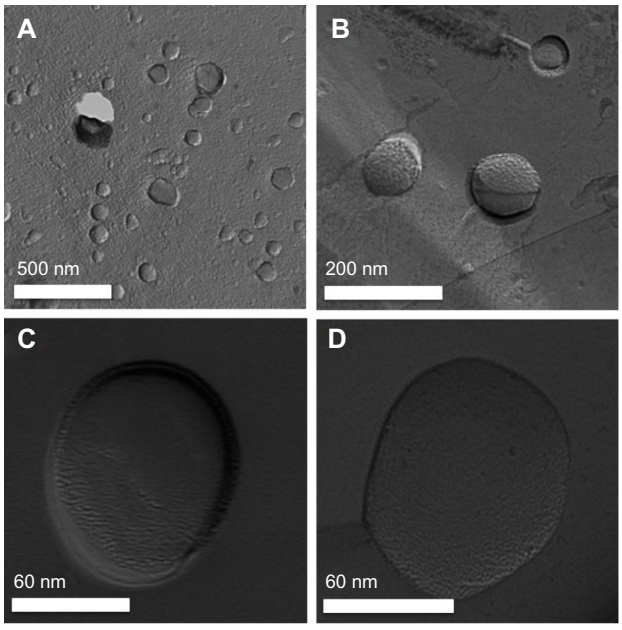

Figure 3 Freeze-fractured transmission electron microscopy images of the optimized meloxicam-loaded vesicle formulation.
Notes: (**A**) 5,000×; (**B**) 30,000×; (**C**) 100,000×; (**D**) 100,000×.

Effect of surfactant charge

The physicochemical characteristics of the A-TFS, N-CLP, and C-TFS outlined in Table 2 reveal that the addition of anionic surfactant, ie, SHS in A-TFS, and cationic surfactant, ie, CPC in C-TFS, produced significant differences in vesicle size (nm), zeta potential (mV), elasticity ($mg \cdot sec^{-1} \cdot cm^{-2}$) and EE (%) compared with N-CLP. A-TFS displayed a large vesicle size (~164 nm) with a negative charge (~−60.8 mV). In contrast, C-TFS exhibited a small vesicle size (~90 nm) with a positive charge (~+48.3 mV). Moreover, the elasticity and EE of both types of transfersome (A-TFS and C-TFS) were higher than that of N-CLP. The neutralization of the anionic drug (MX) and cationic vesicles (C-TFS) may have resulted in smaller vesicle sizes due to a reduction in the repulsive forces in the C-TFS bilayer. In contrast, the synergistic effects of the anionic drug (MX) and anionic vesicles (A-TFS) may have resulted in large vesicle sizes due to the induction of repulsive forces in the A-TFS bilayer.[13] The vesicle formulations were composed of neutral material, ie, Chol, and positively and negatively charged surfactants, ie, CPC and SHS, respectively. Under the experimental condition of pH 5.5, the isoelectric point (PI) of PC (PI =6) was higher than the pH. However, the PI of MX (PI =2.6) was lower than the pH. Therefore, PC and MX displayed a net positive charge and a net negative charge, respectively. Thus,

Table 2 Effect of the surfactant on vesicle size, zeta potential, elasticity and entrapment efficiency of the vesicle formulation (mean ± standard error)

	Vesicle size (nm)	Zeta potential (mV)	Elasticity ($mg \cdot sec^{-1} \cdot cm^{-2}$)	Entrapment efficiency (%)
Effect of surfactant charge				
A-TFS	164.3±3.2	−60.8±0.51	19.2±1.68	54.11±0.33
N-CLP	108.8±10.6	1.3±1.01	11.6±1.64	26.36±0.26
C-TFS	90.6±9.2	48.3±0.67	88.7±0.98	68.06±0.84
Effect of surfactant carbon chain length				
C4	113.3±3.5	10.9±3.21	120.1±2.87	9.92±0.41
C12	94.5±2.0	26.9±2.63	108.7±1.74	46.11±0.29
C16	90.6±9.2	48.3±0.67	88.7±0.98	68.06±0.84
Effect of surfactant content				
0% CPC	108.8±10.6	1.3±1.01	11.6±1.64	26.36±0.26
10% CPC	78.8±9.2	36.6±1.37	23.6±2.40	29.51±0.98
20% CPC	81.6±1.0	39.7±3.98	52.6±1.32	47.25±0.67
29% CPC	90.6±9.2	48.3±0.67	88.7±0.98	68.06±0.84

Abbreviations: A-TFS, anionic transfersomes; CPC, cetylpyridinium chloride; C-TFS, cationic transfersomes; N-CLP, neutral conventional liposomes.

the net charges of A-TFS, N-CLP, and C-TFS were negative, neutral, and positive, respectively, as a result of the intrinsic properties of their surfactants and the total net charge of the liposome composition. SHS and CPC exhibit a high radius of curvature, which can destabilize and increase the deformability of the vesicle bilayer, thus increasing its fluidity or elasticity.[22] The carbon chain lengths of CPC and SHS were the same, but C-TFS exhibited a stronger interaction with the bilayer than SHS due to its significantly higher elasticity. This result suggests that the hydrophilic head group of the surfactant directly affects the elasticity of the vesicle bilayer. The beneficial roles of SHS and CPC within transfersomes were readily apparent, as the intrinsic properties of the surfactants led to the increased solubility of MX in the vesicle bilayer and therefore EE values for A-TFS and C-TFS that were significantly higher than that of N-CLP. Our results were consistent with a previous study that demonstrated that the EE of a drug in phosphatidylethanolamine vesicles is significantly increased when sodium stearate (anionic surfactant) is incorporated into the vesicles.[23]

Effect of surfactant carbon chain length

The physicochemical characteristics of MX-loaded vesicle formulations containing short-chain (butylpyridinium chloride [C4]), medium-chain (laurylpyridinium chloride [C12]) and long-chain (cetylpyridinium chloride [C16]) carbons are shown in Table 2. The vesicle size and elasticity decreased slightly with increasing carbon chain length in the order of C4, C12, and C16. The vesicle size and elasticity decreased approximately 20% and 26%, respectively, as C4 was substituted by C16. Surfactants with longer carbon chains may increase vesicle rigidity by inserting deeper into the bilayer; thus, increasing the carbon chain length led to decreased vesicle size. Meanwhile, the vesicle size and zeta potential of liposomes containing 1,2-dimyristoyl-sn-glycero-3-phosphocholine ([DMPC] C14), 1,2-dipalmitoyl-sn-glycero-3-phosphocholine (C16), and 1,2-disteroyl-sn-glycero-3-phosphocholine ([DSPC] C18) and loaded with midazolam or propofol were not significantly influenced by the lipids having the same head group.[24] The insertion of C8 (short-chain carbon) resulted in decreased vesicle sizes in the order of poly(asparagines) grafted with C8, C12, C18, and C22.[25] These results suggest that varying trends in vesicle size may be influenced by the hydrophilic head group of the surfactant and the method of preparation. The zeta potential increased significantly with increasing carbon chain length in the order of C4, C12, and C16, with an increase of approximately 77% when C4 was substituted with C16. These results could be due to the intrinsic properties of each surfactant. The hydrophobicity of long-chain carbons is greater than that of short-chain carbons, and long-chain carbons could have led to increased solubility of the surfactant molecule in the PC bilayer. The amount of long-chain carbons in the PC bilayer was greater than the amount of short-chain carbons, and long-chain carbons might therefore exhibit stronger electrostatic interactions and zeta potentials than short-chain carbons. The elasticity of the vesicle increased in the order of C16, C12, and C4. These results are consistent with the findings of Park et al, in which the elasticity was observed to increase with decreasing carbon chain length (increased in the order of C22, C18, C12, and C8).[25] Because long-chain carbons exhibit strong hydrophobic interactions with PC, the PC bilayer of the vesicles becomes tighter. Long-chain carbons decrease the

elasticity of the vesicle through their deep insertion into the PC bilayer. Furthermore, short-chain carbons increase the elasticity of the vesicle through their shallow insertion into the PC bilayer. Therefore, the EE significantly increased with increasing carbon chain length in the order of C4, C12, and C16, with an ~85% increase when C4 was substituted with C16. These results are consistent with Ali et al, who demonstrated that an increase in carbon chain length led to an increase in the encapsulation of hydrophobic drugs, such as propofol and midazolam, into vesicles.[24] Increasing the carbon chain length was also found to increase the encapsulation of water-insoluble drugs, such as ibuprofen, into vesicles in the order of DMPC (C14); DSPC (C18); and dilignoceroyl PC (C24).[10] The increase in the EE values of long-chain carbons could be attributed to the increased hydrophobic area within the PC bilayer.[10,26]

Effect of surfactant content

The physicochemical characteristics of MX-loaded vesicles composed of varying contents of surfactant, including the control (0% CPC) and low (10% CPC), medium (20% CPC), and high (29% CPC) surfactant contents, are shown in Table 2. The vesicle size and zeta potential tended to increase slightly, while the elasticity and EE significantly increased in the order of 10% CPC, 20% CPC, and 29% CPC. The vesicle size, zeta potential, elasticity, and EE increased by approximately 13%, 23%, 73%, and 56%, respectively, when 10% CPC was substituted with 29% CPC. The trends in increasing vesicle size, zeta potential, elasticity, and EE were recognized as intrinsic properties of the surfactant. Liu et al demonstrated that an increase in the biosurfactant produced by some *Bacillus subtilis* strains from 0.05–0.24 mg/mL resulted in a decrease in the vesicle size of soy PC liposomes.[27] However, Mohammed et al demonstrated that an increase in stearylamine (cationic surfactant) from 1–6 μM resulted in an increase in the vesicle size of egg PC liposome.[10] The insertion of surfactant into the vesicle bilayer can increase its curvature and result in decreased vesicle size.[25] However, the net effect on vesicle size in the present study was influenced by other factors. In addition to the method of preparation, the drug loading in the vesicle bilayer may result in increased vesicle size, as confirmed by the study of Mohammed et al.[10]

In vitro skin permeation

Figure 4 shows the graphic plot of the cumulative skin permeation per unit area and the steady-state flux of various MX-loaded vesicle formulations over an incubation period

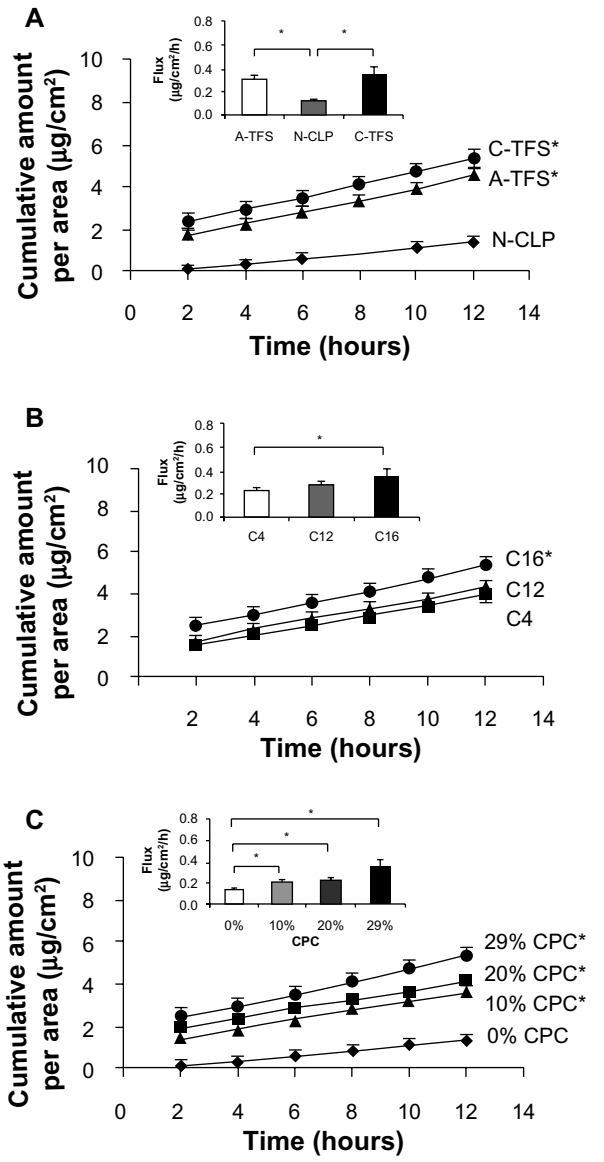

Figure 4 The influence of (**A**) surfactant charge, (**B**) surfactant carbon chain length, and (**C**) surfactant content on the skin permeation profile and the steady-state flux of the vesicle formulation (n=3). *is statistical significance (*P*-value <0.05).
Abbreviations: A-TFS, anionic transfersomes; CPC, cetylpyridinium chloride; C-TFS, cationic transfersomes; h, hour; N-CLP, neutral conventional liposomes.

of 2–12 hours. The skin permeabilities (skin permeation profile and steady-state flux) of A-TFS and C-TFS were not significantly different, while the skin permeabilities of the charged transfersomes were significantly greater than those of the non-charged liposomes (N-CLP). The steady state flux of A-TFS and C-TFS were significantly higher than N-CLP, at approximately 58% and 63%, respectively. The surfactants SHS and CPC in A-TFS and C-TFS can open the dense keratin structures in corneocytes, and both anionic and cationic surfactants swell the SC and interact with the intercellular keratin, thus increasing the skin permeation of various drugs (eg, hydrocortisone, lidocaine).[28] Surfactants can interact with

skin constituents in many ways. For example, surfactants are widely known to interact with proteins, and thus can inactivate enzymes and bind strongly within the SC. They can swell the SC (most likely by uncoiling the keratin fiber and altering the α-helices to a β-sheet conformation) and are able to modify the binding of water to the SC. Anionic surfactant-treated SC is somewhat brittle, possibly due to the extraction of natural moisturizing factor. Cationic surfactants are also able to extract lipids from the SC and can disrupt the lipid bilayer packing within the tissue.[29] Clearly, cationic surfactants cause a greater increase in the steady-state flux of MX than anionic surfactants, which, in turn, cause a greater increase in the flux than N-CLP. Ashton et al[30] compared the effects of dodecyltrimethylammonium bromide (as cationic surfactant), sodium lauryl sulfate (as anionic surfactant), and dodecoxyethanol (Brij 36T) (as non-ionic surfactant) on the in vitro flux of methylnicotinamide across excised human skin and reported that permeation enhancement occurred in the following order: cationic, anionic, neutral. However, Brij 36T was shown to exert a small effect on the permeability but a more immediate effect on skin permeation.[28] This result revealed that the anionic and/or cationic surfactants significantly affected the skin permeation of MX across the skin by swelling the SC and interacting with intercellular keratin. However, the crossing of transfersomes across the skin was attributed to the high deformability of these specialized vesicles due to the accumulation of these single-chain surfactants at sites of high stress as a result of their increased propensity to form high-curvature structures. This rearrangement was claimed to reduce the energy required for deformation; the stress was reportedly produced upon drying of the vesicles, which, being flexible, were able to follow the transdermal hydration gradient.[7]

In our study, the skin permeability of the transfersomes increased when the carbon chain length of the surfactant increased. The skin permeability of the vesicle formulation increased with increasing chain length in the order C4, C12, and C16. The skin permeability of C16 was significantly greater than C4, with an approximately 17% increase when C4 was substituted with C16. These results are consistent with a previous study,[31] which demonstrated that, as the carbon chain length in the vesicle increased from C7 to C12, the permeation of naloxone increased. Ogiso and Shintani revealed that C12–C14 were the most effective carbon chain lengths used in increasing the permeation of propranolol.[32] Duangjit et al reported that C18–C24 were more effective than C32 in the permeation of MX.[18] Short-chain carbons may suffer from insufficient lipophilicity for skin permeation, whereas longer-chain fatty acids might have much higher affinities for lipids in the SC, thereby hindering their permeation. Our study suggests that C16 possesses an optimal balance between partition coefficient and affinity to the skin. The results revealed that skin permeability is also affected by the carbon chain length of the surfactant.

The surfactant content affected skin permeability, with the skin permeability of the transfersomes increasing with increasing surfactant content. The skin permeability of the vesicle formulation increased in the order 0% CPC, 10% CPC, 20% CPC, and 29% CPC. The skin permeabilities of the 29% CPC, 20% CPC, and 10% CPC formulations were significantly higher than that of 0% CPC, by approximately 63%, 41%, and 35%, respectively. This result reveals that the surfactant content significantly affected the skin permeability of the vesicle formulation due to the intrinsic properties of the surfactant (CPC), as reported above.

The present studies demonstrated that the surfactant factor (ie, charge, carbon chain length, and content of surfactant) directly affected the skin permeability of MX.

Stability evaluation

The physicochemical stabilities of MX-loaded vesicle formulations from day 1 to day 120 at 4°C and 25°C were evaluated for recommended storage conditions. After storage at 4°C for 30 days, the MX content had slightly decreased but remained at 90% of the initial formulation. After storage at 25°C for 30 days, the MX remaining in nearly all of the formulations had decreased slightly but remained at 90% and 80% of the initial formulation at day 15 and day 30, respectively. However, after storage at 4°C and 25°C for 120 days, the MX remaining in nearly all of the formulations had decreased by approximately 70%–80% and 80%–90% from the initial formulation, respectively (Figure 5). The physicochemical stabilities (ie, vesicle size and zeta potential) of the vesicle formulations were not significantly different between the experimental temperatures of 4°C and 25°C over a period of 30 days. The physicochemical stabilities of nearly all of the vesicle formulations exhibited similar trends to the MX-remaining results, indicating the good physicochemical stability of our vesicle formulations at 4°C for 30 days as well as at 25°C for 15 days. In our study, the addition of Chol was essential to the vesicle formulation, which can be attributed to Chol's stabilizing effects.[33,34] The physicochemical stability of the vesicle formulation was not significantly different between the experimental temperatures of 4°C and 25°C over 30 days, while the physicochemical stability of the vesicle formulation at the two experimental temperatures (ie, 4°C and 25°C) was significantly different between day 1 and

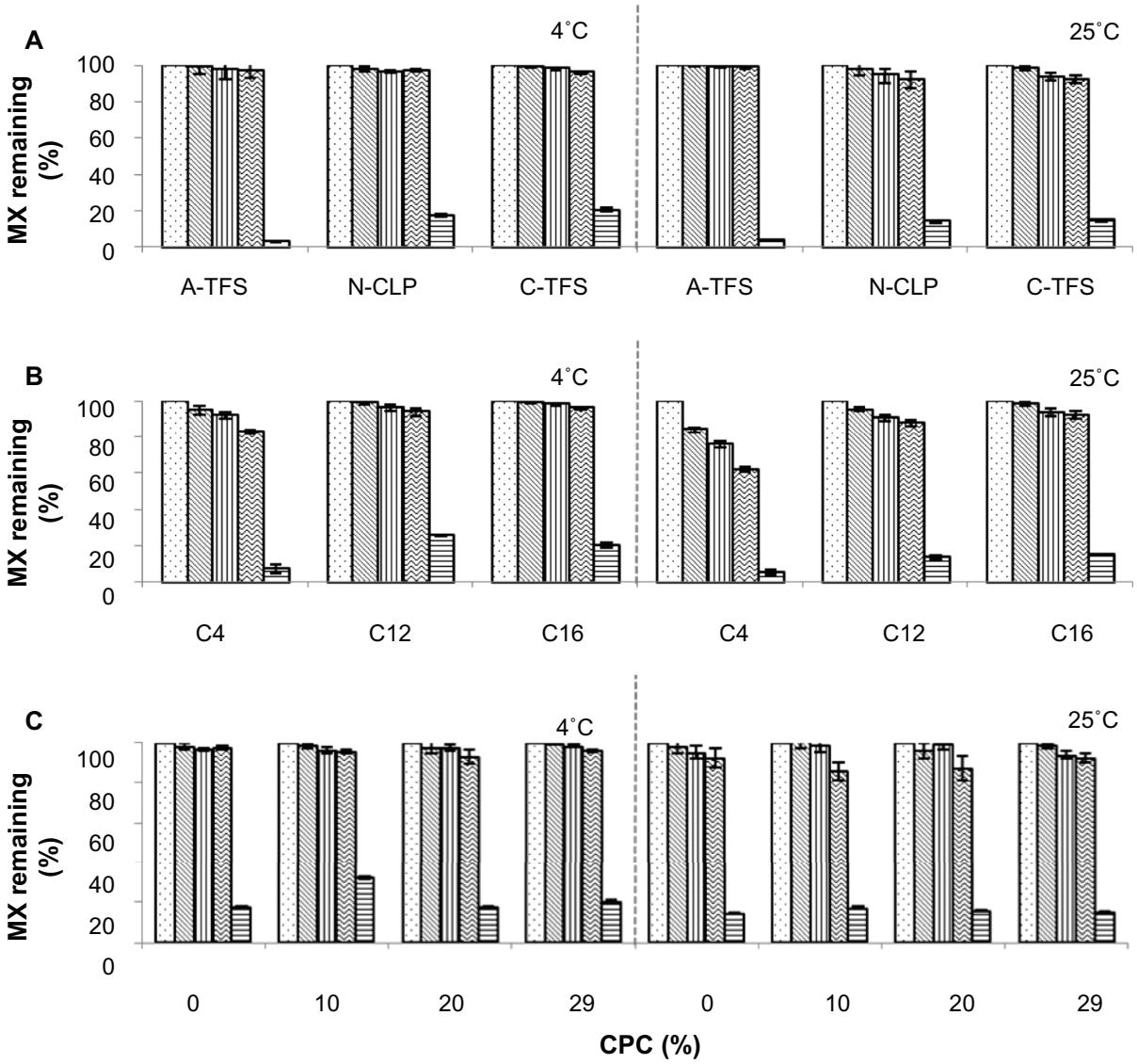

Figure 5 The influence of (**A**) surfactant charge, (**B**) surfactant carbon chain length, and (**C**) surfactant content on the remaining MX at different days (n=3).
Notes: Day 1; day 7; day 15; day 30; day 120.
Abbreviations: A-TFS, anionic transfersomes; C-TFS, cationic transfersomes; MX, meloxicam; N-CLP, neutral conventional liposomes; CPC, cetylpyridinium chloride.

day 120 of storage. Therefore, the storage duration was the primary factor affecting the physicochemical stability of the vesicle formulation in this study. The recommended storage conditions for the vesicle formulation are therefore 4°C for 30 days and/or 25°C for 15 days.

The mechanisms of liposomes on skin permeation

Changes in the ultra-structures of the intercellular lipids occurred following the treatment of skin with the vesicle formulation, as shown in the FTIR spectra and DSC thermograms (Figure 6). The FTIR peaks from the absorption-broadened C–H (CH_2) symmetric and asymmetric stretches are near 2,850 cm^{-1} and 2,920 cm^{-1}, respectively. These peaks in the FTIR spectra of the skin treated with the vesicle formulation shifted from 2,850 cm^{-1} to 2,850.7–2851.3 cm^{-1} and from 2,920 cm^{-1} to 2,920.3–2,920.9 cm^{-1}, respectively. Meanwhile, the DSC thermograms also displayed peak shifts, from 231.72°C for the skin sample treated with the MX suspension (control) to a lower transition temperature for the skin sample treated with the vesicle formulations. The SC lipid of the skin sample existed in the liquid state. The shifted peak of the skin samples were in range of 229.18 °C–230.53°C, depending on vesicle formulation. These results are consistent with previous studies,[35–38] which demonstrated that liposome vesicles do not penetrate into the SC but rather that the lipid components of the vesicles can penetrate and change the enthalpy of the SC lipid-related

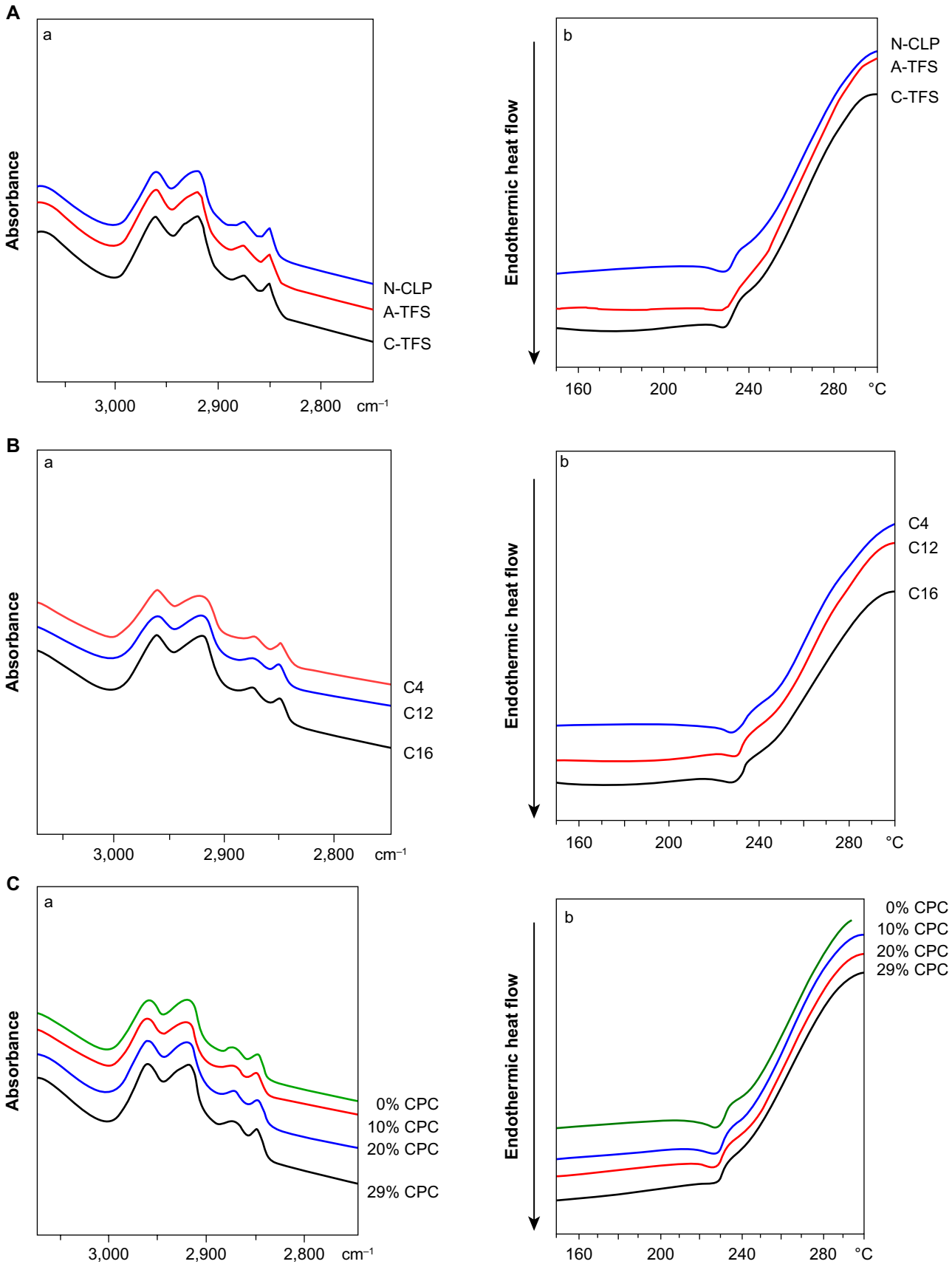

Figure 6 The influence of (**A**) surfactant charge, (**B**) surfactant carbon chain length, and (**C**) surfactant content of the shed snake skin after skin permeation.
Notes: (**a**) Fourier transform infrared spectra; (**b**) differential scanning calorimetry thermograms.
Abbreviations: A-TFS, anionic transfersomes; CPC, cetylpyridinium chloride; C-TFS, cationic transfersomes; N-CLP, neutral conventional liposomes.

transitions of the skin. The present study suggested that the SC lipid arrangement of the skin sample treated with the vesicle formulation was disrupted by altering the fluidity or flexibility of the SC lipids. The interruption of the SC lipids by vesicle formulation or by the vesicle components caused an increase in the skin permeability of MX; the FTIR spectra and DSC thermograms also support the conclusions of this in vitro skin permeation study.

The vesicles may adsorb to the SC surface with subsequent transfer of the drug directly from the vesicles to the skin, or the vesicles may fuse and mix with the SC lipid matrix, increasing drug partitioning into the skin. Our results indicate that the vesicles can be taken into the skin but cannot penetrate through the intact, healthy SC; instead, they dissolve and form a unit membrane structure with the skin sample, as evidenced by the alteration and rearrangement of the lipid structures of the skin sample treated with the vesicles, as revealed by FTIR and DSC characterization (Figure 6).

Conclusion

In this study, surfactant charge, surfactant carbon chain length, and surfactant content directly affected the physicochemical characteristics of vesicles and their skin permeability. The incorporation of a high content (29%) of cationic surfactant (CPC) with a long-chain carbon (C16) into the vesicle formulation improved the skin permeability of MX. The optimal formulation comprised PC/Chol/CPC/MX in a 0.77%:0.04%:0.10%:0.07% w/v ratio and is recommended as the optimal liposome for the skin delivery of MX. The possible mechanisms by which these liposomes improved the skin delivery of MX encompassed the penetration-enhancing mechanism and the vesicle adsorption to and/or fusion with the SC. Our findings provide useful fundamental information for the development and design of novel liposome formulations for enhancing the TDD of lipophilic drugs.

Acknowledgments

The authors are grateful to the Thailand Research Funds through the Royal Golden Jubilee PhD Program (grant number PHD/0141/2552), and the Basic Research Grant (grant number BRG 5680016), Faculty of Pharmacy, Silpakorn University, Thailand and Department of Pharmaceutics, Hoshi University, Japan for facilities and support. The authors gratefully acknowledge Professor Yoshie Maitani and Dr Kumi Kawano of the Department of Drug Delivery Research, Hoshi University for their helpful assistance with determination of liposome elasticity, and also Professor Satoru Kato and Tsubasa Miyoshi for their helpful assistance of liposomes characterization using freeze-fractured transmission electron microscopy at the Department of Physics, Kwansei Gakuin University, Hyogo, Japan. Finally, the authors would like to acknowledge Assistant Professor Dr Warisada Sila-on of the Faculty of Pharmaceutical Sciences, Ubon Ratchathani University, Ubon Ratchathani, Thailand for facilities and support.

Disclosure

The authors report no conflicts of interest in this work.

References

1. Engelhardt G, Homma D, Schlegel K, Utzmann R, Schnitzer C. Anti-inflammatory, analgesic, antipyretic and related properties of meloxicam, a new non-steroidal anti-inflammatory agent with favourable gastrointestinal tolerance. *Inflamm Res*. 1995;44:423–433.
2. Luger P, Daneck K, Engel W, Trummlitz G, Wagner K. Structure and physicochemical properties of meloxicam, a new NSAID. *Eur J Pharm Sci*. 1996;4:175–187.
3. Degner F, Sigmund R, Zeidler H. Efficacy and tolerability of meloxicam in an observational, controlled cohort study in patients with rheumatic disease. *Clin Ther*. 2000;22:400–410.
4. Bjarnason I, Hayllar J, MacPherson AJ, Russell AS. Side effects of nonsteroidal anti-inflammatory drugs on the small and large intestine in humans. *Gastroenterology*. 1993;104(6):1832–1847.
5. Yuan Y, Li SM, Mo FK, Zhong DF. Investigation of microemulsion system for transdermal delivery of meloxicam. *Int J Pharm*. 2006;321:117–123.
6. Jantharaprapap R, Stagni G. Effects of penetration enhancers on in vitro permeability of meloxicam gels. *Int J Pharm*. 2007;343:26–33.
7. Cevc G, Schätzlein A, Blume G. Transdermal drug carriers: basic properties, optimization and transfer efficiency in the case of epicutaneously applied peptides. *J Control Release*. 1995;36:3–16.
8. Montenegro L, Panico AM, Ventimiglia A, Bonina FP. In vitro retinoic acid release and skin permeation from different liposome formulations. *Int J Pharm*. 1996;133:89–96.
9. Katahira N, Murakami T, Kugai S, Yata N, Takano M. Enhancement of topical delivery of a lipophilic drug from charged multilamellar liposomes. *J Drug Target*. 1999;6:405–414.
10. Mohammed AR, Weston N, Coombes AG, Fitzgerald M, Perrie Y. Liposome formulation of poorly water soluble drugs: optimisation of drug loading and ESEM analysis of stability. *Int J Pharm*. 2004;285:23–34.
11. Song YK, Kim CK. Topical delivery of low-molecular-weight heparin with surface-charged flexible liposomes. *Biomaterials*. 2006;27(2):271–280.
12. Sinico C, Manconi M, Peppi M, Lai F, Valenti D, Fadda AM. Liposomes as carriers for dermal delivery of tretinoin: in vitro evaluation of drug permeation and vesicle-skin interaction. *J Control Release*. 2005;103:123–136.
13. Manosroi A, Khanrin P, Lohcharoenkal W, et al. Transdermal absorption enhancement through rat skin of gallidermin loaded in niosomes. *Int J Pharm*. 2010;392:304–310.
14. Gillet A, Compère P, Lecomte F, et al. Liposome surface charge influence on skin penetration behaviour. *Int J Pharm*. 2011;411:223–231.
15. Takayama K, Nagai T. Simultaneous optimization for several characteristics concerning percutaneous absorption and skin damage of ketoprofen hydrogels containing d-limonene. *Int J Pharm*. 1991;74(2–3):115–126.
16. Ueda N, Nakano R. Estimating expected error rates of neural network classifiers in small sample size situations: a comparison of cross-validation and bootstrap. IEEE International Conference Neural Networks Proceeding; 27 Nov 1995–01 Dec 1995, 1995; Perth, WA.
17. Dupret G, Koda M. Bootstrap resampling for unbalanced data in supervised learning. *Eur J Oper Res*. 2001;134:141–156.

18. Duangjit S, Opanasopit P, Rojanarata T, Ngawhirunpat T. Characterization and in vitro skin permeation of meloxicam-loaded liposomes versus transfersomes. *J Drug Deliv*. 2011;2011:418316.
19. Shotton DM, Servers NJ. An introduction to freeze fracture and deep etching. In: Servers NJ, Shotton DM, editors. Rapid freezing, freeze fracture, and deep etching. New York: Wiley-Liss; 1995:1–31.
20. Cevc G. Material Transport Across Permeability Barriers by Means of Lipid Vesicles. In: Lipowsky R, Sackmann E, editors. Handbook of Biological Physics. Amsterdam: Elsevier; 1995:465–490.
21. Ngawhirunpat T, Panomsuk S, Opanasopit P, Rojanarata T, Hatanaka T. Comparison of the percutaneous absorption of hydrophilic and lipophilic compounds in shed snake skin and human skin. *Pharmazie*. 2006;61:331–336.
22. Elsayed MM, Abdallah OY, Naggar VF, Khalafallah NM. Lipid vesicles for skin delivery of drugs: reviewing three decades of research. *Int J Pharm*. 2007;332:1–16.
23. Fang YP, Tsai YH, Wu PC, Huang YB. Comparison of 5-aminolevulinic acid-encapsulated liposome versus ethosome for skin delivery for photodynamic therapy. *Int J Pharm*. 2008(356):144–152.
24. Ali MH, Moghaddam B, Kirby DJ, Mohammed AR, Perrie Y. The role of lipid geometry in designing liposomes for the solubilisation of poorly water soluble drugs. *Int J Pharm*. 2013;453(1):225–232.
25. Park SI, Lee EO, Kim JW, Kim YJ, Han SH, Kim JD. Polymer-hybridized liposomes anchored with alkyl grafted poly(asparagine). *J Colloid Interface Sci*. 2011;364:31–38.
26. Dan N. Lipid tail chain asymmetry and the strength of membrane-induced interactions between membrane proteins. *Biochim Biophys Acta*. 2007;1768:2393–2399.
27. Liu J, Zou A, Mu B. Surfactin effect on the physicochemical property of PC liposome. *Colloids Surf A Physicochem Eng Asp*. 2010;361:90–95.
28. Barry BW. Penetration enhancer classification. In: Smith, Maibach HI, editors. *Percutaneous Penetration Enhancers*. 2nd ed. Boca Raton, FL: CRC Press; 2006:3–15.
29. Williams AC. *Transdermal and Topical Drug Delivery: From Theory to Clinical Practice*. London: Pharmaceutical Press; 2003.
30. Ashton P, Walters KA, Brain KR, Hadgraft J. Surfactant effects in percutaneous absorption. I. Effects on the transdermal flux of methyl nicotinate. *Int J Pharm*. 1992;87:261.
31. Aungst BJ, Rogers NJ, Shefter E. Enhancement of naloxone penetration through human skin in vitro using fatty acids, fatty alcohols, surfactants, sulfoxides and amides. *Int J Pharm*. 1986;33:225–234.
32. Ogiso T, Shintani M. Mechanism for the enhancement effect of fatty acids on the percutaneous absorption of propranolol. *J Pharm Sci*. 1990;79:1065.
33. Liu D, Chen W, Tsai L, Yang S. Microcalorimetric and shear studies on the effects of cholesterol on the physical stability of lipid vesicles. *Colloids Surf A Physicochem Eng Asp*. 2000;172:57–67.
34. Nasseri B. Effect of cholesterol and temperature on the elastic properties of niosomal membranes. *Int J Pharm*. 2005;300:95–101.
35. Kato A, Ishibashi Y, Miyake Y. Effect of egg yolk lecithin on transdermal delivery of bunazosin hydrochloride. *J Pharm Pharmacol*. 1987;39:399–400.
36. Zellmer S, Pfeil W, Lasch J. Interaction of phosphatidylcholine liposomes with the human stratum corneum. *Biochim Biophys Acta*. 1995;1237:176–182.
37. Kirjavainen M, Urtti A, Jääskeläinen I, et al. Interaction of liposomes with human skin in vitro – the influence of lipid composition and structure. *Biochim Biophys Acta*. 1996;1304:179–189.
38. Obata Y, Utsumi S, Watanabe H, et al. Infrared spectroscopic study of lipid interation in stratum corneum treated with transdermal absorption enhancers. *Int J Pharm*. 2010;389:18–23.

International Journal of Nanomedicine

Dovepress
open access to scientific and medical research

Open Access Full Text Article

ORIGINAL RESEARCH

Investigation of the mechanism of enhanced skin penetration by ultradeformable liposomes

Thirapit Subongkot
Boonnada Pamornpathomkul
Theerasak Rojanarata
Praneet Opanasopit
Tanasait Ngawhirunpat

Faculty of Pharmacy, Silpakorn University, Nakhon Pathom, Thailand

Abstract: This study aimed to determine the mechanism by which ultradeformable liposomes (ULs) with terpenes enhance skin penetration for transdermal drug delivery of fluorescein sodium, using transmission electron microscopy (TEM) and confocal laser scanning microscopy (CLSM). Skin treated with ULs containing d-limonene, obtained from in vitro skin penetration studies, was examined via TEM to investigate the effect of ULs on ultrastructural changes of the skin, and to evaluate the mechanism by which ULs enhance skin penetration. The receiver medium collected was analyzed by TEM and CLSM to evaluate the mechanism of the drug carrier system. Our findings revealed that ULs could enhance penetration by denaturing intracellular keratin, degrading corneodesmosomes, and disrupting the intercellular lipid arrangement in the stratum corneum. As inferred from the presence of intact vesicles in the receiver medium, ULs are also able to act as a drug carrier system. CLSM images showed that intact vesicles of ULs might penetrate the skin via a transappendageal pathway, potentially a major route of skin penetration.

Keywords: ultradeformable liposomes, mechanism of enhanced skin penetration, transmission electron microscopy, confocal laser scanning microscopy

Introduction

A transdermal drug delivery system utilizes skin to deliver drug into the circulation system. The main obstacle in this system is poor percutaneous absorption, because the uppermost layer of the skin (the stratum corneum) acts as a barrier. To improve percutaneous absorption of drug, many techniques have been applied, such as iontophoresis,[1] sonophoresis,[2] microneedles,[3] and lipid vesicle carriers.[4,5] Among the group of lipid vesicle carriers, ultradeformable liposomes (ULs) have received considerable attention in transdermal drug delivery research. Introduced by Cevc and Blume,[6] ULs are a type of elastic liposome, created by incorporating edge activators into liposomes. ULs have been shown to be effective for transdermal delivery of macromolecules, which are difficult to permeate through the skin.[7–11]

Two possible mechanisms proposed for the enhancement of skin penetration by ULs are a penetration-enhancing effect and a drug carrier system. The first mechanism suggests that ULs increase drug penetration into the skin by acting as a penetration enhancer.[12,13] The second mechanism proposes that ULs act as a drug carrier system.[6,14–18] To investigate the penetration-enhancing effect, various techniques have been used, such as infrared spectroscopy, differential scanning calorimetry, and skin penetration study. Although these techniques proved to be convenient and simple, they could not reveal the ultrastructural changes in skin caused by penetration enhancers. To assess the drug carrier system mechanism, drug-loaded vesicles must be able to pass through the skin into systemic circulation as intact vesicles. Cevc et al[15] reported the presence of drug-loaded vesicles in the blood of mice after fluorescently-labeled

Correspondence: Tanasait Ngawhirunpat
Department of Pharmaceutical Technology, Faculty of Pharmacy, Silpakorn University, 6 Racchamakkanai Road, Muang, Nakhon Pathom 73000, Thailand
Tel +66 34 255 800
Fax +66 34 255 801
Email tanasait@su.ac.th

submit your manuscript | www.dovepress.com
Dovepress
http://dx.doi.org/10.2147/IJN.S65287

transfersomes were applied to the skin. This finding was evidence that ULs penetrated the skin and entered the systemic circulation as intact vesicles. Regarding in vivo and in vitro experiments of human skin treated with elastic vesicles, Honeywell-Nguyen et al[16] suggested that penetration of intact vesicles into viable epidermis is unlikely to happen, because little vesicle material was found in the deepest layers of stratum corneum.

Understanding the mechanism of action of vesicle–skin interaction is a prerequisite for transdermal drug delivery development and optimization. However, the mechanism of action of vesicle–skin interaction has not been clearly investigated. Therefore, we performed an in vitro skin penetration study, using porcine skin treated with ULs to evaluate the penetration enhancement mechanism, focusing on changes in the ultrastructure of skin affected by vesicle interaction. A UL with d-limonene was selected as a candidate to examine both proposed mechanisms.[19,20] Transmission electron microscopy (TEM) was used to visualize changes in cellular components caused by UL interaction, inside both stratum corneum and viable tissues, in order to assess the penetration-enhancing mechanism. TEM and confocal laser scanning microscopy (CLSM) were also used to investigate vesicle penetration and drug entrapment in tissue cross-sections and in receiver medium. Vesicles were probed with 1,2-dihexadecanoyl-sn-glycero-3-phosphoethanolamine triethylammonium salt (Rh-PE) and fluorescein sodium (NaFl) – which fluoresce red and green, respectively – to determine the penetration of ULs into tissue and receiver medium.

Materials and methods

Materials

Non-hydrogenated egg phosphatidylcholine (PC), Coatsome® NC-50, (with ≥95% purity) was obtained from NOF Corp (Tokyo, Japan). NaFl and d-limonene were purchased from Sigma-Aldrich Corp (St Louis, MO, USA). Tween® 20 was obtained from Ajax Finechem Pty Ltd (Auckland, New Zealand). Lissamine™ rhodamine B (Rh-PE) and 4′,6-diamino-2-phenylindole dihydrochloride (DAPI) were purchased from Thermo Fisher Scientific (Waltham, MA, USA). Cholesterol (Chol) was obtained from Carlo Erba Reagents (Cornaredo, Italy). All other reagents were of analytical grade.

Preparation of liposomes

The UL formulation (consisting of PC, d-limonene, Chol, Tween 20, and NaFl) was prepared using a sonication method, as described in our previous study.[20] Briefly, PC and Chol were dissolved in a mixture of methanol and chloroform (1:2, by volume). The mixture of PC and Chol was dried, using nitrogen stream, until a thin, homogeneous film was created. The thin film obtained in a test tube was then stored for 6 hours in a desiccator connected to a vacuum pump. Afterwards, the dried thin lipid film was hydrated with phosphate buffered saline (PBS) and NaFl solution. Then, the hydrated lipid film was dispersed, using a sonicator bath, for 30 minutes. Tween 20 and d-limonene were added to the dispersion before sonication with a probe sonicator, for size reduction of the liposomes.

Size and shape of the liposomes

Particle size and surface charge

Distilled water was used to dilute the ULs. Then, the particle size, size distribution, and zeta potential were measured using a photon correlation spectroscopy particle size analyzer (Zetasizer Nano ZS, Malvern Instruments Ltd, Malvern, UK) with a 4 mW helium–neon laser at a scattering angle of 173 degrees. All measurements were performed under ambient conditions, in triplicate.

Transmission electron microscopy

The ULs were observed using TEM for particle size and shape assessment. The sample was diluted with distilled water, then placed in sonicator bath for 10 minutes. The sample was then dropped onto a formvar-coated copper grid. The excess liposome sample on the copper grid was gently removed using filter paper. Afterwards, the sample was observed using an 80 kV microscope (JEM 1230, JEOL Ltd, Tokyo, Japan).

In vitro skin penetration study for TEM investigation

Skin preparation

Abdominal porcine skin (obtained from intrapartum stillbirth animals provided by a farm in Nakhon Pathom) was used as a barrier membrane in this study. Subcutaneous fat was removed using surgical blades and scissors. The thickness of the abdominal skin was about 0.6–0.7 mm. The prepared porcine skin was then stored in a refrigerator at –20°C until use. Prior to the experiments, the skin was thawed using PBS at room temperature.

Skin penetration study

The skin penetration study was conducted using a 2.31 cm^2 penetration area of Franz diffusion cells, connected

to a circulating water bath. The temperature of the water bath was maintained at 32°C. The porcine skin was mounted between the donor and receptor compartments of the diffusion chamber, with the stratum corneum facing the donor compartment. PBS was used as the receiver medium, filling the receiver compartment with 6.5 mL. The receiver medium was stirred with a magnetic bar at a rate of 500 rpm. Two milliliters of ULs were placed into the donor compartment. The experiment was performed under occlusive conditions. At predetermined times of 30 minutes, 1 hour, 2 hours, and 4 hours, 0.5 mL of receiver medium was withdrawn for vesicle visualization, and the same volume of PBS was added to the receiver compartment, to maintain a constant volume. At the end of the skin penetration experiment, the skin samples were taken from the diffusion cells and washed with PBS. The skin samples were stored at −20°C prior to TEM investigation.

Skin preparation for TEM

The treated skin samples were investigated for ultrastructural changes using TEM visualization. Intact skin was used as a control. The skin samples were cut into small pieces and fixed overnight (at 4°C) with 2.5% glutaraldehyde (by volume), and 1% osmium tetroxide (weight to volume) in 0.1 M PBS for 2 hours. After fixation, the samples were dehydrated in a range of ethanol solutions (35%, 50%, 70%, 95%, and 100%) and infiltrated with Spurr's resin. The resin-embedded samples were incubated at 70°C for 8 hours. Ultrathin sections were cut using an ultramicrotome (2088 Ultrotome V; LKB-Produkter AB, Bromma, Sweden) using a diamond knife (Ultra 45°, Diatome AG, Biel, Switzerland), collected on copper grids, and intensified with uranium acetate and lead citrate. The samples were visualized using TEM (JEM 1230). Ultrathick sections were cut by an ultramicrotome, stained with toluidine blue, and observed by light microscope.

Receiver medium visualization by TEM

The receiver medium was visualized to assess the penetration of vesicles through the skin – as intact or disintegrated vesicles. The receiver medium was filtered through a nylon membrane (0.45 µm pore size) to remove contaminants. The filtrate was placed in a sonicator bath for 10 minutes before being dropped onto a formvar-coated copper grid. After drying, the sample was visualized under the microscope (JEM 1230) at 100 K magnification. Microscopy was performed at 80 kV.

Confocal laser scanning microscopy study

Liposome preparation

The fluorescent probe, Rh-PE, was dissolved in a mixture of methanol and chloroform (1:2, by volume) before being added to a test tube containing a mixture of PC and Chol. The ratio of PC to Rh-PE was 100:1 M. The mixture of Rh-PE, PC, and Chol was then prepared for thin film formation, according to the process described above.

Separation of non-entrapped NaFl from ULs

A filtration technique using Amicon® Ultra-0.5 centrifugal devices (Millipore Corporation, Billerica, MA, USA) was utilized to separate non-entrapped drug from UL-labeled Rh-PE. The UL-labeled Rh-PE (0.5 mL) was added into an ultrafiltration tube, with a cut-off molecular weight of 3,000 Da, and then the mixture was centrifuged at 14,000× *g*, at 4°C, for 30 minutes. The filtrate was removed, and then the retentate tube was inverted in a new collection tube, to collect the entrapped NaFl-loaded, UL-labeled Rh-PE via centrifugation at 1,000× *g*, at 4°C, for 2 minutes. The entrapped NaFl-loaded, UL-labeled Rh-PE obtained was immediately used in the skin penetration experiments.

Skin penetration study

The skin penetration of NaFl-loaded, UL-labeled Rh-PE was studied using the method described above. The donor compartment was filled with 150 µL of the entrapped NaFl-loaded, UL-labeled Rh-PE. The receiver medium and the treated skin samples were collected for analysis.

Skin histology preparation

The cross-sectional tissue samples of skin treated with NaFl-loaded, UL-labeled Rh-PE were prepared using a cryomicrotome (CM1850, Leica Microsystems GmbH, Wetzlar, Germany). Each treated skin sample was embedded in cryosection embedding medium (Neg 50™, Microm International GmbH, Waldorf, Germany) onto a metal sample holder inside a cryomicrotome, at −30°C. The embedded skin was sectioned into 10 µm slices by microtome blades (High-profile Disposable Blade 818, Leica Microsystems GmbH, Wetzlar, Germany) before being placed onto adhesion slides (SuperFrost® Plus, Menzel-Gläser, Braunschweig, Germany). These sectioned tissues were stained with 3 µM DAPI for 2 minutes (to stain the living cell layer of the skin), washed with PBS, mounted with mounting medium, and covered with a cover slip.

Receiver medium preparation

The receiver medium was filtered through a nylon membrane (0.45 µm pore size) to remove any contaminants. The filtrate was dropped onto a glass slide and dried at room temperature. After drying, the sample was mounted with mounting medium and covered with a cover slip, prior to investigation with CLSM.

CLSM imaging

CLSM, using a colocalization technique, was employed to analyze the presence of NaFl-loaded, UL-labeled Rh-PE in the receiver medium, to elucidate the skin penetration route of ULs in tissue cross-sections. Different fluorescence colors of compounds among rhodamine-probed liposomes (red), NaFl as entrapped drug (green), and from living cells (blue) were applied to visualize the vesicle and drug distribution in the treated skin sample. The 10× objective lens of an inverted Zeiss LSM 510 Meta confocal microscope (Carl Zeiss Microscopy GmbH, Jena, Germany) equipped with a helium–neon laser (excitation wavelength: 543 nm) for Rh-PE, an argon laser (excitation wavelength: 488 nm) for NaFl, and a diode laser (excitation wavelength: 358 nm) for DAPI was used for receiver medium and cross-sectional tissue visualization. To investigate the possible skin penetration pathways of ULs, the mean fluorescence intensities from follicular and nonfollicular regions were compared. The fluorescence intensities obtained from the middle vertical line of each image were calculated using Zeiss LSM 5 operating software.

Data analysis and statistics

Statistical significance of differences was examined using the Student's *t*-test. The significance level was set at $P<0.05$.

Results and discussion

Size and shape of ULs

The size, shape, and surface charge of ULs were measured using a particle size analyzer. The average size of ULs was 37.23±0.2 nm, with a narrow size distribution (polydispersity index: 0.22). The zeta potential was negative (−10.6±0.65 mV). The zeta potential of liposomes composed of PC and Chol only was −3.78±0.11 mV (data not shown). NaFI is an anionic compound. PC is a zwitterionic compound, with an isoelectric point (pl) between 6–6.7.[21] The pH in our experimental conditions (pH: 7.4) was higher than the pI. Therefore, the PC vesicles had negative charge; therefore, NaFI-loaded ULs exhibited a negative charge. A TEM image of the ULs (Figure 1) shows that UL vesicles were nanospheres. The average size of ULs, as determined by TEM, was 34.08±2.96 nm. The average size of ULs obtained from dynamic light scattering and TEM techniques was not significantly different. A small UL particle size is desired for vesicle penetration of skin.[22]

Mechanism of enhanced skin penetration

TEM study of treated skin

The prepared skin samples were observed via TEM, to evaluate the mechanism of enhanced penetration by ULs. The ultrathick sections of intact skin and skin treated with ULs, observed via light microscopy, are shown in Figure 2. Figure 2A shows intact skin; Figures 2B and 2C show regions of follicular and nonfollicular skin, respectively, treated with ULs, at 4 hours. The stratum corneum of intact skin (Figure 2A) was normal. In the treated skin, it was detached (Figures 2B and 2C).

Figure 3 shows TEM images of intact skin. Figures 3A and 3B show an overview of the stratum corneum and stratum granulosum in the epidermis. In Figure 3C, intercellular lipid lamellae were observed in the intercellular space as electron lucent bands. Corneocytes were visualized by their characteristic flattened shape, absence of organelles, and presence of electron-dense keratin filaments. Moreover, corneodesmosomes were observed, connecting corneocytes between layers of the stratum corneum. Figure 3D shows corneodesmosomes connecting cornified cells in the stratum corneum to one another, as well as to keratinocyte cells in the stratum granulosum.

Figure 4 shows TEM images of ultrathick sections of porcine skin treated with ULs (from Figure 2B).

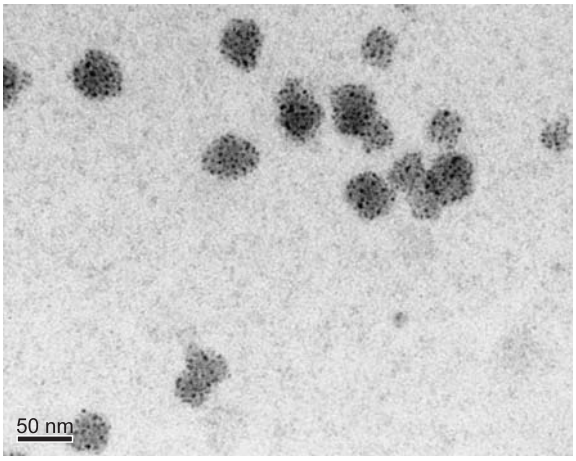

Figure 1 Transmission electron microscopy images of ultradeformable liposomes.
Notes: Magnification: 200 K. Scale bar represents 50 nm.

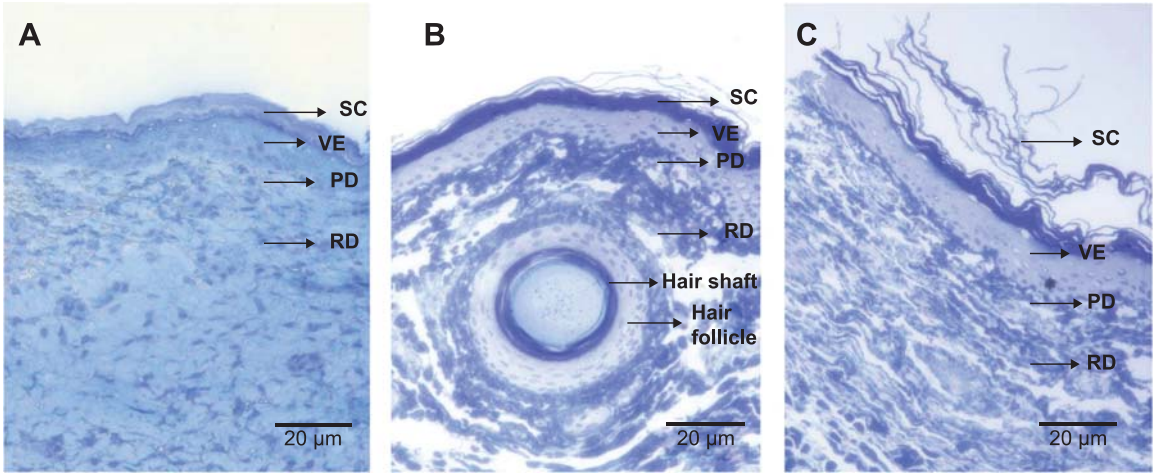

Figure 2 Ultrathick sections observed by light microscopy.
Notes: (**A**) Intact pig skin, (**B**) and (**C**) pig skin treated with ultradeformable liposomes at 4 hours, from follicular and nonfollicular regions, respectively. Each scale bar represents 20 μm.
Abbreviations: SC, stratum corneum; VE, viable epidermis; PD, papillary dermis; RD, reticular dermis.

Figures 4A and 4B show the upper and lower stratum corneum, respectively, at the same magnification. The upper stratum corneum (Figure 4A) had broader-shaped corneocytes than in the lower stratum corneum (Figure 4B). Figure 4C shows that porcine skin treated with ULs had obviously less electron-dense keratin filaments, compared against intact skin (Figure 3C). The broad shape and the fewer electron-dense keratin filaments of the corneocytes in

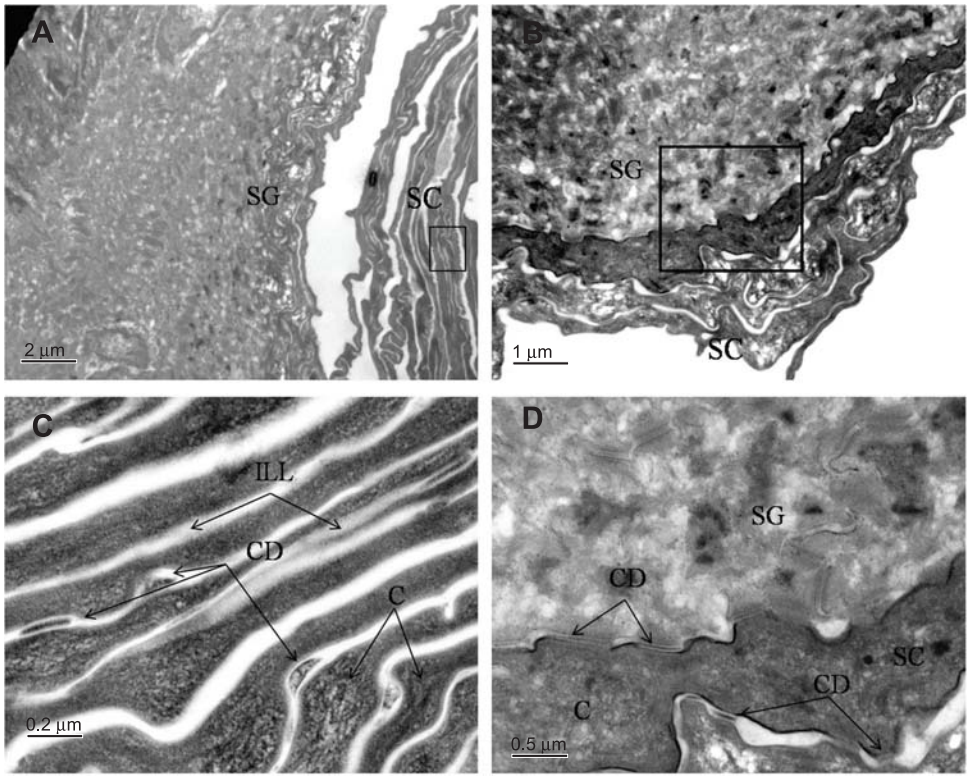

Figure 3 Transmission electron microscopy images of intact pig skin.
Notes: (**A**) Overview of SC and SG; scale bar represents 2 μm. (**B**) Overview of SC and SG; scale bar represents 1 μm. (**C**) Magnification of marked area in (**A**); scale bar represents 0.2 μm. (**D**) Magnification of marked area in (**B**); scale bar represents 0.5 μm.
Abbreviations: SC, stratum corneum; SG, stratum granulosum; C, corneocyte; ILL, intercellular lipid lamellae; CD, corneodesmosome.

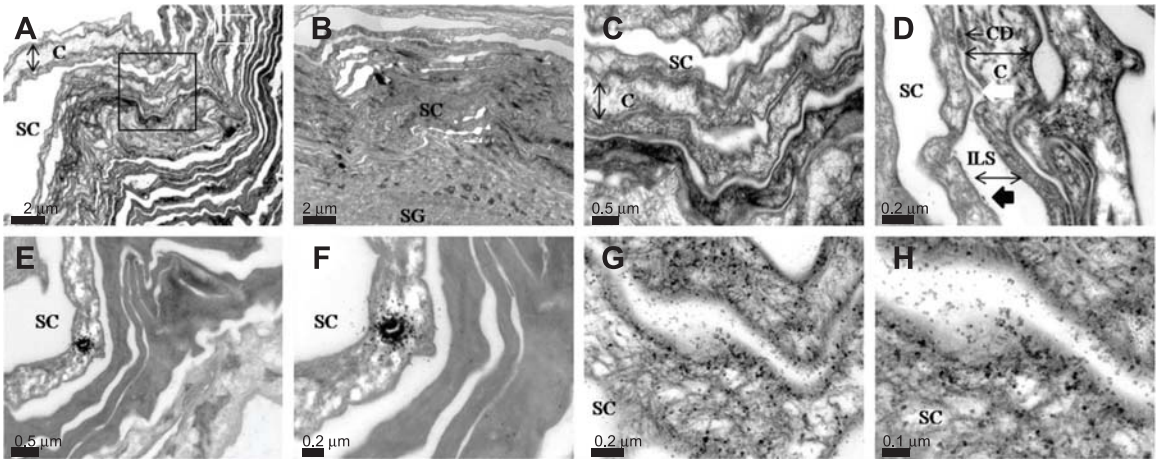

Figure 4 Transmission electron microscopy images of pig skin treated with ultradeformable liposomes obtained from ultrathick section of pig skin treated with ultradeformable liposomes at 4 hours.
Notes: (**A**) Corneocytes in SC; scale bar represents 2 μm. (**B**) SC and SG; scale bar represents 2 μm. (**C**) Magnification of area in (**A**) marked with black rectangle; scale bar represents 0.5 μm. (**D**) Magnification of area in (**A**) marked with white rectangle; black arrow indicates degraded corneodesmosome; white arrow indicates degrading corneodesmosome in SC; scale bar represents 0.2 μm. (**E**) Vesicle penetration into corneocyte; scale bar represents 0.5 μm. (**F**) Magnification of (**E**); scale bar represents 0.2 μm. (**G**) Vesicle fragmentation in SC; scale bar represents 0.2 μm. (**H**) Magnification of (**G**); scale bar represents 0.1 μm.
Abbreviations: SC, stratum corneum; SG, stratum granulosum; C, corneocyte; CD, corneodesmosome; ILS, intercellular space.

the stratum corneum resulted from denaturation of keratin inside the corneocytes. At the same magnification, the intercellular spaces of porcine skin treated with ULs (Figure 4D) were wider than those of intact skin (Figure 3C), because the corneodesmosomes that connected the corneocytes between each stratum corneum layer were degraded. As a result of the degradation of corneodesmosomes, the stratum corneum layers of treated skin were detached, as seen in ultrathick sections (Figures 2B and 2C). Since the hydration effect of PBS resulted in corneocyte swelling and intercellular lipid lamellae disruption,[23,24] the detachment of the stratum corneum layers in Figures 2B and 2C might result from both liposome-induced corneodesmosome degradation and the hydration effect. Some corneodesmosomes are present in the upper part of Figure 4D, whereas the lower part shows degrading (white arrow) and degraded (black arrow) corneodesmosomes. These images indicate that the degradation of corneodesmosomes depends on the rate at which ULs penetrate the skin.

Figure 4E shows a UL particle and denatured keratin inside a corneocyte. When observed at higher magnification (Figure 4F), it was obvious that the particle was disintegrating into smaller pieces. Figures 4G and 4H show many disintegrated particles inside corneocytes and in the intercellular space of the stratum corneum. Keratin inside corneocytes was denatured, and no corneodesmosomes were observed. Figures 4E and 4F reveal that when particles penetrated the corneocyte, they gradually disintegrated into smaller pieces of phospholipid bilayer, denatured keratin, and disrupted corneodesmosomes – thereby enhancing the penetration of entrapped drugs. Figures 4G and 4H also show particle fragmentation to be mostly confined to the inner cellular membrane and intercellular lipid of corneocytes. Because the inside of corneocytes contains keratin, while inner and outer cellular membranes of corneocytes are lipid and protein, respectively, most of the lipid vesicles were confined to the inner cellular envelope and extracellular lipid matrix.

Figure 5 shows TEM images of ultrathick sections of porcine skin treated with ULs (from Figure 2C). Figures 5A and 5B show the degraded corneodesmosomes at the interface of the stratum corneum and stratum granulosum (black arrow). In Figure 5B, disintegrated particles were observed near the desmosomes. In viable epidermis (Figure 5C), desmosomes and hemidesmosomes, which connect stratum basale and papillary dermis (Figure 5D), were normal. From Figures 5A through 5D, it is apparent that only corneodesmosomes were degraded, whereas the desmosomes in viable epidermis and hemidesmosomes in the epidermis–dermis interface were normal. Desmosomes are intercellular junctions that maintain tissue integrity of the epidermis. The main components of desmosomes are cadherins, armadillo proteins, and plakins. Corneodesmosomes are cellular junctions, derived from desmosomes, that provide strong intercorneocyte cohesion within the stratum corneum. The extracellular proteins of corneodesmosomes, which mediate corneocyte cohesion, are desmoglein 1, desmocollin 1, and corneodesmosin – a secreted glycoprotein that is incorporated into desmosomes prior to their conversion to corneodesmosomes in the

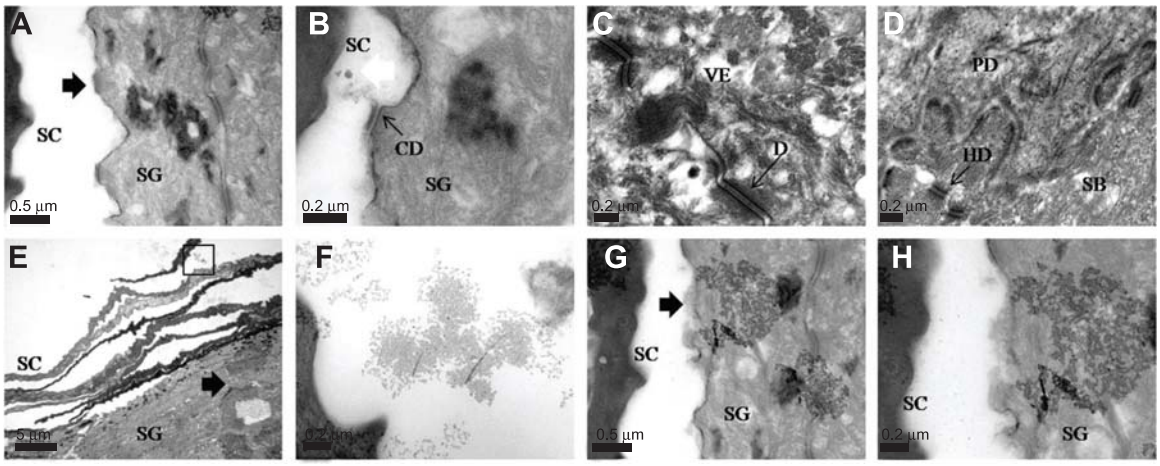

Figure 5 Transmission electron microscopy images of pig skin treated with ultradeformable liposomes, obtained from ultrathick section of pig skin treated with ultradeformable liposomes at 4 hours.

Notes: (**A**) Corneodesmosome degradation (black arrow) between SC and SG; scale bar represents 0.5 μm. (**B**) Corneodesmosome degradation (black arrow) and disintegrated particle (white arrow) between SC and SG; scale bar represents 0.2 μm. (**C**) Desmosome in viable epidermis; scale bar represents 0.2 μm. (**D**) Hemidesmosome at stratum basale and papillary dermis; scale bar represents 0.2 μm. (**E**) Ultradeformable liposome penetration into the skin (black arrow); scale bar represents 5 μm. (**F**) Magnification of marked area in (**E**); scale bar represents 0.2 μm. (**G**) Disrupted cell membrane (black arrow) from penetration of intact vesicles into SG; scale bar represents 0.5 μm. (**H**) Magnification of (**G**); scale bar represents 0.2 μm.

Abbreviations: SC, stratum corneum; SG, stratum granulosum; SB, stratum basale; PD, papillary dermis; D, desmosome; CD, corneodesmosome; HD, hemidesmosome; VE, viable epidermis.

stratum corneum.[25,26] We suggest that corneodesmosomes are degraded by their interaction with UL vesicles. Other desmosomes and hemidesmosomes are unaffected, which may be due to the difference in desmosomal protein structures between the stratum corneum and viable epidermis, as mentioned above.

Figure 5E shows the penetration of ULs through the stratum corneum into viable epidermis. The area of penetration shows obvious detachment of the stratum corneum, which resulted from corneodesmosome degradation. In the upper portion of the penetrated area, intact vesicles were observed, as shown in Figure 5F. Several upper stratum corneum layers were loosened, due to a desquamation process. As a result, intact vesicles were found in the intercellular region.

The presence of intact vesicles in the stratum granulosum (Figures 5G and 5H) indicates that ULs can penetrate viable epidermis as intact vesicles. The uppermost keratinocyte membrane in the stratum granulosum was disrupted by the penetration of ULs (Figures 5G and 5H). The presence of intact vesicles found in viable epidermis may be caused by the denaturing of keratin inside corneocytes and the degradation of corneodesmosomes by interactions with UL vesicles.

From our TEM images (Figures 4 and 5), it is apparent that ULs increase drug penetration by acting as a penetration enhancer and drug carrier system. The ULs enhanced skin penetration by entering corneocytes before disintegrating into small fragments and interacting with the protein and lipid barrier structure of the stratum corneum. The vesicles denatured keratin filaments inside corneocytes and degraded corneodesmosomes, resulting in vesicle and drug penetration into viable epidermis and dermis. Intracellular proteins and protein structures may become denatured as a result of their interactions with the surfactants in vesicles (Tween 20 and phospholipid).[27,28] d-limonene is a monoterpene skin penetration enhancer, incorporated in ULs, that could break interlamellar hydrogen bonding within the lipid bilayer. This interaction leads to widening of the aqueous region near polar head groups, and results in increased diffusion of polar molecules.[29] Our findings also support the lipid protein partitioning theory, which proposes that penetration enhancers act by disrupting intercellular lipid organization, modifying intracellular proteins, resulting in increased drug penetration into viable epidermis.[30]

A distinct difference between follicular and nonfollicular regions of skin interacting with vesicles was that there were more vesicle fragments found in the stratum corneum of the follicular region, as shown in Figures 4G and 4H. The presence of more vesicle fragments in the follicular region, as observed by TEM, confirmed our previous suggestion that the follicular pathway was the main permeation pathway of ULs.[21]

Receiver medium observation and CLSM study

The collected receiver medium was investigated using TEM and CLSM, to determine the mechanism of the drug carrier system.

TEM was used to investigate the receiver medium from TEM visualization, at time points of 30 minutes, 1 hour, 2 hours, and 4 hours; those images are shown in Figures 6A through 6D, respectively. The receiver medium showed the spherical shape and nanoscale of vesicles, indicating that ULs could penetrate through skin to the receiver medium as intact vesicles.

Figures 7A through 7D show CLSM images of receiver medium at time points of 30 minutes, 1 hour, 2 hours, and 4 hours. The presence of red fluorescence and green fluorescence in the receiver medium indicated that both ULs and NaFl could penetrate through skin. The ULs found in the receiver medium could be both intact vesicles and phospholipid bilayer. Regarding the presence of intact vesicles in the receiver medium, as observed by TEM (Figures 6A–6D), NaFl found in the receiver medium could be both entrapped drug and free drug. The presence of both colors of fluorescence at the same point could also be used to investigate the release behavior of ULs. It is assumed that red fluorescence in receiver medium is intact vesicle. If the green fluorescence intensity is less than the red fluorescence intensity, the entrapped drug was released. Inside the white circles of Figures 7A-1, 7A-3, and 7A-4, the green fluorescence intensity was markedly less than the red fluorescence intensity, indicating that the vesicles had released some part of the entrapped drug into the skin. If both the green fluorescence and red fluorescence appeared equal, the entrapped drug was not released, or a significant amount was not released. In Figures 7B-1, 7B-3, 7B-4, 7C-1, 7C-3, and 7C-4, both green fluorescence and red fluorescence were equal, indicating that the entrapped drug was not released, or a significant amount was not released. If green fluorescence appears while red fluorescence does not, there is free drug. Inside the white circles of Figures 7D-1, 7D-3, and 7D-4, green fluorescence appeared, whereas red fluorescence did not appear, indicating there was free drug in the receiver medium. Supported by the presence of intact vesicles in the receiver medium (Figures 6 and 7), we suggest that ULs might penetrate through skin to the systemic blood circulation as intact vesicles. Pegylated or stealth liposomes should be applied for transdermal drug delivery, instead of conventional liposomes, to reduce reticuloendothelial system uptake and to prolong circulation time in blood.

Using CLSM and size exclusion chromatography, Cevc et al[15] compared the vesicle size of phospholipid ULs from

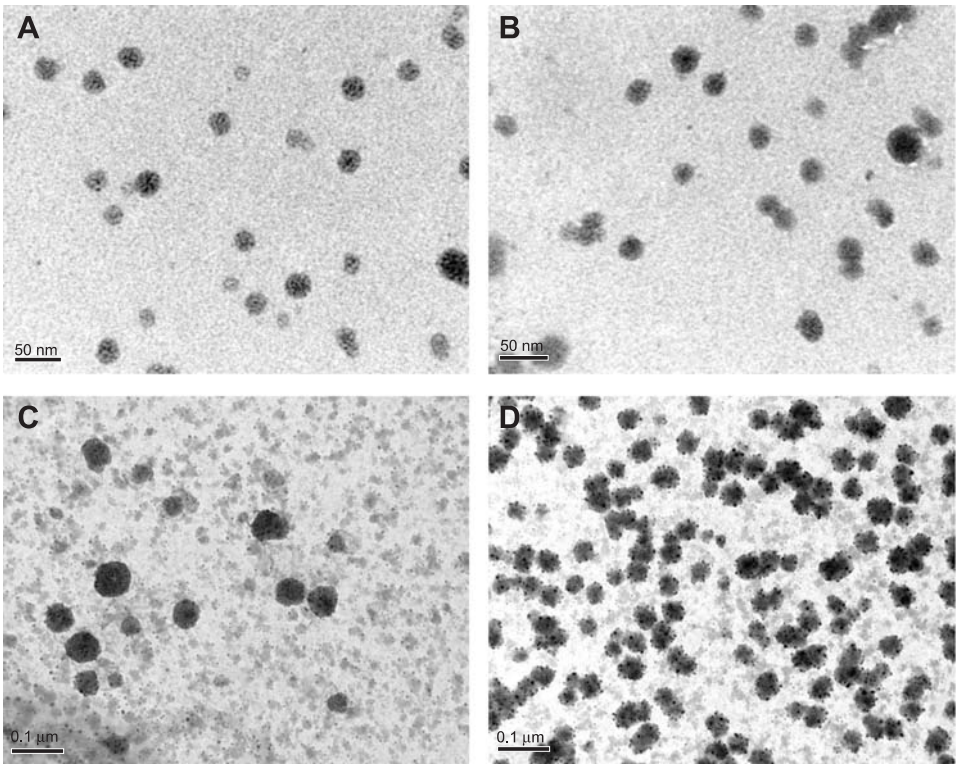

Figure 6 Transmission electron microscopy images of the receiver medium after skin penetration study of the NaFl-loaded, Rh-PE-labeled ultradeformable liposomes at different time points.
Notes: (**A**) 30 minutes; scale bar represents 50 nm. (**B**) 1 hour; scale bar represents 50 nm. (**C**) 2 hours; scale bar represents 100 nm. (**D**) 4 hours; scale bar represents 100 nm.
Abbreviations: NaFl, fluorescein sodium; Rh-PE, rhodamine B 1,2-dihexadecanoyl-sn-glycero-3-phosphoethanolamine triethylammonium salt.

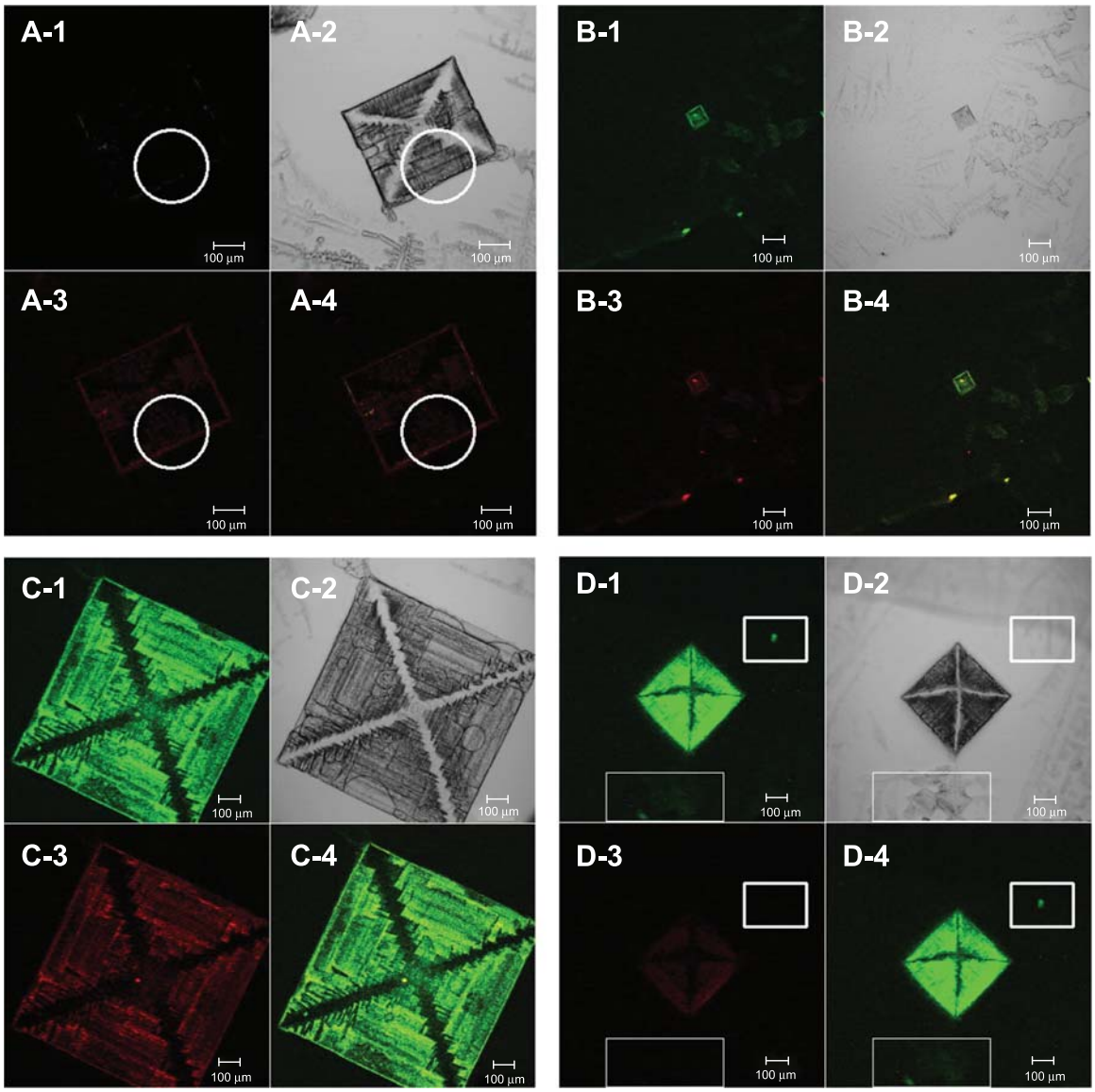

Figure 7 Confocal laser scanning microscopy images of receiver medium from the skin penetration study of NaFl-loaded, Rh-PE-labeled ultradeformable liposomes at different time points.
Notes: (**A**) 30 minutes; (**B**) 1 hour; (**C**) 2 hours; (**D**) 4 hours. Each image is divided into four parts: **-1**, green fluorescence of NaFl; **-2**, bright field image; **-3**, red fluorescence of Rh-PE; **-4**, overlay of **-1** and **-3**. Scale bars represent 100 µm.
Abbreviations: NaFl, fluorescein sodium; Rh-PE, rhodamine B 1,2-dihexadecanoyl-sn-glycero-3-phosphoethanolamine triethylammonium salt.

their original preparation with those collected from the serum of mice who had the ULs applied to their skin. The size of vesicles from the original preparation did not differ from those obtained from the mouse serum. The authors concluded that ULs penetrated through the skin to the circulation system as intact vesicles, without permanent disintegration. Therefore, based on our TEM images of intact vesicles found in viable epidermis (Figures 5G and 5H) and receiver medium (Figures 6A through 6D), as well as CLSM images of receiver medium (Figures 7A through 7D), we agreed with Cevc et al[7] – that ULs could penetrate the skin and enter the blood circulation system as intact vesicles. Honeywell-Nguyen et al[16,17] studied in vivo and in vitro interactions between nonionic elastic vesicles and human skin, using tape stripping techniques. TEM images revealed that little vesicle material was found in the deepest layers of the stratum corneum. Thus, the authors suggested that penetration of intact vesicles into viable epidermis might not be possible. Because the specimen used for TEM preparation was a very small piece, the probability of finding intact vesicles in viable epidermis was also very small. To confirm the penetration of intact vesicles into viable epidermis or into the blood circulation system,

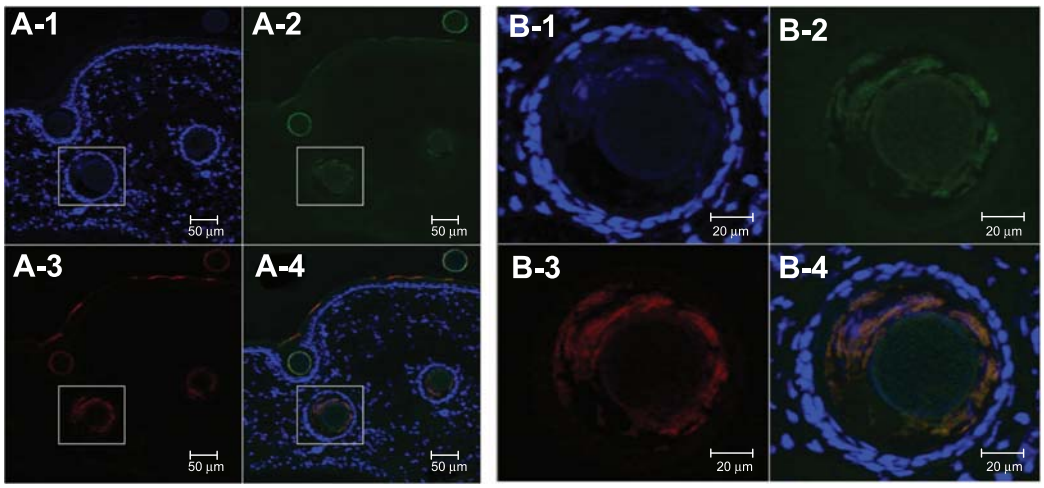

Figure 8 Confocal laser scanning microscopy cross-sectional images of porcine skin treated with NaFl-loaded, Rh-PE-labeled ultradeformable liposomes, at 2 hours.
Notes: (**A**) Scale bars represent 50 μm. (**B**) Magnification of marked area in (**A**); scale bars represent 20 μm. Each image is divided into four parts: **-1**, blue fluorescence of DAPI, **-2**, green fluorescence of NaFl; **-3**, red fluorescence of Rh-PE; **-4**, overlay of **-1**, **-2**, and **-3**.
Abbreviations: NaFl, fluorescein sodium; Rh-PE, rhodamine B 1,2-dihexadecanoyl-sn-glycero-3-phosphoethanolamine triethylammonium salt; DAPI, 4′,6-diamidino-2-phenylindole.

the receiver medium (or collected serum) also should be investigated.

Figures 8A and 8B show cross-sections of skin treated with NaFl-loaded, Rh-PE-labeled ULs at 2 hours. Both green fluorescence and red fluorescence were seen throughout the tissue cross-section, with high-intensity deposits in the follicular region, indicating that NaFl and ULs could permeate from the stratum corneum to the dermis and accumulate in the hair follicles, more than in other regions, as shown in Figures 8A-2, 8A-3, and 8A-4. Figures 8B-2, 8B-3, and 8B-4 show the hair follicle at higher magnification. The orange fluorescence inside the hair follicle, seen in the merged image (Figure 8B-4), occurred due to green fluorescence and red fluorescence at the same region, which indicated that NaFl was still entrapped in ULs when it had penetrated via the hair follicles.

Sequential cross-sectional images of follicular and nonfollicular regions of porcine skin treated with NaFl-loaded,

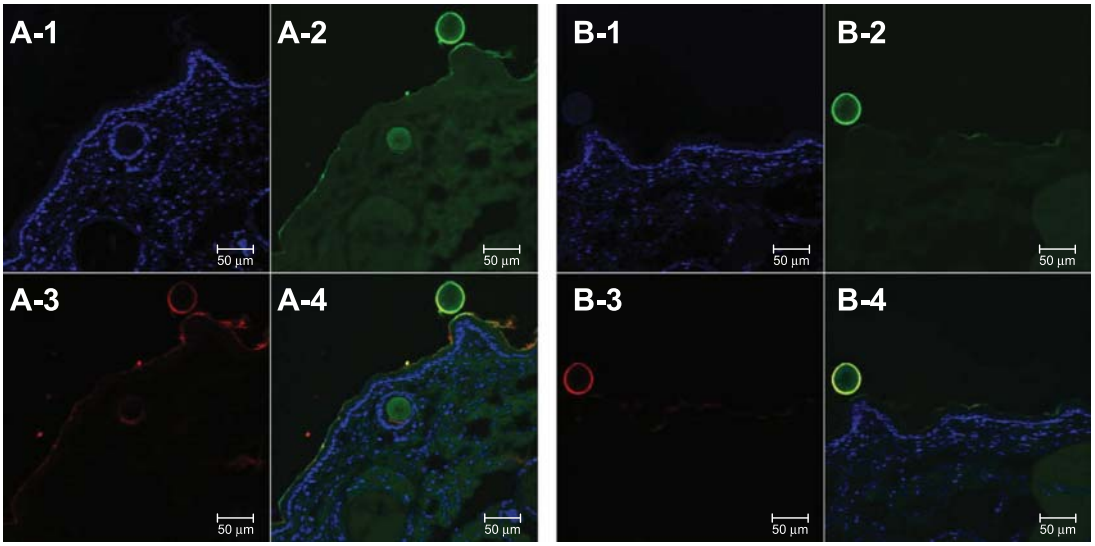

Figure 9 Confocal laser scanning microscopy cross-sectional images of porcine skin treated with NaFl-loaded Rh-PE–labeled ULs and stained with DAPI, at 4 hours.
Notes: (**A**) Follicular region; (**B**) nonfollicular region. Each image is divided into four parts: **-1**, blue fluorescence of DAPI; **-2**, green fluorescence of NaFl; **-3**, red fluorescence of Rh-PE; **-4**, overlay of **-1**, **-2**, and **-3**. Scale bar represents 50 μm.
Abbreviations: ULs, ultradeformable liposomes; NaFl, fluorescein sodium; Rh-PE, rhodamine B 1,2-dihexadecanoyl-sn-glycero-3-phosphoethanolamine triethylammonium salt; DAPI, 4′,6-diamidino-2-phenylindole.

Table 1 Fluorescence intensities of NaFl and Rh-PE at follicular and nonfollicular regions

Region	NaFl	Rh-PE
Follicular region	425.60±210.07*	103.12±57.78*
Nonfollicular region	255.01±61.43	80.41±29.37

Notes: *$P<0.05$, compared against nonfollicular region. Each value represents the mean ± standard deviation.
Abbreviations: NaFl, fluorescein sodium; Rh-PE, rhodamine B 1,2-dihexadecanoyl-sn-glycero-3-phosphoethanolamine triethylammonium salt.

Rh-PE-labeled ULs (at 4 hours) are shown in Figures 9A and 9B. Both green fluorescence and red fluorescence intensities at follicular regions (Figures 9A-2 and 9A-3) were significantly higher than at nonfollicular regions (Figures 9B-2 and 9B-3) (Table 1), indicating that NaFl and ULs penetrated via the follicular region more than via the nonfollicular region.

Theoretically, molecules permeate the skin through intercellular, intracellular (transcellular), and follicular (transappendageal) pathways.[31] Follicular channels offer a large space for drug and vesicle transportation, bypassing the barrier function of the stratum corneum. The interaction of vesicle and intracellular protein in the transcellular pathway resulted in vesicle fragmentation, as shown in Figures 4E through 4H. Regarding our TEM and CLSM investigation, we suggest that the intact vesicles found in receiver medium might penetrate skin using a transappendageal pathway as the main transportation route.

Conclusion

Our TEM investigation revealed that ULs employed both a penetration-enhancing effect and a drug carrier system mechanism for enhancement of skin penetration. ULs act as penetration enhancers by denaturing intracellular protein and corneodesmosomes, and disrupting intercellular lipid organization, which results in enhancement of penetration via intracellular and intercellular pathways, respectively. ULs also act as a drug carrier system, by penetrating through skin into receiver medium as intact vesicles, as observed by TEM and CLSM. We suggest that a transappendageal pathway is the major penetration route of intact vesicles.

Acknowledgments

The authors are thankful for the financial support of Thailand Research Funds, through the Golden Jubilee PhD Program (Grant number: PHD/0057/2551), and the TRF Basic Research Grant (Grant number: BRG 5680016).

Disclosure

The authors report no conflicts of interest in this work.

References

1. Wang Y, Thakur R, Fan Q, Michniak B. Transdermal iontophoresis: combination strategies to improve transdermal iontophoretic drug delivery. *Eur J Pharm Biopharm.* 2005;60(2):179–191.
2. Herwadkar A, Sachdeva V, Taylor LF, Silver H, Banga AK. Low frequency sonophoresis mediated transdermal and intradermal delivery of ketoprofen. *Int J Pharm.* 2012;423(2):289–296.
3. Kolli CS, Banga AK. Characterization of solid maltose microneedles and their use for transdermal delivery. *Pharm Res.* 2008;25(1):104–113.
4. Shah KA, Date AA, Joshi MD, Patravale VB. Solid lipid nanoparticles (SLN) of tretinoin: potential in topical delivery. *Int J Pharm.* 2007;345(1–2):163–171.
5. Dragicevic-Curic N, Scheglmann D, Albrecht V, Fahr A. Temoporfin-loaded invasomes: development, characterization and in vitro skin penetration studies. *J Control Release.* 2008;127(1):59–69.
6. Cevc G, Blume G. Lipid vesicles penetrate into intact skin owing to the transdermal osmotic gradients and hydration force. *Biochim Biophys Acta.* 1992;1104(1):226–232.
7. Cevc G, Gebauer D, Stieber J, Schätzlein A, Blume G. Ultraflexible vesicles, Transfersomes, have an extremely low pore penetration resistance and transport therapeutic amounts of insulin across the intact mammalian skin. *Biochim Biophys Acta.* 1998;1368(2):201–215.
8. Cevc G. Transdermal drug delivery of insulin with ultradeformable carriers. *Clin Pharmacokinet.* 2003;42(5):461–474.
9. Mishra D, Dubey V, Asthana A, Saraf DK, Jain MK. Elastic liposomes mediated transcutaneous immunization against Hepatitis B. *Vaccine.* 2006;24(22):4847–4855.
10. Cevc G, Mazgareanu S, Rother M. Preclinical characterization of NSAIDs in ultradeformable carriers or conventional topical gels. *Int J Pharm.* 2008;360(1–2):29–39.
11. Rother M, Seidel EJ, Clarkson PM, Mazgareanu S, Vierl U, Rother I. Efficacy of epicutaneous Diractin (ketoprofen in Transfersome gel) for the treatment of pain related to eccentric muscle contractions. *Drug Des Devel Ther.* 2009;3:143–149.
12. El Maghraby GM, Williams AC, Barry BW. Skin delivery of oestradiol from deformable and traditional liposomes: mechanistic studies. *J Pharm Pharmacol.* 1999;51(1):1123–1134.
13. van den Bergh BA, Bouwstra JA, Junginger HE, Wertz PW. Elasticity of vesicles affects hairless mouse skin structure and permeability. *J Control Release.* 1999;62(3):367–379.
14. Cevc G, Blume G. New, highly efficient formulation of diclofenac for the topical, transdermal administration in ultradeformable drug carriers, Transfersomes. *Biochim Biophys Acta.* 2001;1514(2):191–205.
15. Cevc G, Schätzlein A, Richardsen H. Ultradeformable lipid vesicles can penetrate the skin and other semi-permeable barriers unfragmented. Evidence from double label CLSM experiments and direct size measurements. *Biochim Biophys Acta.* 2002;1564(1):21–30.
16. Honeywell-Nguyen PL, de Graaff AM, Groenink HW, Bouwstra JA. The in vivo and in vitro interactions of elastic and rigid vesicles with human skin. *Biochim Biophys Acta.* 2002;1573(2):130–140.
17. Honeywell-Nguyen PL, Bouwstra JA. The in vitro transport of pergolide from surfactant-based elastic vesicles through human skin: a suggested mechanism of action. *J Control Release.* 2003;86(1):145–156.
18. Honeywell-Nguyen PL, Bouwstra JA. Vesicles as a tool for transdermal and dermal delivery. *Drug Discov Today.* 2005;2:67–74.
19. Subongkot T, Duangjit S, Rojanarata T, Opanasopit P, Ngawhirunpat T. Ultradeformable liposomes with terpenes for delivery of hydrophilic compound. *J Liposome Res.* 2012;22(3):254–262.
20. Subongkot T, Wonglertnirant N, Songprakhon P, Rojanarata T, Opanasopit P, Ngawhirunpat T. Visualization of ultradeformable liposomes penetration pathways and their skin interaction by confocal laser scanning microscopy. *Int J Pharm.* 2013;441(1–2):151–161.
21. Chain E, Kemp I. The isoelectric points of lecithin and sphingomyelin. *Biochem J.* 1934;28(6):2052–2055.
22. Verma DD, Verma S, Blume G, Fahr A. Particle size of liposomes influences dermal delivery of substances into skin. *Int J Pharm.* 2003;258(1–2):141–151.

23. Warner RR, Stone KJ, Boissy YL. Hydration disrupts human stratum corneum ultrastucture. *J Invest Dermatol*. 2003;120(3):275–284.
24. Bouwstra JA, de Graaff A, Gooris GS, Nijsse J, Wiechers JW, van Aelst AC. Water distribution and related morphology in human stratum corneum at different hydration levels. *J Invest Dermatol*. 2003;120(5):750–758.
25. Caubet C, Jonca N, Brattsand M, et al. Degradation of corneodesmosome proteins by two serine proteases of the kallikrein family, SCTE/KLK5/hK5 and SCCE/KLK7/hK7. *J Invest Dermatol*. 2004;122(5):1235–1244.
26. Garrod D, Chidgey M. Desmosome structure, composition and function. *Biochim Biophys Acta*. 2008;1778(3):572–587.
27. Williams AC, Barry BW. Penetration enhancers. *Adv Drug Deliv Rev*. 2004;56(5):603–618.
28. Som I, Bhatia K, Yasir M. Status of surfactants as penetration enhancers in transdermal drug delivery. *J Pharm Bioallied Sci*. 2012;4(1):2–9.
29. Narishetty ST, Panchagnula R. Transdermal delivery of zidovudine: effect of terpenes and their mechanism of action. *J Control Release*. 2004;95(3):367–379.
30. Barry BW. Lipid-Protein-Partitioning theory of skin penetration enhancement. *J Control Release*. 1991;15:237–248.
31. Barry BW. Novel mechanisms and devices to enable successful transdermal drug delivery. *Eur J Pharm Sci*. 2001;14(2):101–114.

Bootstrap Resampling Technique to Evaluate the Reliability of the Optimal Liposome Formulation: Skin Permeability and Stability Response Variables

Sureewan Duangjit,[a,c] Praneet Opanasopit,[a] Theerasak Rojanarata,[a] Jun Takayama,[b] Kozo Takayama,[c] and Tanasait Ngawhirunpat*[,a]

[a] *Faculty of Pharmacy, Silpakorn University; Sanamchandra Palace Campus, Nakhon Pathom 73000, Thailand:* [b] *Research Fellow of Japan Society for the Promotion of Science; 5–3–1 Kojimachi, Chiyoda-ku, Tokyo 102–0083, Japan: and* [c] *Department of Pharmaceutics, Hoshi University; 2–4–41 Ebara, Shinagawa-ku, Tokyo 142–8501, Japan.*
Received May 9, 2014; accepted June 22, 2014; advance publication released online July 9, 2014

A nonlinear response surface method incorporating multivariate spline interpolation (RSM-S) is a useful technique for the optimization of pharmaceutical formulations, although the direct reliability of the optimal formulation must be evaluated. In this study, we demonstrated the feasibility of using the bootstrap (BS) resampling technique to evaluate the direct reliability of the optimal liposome formulation predicted by RSM-S. The formulation characteristics (X_n), including vesicle size (X_1), size distribution (X_2), zeta potential (X_3), elasticity (X_4), drug content (X_5), entrapment efficiency (X_6), release rate (X_7), and the penetration enhancer (PE) factors as formulation factors (Z_n), with the type of PE (Z_1) and content of PE (Z_2) were used as causal factors of the response surface analysis. The intended responses were high skin permeability (flux, Y_1) and high stability formulation (drug remaining, Y_2). Based on the dataset obtained, the simultaneous optimal solutions were estimated using RSM-S. Leave-one-out-cross-validation showed satisfying reliability of the optimal solution. Concurrently, similar BS optimal solutions were estimated from the BS dataset that was generated from the original dataset through BS resampling at frequencies of 250, 500, 750, and 1000. The analysis and simulation indicated that X_4, X_5, and Z_2 were the prime factors affecting Y_1 and Y_2. These findings suggest that this approach could also be useful for evaluating the reliability of an optimal liposome formulation predicted by RSM-S and would be beneficial for the pharmaceutical development of liposomes for transdermal drug delivery.

Key words bootstrap; response surface; simultaneous optimal solution; transdermal drug delivery

Optimization techniques using computer-based rationales to research and develop pharmaceutical formulations have recently become attractive and interesting. A non-linear response surface method incorporating multivariate spline interpolation (RSM-S) is a powerful method for pharmaceutical optimization.[1] RSM-S has shown that the complex relationships between causal factors and response variables could be simply comprehended and that the simultaneous optimal solutions obtained would be stable and reproducible.[2] Several intensive studies successfully developed novel pharmaceutical formulations using RSM-S (*e.g.*, water-in-oil-water multiple emulsion of insulin for intestinal delivery,[3] sustained release of diltiazem tablets for oral delivery[4] and ultra-deformable liposome of meloxicam for transdermal delivery[5]). RSM-S was determined to be a promising technique for formulation optimization.[3–7] Simultaneously, it is considerable to evaluate the accuracy and reliability of each optimal formulation estimated by RSM-S. The leave-one-out-cross-validation (LOOCV) method was also employed. The LOOCV method can evaluate the generalization error of a given response surface.[8] Moreover, the reliability of optimal formulation estimated by certain response surface can be directly evaluated using bootstrap (BS) resampling methods. The BS method is a simulation technique based on the empirical distribution of the experimental data that introduced by Efron.[9] BS resampling is generally used to estimate confidence intervals and the bias and variance of an estimator. The basic idea of BS resampling is randomly sampling from original dataset (experimental data). A BS samples ($X^*=X_1^*,X_2^*,\cdots,X_n^*$) is randomly sampled that replacement from the original data ($X=X_1,X_2,\cdots,X_n$) by reproducing the BS resampling procedure.

When designing and developing liposome for transdermal drug delivery, the safety, stability and efficacy of formulation must be simultaneously optimized. Generally, the liposome formulation is composed of various formulation characteristics and several formulation factors. The formulation characteristics and formulation factors are the major parameters directly affecting the skin permeability of a liposome formulation.[10] The development of liposomes has previously been based primarily on trial and error to obtain an appropriate formulation for satisfying multiple characteristics of the formulation. Designing and testing on a case-by-case basis (or by trial and error techniques) was considered a wasteful method for designing each liposome formulation. The acceptable liposome formulation for one characteristic was often not satisfactory for other characteristics. Thus, these restrictions incurred difficulties in the design and development of liposome formulations. The optimal liposome formulation is generally influenced by a mixture of acceptable formulation characteristics and formulation factors. Therefore, an understanding of the actual relationships between causal factors (*e.g.*, formulation characteristics and formulation factors) and pharmaceutical responses (*e.g.*, skin permeability and stability of formulation) is required to develop satisfying liposome for transdermal drug delivery.

In this study, the original dataset used was obtained from the experiment. The formulation characteristics (X_n) and formulation factors (Z_n) of 30 model liposome formulations

The authors declare no conflict of interest.

* To whom correspondence should be addressed. e-mail: tanasait@su.ac.th

were selected as causal factors of response variables (Y_n). Using multivariate statistical techniques, the significant causal factors were chosen as effective causal factors for certain response analyses. When developing an optimal liposome formulation for transdermal drug delivery, having a proper mixture of high skin permeability and good stability formulation should be considered. For this objective, RSM-S was applied in our study. The LOOCV and BS resampling methods were also used to evaluate the reliability of the simultaneous optimal solutions predicted by RSM-S.

MATERIALS AND METHODS

Materials Phosphatidylcholine (PC) was obtained from LIPOID GmbH (Ludwigshafen, Germany). Sodium hexadecyl sulfate (SHS) was purchased from Tokyo Chemical Industry (Tokyo, Japan). Hexadecylpyridinium chloride (HPC), dodecylpyridinium chloride (DPC), and butylpyridinium chloride (BPC) were purchased from MP Biomedicals (Santa Ana, CA, U.S.A.). Meloxicam (MX) was supplied by Sigma-Aldrich Production GmbH (Buchs, Switzerland). Cholesterol (Chol) was obtained from Wako Pure Chemical Industries, Ltd. (Osaka, Japan). All other chemicals used were of reagent grade.

Preparation of Model Liposome Formulation Thirty model formulations were prepared according to the optimal liposome formulation obtained in our previous study.[11] As shown in Table 1, model formulations that were composed of a controlled amount of PC, Chol, MX, and various types and content of penetration enhancers (PE) (*e.g.*, SHS, HPC, DPC, BPC) were prepared using a sonication method. A previous study reported that alkyl pyridinium surfactants exhibit the ability for saturation and solubilization of the bilayer,[12] which could enhance the transdermal delivery of anti-inflammatory drugs.[13] Briefly, all ingredients were dissolved and mixed in methanol–chloroform (1 : 2, v/v), and the solvent was evaporated under a nitrogen gas stream. The lipid thin film was dried in a desiccator for 6 h to remove the remaining solvent. The dried lipid film was hydrated with an acetate buffer solution (pH 5.5). Model vesicle formulations were subsequently sonicated for 30 min using a sonicator bath (5510J-DTH; Branson Ultrasonics, Danbury, CT, U.S.A.). All model liposome formulations were freshly prepared or preserved in airtight containers at 4°C prior to further studies.

Determination of Vesicle Size, Size Distribution and Zeta Potential of Liposomes The vesicle size, size distribution and zeta potential of model formulation were measured by photon correlation spectroscopy (Zetasizer Nano series, Malvern Instrument, U.K.). Twenty microliters of liposomes was diluted with 1480 μL of deionized water. All determinations were performed at room temperature, at least three independent samples were collected and the vesicle size, size distribution and zeta potential were measured in triplicate.

Table 1. Formulation of Model Liposome Formulation for Simultaneous Optimization

Formula	mM
Phosphatidylcholine[a)]	10.00
Cholesterol[b)]	1.05
Meloxicam	2.20
Penetration enhancers[c–f)]	0.00–2.90

a) Bilayer forming liposome. *b*) Membrane stabilizer. *c*) Sodium hexadecyl sulfate. *d*) Hexadecylpyridinium chloride. *e*) Dodecylpyridinium chloride. *f*) Butylpyridinium chloride.

Determination of Elasticity of Liposomes The elasticity value of the model liposomes formulation was directly proportional to $J_{Flux} \times (r_v/r_p)^2$, which was obtained from the previous study.[14,15]

$$\text{Elasticity value} = J_{Flux} \times \left(\frac{r_v}{r_p} \right)^2 \quad (1)$$

where J_{Flux} is the rate of penetration through a permeable barrier ($mg \cdot s^{-1} \cdot cm^{-2}$), r_v is the average liposome size after extrusion (nm) and r_p is the pore size of the membrane (nm). To measure J_{Flux}, the liposomes were extruded through a polycarbonate membrane (Nuclepore, GE Healthcare Life Sciences, Buckinghamshire, U.K.) with a pore diameter of 50 nm (r_p) at a pressure of 0.5 MPa. Five minutes after extrusion, the extrudate was weighed (J_{Flux}), and the average liposome diameter (r_v) was measured by photon correlation spectroscopy.

Determination of Drug Content in Liposome Formulations and Entrapment Efficiency The MX content in the liposome formulations and entrapment efficiency were determined by HPLC. The liposome vesicles were broken down with Triton® X-100 (0.1% w/v) at a 1 : 1 v/v ratio and appropriately diluted with phosphate buffer solution (PBS, pH 7.4). The liposome/Triton® X-100 was centrifuged at 10000×***g*** at 4°C for 10 min. The supernatant was filtered with a 0.45 μm nylon syringe filter. The entrapment efficiency of the MX loaded in the liposome formulations was calculated according to the following Eq. 2:

$$\% \text{ Entrapment efficiency} = \left(\frac{C_L}{C_i} \right) \times 100 \quad (2)$$

where C_L is the concentration of MX loaded in the liposome formulations, as described in the above methods, and C_i is the initial concentration of MX added to the liposome formulations.

Evaluation of the Release Profile of Liposomes The release profile of MX from the MX loaded liposome formulation was determined using a dialysis bag with a molecular weight cut off; MWCO 6000–8000. Fifty milliliters of PBS at a control temperature of 32±1°C was used as the receiving medium and was constantly stirred at 150 rpm. This condition was chosen to obtain sink condition in the receiving medium. Five hundred microliters of MX loaded liposome formulation was filled in a dialysis bag and immersed in the receiving medium. The samples were withdrawn and filtered at intervals of 5, 10, 15, 20, 30, 45, and 60 min and 2, 4, 6, 8, 10, and 12 h. The concentration of MX was determined by HPLC.

Determination of the Response Variables The skin permeability (flux, Y_1) and stability of the formulation (drug remaining, Y_2) were selected as the response variables to be evaluated in the resulting liposome formulation.

a) Skin Permeability of Liposomes: The excised skins of hairless mice (Laboskin®, HOS: HR-1 Male, 7 weeks, Sankyo Labo Service Corporation, Inc., Tokyo, Japan) were used as skin models for the *in vitro* skin permeation study. This animal study was performed at Hoshi University and complied with the regulations of the committee on Ethics in the Care and Use of Laboratory Animals. Side-by-side diffusion cells

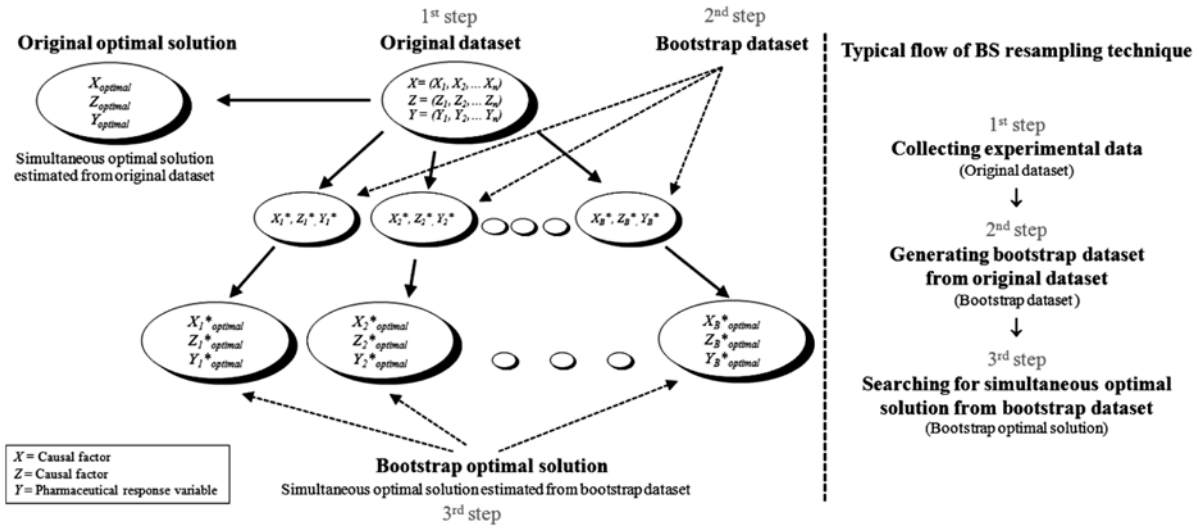

Fig. 1. The Process of Bootstrap Resampling Technique to Evaluate the Reliability of Simultaneous Optimal Solutions

with an available diffusion area of 0.95 cm^2 were employed. The receiving chambers were filled with 3 mL of PBS (pH 7.4 at 32°C), and the donor chambers were filled with 3 mL of the MX loaded liposome formulation. At the appropriate times, the receiving medium was withdrawn, and the same volume of fresh buffer solution was replaced in the receiving chambers. The concentration of MX in the aliquot was analyzed using HPLC. The cumulative amount of MX per area was plotted against time, and the flux value (Y_1) was determined as the slope of linear portion of the plot.

b) Stability of Liposomes: The MX loaded liposome formulations were kept in glass bottles with plastic plugs and stored at 25±1°C for 30 d. The drug remaining in the MX loaded liposome formulations (Y_2) was determined by HPLC. The concentration of MX in the liposome formulation after preparation at day 0 was normalized to 100%.

HPLC Analysis The HPLC system consisted of a SIL-20 A autosampler, an LC-20AT liquid chromatography and an SPD-20AUV detector (Shimadzu Corporation, Kyoto, Japan). The analytical column was YMC-Pack ODS-A (150 mm×4.6 mm i.d., S-5, YMC Co., Ltd., Kyoto, Japan). The mobile phase was composed of methanol–acetate buffer solution (pH 4.6) (50 : 50, v/v). The flow rate was set at 0.8 mL/min, and the wavelength used was UV-detected at 272 nm. All samples were freshly prepared or stored at 4°C until analysis. The calibration curve for MX was in the range of 1–100 μg/mL, with a correlation coefficient of 0.9997. The percent recovery ranged from 99.9–100.3%, and the relative standard deviations for both the intra- and inter-day measurements were less than 2%.

Simultaneous Optimization and Reliability Evaluation of the Optimal Solution Using DataNESIA and BS Resampling The formulation characteristics (X_n) (*e.g.*, vesicle size (X_1), size distribution (X_2), zeta potential (X_3), elasticity (X_4), drug content (X_5), entrapment efficiency (X_6), release rate (X_7)) and penetration enhancers (PE) used in the model formulations as formulation factors (Z_n) (*e.g.*, type of PE (Z_1) and content of PE (Z_2)) were used as causal factors of the response variables. The model formulation of sufficient skin permeability (Y_1) and good stability formulation (Y_2) was defined as the optimal liposome formulation. High skin permeability and high stability formulation were considered ideal for seeking simultaneous optimal solution. The significant causal factors were selected as effective causal factors for dataNESIA analysis using the multiple regression analysis (MRA) incorporating the stepwise way of factor selection. The software JMP (Version 8, SAS Institute Inc., Cary, NC, U.S.A.) was employed for MRA. The simultaneous optimal solution was estimated using the dataNESIA software (Version 3.2, Azbil Corp., Fujisawa, Japan), which was based on a RSM-S, using the original dataset obtained from 30 model formulations. As shown in Fig. 1, the simultaneous optimal solution from the original dataset was called "the original optimal solution." The accuracy and reliability of the original optimal solution were also determined by LOOCV. The statistical significance of accuracy and reliability was tested based on Pearson's R test. Finally, the BS resampling method was employed to estimate confidence ranges of the original optimal solution. An enormous number of BS samples was generated from the original dataset through BS resampling at a frequency of 250, 500, 750, and 1000. The simultaneous optimal solutions for all BS samples were also estimated using RSM-S. The simultaneous optimal solutions from the BS samples dataset are hereafter called "the BS optimal solution." The details of the reliability assessment of the original optimal solution and the BS optimal solutions have been fully described in previous studies.[1,16)]

RESULTS AND DISCUSSION

Prediction of Response Variables and Simultaneous Optimization In this study, the formulation characteristics (*e.g.*, vesicle size (X_1), size distribution (X_2), zeta potential (X_3), elasticity (X_4), drug content (X_5), entrapment efficiency (X_6), release rate (X_7)) and formulation factors (*e.g.*, type of PE (Z_1) and content of PE (Z_2)) were used as the causal factors of the response variables. The selection of significant causal factors as the original dataset for the dataNESIA analysis was key to generating an accurate optimal solution because the evaluation of the precise optimal solution depended significantly on the integrity and the correctness of the original dataset. The result indicated that the elasticity (X_4), drug content (X_5), and content

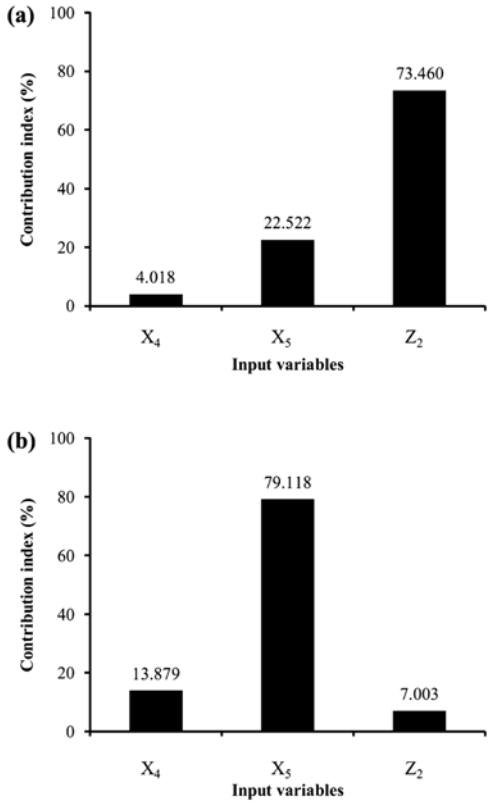

Fig. 2. The Contribution Index of Effective Causal Factor for Predicting Response Variables

(a) Skin permeability (Y_1) and (b) stability of formulation (Y_2).

of PE (Z_2) were selected as effective causal factors for RSM-S by MRA, incorporating a stepwise way of factor selection. The correlation coefficients for the skin permeability (Y_1) and the stability of formulation (Y_2) were sufficiently high (0.7601 and 0.9700, respectively), suggesting that X_5 and Z_2 and X_4, X_5 and Z_2 were important to Y_1 and Y_2, respectively. The contribution index of the effective causal factor for predicting Y_1 and Y_2 is shown in Fig. 2.

The liposome formulation was optimized based on the original dataset using RSM-S. X_4=74.5 ($mg \cdot s^{-1} \cdot cm^{-2}$), X_5=514 (μg/mL), and Z_2=0.0689 (%mol) were estimated as optimal formulation characteristics and formulation factors variables. The following were predicted to be the optimal response variables: Y_1=0.269 ($\mu g/cm^2/h$) and Y_2=375 (μg/mL). The results indicated that the original optimal solution, which was considered ideal, had a relatively high elasticity (X_4), high drug content (X_5), and high content of PE (Z_2). The formulation characteristics and formulation factors could directly affect the effectiveness of liposome formulation for improving skin permeability, as reported in a previous study.[17] The stability of liposome formulation could be modified by altering aspects of the composition of the liposome, such as the presence of cholesterol.[18] Thus, these effective causal factors might be factors affecting both the efficacy and stability of liposome formulation. The approximate actual relationship between causal factors (formulation characteristics and formulation factors) on response variables (skin permeability and stability of formulation) is shown in Fig. 3.

Figures 3a, b and c show the response surfaces of the skin permeability estimated by RSM-S. Each response surface exhibited relationships among three effective causal factors (X_4, X_5, Z_2) and response variables (Y_1, Y_2) by fixing one effective causal factor at an optimal constant value and then generating the response surface of two remain causal factors to one response variable. The results indicated that as the elasticity (X_4) was held constant (74.5 $mg \cdot s^{-1} \cdot cm^{-2}$), the increase in the drug content (X_5) and the content of PE (Z_2) to high values (over 350 μg/mL and 0.06%mol, respectively) resulted in higher skin permeability, as shown in Figs. 3a and c, respectively. When the drug content (X_5) was constant, as shown in Fig. 3b, the content of PE (Z_2) was demonstrated to be a major factor inducing higher skin permeability. Zucker *et al.* noted that the capability to entrap sufficient drug content in the formulation was necessary in pharmaceutical liposome formulation to achieve therapeutic efficacy.[19] These results indicated that the skin permeability of the liposome formulation in our study was influenced by the drug content (X_5) and the content of PE (Z_2); thus, these responses were confirmed by the contribution index shown in Fig. 2a.

Figures 3d, e and f show the response surfaces of the stability of formulation predicted by RSM-S. The results revealed that as the content of PE (Z_2) was kept steady, the increase in elasticity (X_4) and drug content (X_5) to high values (over 60 $mg \cdot s^{-1} \cdot cm^{-2}$ and 350 μg/mL, respectively) tended to increase both the drug content remaining in the formulation and the stability of the formulation, as shown in Fig. 3d. Good stability of formulation was exhibited when the elasticity (X_4) and the content of PE (Y_2) was higher than 60 $mg \cdot s^{-1} \cdot cm^{-2}$ and 0.06%mol, respectively, as shown in Fig. 3e. Elsayed *et al.* revealed that a single-chain surfactant (as PE) with a high radius of curvature could destabilize or increase the deformability of the vesicle.[20] The present results suggested that our liposome formulation still displayed good stability; The present results suggested that our liposome formulation had high elasticity characteristics but still displayed good stability because all of the model liposome formulations used in this study contained an optimal amount of cholesterol as a membrane stabilizer.[18,21] Liposome formulations with high elasticity values could improve the *in vitro* and *in vivo* skin permeability of various drugs.[22–24] Moreover, the level of high drug content remaining in the formulation after storage at 25°C for 30 d was obtained (Fig. 3f) as the content of PE (Y_2) decreased and the drug content (X_5) increased. These results could be summarized as follows: the stability of liposome formulation in our study was affected by the elasticity (X_4), the drug content (X_5) and the content of PE (Z_2). These responses were also confirmed by the contribution index shown in Fig. 2b.

The approximate relationships obtained from our study were consistent with the results of a previous study: the formulation characteristics and formulation factors directly affected the skin permeability effectiveness of the liposome formulation. Furthermore, the present findings could provide beneficial basic knowledge and help determine the essential causal factor information for the further development of liposome in transdermal drug delivery. An effective liposome formulation should contain both acceptable skin permeability and good stability in one liposome formulation. The elasticity (X_4), drug content (X_5), and content of PE (Z_2) were significant factors that should be considered in liposome optimization. Therefore, the chosen liposome composition should extremely affect these significant factors, and this technique can be ap-

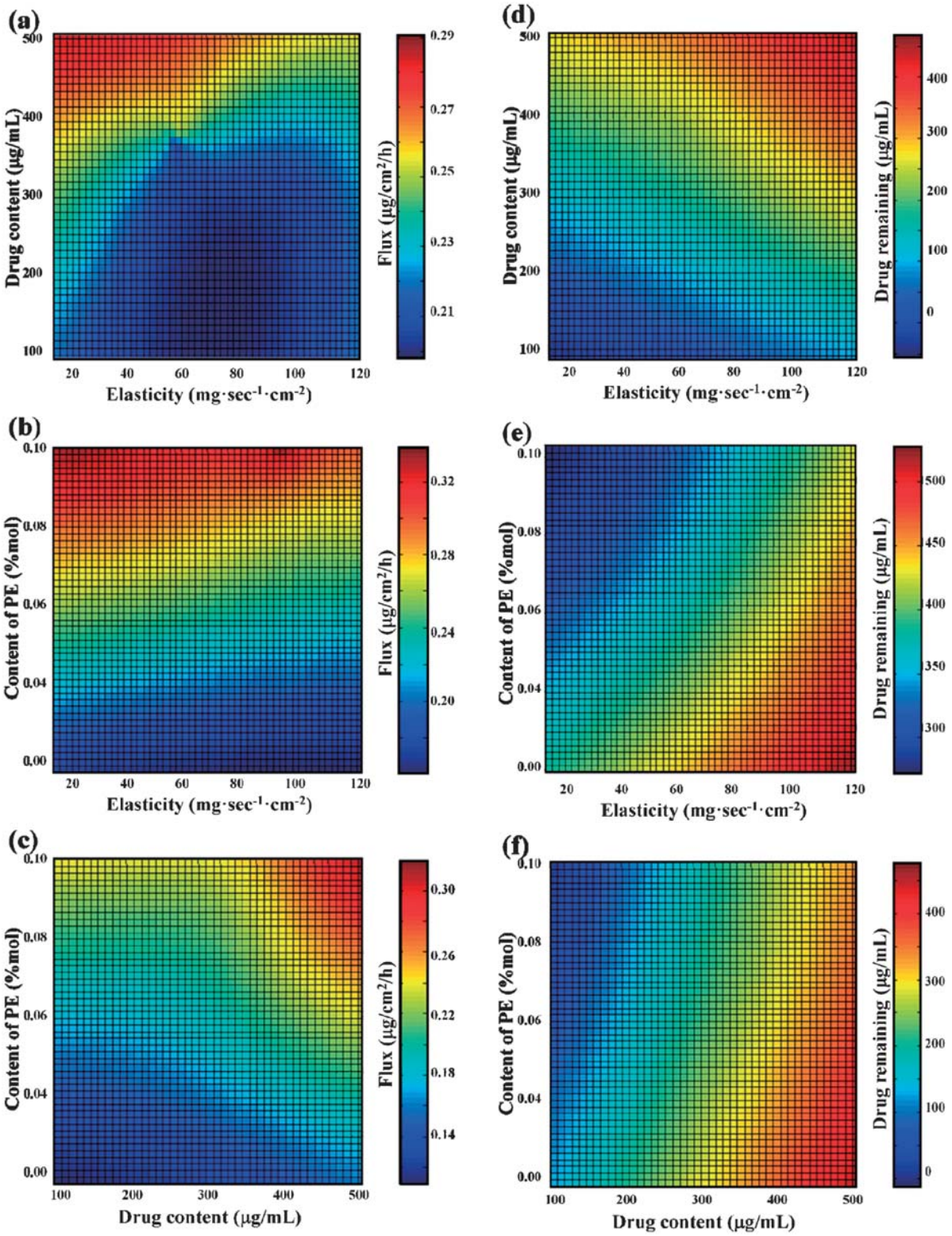

Fig. 3. The Response Surface of Skin Permeability (Flux, Y_1) (Left) and Stability of Formulation (Drug Remaining, Y_2) (Right) as Function of X_4 and X_5 (a, d), X_4 and X_9 (b, e) and X_5 and X_9 (c, f) at a Constant of Z_2 (0.0689%mol), X_5 (514 μg/mL) and X_4 (74.5 mg·s^{-1}·cm^{-2}), Respectively

plied for selecting the liposome composition. To date, it has been difficult to interpret all of the influences on the confounded relationships between formulation characteristics (as latent variables) and formulation factors,[5] although several recent pharmaceutical studies have been successful in formulation optimization. However, our study was successful in achieving this purpose by using both formulation characteristics and formulation factors as causal factors for RSM-S analysis, to understand the relationships of formulation characteristics (as latent variables), formulation factors and pharmaceutical response variables.

The accuracy and reliability of the response surface of original optimal solution were determined by LOOCV, as shown in Fig. 4. The correlation coefficients of the estimated and

experimental values for the skin permeability (Y_1) and the stability of formulation (Y_2) were extremely high (R_{LOOCV}=0.9653 and 0.9984, respectively). These results suggested that RSM-S successfully predicted the relationship between the causal factors (formulation characteristic and formulation factors) and pharmaceutical response variables.[6,7] These results indicated that an original optimal solution with acceptable characteristics (*e.g.*, high skin permeability and good stability formulation) could be estimated with RSM-S.

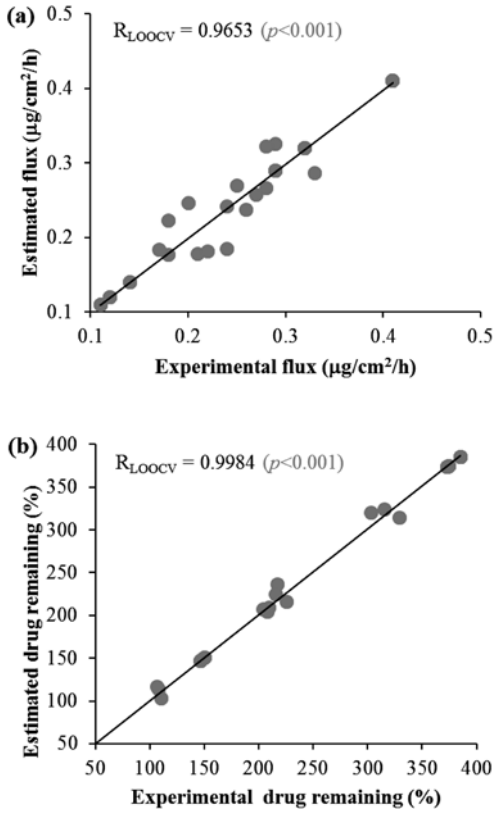

Fig. 4. The Leave-One-Out-Cross-Validation (LOOCV) Estimated Accuracy and Reliability of the Response Surface Variables

(a) Skin permeability (flux) and (b) stability of formulation (drug remaining at 25°C for 30 d) predicted by X_4, X_5, and Z_2.

Evaluation of the Reliability of the Optimal Solution Using BS Resampling In evaluating the reliability of the optimal solution, the LOOCV method efficiently provided a versatile assessment of the response surfaces.[25] The correlation coefficients are values that indicate the stability of the response surface. Thus, the reliability of the original optimal solution cannot be quantitatively evaluated using these values.[13] Therefore, BS resampling was needed to evaluate the reliability of the optimal solution[8,26,27] estimated by RSM-S. The BS datasets were generated from the original datasets through BS resampling at a frequency of 250, 500, 750, and 1000. The BS optimal solution and predicted responses are shown in Table 2. The BS optimal solutions and their standard deviation were stable, regardless of altering the frequency of resampling, indicating that a resampling frequency of more than 250 was adequate to determine the stability of the optimal solutions. Consistent with a previous study,[16] a small frequency size of more than 50 resamplings was also sufficient to evaluate the stability of the optimal pharmaceutical formulation.

The confidence intervals of the original optimal solution are shown in Table 3. The ranges of confidence intervals of most of the factors (X_4, X_5, and Z_2) were quite narrow for practical studies of liposome formulations. While further study is required to confirm the potential of the optimal solution predicted by RSM-S compared with the optimal formulation found in the experiment, a previous study[25] suggested that the characteristic values predicted by RSM-S were quite similar to the experimental values. Therefore, these results support the hypothesis that the RSM-S method can be employed to estimate simultaneous optimal solutions. The reliability of the optimal solution improved with an increase in the size of the experimental original dataset, although the precision of

Table 2. Bootstrap Optimal Solutions and Bootstrap Standard Deviations by Different Frequencies of Bootstrap Resampling

BS resampling frequency	Optimized formulations			Predicted responses	
	X_4[c] ($mg \cdot s^{-1} \cdot cm^{-2}$)	X_5[d] (μg/mL)	Z_2[e] (%mol)	Y_1[f] ($\mu g/cm^2/h$)	Y_2[g] (μg/mL)
N=0[a]	74.5	514	0.0689	0.2692	375
N=250[b]	74.4 (0.194)	514 (0.202)	0.0690 (0.0001)	0.2690 (0.0000)	375 (0.266)
N=500[b]	74.3 (0.189)	514 (0.219)	0.0689 (0.0001)	0.2690 (0.0001)	375 (0.210)
N=750[b]	74.3 (0.185)	514 (0.217)	0.0689 (0.0001)	0.2690 (0.0001)	375 (0.215)
N=100[b]	74.4 (0.187)	514 (0.200)	0.0689 (0.0001)	0.2690 (0.0001)	375 (0.213)

a) Original optimal solution. *b*) BS optimal solution. *c*) Elasticity. *d*) Drug content. *e*) Content of penetration enhancer. *f*) Skin permeation flux. *g*) Drug remaining at 25°C, 30 d. ( ) bootstrap standard deviation.

Table 3. Confidence Interval of Simultaneous Optimal Solution Estimated by RSM-S

Causal factor	Original optimal solution	250[a]		500[b]		750[c]		1000[d]	
		Lower	Upper	Lower	Upper	Lower	Upper	Lower	Upper
X_4 ($mg \cdot s^{-1} \cdot cm^{-2}$)	74.5	74.2	75.0	73.8	74.8	73.9	74.9	73.8	74.9
X_5 (μg/mL)	514	513	514	513	515	513	515	513	514
Z_2 (%mol)	0.0689	0.0688	0.0691	0.0687	0.0691	0.0688	0.0692	0.0688	0.0691
Y_1 ($\mu g/cm^2/h$)	0.269	0.2689	0.2690	0.2688	0.2692	0.2689	0.2692	0.2689	0.2691
Y_2 (μg/mL)	375	374	376	374	375	374	376	374	375

a) BS resampling frequency at 250. *b*) BS resampling frequency at 500. *c*) BS resampling frequency at 750. *d*) BS resampling frequency at 1000.

the optimal solutions was ensured, even with a small size of original dataset.

CONCLUSION

The multivariate statistical technique based on the BS resampling method was useful to evaluate the accuracy and reliability of the optimal solution determined by RSM-S. In our study, the elasticity (X_4), drug content (X_5), and content of PE (Z_2) were primary causal factors that should be intensively considered in the development of a liposome formulation for transdermal drug delivery because these were the most important factors that significantly correlated with efficient and effective simultaneous optimal liposome formulation.

Acknowledgments The authors gratefully acknowledge the Thailand Research Funds through the Basic Research Grant (No. 5680016) for financial support and thank the Faculty of Pharmacy, Silpakorn University, Nakhon Pathom, Thailand.

REFERENCES

1) Onuki Y, Ohyama K, Kaseda C, Arai H, Suzuki T, Takayama K. Evaluation of the reliability of nonlinear optimal solutions in pharmaceuticals using a bootstrap resampling technique in combination with Kohonen's self-organizing maps. *J. Pharm. Sci.*, **97**, 331–339 (2008).
2) Takayama K, Obata Y, Morishita M, Nagai T. Multivariate spline interpolation as a novel method to optimize pharmaceutical formulations. *Pharmazie*, **59**, 392–395 (2004).
3) Onuki Y, Morishita M, Takayama K. Formulation optimization of water-in-oil-water multiple emulsion for intestinal insulin delivery. *J. Control. Release*, **97**, 91–99 (2004).
4) Kikuchi S, Takayama K. Multivariate statistical approach to optimizing sustained-release tablet formulations containing diltiazem hydrochloride as a model highly water-soluble drug. *Int. J. Pharm.*, **386**, 149–155 (2010).
5) Duangjit S, Obata Y, Sano H, Kikuchi S, Onuki Y, Opanasopit P, Ngawhirunpat T, Maitani Y, Takayama K. Menthosomes, novel ultradeformable vesicles for transdermal drug delivery: Optimization and characterization. *Biol. Pharm. Bull.*, **35**, 1720–1728 (2012).
6) Onuki Y, Hoshi M, Okabe H, Fujikawa M, Morishita M, Takayama K. Formulation optimization of photocrosslinked polyacrylic acid modified with 2-hydroxyethyl methacrylate hydrogel as an adhesive for a dermatological patch. *J. Control. Release*, **108**, 331–340 (2005).
7) Surini S, Akiyama H, Morishita M, Nagai T, Takayama K. Release phenomena of insulin from an implantable device composed of a polyion complex of chitosan and sodium hyaluronate. *J. Control. Release*, **90**, 291–301 (2003).
8) Ueda N, Nakano R. Estimating expected error rates of neural network clasifiers insmall sample size situations: a comparison of cross-validation and bootstrep. *IEEE International Conference Neural Networks Proceeding.* Vol. 1, IEEE, Perth, WA, pp. 101–104 (1995).
9) Efron B, Tibchirani RJ. *An Introduction to the Bootstrap.* Chapman and Hall, New York (1993).
10) Duangjit S, Opanasopit P, Rojarata T, Obata Y, Oniki Y, Takayama K, Ngawhirunpat T. The role of deformable liposome characteristics on skin permeability of meloxicam: Optimal transfersome as transdermal delivery carriers. *The Open Conference Proceedings Journal*, **4**, 87–92 (2013).
11) Duangjit S, Obata Y, Sano H, Onuki Y, Opanasopit P, Ngawhirunpat T, Miyoshi T, Kato S, Takayama K. Comparative study of novel ultradeformable liposomes: menthosomes, transfersomes and liposomes for enhancing skin permeation of meloxicam. *Biol. Pharm. Bull.*, **37**, 239–247 (2014).
12) de la Maza A, Parra JL. Solubilization of liposomes formed by lipids modeling the stratum corneum caused by alkyl pyridinium surfactants. *Chem. Phys. Lipids*, **87**, 159–169 (1997).
13) Duangjit S, Opanasopit P, Rojanarata T, Ngawhirunpat T. Effect of edge activator on characteristic and *in vitro* skin permeation of meloxicam loaded in elastic liposomes. *Adv. Mat. Res.*, **194–196**, 537–540 (2011).
14) van den Bergh BA, Wertz PW, Junginger HE, Bouwstra JA. Elasticity of vesicles assessed by electron spin resonance, electron microscopy and extrusion measurements. *Int. J. Pharm.*, **217**, 13–24 (2001).
15) Cevc G. Material Transport Across Permeability Barriers by Means of Lipid Vesicles. *Handbook of Biological Physics.* (Lipowsky R, Sackmann E eds.) Elsevier Science B.V., pp. 465–490 (1995).
16) Arai H, Suzuki T, Kaseda C, Ohyama K, Takayama K. Bootstrap re-sampling technique to evaluate the optimal formulation of theophylline tablets predicted by non-linear response surface method incorporating multivariate spline interpolation. *Chem. Pharm. Bull.*, **55**, 586–593 (2007).
17) Duangjit S, Opanasopit P, Rojanarata T, Ngawhirunpat T. Evaluation of meloxicam-loaded cationic transfersomes as transdermal drug delivery carriers. *AAPS PharmSciTech*, **14**, 133–140 (2013).
18) Mohammed AR, Weston N, Coombes AGA, Fitzgerald M, Perrie Y. Liposome formulation of poorly water soluble drugs: optimisation of drug loading and ESEM analysis of stability. *Int. J. Pharm.*, **285**, 23–34 (2004).
19) Zucker D, Marcus D, Barenholz Y, Goldblum A. Liposome drugs' loading efficiency: A working model based on loaded conditions and drugs' physicochemical properties. *J. Control. Release*, **139**, 73–80 (2009).
20) Elsayed MMA, Abdallah OY, Naggar VF, Khalafallah NM. Lipid vesicles for skin delivery of drugs: Reviewing three decades of research. *Int. J. Pharm.*, **332**, 1–16 (2007).
21) Chen L-Y, Cheng C-W, Lin J-J, Chen W-Y. Exploring the effect of cholesterol in lipid bilayer membrane on the melittin penetration mechanism. *Anal. Biochem.*, **367**, 49–55 (2007).
22) Gupta PN, Mishra V, Rawat A, Dubey P, Mahor S, Jain S, Chatterji DP, Vyas SP. Non-invasive vaccine delivery in transfersomes, niosomes and liposomes: a comparative study. *Int. J. Pharm.*, **293**, 73–82 (2005).
23) Ahad A, Aqil M, Kohli K, Sultana Y, Mujeeb M, Ali A. Formulation and optimization of nanotransfersomes using experimental design technique for accentuated transdermal delivery of valsartan. *Nanomedicine*, **8**, 237–249 (2012).
24) Uchino T, Lefeber F, Gooris G, Bouwstra J. Physicochemical characterization of drug-loaded rigid and elastic vesicles. *Int. J. Pharm.*, **412**, 142–147 (2011).
25) Bourquin J, Schmidli H, van Hoogevest P, Leuenberger H. Comparison of artificial neural networks (ANN) with classical modelling techniques using different experimental designs and data from a galenical study on a solid dosage form. *Eur. J. Pharm. Sci.*, **6**, 287–300 (1998).
26) Dupret G, Koda M. Bootstrep re-sampling for unbalanced data in supervised learning. *Eur. J. Oper. Res.*, **134**, 141–156 (2001).
27) Zhang J. Inferential estimation of polymer quality using bootstrep aggregated neural networks. *Neural Netw.*, **12**, 927–938 (1999).

Advanced Materials Research Vol. 1060 (2015) pp 21-24
© (2015) Trans Tech Publications, Switzerland
doi:10.4028/www.scientific.net/AMR.1060.21

Submitted: 15.07.2014
Revised: 22.08.2014
Accepted: 12.09.2014

Development and Evaluation of Tamarind Seed Xyloglucan for Transdermal Patch of Clindamycin

Sureewan Duangjit,[1,a] Parin Buacheen,[1,b]
Pongsakorn Priebprom,[1,c] Sittikun Limpanichkul,[1,d]
Panida Asavapichayont,[1,e] Porntip Chaimanee,[2,f]
and Tanasait Ngawhirunpat,[1,g]

[1]Faculty of Pharmacy, Silpakorn University, Nakhon Pathom 73000 Thailand

[2]Faculty of Science, Silpakorn University, Nakhon Pathom 73000 Thailand

[a]dsureewan@hotmail.com, [b]parin.docu@gmail.com, [c]prieprom802@hotmail.com,
[d]sittikun.t@hotmail.com, [e]apanida@su.ac.th, [f]porntip@su.c.th, [g]tanasait@su.ac.th

Keywords: Tamarind seed extract, Xyloglucan, Clindamycin, Transdermal patch, Acne vulgaris, Staphyllococus aureus

Abstract. The object of this study was to develop the clindamycin transdermal patch using extracts of tamarind seeds as novel gelling agent for transdermal delivery. The patch was composed of tamarind seed extracts having xyloglucan as a main composition, 1% clindamycin, and various ratios of glycerin and propylene glycol i.e. 10:0, 8:2, 6:4, 5:5, 4:6, 2:8 and 0:10, as plasticizer and penetration enhancer, respectively. The clindamycin patch was prepared by casting method. The content of clindamycin in the patch, the tensile strength and the drug release from the patch were evaluated. Moreover, the cup and plate method was used to determine the antimicrobial activity of clindamycin patch compared with commercial available clindamycin gel in the market, and *Staphyllococcus aureus* was used as test organism in this study. The results showed that the good physical stability of clindamycin patches were successfully prepared. The ratio of composition in the formulation affected the tensile strength and the drug release. As the ratio of propylene glycol to glycerin in the formulation was increased, the tensile strength and the drug release increased. The formulation composed of the ratio of glycerin and propylene glycol (4:6) showed the highest drug release and the best efficiency in antibiotic test. Our results indicated that the extracts of tamarind seeds could be a potential biopolymer and also applied as controlled release in transdermal delivery system.

Introduction

Natural polymers have been extensively used as biopolymers in pharmaceutics because of their naturalness and non-toxicity materials. Xyloglucan (XG) is a natural glucosaminoglycan polysaccharide derived from the tamarind seed (*Tamarindus indica*). Thus, tamarind seed XG was used as binder, stabilizer, plasticizers, thickening agent and gelling agent in various drugs delivery system such as oral [1], buccal [2] or rectal [3] drug delivery, because of its biodegradability and biocompatibility properties. Acne vulgaris is a common chronic inflammatory disease of the pilosebaceous units. Standard therapies were available for acne vulgaris e.g. oral and topical antibiotics. Clindamycin phosphate is the most common topical antibiotic used in the treatment of acne vulgaris for over 20 years [4]. However, poor patient compliance was a major cause of treatment failure because of low efficacy, slow onset of action, adverse effects [5]. The new formulation of topical acne treatment to improve patient adherence with medication, which is ease of use, prolong release, reduce lesion counts and conceal redness is extremely interested. In this study, novel transdermal patch of clindamycin was developed using extracts from tamarind seed to overcome acne treatment failures. Moreover, the content of clindamycin in the patch, the tensile strength, the drug release from the patch and the antimicrobial activity were evaluated.

Materials Tamarind seed xylogluxan (XG) was gifted by Faculty of Science, Silpakorn University, Thailand. Clindamycin phosphate (CM) was obtained as a gift sample from Bangkoklab and Cosmetics Co., Ltd. (Ratchaburi, Thailand). All other chemicals and solvents were of analytical grade.

Methods

Preparation of CM transdermal patch. CM patches using XG as gelling agent were prepared by casting method. The dispersion of 1% XG and 1% CM in purified water were mixed with the various ratios of glycerin (Gly) and propylene glycol (PG) at 10:0, 8:2, 6:4, 5:5, 4:6, 2:8 and 0:10. The polymer mixture of XG and CM were stirred for 12 h at room temperature (25 °C), then they were poured and dried on the petri-dish at 60 °C for 12 h.

Evaluation of transdermal patch.

Drug content. The content of CM was extracted from the transdermal patches to potassium phosphate solution (PS, pH 2.5). Two mg of CM in the patch samples were immersed in 15 mL of PS and stirred for 2 h. The solution was centrifuged at 10,000 rpm at 25 °C for 30 min. The supernatant was filtered with 0.45 μm nylon syringe filter. Then, CM in each sample was determined by HPLC.

Tensile strength. The tensile strength of the patches was evaluated by Texture Analyzer (TA.XT plus, stable Micro Systems, Inc., NY, USA) with a 5 kg load cell equipped with tensile grip holder. The patches were cut into rectangular shape (5 x 25; mm). The thickness of each patches ranged from 0.2-0.4 mm. The tensile strength at break value was calculated.

***In vitro* release of CM from transdermal patch.** The Franz's diffusion cell with an available release area of 1.85 cm^2 was employed. The membrane with MWCO 6,000-8,000 (Nuclepore; Whatman Inc., MA, USA) was used as a membrane for *in vitro* release study. The receiver chamber was filled with 6.5 mL of phosphate buffer saline (PBS; pH 7.4, 37 °C) and the donor chamber was mounted with the round patch sample (7.07 cm^2). At appropriate times (0-8 h), 1 mL of the release medium was withdrawn, and the same volume of fresh buffer solution was replaced in the receiver chamber. The concentration of CM in the aliquot was analyzed using HPLC (Agilent 1100 series, Agilent Technologies, USA). The analytical column was VertiSep® C8 column (250 mm × 4.6 mm, 5 μm particle size), and the mobile phase consisted of PS (pH 2.5)/acetronitrile (77.5:22.5, v/v). The flow rate was set at 1 mL/min, and the wavelength used in this determination was 210 nm.

Antimicrobial test. The antimicrobial activity of the transdermal patch was tested against *Staphyllococus aureus* (*S. aureus*) using the cup and plate method. The cylinder cups were placed onto the top of the TSB plates. The release medium after 8 h of each sample (CM patch, CM gel, blank-patch, standard CM solution (as positive control) and PBS (as negative control)) was poured into the cups and then incubated at 37 °C for 24 h. The inhibition zone were observed and evaluated.

Results and discussion.

Physical properties of CM transdermal patch. The physical appearance of the CM patch with various ratios of Gly and PG are shown in Fig. 1. The Gly in the patch formulation affected the appearance of the patch e.g. softness, smoothness, moistness, toughness and beauty patch as its plasticizer and humectant property. The Gly and PG patch of 4:6 showed the optimal ratio and had good appearance, while the patches of 0:10 and 2:8 were the most roughness, brittleness and moistureless patch, respectively.

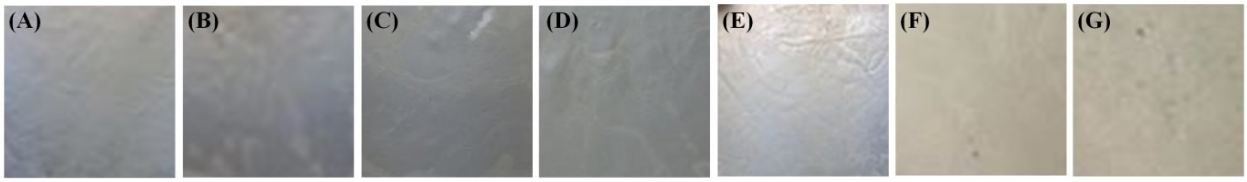

Fig. 1. The physical appearance of the CM patch with differenct ration of Gly and PG: (A) 10:0, (B) 8:2, (C) 6:4, (D) 5:5, (E) 4:6, (F) 2:8 and (G) 0:10.

Drug content, tensile strength and drug release study. The ratio of Gly and PG in the formulation also affected the drug content, tensile strength and drug release of the CM patches. As shown in Fig. 2, Gly and PG not only affected the tensile strength, but also the *in vitro* drug release. The patch with Gly and PG at the ratio of 4:6 showed the optimal tensile strength and maximum drug release when compared to other formulations, whereas, the patch with Gly and PG at the ratio of 2:8 became very brittle. Our results corresponded well with the study of Song and Zheng [6]. This could be explained by the poor plasticity effect of Gly at low concentration and the plenty nanopores existed in the patch formulation. Moreover, the CM release from the patch increased when the PG ratio was increased. Shingade G. reported that the nabumetone release from the gels increased with increase the concentration of PG in the formulation [7].

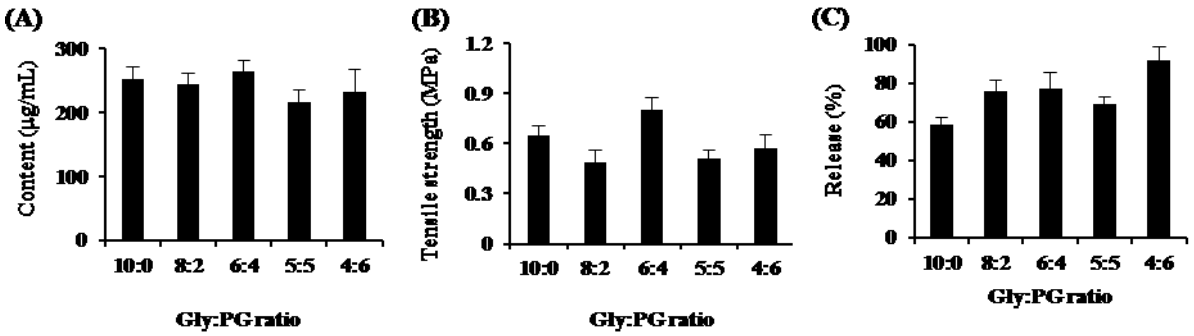

Fig. 2. Effect of glycerin and propylene glycol on the CM transdermal patch: (A) the drug content, (B) the tensile strength and (C) the in vitro drug release.

The influence of Gly and PG on the release kinetic CM from the transdermal patch using tamarind seed XG as gelling agent is illustrated in Table 1. The results suggested that the linear relationship was obtained, when the percentage of CM release was plotted against the square root of time, indicating that the release of CM from the transdermal patches was described by the Higuchi model. The CM release from the patch formulation could be controlled by the XG transdermal patch. The rate limiting step was the process of diffusion through the XG transdermal patch matrix; thus this system was observed in the delivery system that the drug is freely soluble in the formulation, and the membrane does not significantly affect the release of the drug [7].

Table 1. The release kinetics of CM from different formulations

Model of release kinetics (R^2)	**Formulation (Gly : PG)**				
	10:0	**8:2**	**6:4**	**5:5**	**4:6**
Zero-order $Q = k\,[8]^0$	0.9387	0.9707	0.8934	0.8344	0.8899
First-order $Q = [8]^0 e^{-kt}$	0.8738	0.9076	0.8274	0.7733	0.8188
Higuchi-model $Q = kt^{1/2}$	0.9853	0.9910	0.9593	0.9117	0.9573

Antimicrobial activities of CM transdermal patch. 1% CM is a topical antibiotic approved for the commercial product for treatment of acne vulgaris. Fig. 3 shows the inhibition zone of bacteria growth by the CM patch of Gly and PG (4:6) compared with CM gel, blank-patch, PBS and standard CM solution after 24 h incubation with *S. aureus*. The CM patch inhibited *S. aureus* growth as well as the CM gel. Because, CM inhibits bacteria protein synthesis at the ribosomal level by binding to the 50s ribosomal subunit, and proceeds the peptide chain initiation. This result indicated that the CM transdermal patch using tamarind seed XG as gelling agent showed a good efficiency in antimicrobial test, and its antimicrobial activity was not significantly different from the commercial product of CM.

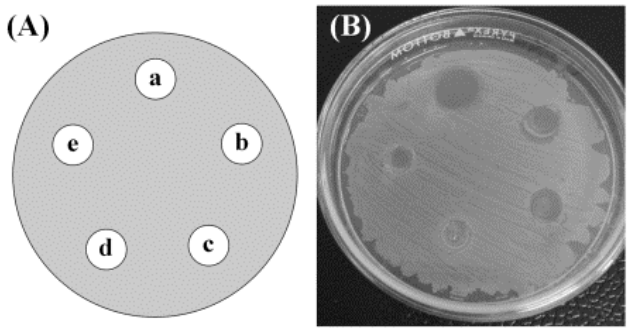

Fig. 3. The antimicrobial activity of CM transdermal patch (4:6): (A) the position of each sample (a) standard CM solution, (b) CM patch, (c) CM commercial gel, (d) blank-patch and (e) phosphate solution, and (B) the inhibition zone observed after incubated at 37 °C for 24 h.

Summary

The 1% clindamycin transdermal patches composed of tamarind seed extracts, glycerin and propylene glycol was successfully prepared. The incorporation Gly and PG in the tamarind seed XG patch affected the physical properties of CM transdermal patch. The patch composed of Gly and PG (4:6) provided the highest drug release and the best efficiency in antibiotic test. Our results indicated that the extracts of tamarind seeds could act as a potential biopolymer and could also be applied as controlled release in transdermal delivery system.

Acknowledgements

The authors are grateful to the Thailand Research Funds through the Basic Research Grant (BRG 5680016) and the Faculty of Pharmacy, Silpakorn University, Thailand for the financial and facilities support.

References

[1] K. Itoh, M. Yahaba, A. Takahashi, R. Tsuruya, S. Miyazaki, M. Dairaku, M. Togashi, R. Mikami, and D. Attwood: Int J Pharm Vol. 356 (2008), p. 95–101

[2] D. R. Nisbet, K. E. Crompton, S. D. Hamilton, S. Shirakawa, R. J. Prankerd, D. I. Finkelstein, M. K. Horne, and J. S. Forsythe: Biophy Chem Vol. 121 (2006), p. 14-20

[3] Miyazaki S, Suisha F, Kawasaki N, Shirakawa M, Yamatoya K, and Attwood D: J Control Release. Vol. 56 (1998), p. 75-83

[4] J. A. Myers, M. Spellman, A. Yaroshinsky, and A. Shalit: J Am Acad Dermatol Vol. 50 (2004), p. 24

[5] B. Dréno, F. Nantes, and A. Layton: J Am Acad Dermatol Vol. 68 (2013), p. AB17

[6] Y. Song and Q. Zheng: Bioresource Technol Vol. 99 (2008), p. 7665–7671

[7] G. Shingade: World J Pharm Res Vol. 1 (2012), p. 776-785

[8] T. N. C. Dantas, H. S. R. C. Silva, A. A. D. Neto, M. C. Marcucci, and M. A. M. Maciel: Braz J Pharmacogn Vol. 20 (2010), p. 368–375

International Journal of Nanomedicine

Dovepress
open access to scientific and medical research

Open Access Full Text Article

ORIGINAL RESEARCH

Mechanistic study of decreased skin penetration using a combination of sonophoresis with sodium fluorescein-loaded PEGylated liposomes with D-limonene

This article was published in the following Dove Press journal:
International Journal of Nanomedicine
15 December 2015
Number of times this article has been viewed

Worranan Rangsimawong
Praneet Opanasopit
Theerasak Rojanarata
Tanasait Ngawhirunpat

Faculty of Pharmacy, Silpakorn University, Nakhon Pathom, Thailand

Abstract: The effect of low frequency sonophoresis (SN, 20 kHz) on the skin transport of sodium fluorescein (NaFI)-loaded liposomes was investigated. An in vitro skin penetration study in open and blocked hair follicles was performed, and confocal laser scanning microscopy and scanning electron microscopy were used to visualize the penetration pathways. The results showed that SN significantly increased the flux of NaFI solution, whereas it significantly decreased the flux of NaFI-loaded polyethylene glycol-coated (PEGylated) liposomes with D-limonene (PL-LI). SN did not significantly affect the flux of NaFI-loaded conventional liposomes and PEGylated liposomes. In the blocked follicles, the flux of NaFI-loaded PL-LI both with and without SN decreased, indicating that NaFI-loaded PL-LI penetrated the skin via the transfollicular pathway. A confocal laser scanning microscopy image showed that in the skin without SN, the fluorescence intensity of NaFI-loaded PL-LI was observed in the skin and along the length of hair inside the skin, whereas in the skin with applied SN, the fluorescence intensity was detected only on the top of hair outside the skin. From scanning electron microscopy images, SN dislocated the corneocytes and reduced the deposition of PL-LI around hair follicles. These results revealed that SN may partially plug hair follicle orifices and reduce percutaneous absorption through the follicular pathway.

Keywords: sonophoresis, PEGylated liposomes, hydrophilic compound, follicular pathway

Introduction

Sonophoresis (SN) is a non-invasive technique for increasing the skin permeability of various medications, including hydrophilic and large molecular weight compounds such as caffeine,[1,2] hydrocortisone,[3] calcein, and FITC-labeled dextrans. The transdermal delivery of hydrophilic solutes with low-frequency ultrasound is likely to occur as non-specific transport across the stratum corneum (ie, both the intracellular lipid regions and the corneocytes).[4] Several possible mechanisms for SN as a transport pathway have been suggested, such as thermal effects by absorption of ultrasound energy and cavitation effects caused by collapse and oscillation of cavitation bubbles in the ultrasound field.[5,6] Cavitation has been found to be the main factor in creating aqueous pathways across the stratum corneum by distorting the lipid bilayer, which can lead to enhancing the transport of hydrophilic drugs across the skin.[7]

Low-frequency SN typically enhances the transport of hydrophilic molecules in solution across the skin. It can easily be coupled with other transdermal drug delivery techniques such as tape stripping,[8] microneedle,[9] electroporation,[10] iontophoresis,[11] and chemical enhancement to produce a synergistic effect on transdermal

Correspondence: Tanasait Ngawhirunpat
Faculty of Pharmacy, Silpakorn University, 6 Racchamakka Nai Road, Nakhon Pathom 73000, Thailand
Fax +66 3 425 5801
Email ngawhirunpat_t@su.ac.th

drug delivery through an intracellular pathway.[12] The combination of SN and liposomes in skin permeation has rarely been studied, and whether these methods have a synergistic effect is still controversial. Vyas et al showed that the application of ultrasound and an ointment containing liposomes enhanced diclofenac-entrapped liposome permeation across the skin.[13] However, Dahlan et al reported that the liposome application to sonicated skin prior to application of bovine serum albumin solution reduced bovine serum albumin penetration and transepidermal water loss due to the repair of sonication-induced skin disruption.[14] Moreover, no mechanistic study for liposome penetration into skin combined with SN has yet been reported in term of skin penetration pathway, particularly for the utilization of liposomes as a transfollicular drug delivery system.

D-limonene ($C_{10}H_{16}$) is one of the most common terpenes in nature that has been widely used as skin penetration enhancers. It can be remained in the lipid portion of the stratum corneum, and can fluidize or perturb the integrity of the barrier function of the stratum corneum for enhanced transport of both hydrophilic and hydrophobic drugs through the skin.[15] Polyethylene glycol (PEG), a hydrophilic polymer, grafted onto the surface of the liposomes (PEGylated liposomes, PL), was reported to enhance skin penetration of zidovudine by binding to water molecules, increasing the hydration of the stratum corneum.[16] In addition, our previous work reported that D-limonene containing PL provided a synergistic effect to enhance penetration of hydrophilic compounds into and through the skin.[17]

Therefore, the aim of this study was to investigate the effect of low frequency SN (20 kHz) on the follicular pathway for transport of sodium fluorescein (NaFI)-loaded PL into porcine skin. PL containing D-limonene has been used as a carrier to enhance transdermal delivery of hydrophilic NaFI, with the transfollicular pathway as the major penetration pathway.[17] NaFI was used as a hydrophilic fluorescent compound entrapped in vesicles. Liposomal formulations were prepared by the sonication method. The particle size, shape, and in vitro skin penetration were investigated. Selectively blocked hair follicles were prepared to compare with open hair follicles. Confocal laser scanning microscopy (CLSM) and scanning electron microscopy were used to visualize the skin penetration pathways of the vesicles.

Methods

Materials

Egg phosphatidylcholine (PC) and Na-salt *N*-(carbonyl-methoxypolyethylen glycol-2000)-1,2-distearoyl-*sn*-glycero-3-phosphoethanolamine (PEG_{2000}-DSPE) were purchased from Lipoid GmbH, Ludwigshafen, Germany. Cholesterol (Chol) was purchased from Carlo Erba Reagent, Ronado, Italy. Tween 20 was purchased from Ajax Finechem, Auckland, New Zealand. NaFI and D-limonene were purchased from Sigma-Aldrich, St Louis, MO, USA. Lissamine™ rhodamine B 1,2-dihexadecanoyl-*sn*-glycero-3-phosphoethanolamine triethylammonium salt (Rh-PE) was purchased from Invitrogen, Carlsbad, CA, USA.

Liposome preparation

The formulations of the liposomes containing PC, Chol, PEG_{2000}-DSPE, Rh-PE, NaFl, and D-limonene are shown in Table 1. The liposomes were prepared using the sonication method. Briefly, a mixture of PC, Chol, PEG_{2000}-DSPE, and Rh-PE (as fluorescence probe) dissolved in chloroform/methanol (2:1, v/v) was evaporated using the flow of N_2 gas in tubes and placed in a desiccator at 6 hours. The lipid film was hydrated with NaFI solution and mixed with D-limonene in 2% (w/v) Tween 20 solution. PL and conventional liposomes (CL) were prepared using the same process described earlier. The particle size of all formulations was reduced following probe-sonication for 30 minutes. The particle size of all formulations was reduced following probe-sonication (Vibracell™, VCX 130 PB, Sonics and Materials, Inc., Newtown, CT, USA) with a frequency of 40 kHz at 40% amplitude for one cycle of 30 minutes under ice bath. An excess lipid composition was separated from vesicle formulation by centrifugation at 15,000 *g* at 4°C for 15 minutes.

Table 1 The composition of the different liposomal formulations

Formulations	NaFI (mM)	PC:Chol:PEG_{2000}-DSPE (mM)	PC:Rh-PE (mM)	D-limonene (mM)
CL	5.59	10:2	100:1	–
PL	5.59	10:2:0.12	100:1	–
PL-LI	5.59	10:2:0.12	100:1	73.41

Abbreviations: CL, conventional liposome; Chol, cholesterol; NaFI, sodium fluorescein; PC, phosphatidylcholine; PEG_{2000}-DSPE, Na-salt *N*-(carbonyl-methoxypolyethylen glycol-2000)-1,2-distearoyl-*sn*-glycero-3-phosphoethanolamine; PL, PEGylated liposome; PL-LI, PEGylated liposome with D-limonene; Rh-PE, Lissamine™ rhodamine B 1,2-dihexadecanoyl-*sn*-glycero-3-phosphoethanolaminetriethylammonium salt.

Characterization of liposomal formulations

Particle size and surface charge

Each liposome formulation was diluted with an appropriate amount of water and measured for particle size, size distribution, and zeta potential, using a dynamic light scattering particle size analyzer (Zetasizer Nano-ZS, Malvern Instrument, Malvern, UK) with a 4 mW He–Ne laser at a scattering angle of 173°.

Particle size and shape by transmission electron microscopy

Each liposome formulation was diluted with an appropriate amount of distilled water and placed in a sonicator bath for 10 minutes and then dropped onto a formvar-coated copper grid. The sample was observed using transmission electron microscopy (JEM 1230, JEOL Ltd, Tokyo, Japan) at 80 kV for particle size and shape measurements. The image analysis software (JMicroVision V.1.2.7, University of Geneva, Geneva, Switzerland) was used to determine the diameter of the particle.

Drug entrapment efficiency

The NaFI entrapped liposomes was established by using an ultrafiltration tube with a molecular weight cutoff of 3,000 Da (Microcon YM-3; Millipore, Billerica, MA, USA). Briefly, liposomes in ultrafiltration tube were centrifuged at 4°C at 10,000× *g* for 60 minutes. 0.25 mL of phosphate-buffered saline (PBS) was added to the retentate and centrifuged at 4°C at 10,000× *g* for 40 minutes. The retentate was disrupted with 0.2 mL of 0.1% (w/v) Triton X-100 and centrifuged at 4°C at 10,000× *g* for 10 minutes. The NaFI content of the supernatant was determined by fluorescence analysis and calculated with the following:

$$\% \text{ EE} = (\text{CL}/\text{Ci}) \times 100 \quad (1)$$

where % EE is the entrapment efficiency, CL is the concentration of NaFI in the liposomal formulation, and Ci is the initial concentration of NaFI added.

In vitro skin permeation study

Preparation of the porcine skin

Abdominal porcine skin was taken from intrapartum stillbirth animals provided by a farm in Nakhon Pathom. Subcutaneous fat was carefully removed using medical scissors and surgical blades (thickness ~0.6–0.7 mm). The skin samples were frozen at −20°C until use. The skin samples were thawed at room temperature using PBS (pH 7.4) prior to the experiments.

Selectively blocked hair follicle

All hair follicles in the skin sample were blocked by using the follicular closing technique.[15] Each skin sample had a hair follicle density on average between 30 and 40 follicles per application area (1.96 cm^2). One microdrop of nail varnish using a blunt 27-gauge needle was carefully placed beside each hair follicle orifice and dried for 5 minutes to completely block the follicular shunt. Then, the skin samples were washed with PBS and mounted on Franz cells.

Skin permeation study

In vitro permeation studies of NaFI through porcine skin were performed using Franz diffusion cells. Briefly, ~2 mL of NaFI-loaded liposomes was added to the skin surface in the donor compartment (an average diffusion area of 2.022 cm^2), and the receptor compartment of the cell was filled with 6 mL of PBS. The skin samples, which were mounted on the Franz cells, were treated with ultrasound. The diffusion studies were performed for 24 hours. The 0.5 mL of receiver medium was withdrawn at predetermined time points of 1, 2, 4, 6, 8, and 24 hours for analysis by the fluorescence-detection method, and an identical volume of PBS was added into the receiver compartment to maintain a constant volume. The cumulative amount profile was plotted against time. The steady-state flux was determined as the slope of the linear portion of the plot. Each sample was analyzed in triplicate.

For passive delivery studies, a similar procedure to the SN-treated skin studies was followed, except that the skin samples were not subjected to ultrasound treatment.

Sonophoresis-treated skin

Low frequency SN at 20 kHz was generated by using an ultrasonic transducer (Vibra-cell™, VCX130 PB, Sonics and Materials, Inc.), which has a transducer probe with a radiating diameter of 6 mm. The ultrasound transducer probe was placed inside the donor compartment with its active horn face located 3 mm above the skin surface. NaFI-loaded liposomes (as a coupling medium) were placed in the donor chamber. The skin was then continuously sonicated for 2 minutes (100% duty cycle, 25% amplitude). The acoustic intensity applied was 1.90 W/cm^2, which was calculated from the following equation:

$$\text{Intensity } (\text{Watts/cm}^2) = \frac{\text{Power (Watts)}}{\text{Area of skin } (\text{cm}^2)} = \frac{\text{Sound energy (joules)}}{\text{Area of skin } (\text{cm}^2) \times \text{Application time (second)}} \quad (2)$$

Fluorescence analysis

The NaFI concentration was analyzed using a fluorescence spectrophotometer (Fusion™ Universal Microplate Analyzer, Packard Instrument Company, Inc., Downers Grove, IL, USA). The excitation wavelength was 485 nm, and the emission wavelength was 535 nm. One hundred µL of the sample was pipetted into a black 96-well plate, and fluorescence was detected for three replicates of each sample.

Confocal laser scanning microscopy

After 4 hours of in vitro skin penetration study, the whole skins were cross-sectioned using a cryostat (Leica 1850, Leica Instrument). Each skin sample was mounted on a metal sample holder using a frozen section medium (Neg50, Microm International, Waldorf, Germany). The frozen skin was sectioned into 10 µm slices and placed on glass microscope slides. The skin tissues were mounted with mounting medium and covered with a cover slip. Confocal images were obtained using the 10× objective lens system of an inverted Zeiss LSM 510 META microscope (Carl Zeiss AG, Jena, Germany) with a He–Ne laser (excitation wavelength 543 nm; emission wavelength 580 nm), Ar laser (excitation wavelength 488 nm; emission wavelength 514 nm), and diode laser (excitation wavelength 358 nm; emission wavelength 461 nm).

Scanning electron microscopy

After 4 hours in vitro skin penetration study, porcine skin was visualized to study the effect of liposomal formulations and SN on epidermal structure. Each skin sample was cut into pieces (1×2 mm) from the central area. The samples were rapidly frozen in liquid nitrogen and dried using a Freeze-Dry System (FreeZone 2.5; Labconco, Kansas City, MO, USA) for 24 hours. The dried specimens were gold coated using a sputtering device. Specimens were then observed with a scanning electron microscope (Camscan Mx2000; Obducat Camscan Ltd, Cambridge, UK).

Statistical analysis

One-way analysis of variance followed by a least significant difference post hoc test was used to analyze the statistical significance of observed differences. The significance level was set at $P<0.05$.

Results and discussion

Physicochemical characterization of liposomal formulations

The average size of CL, PL, and PEGylated liposomes with D-limonene (PL-LI) was 105.40±4.50, 71.30±1.22, and 43.59±1.37 nm, respectively, with a narrow size distribution (polydispersity index below 0.3). Similar to the observed particle size from transmission electron microscopy technique, the average particle size of CL, PL, and PL-LI was 112.95±14.01, 58.62±6.93, and 44.81±6.55 nm, respectively, with a spherical shape (Figure 1). In a previous study, the particle sizes of PL and PL-LI were significantly lower than CL because PEG molecules at the surface of the liposome provided a significant reduction in attractive force (van der Waals) and an increase in the repulsive forces (steric, electrostatic, and hydration) for formation. In addition, Tween 20 added into PL-LI formulations can decrease the size of the liposome vesicle. All liposomes formulations showed a negative surface charge (−8.74 to −12.65 mV). As the pH of

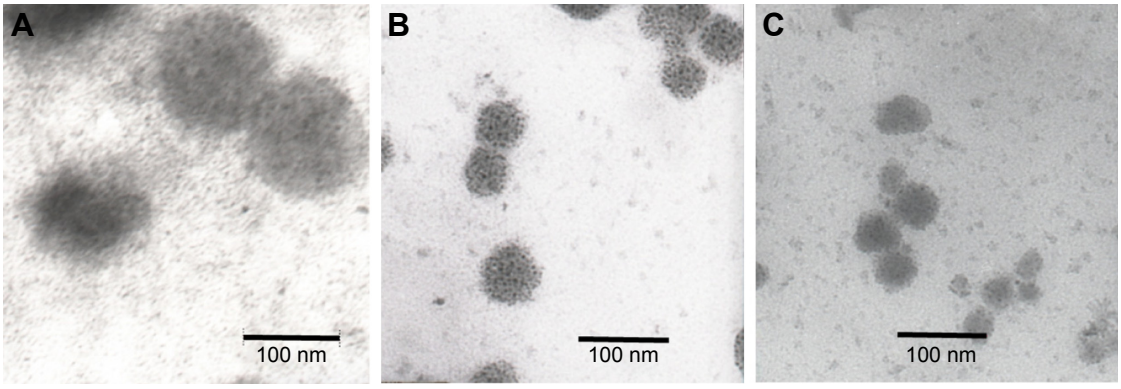

Figure 1 Transmission electron microscopy images of NaFI-loaded liposomes.
Notes: (**A**) CL, (**B**) PL, and (**C**) PL-LI.
Abbreviations: CL, conventional liposome; NaFI, sodium fluorescein; PL, PEGylated liposome; PL-LI, PEGylated liposome with D-limonene.

study condition (pH 7.4) was higher than the isoelectric point of PC (isoelectric point between 6 and 6.7), the PC vesicle exhibited a negative charge.[17]

The drug entrapment efficiency of CL, PL, and PL-LI was 17.33%±1.13%, 21.76%±1.56%, and 29.60%±2.35%, respectively. According to the presence of PEG-lipids in the liposome formulation, the membrane bilayer became more polar and the efficiency of incorporation of the hydrophilic drug increased.[16] In addition, edge activator and terpenes may lead to formation of pores in the bilayer, destabilize the lipid bilayers of vesicles, and increase the flexibility of the membrane.[18–24]

In vitro skin penetration study

Figure 2A presents the cumulative amount of NaFI permeated into the skin at different time points, in which the amount of NaFI through the skin was in the following order: PL-LI without SN>NaFI solution with SN>PL-LI with SN>PL without SN>PL with SN>CL with SN>CL without SN>NaFI solution without SN. For skin without SN, PL-LI showed the highest cumulative amount of NaFI, followed by PL, CL, and NaFI solution. In our previous study, liposomes containing Tween 20 (as an edge activator) increased deformability of vesicle bilayer, thus resulting in increased skin permeability of NaFI. As D-limonene (as skin penetration enhancers) was incorporated into liposomes containing an edge activator a synergistic enhancement of skin penetration of NaFI was observed.[20] In SN-treated skin, the NaFI solution showed higher cumulative penetration than other formulations. However, there was no significant difference in skin permeation of NaFI-loaded CL or PL with or without SN.

From these results, the steady-state flux of NaFI was used to determine the effect of SN on each formulation (Figure 2B). SN significantly increased the NaFI flux in NaFI solution from 0.0058 (without SN) to 0.2999 µg/cm²/h (with SN), indicating that using SN resulted in a 51.7-fold enhancement in permeation over passive delivery. SN is a more effective technique in enhancing transdermal delivery of small hydrophilic molecules,[2] as the NaFI solution permeated better through the skin with SN than with liposomal formulations. The mechanism of SN is acoustically induced cavitation to create intercellular lipid channels and defects in the stratum corneum both in the lipid bilayer and in the corneocyte, which induces aqueous permeation pathways at discrete sites.[4,9,25] In SN, both cavitation and temperature affect the solute diffusivity. Thermal energy provides a doubling of permeability for every 10°C of increase in temperature.[26] However in this study, there was no significant rise in temperature of the donor solutions in contact with the sonicated skin (increased ~1°C–2°C); therefore, the NaFI diffusity was mainly due to cavitation from SN.

In contrast, SN significantly decreased the NaFI flux of PL-LI from 0.5380 (without SN) to 0.1914 µg/cm²/h, indicating that using SN resulted in a 2.81-fold decrease in skin permeation compared with passive delivery. Similarly to PL, SN decreased the NaFI flux of PL from 0.0600 (without SN) to 0.0427 µg/cm²/h (1.41-fold), while SN increased the NaFI flux of CL from 0.0250 (without SN) to 0.0418 µg/cm²/h (5.36-fold). However, the NaFI flux of CL and PL between with and without SN was not significantly different, indicating that SN had no effect on the penetration route of CL and PL. According to Vyas et al,[13] in the application of diclofenac-loaded liposomal ointment, with ultrasound enhancement diclofenac permeated across the skin better than liposome ointment alone. The improved diffusion is probably due to the breaking of lamellae on

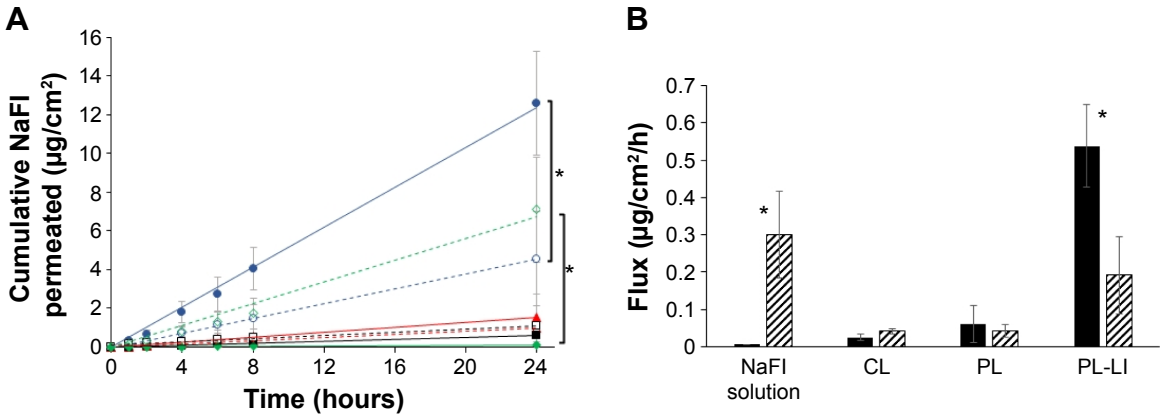

Figure 2 The skin permeation profile and flux of NaFI solution and NaFI loaded in different liposomal formulation with and without SN.
Notes: (**A**) The cumulative amount-time profiles of NaFI in different liposomal formulations with and without SN. Symbols: PL-LI with SN (○) and without SN (●), PL with SN (△) and without SN (▲), CL with SN (□) and without SN (■), and NaFI solution with SN (◇) and without SN (◆). (**B**) Comparison of NaFI flux (µg/cm²/h) of each liposome formulation with (▨) and without SN (■). Each value represents the mean ± SD (n=3). *Indicates significant difference between groups ($P<0.05$).
Abbreviations: CL, conventional liposome; NaFI, sodium fluorescein; PL, PEGylated liposome; PL-LI, PEGylated liposome with D-limonene; SN, sonophoresis.

sonication.[13] After releasing the entrapped drug, hydrophilic molecules were transported through the pore pathway in the stratum corneum.[20] When sonication energy was terminated, phospholipid bilayer fragments were rapidly fused and closed to form liposome vesicles.[27] Liposomes repair ultrasound-induced skin disruption by adsorption onto and fusion with the skin surface defect to reduce permeability.[14] Moreover, the penetration pathway of PL-LI was reported to be transfollicular rather than intercellular or intracellular.[16] Therefore, if ultrasound can lead to changes in the structure of the skin surface, the penetration route of NaFI-loaded PL-LI will also be affected. However, PL-LI showed higher NaFI permeation through the skin than CL and PL because D-limonene in PL-LI caused greater skin disruption than that can be repaired by liposome vesicles.

For skin penetration pathways, the delivery of the substances into the skin primarily occurs by two routes, the transfollicular route and the transepidermal routes (intercellular and intracellular penetration).[24] The blocked hair follicles skin (blocked by the nail varnish) presented only the transepidermal route. Therefore, the difference in permeated flux between the open hair follicles skin (transfollicular and transepidermal route) and the blocked hair follicles skin (only transepidermal route) was calculated as the transfollicular penetration flux.[15] For comparison of the blocked and open hair follicles skin, the cumulative amount and the flux of NaFI-loaded PL-LI between with SN and without SN were evaluated (Figure 3). In the blocked hair follicles skin, the flux of NaFI in PL-LI using SN and without SN was very small, thus there was no significant difference in the flux between using SN and without SN.

In the open hair follicle skin, skin without SN exhibited significantly higher cumulative amounts of NaFI than skin with SN. According to our previous study, the major penetration pathway of PL with D-limonene is the transfollicular pathway, while the intercellular and intracellular pathways are minor pathways.[16] Using ultrasound leads to changes in the corneocyte layers in the uppermost layer of skin causing opening up of the continuous surface together with partially sloughing off of the hair follicle orifices, and thus the follicular route of absorption is reduced.[3,24] Therefore, PL-LI that mainly permeated through the follicular route had a higher passive permeability than SN. While the flux of NaFI solution treated with SN and without SN was not significantly different between the open and blocked hair follicle skin (data not shown). These might be caused from that NaFI transported via transepidermal route as a major route.

Visualization of fluorescence dye permeation through SN-treated skin

CLSM images were used to visualize the fluorescence compound, NaFI-loaded liposomes and Rh-PE-probed phospholipid membrane, and demonstrate their skin penetration. Figure 4 shows cross sections of the skin after 4 hours in vitro skin permeation with and without SN of NaFI solution and NaFI-loaded-Rh-PE-labeled liposomes: CL, PL, and PL-LI. In these results, the NaFI and Rh-PE accumulated in the follicle openings, covered the hair and penetrated into the follicular duct. PL-LI without SN showed brighter fluorescence intensity of NaFI and Rh-PE in the skin and the hair follicle than other formulations.

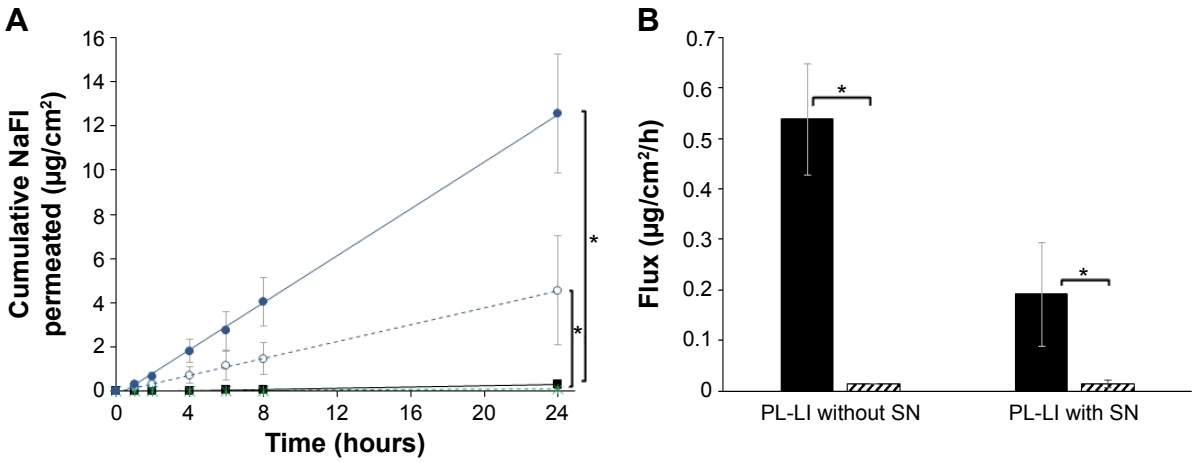

Figure 3 The skin permeation profile and flux of NaFI-loaded PL-LI through blocked hair follicles skin with SN and without SN.
Notes: (**A**) The skin permeation profiles of NaFI-loaded PL-LI permeated through blocked hair follicles skin (with SN [■] and without SN [*]) and open hair follicles skin (with SN [○] and without SN [●]). (**B**) Comparison of NaFI flux (µg/cm²/h) of NaFI-loaded PL-LI permeated through blocked hair follicles skin (▨) and open hair follicles skin (■). Each value represents the mean ± SD (n=3). *Indicates significant difference from other groups ($P<0.05$).
Abbreviations: NaFI, sodium fluorescein; PL-LI, PEGylated liposome with D-limonene; SN, sonophoresis.

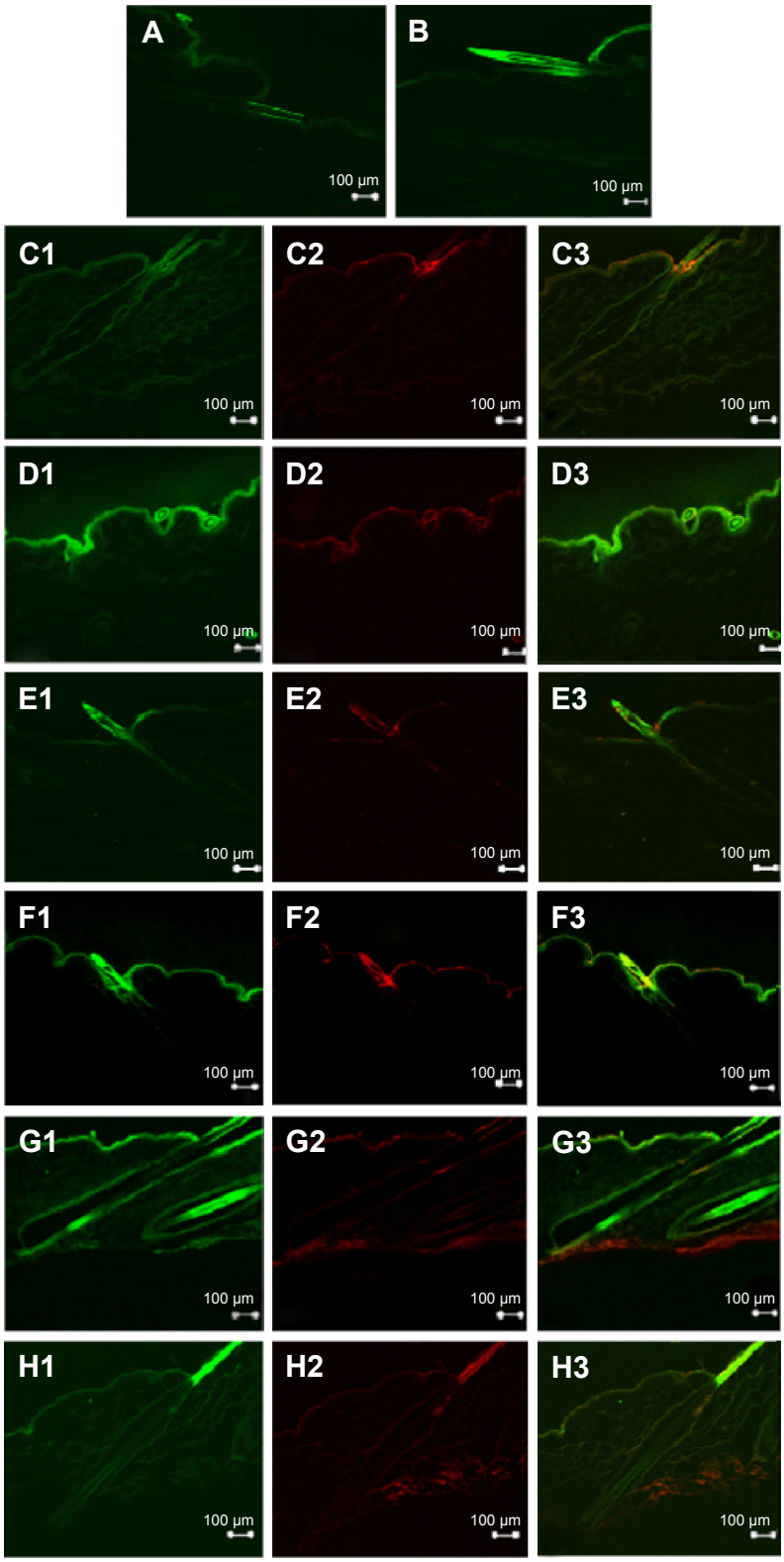

Figure 4 Confocal images of the skin cross section obtained at 4 hours after deposition of (**A**) NaFl solution without SN, (**B**) NaFl solution with SN, (**C**) NaFl-loaded-Rh-PE-labeled liposomes: CL without SN, (**D**) NaFl-loaded-Rh-PE-labeled liposomes: CL NaFl-loaded-Rh-PE-labeled liposomes: CL with SN, (**E**) NaFl-loaded-Rh-PE-labeled liposomes: PL without SN, (**F**) NaFl-loaded-Rh-PE-labeled liposomes: PL with SN, (**G**) NaFl-loaded-Rh-PE-labeled liposomes: PL-LI without SN, and (**H**) NaFl-loaded-Rh-PE-labeled liposomes: PL-LI with SN.

Notes: In images **C** to **H**, it is divided into 3 parts: 1) green fluorescence of NaFl; 2) red fluorescence of Rh-PE; and 3) overlay of green fluorescence of NaFl and red fluorescence of Rh-PE. The scale bar represents 100 μm. All confocal images were obtained at a magnification of ×10.

Abbreviations: CL, conventional liposome; NaFl, sodium fluorescein; PL, PEGylated liposome; PL-LI, PEGylated liposome with D-limonene; Rh-PE, rhodamine B 1,2-dihexadecanoyl-*sn*-glycero-3-phosphoethanolamine triethylammonium salt; SN, sonophoresis.

The skin with SN of NaFI solution, CL, and PL showed brighter fluorescence intensity for both NaFI and Rh-PE-labeled liposome membrane than the skin without SN. The fluorescence was deposited in the stratum corneum surface, covered the hair and in the follicle opening, but did not penetrate into the deep follicular duct. The skin image of PL-LI with SN exhibited weaker fluorescence intensity for NaFI and Rh-PE than skin without SN, which exhibited high intensity fluorescence on the top of hair outside the skin. While PL-LI without SN showed bright fluorescence intensity at a depth of 10–40 μm of the stratum corneum and exhibited deeper penetration around the hair follicle orifice than other regions of skin surface, the fluorescence was also observed along the length of hair inside the skin, indicating the follicular penetration route was the main penetration route. In addition, the Rh-PE-labeled PL-LI membrane showed the deposition of fluorescence at the same region of NaFI and in the deepest layer of skin, suggesting that the intact vesicles might penetrate into skin. However, the fluorescence of NaFI was observed in only some parts of the skin, suggesting that some vesicles might release the entrapped drug before attaching to any part of the skin. These results indicated three mechanisms of skin penetration for the NaFI-loaded PL-LI: i) penetration associated with the liposomal bilayer (intact vesicles), ii) penetration associated with a liposomal bilayer fragment, or iii) penetration solitarily.[28]

The fluorescence intensity of NaFI-loaded-Rh-PE-labeled PL-LI in skin decreased when using SN, indicating that the mechanical effect of ultrasound changed the transport pathway of drug-loaded lipid vesicles. Morimoto et al reported that the differences in the physicochemical properties of the solutes, such as lipophilicity or hydrophilicity, may be affected when using low frequency ultrasound, as the ultrasound increases water transport across the skin. Thus, the distribution of more lipophilic compounds may not be influenced,[4] indicating that PL-LI as a lipid vesicle carrier might not penetrate through hydrophilic transport routes in the intercellular space of the stratum corneum. In addition, liposomes adsorbed onto the skin damage caused by sonication might cause the high fluorescence intensity of both NaFI and Rh-PE-labeled CL and PL at the top of the skin layer.

Scanning electron microscopy

Figure 5 shows scanning electron micrographs of the skin surface for control (PBS), CL, PL, and PL-LI with and without SN. The surface of skin without SN was observed to assess the effect of SN on the transport route of NaFI-loaded liposomal formulations across the skin. Without SN, the surface of the stratum corneum remained relatively flat, intact, and confluent. However, in skin with SN, the corneocytes were lifted up and exhibited crack-like structures. The low-frequency SN induces disruption of the structure of stratum corneum lipid bilayers and enhances skin permeability for hydrophilic molecules in solution into the viable epidermis through an intracellular pathway.[4,8] However, the combination of CL or PL with SN for treated skin showed small corneocytes lifting, indicating that the lipid membrane of liposomes could fill and cover the skin damage. Although liposomes can repair the skin damage, the combination of using a chemical penetration enhancer (D-limonene) in a liposomal formulation (PL-LI) and SN resulted in greater disruption of the skin stratum corneum so the skin damage could not be repaired by liposomes.[13,29]

Figure 6 shows scanning electron micrographs of the skin surface view at the follicular region of the control (PBS), CL, PL, and PL-LI with and without SN. In the absence of SN, only PL-LI was clearly found to be deposited on the top of hair follicles that covered hair follicle orifices (Figure 6G, white arrow), indicating the use of the follicular route as a major penetration route. Therefore, SN had a lower amount of NaFI permeate through the skin than without SN (Figure 2) because the ultrasound changes the ultrastructure of the stratum corneum, dislocating the top layer of corneocytes. Additionally, the follicles constitute a very tiny fraction (≤0.1% approximately) of the total skin surface area; therefore, many detached corneocytes might partially slough off the hair follicle opening,[3] closing the main penetration pathway of NaFI-loaded-PL-LI. Therefore, the partial plugging of the hair follicle orifices caused by ultrasound energy altering the ultrastructure of stratum corneum might reduce the absorption of NaFI and PL-LI via the follicular route.[30]

Conclusion

This work demonstrated that low frequency SN (20 kHz for 2 minutes) affected the skin penetration of NaFI-loaded PL-LI via the transfollicular pathway. SN significantly decreased the NaFI flux of PL-LI compared to skin without SN. In selectively blocked hair follicles, the skin penetration of NaFI-loaded PL-LI decreased both with and without SN, indicating that the follicular pathway was a major penetration pathway. A CLSM study confirmed that a high intensity of NaFI-loaded PL-LI into the skin and along the length of hair inside the skin was found in skin without SN, while a high intensity on the top of hair outside the skin was observed in the skin with SN. In addition, scanning electron microscopy images revealed that SN could partially dislocate corneocytes to plug hair follicle orifices; therefore, it could reduce the

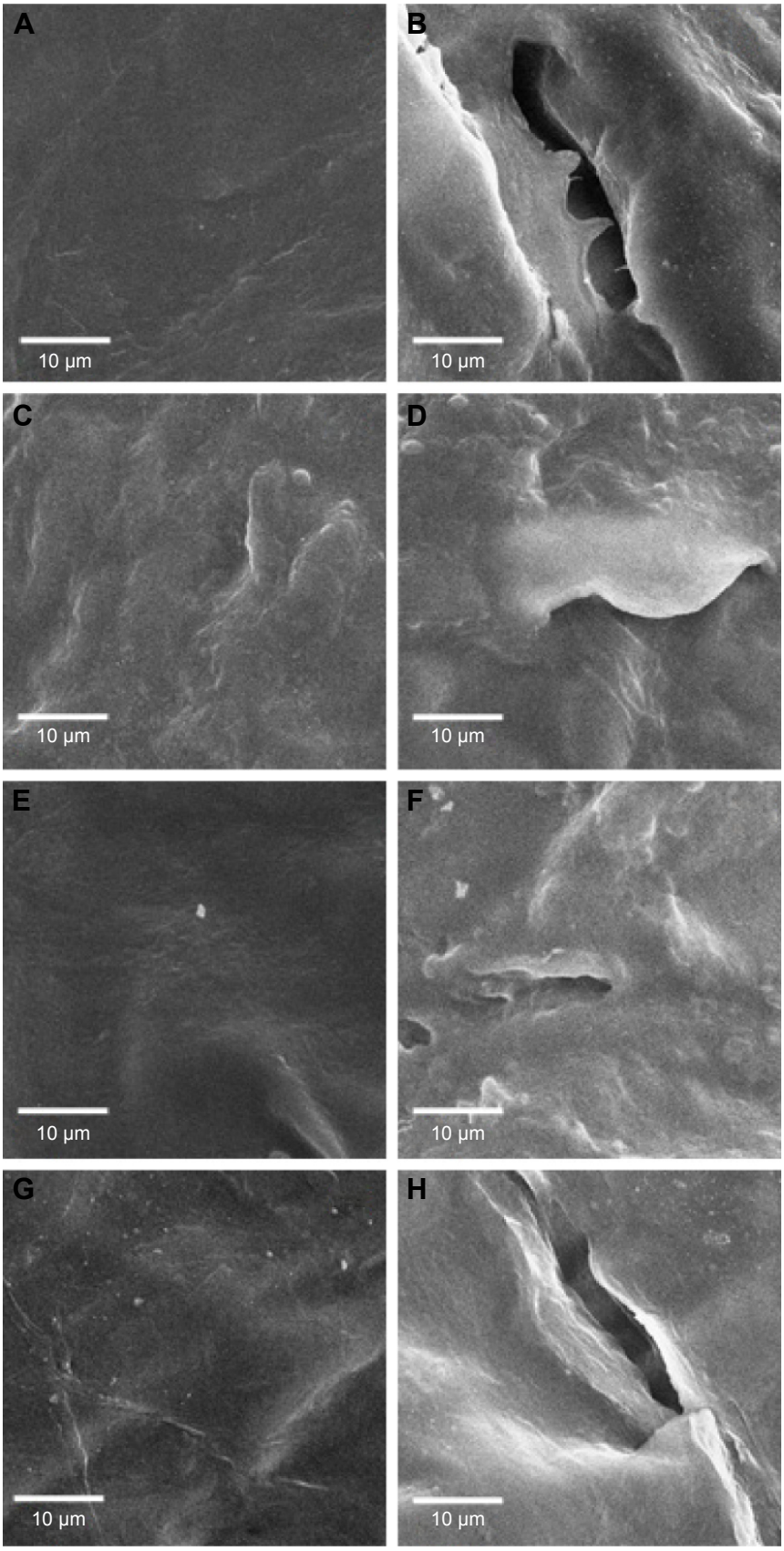

Figure 5 Scanning electron microscopy (SEM) images of porcine skin surface at nonfollicular region (original magnification ×1,000): control (PBS) without SN (**A**) and with SN (**B**), CL without SN (**C**) and with SN (**D**), PL without SN (**E**) and with SN (**F**), and PL-LIs without SN (**G**) and with SN (**H**).
Abbreviations: CL, conventional liposome; PBS, phosphate-buffered saline; PL, PEGylated liposome; PL-LI, PEGylated liposome with D-limonene; SN, sonophoresis.

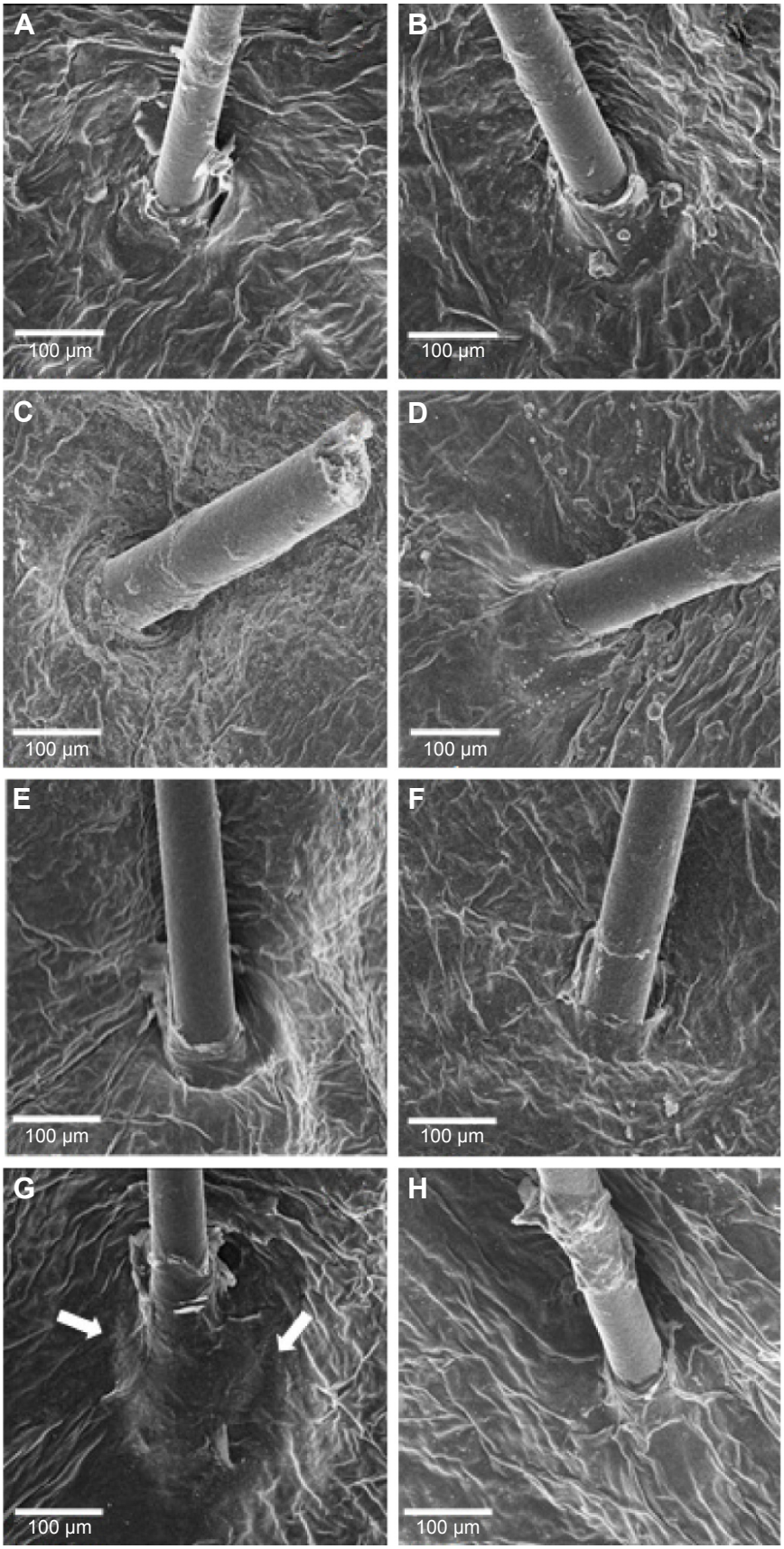

Figure 6 Scanning electron microscopy (SEM) images of porcine skin surface at follicular region (original magnification ×120): control (PBS) without SN (**A**) and with SN (**B**), CL without SN (**C**) and with SN (**D**), PL without SN (**E**) and with SN (**F**), and PL-LIs without SN (**G**) and with SN (**H**).
Note: The white arrows are PL-LI covered hair follicle orifices (**G**).
Abbreviations: CL, conventional liposome; PBS, phosphate-buffered saline; PL, PEGylated liposome; PL-LI, PEGylated liposome with D-limonene; SN, sonophoresis.

percutaneous absorption of NaFI and PL-LI. Therefore, SN might affect the penetration via the follicular pathway.

Acknowledgments

The authors gratefully acknowledge the Thailand Research Funds through the Basic Research Grant (Grant No 5680016) and the Thailand Research Funds through the Royal Golden Jubilee PhD Program (Grant No PHD/0091/2554) for financial support.

Disclosure

The authors report no conflicts of interest in this work.

References

1. Boucaud A, Machet L, Arbeille B, et al. In vitro study of low-frequency ultrasound-enhanced transdermal transport of fentanyl and caffeine across human and hairless rat skin. *Int J Pharm*. 2001;228:69–77.
2. Sarheed O, Abdul Rasool BK. Development of an optimised application protocol for sonophoretic transdermal delivery of a model hydrophilic drug. *Open Biomed Eng J*. 2011;5:14–24.
3. Sarheed O, Frum Y. Use of the skin sandwich technique to probe the role of the hair follicles in sonophoresis. *Int J Pharm*. 2012;423:179–183.
4. Morimoto Y, Mutoh M, Ueda H, et al. Elucidation of the transport pathway in hairless rat skin enhanced by low-frequency sonophoresis based on the solute–water transport relationship and confocal microscopy. *J Control Release*. 2005;103:587–597.
5. Polat BE, Hart D, Langer R, et al. Ultrasound-mediated transdermal drug delivery: Mechanisms, scope, and emerging trends. *J Control Release*. 2011;152:330–348.
6. Park D, Park H, Seo J, et al. Sonophoresis in transdermal drug deliverys. *Ultrasonics*. 2014;54:56–65.
7. Mitragotri S, Blankschtein D, Langer R. Transdermal drug delivery using low-frequency sonophoresis. *Pharm Res*. 1996;13:411–420.
8. Lee SE, Choi KJ, Menon GK, et al. Penetration pathways induced by low-frequency sonophoresis with physical and chemical enhancers: iron oxide nanoparticles versus lanthanum nitrates. *J Invest Dermatol*. 2010;130:1063–1072.
9. Han T, Das DB. Potential of combined ultrasound and microneedles for enhanced transdermal drug permeation: a review. *Eur J Pharm Biopharm*. 2015;89:312–328.
10. Petchsangsai M, Rojanarata T, Opanasopit P, et al. The combination of microneedles with electroporation and sonophoresis to enhance hydrophilic macromolecule skin penetration. *Biol Pharm Bull*. 2014;37:1373–1382.
11. Fang J, Hwang T, Huang Y, et al. Transdermal iontophoresis of sodium nonivamide acetate: V. Combined effect of physical enhancement methods. *Int J Pharm*. 2002;235:95–105.
12. Mutalik S, Parekh HS, Davies NH, et al. A combined approach of chemical enhancers and sonophoresis for the transdermal delivery of tizanidine hydrochloride. *Drug Deliv*. 2009;16:82–91.
13. Vyas SP, Singh R, Asati RK. Liposomally encapsulated diclofenac for sonophoresis induced systemic delivery. *J Microencapsul*. 1995;12:149–154.
14. Dahlan A, Alpar HO, Murdan S. An investigation into the combination of low frequency ultrasound and liposomes on skin permeability. *Int J Pharm*. 2009;379:139–142.
15. Meidan VM, Bonner MC, Michniak BB. Transfollicular drug delivery – is it a reality? *Int J Pharm*. 2005;306:1–14.
16. Jain S, Tiwary A, Jain N. PEGylated elastic liposomal formulation for lymphatic targeting of zidovudine. *Curr Drug Deliv*. 2008;5:275–281.
17. Rangsimawong W, Opanasopit P, Rojanarata T. Terpene-containing PEGylated liposomes as transdermal carriers of a hydrophilic compound. *Biol Pharm Bull*. 2014;37:1936–1943.
18. Manosroi A, Ruksiriwanich W, Abe M, et al. Transfollicular enhancement of gel containing cationic niosomes loaded with unsaturated fatty acids in rice (*Oryza Sativa*) bran semi-purified fraction. *Eur J Pharm Biopharm*. 2012;81:303–313.
19. Kenworthy AK, Simon SA, McIntosh TJ. Structure and phase behavior of lipid suspensions containing phospholipids with covalently attached poly(ethylene glycol). *Biophys J*. 1995;68:1903–1920.
20. Subongkot T, Wonglertnirant N, Songprakhon P, et al. Visualization of ultradeformable liposomes penetration pathways and their skin interaction by confocal laser scanning microscopy. *Int J Pharm*. 2013;441:151–161.
21. Patzelt A, Richter H, Buettemeyer R, et al. Differential stripping demonstrates a significant reduction of the hair follicle reservoir in vitro compared to in vivo. *Eur J Pharm Biopharm*. 2008;70(1):234–238.
22. Jain S, Jain P, Umamaheshwari RB, et al. Transfersomes – a novel vesicular carrier for enhanced transdermal delivery: development, characterization, and performance evaluation. *Drug Dev Ind Pharm*. 2003;29(9):1013–1026.
23. Honeywell-Nguyen PL, Bouwstra JA. Vesicles as a tool for transdermal and dermal delivery. *Drug Discov Today Technol*. 2005;2(1):67–74.
24. Badran M, Shazly G, El-Badry M, et al. Effect of terpene liposomes on the transdermal delivery of hydrophobic model drug, nimesulide: characterization, stability and in vitro skin permeation. *Afr J Pharm Pharmacol*. 2012;6(43):3018–3026.
25. Alvarez-Román R, Merino G, Kalia YN, et al. Skin permeability enhancement by low frequency sonophoresis: lipid extraction and transport pathways. *J Pharm Sci*. 2003;6:1138–1146.
26. Merino G, Kalia YN, Delgado-Charro MB, et al. Frequency and thermal effects on the enhancement of transdermal transport by sonophoresis. *J Control Release*. 2003;88:85–94.
27. Lasic DD. The mechanism of vesicle formation. *Biochem J*. 1998;256:1–11.
28. Grams YY. *Influence of Molecular Properties and Delivery System Design on the Transfollicular Transport Across the Skin* [dissertation]. Leiden: Division of Drug Delivery Technology of the Leiden/Amsterdam Center for Drug Research, Leiden University; 2005.
29. Essa EA, Bonner MC, Barry BW. Electroporation and ultradeformable liposomes; human skin barrier repair by phospholipid. *J Control Release*. 2003;92:163–172.
30. Han T, Das DB. Permeability enhancement for transdermal delivery of large molecule using low-frequency sonophoresis combined with microneedles. *J Pharm Sci*. 2013;102:3614–3622.

International Journal of Nanomedicine

Dovepress
open access to scientific and medical research

Open Access Full Text Article

ORIGINAL RESEARCH

Effect of liposomal fluidity on skin permeation of sodium fluorescein entrapped in liposomes

This article was published in the following Dove Press journal:
International Journal of Nanomedicine
17 July 2015
Number of times this article has been viewed

Thirapit Subongkot[1]
Tanasait Ngawhirunpat[2]

[1]Department of Pharmaceutical Technology, Faculty of Pharmaceutical Sciences, Burapha University, Chonburi, Thailand; [2]Department of Pharmaceutical Technology, Faculty of Pharmacy, Silpakorn University, Nakhon Pathom, Thailand

Abstract: The purpose of this study was to investigate the effect of ultradeformable liposome components, Tween 20 and terpenes, on vesicle fluidity. The fluidity was evaluated by electron spin resonance spectroscopy using 5-doxyl stearic acid and 16-doxyl stearic acid as spin labels for phospholipid bilayer fluidity at the C5 atom of the acyl chain near the polar head group (hydrophilic region) and the C16 atom of the acyl chain (lipophilic region), respectively. The electron spin resonance study revealed that Tween 20 increased the fluidity at the C5 atom of the acyl chain, whereas terpenes increased the fluidity at the C16 atom of the acyl chain of the phospholipid bilayer. The increase in liposomal fluidity resulted in the increased skin penetration of sodium fluorescein. Confocal laser scanning microscopy showed that ultradeformable liposomes with terpenes increase the skin penetration of sodium fluorescein by enhancing hair follicle penetration.

Keywords: ultradeformable liposomes, terpenes, fluidity, electron spin resonance spectroscopy, confocal laser scanning microscopy

Introduction

Transdermal drug delivery systems utilize skin as a transportation route and offer many advantages, including avoidance of first-pass hepatic metabolism, sustained and controlled drug release, and improved patient compliance. However, the stratum corneum, the outermost skin layer, exhibits a rate-limiting step in regulating drug absorption into the skin. Various strategies have been used to increase drug absorption across the skin, such as microneedles,[1] iontophoresis,[2] sonophoresis,[3] electroporation,[4] microdermabrasion,[5] microemulsion,[6] niosomes,[7] and liposomes.[8–10] Ultradeformable liposomes (ULs), also called transfersomes, are a type of elastic vesicle, introduced by Cevc and Blume.[11] ULs generally consist of phospholipids and surfactant as a membrane softening agent. Due to their flexibility, ULs fit through narrow pores approximately one-tenth of their diameter. ULs also penetrate as intact vesicles through the skin into the blood circulation without permanent disintegration.[12] ULs effectively increase the skin penetration of drugs both in vitro and in vivo.[13–15]

Terpenes, a class of penetration enhancers obtained from natural sources, have successfully been used as skin penetration enhancers for percutaneous absorption enhancement in various types of liposomes, specifically invasomes,[16,17] and ULs.[18,19] Electron spin resonance (ESR), also known as electron paramagnetic resonance, is a spectroscopy technique used to study molecular mobility by characterizing the unpaired electron of free radicals, also called spin probes, in an extreme applied magnetic field. This technique has been used to study membrane fluidity,[20,21] the skin penetration enhancement mechanism of penetration enhancers and nanocarriers,[22,23] and antioxidant properties.[24]

Correspondence: Tanasait Ngawhirunpat
Department of Pharmaceutical Technology, Faculty of Pharmacy, Silpakorn University, 6 Rajamankha Nai Road, Muang, Nakhon Pathom 73000, Thailand
Tel +66 34 255 800
Fax +66 34 255 801
Email ngawhirunpat_t@su.ac.th

submit your manuscript | www.dovepress.com
Dovepress
http://dx.doi.org/10.2147/IJN.S86624

According to our previous study,[18] ULs consisting of terpenes as a skin penetration enhancer and Tween 20 as a terpene solubilizer significantly enhanced the skin penetration of sodium fluorescein (NaFl). Since ULs with terpenes penetrated via transfollicular pathway as major skin penetration pathway,[19] we suggested that ULs with terpenes increased NaFl penetration by penetrating through hair follicles to bypass stratum corneum. To develop more effective ULs with terpene formulations and to identify the penetration enhancement mechanism, it is necessary to investigate the correlation between percutaneous penetration enhancement and liposomal fluidity, including the molecular structure of ULs with terpenes, which do not yet exist.

Therefore, we selected ESR to investigate the vesicle fluidity and molecular arrangement of the membrane softening components, terpenes and Tween 20, in UL structures using 5- and 16-doxyl stearic acid (5-DSA and 16-DSA) as spin labels. These spin probes have been widely used to study the membrane fluidity of liposomes[20,25] and niosomes.[26] 5-DSA has a nitroxide radical moiety at the fifth carbon atom of the acyl chain, whereas 16-DSA has a nitroxide radical moiety at the 16th carbon atom of the acyl chain (Figure 1). These selected spin labels, 5-DSA and 16-DSA, oriented their molecules parallel to the phospholipid molecules in a bilayer structure, providing mobility parameters for fluidity detection affected by the incorporated components at the C5 and C16 atoms of the phospholipid acyl chains.

Because the follicular pathway is the major skin penetration pathway of ULs with terpenes,[19] the mechanism of skin penetration enhancement by targeting the follicular penetration was elucidated. Liposomal vesicles were probed with rhodamine B 1,2-dihexadecanoyl-sn-glycero-3-phosphoethanolamine triethylammonium salt (Rh-PE), which exhibits red fluorescence, whereas entrapped compound (NaFl) exhibits green fluorescence. Confocal laser scanning microscopy (CLSM) using a co-localization technique was used to probe the skin penetration of fluorescent-labeled vesicles (UL-labeled Rh-PE) by comparing the fluorescence intensity and skin penetration depths between near follicular and nonfollicular regions. The objective of this study was to determine the correlation between liposomal fluidity and the increased in vitro skin penetration of NaFl and to elucidate the effect of vesicle fluidity on the follicular penetration enhancement of liposomes.

Materials and methods

Materials

Non-hydrogenated egg phosphatidylcholine (PC) (Coatsome NC-50; PC purity ≥95%) was purchased from NOF Corporation (Tokyo, Japan). Cholesterol (Chol) was purchased from Sigma-Aldrich, St Louis, MO, USA. Tween 20 was purchased from Ajax Finechem (Auckland, New Zealand). Sodium fluorescein (NaFl), d-limonene, 1,8-cineole, and geraniol were purchased from Sigma-Aldrich. 5-DSA and 16-DSA were purchased from Sigma-Aldrich. Lissamine™ rhodamine B 1,

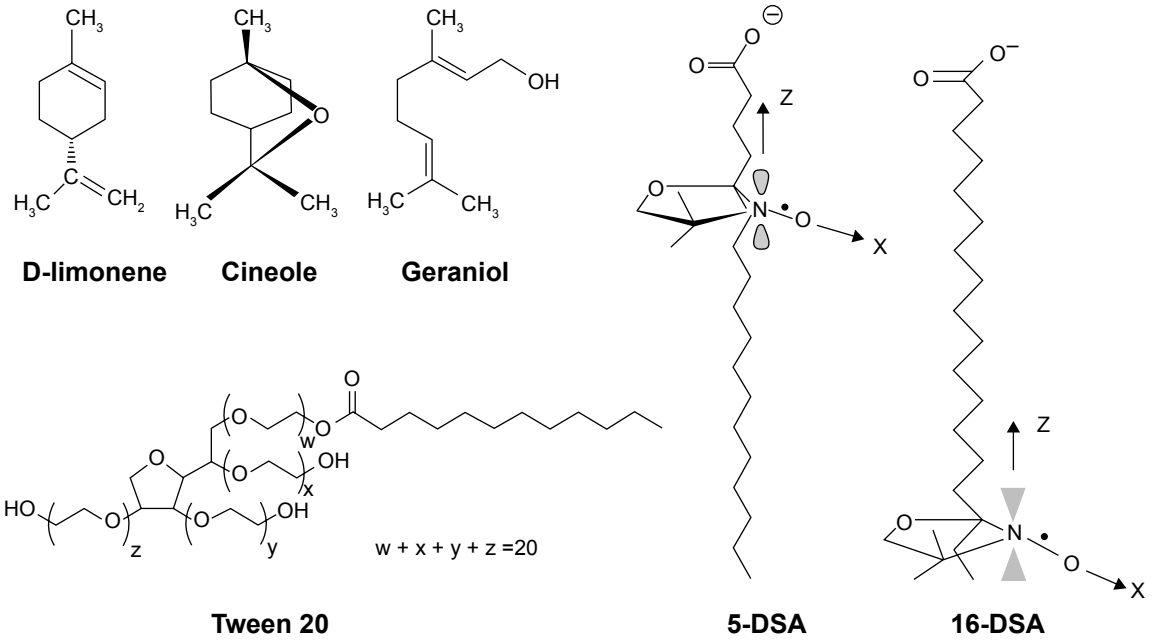

Figure 1 Chemical structures of the terpenes, Tween 20, 5-doxyl stearic acid (5-DSA) and 16-doxyl stearic acid (16-DSA).

2-dihexadecanoyl-sn-glycero-3-phosphoethanolamine triethylammonium salt (Rh-PE) was purchased from Invitrogen, CA, USA. All other reagents were of analytical grade and were commercially available.

Preparation of UL containing monoterpenes

The formulations of the liposomes containing PC, Chol, Tween 20, NaFl, and terpenes are shown in Table 1. The liposomes were prepared using the sonication method. A mixture of PC and Chol was dissolved in chloroform and methanol (2:1 v/v). NaFl solution was prepared by dissolving NaFl to phosphate-buffered saline (PBS) at pH 7.4 as a stock solution. The mixture of PC and Chol was then evaporated using a stream of nitrogen until a thin and homogeneous lipid film was formed. The thin film was placed in a desiccator connected to a vacuum pump for at least 6 hours. Then, the dried thin film was hydrated with PBS and NaFl solution. Tween 20 and each terpene were then added to the liposomal dispersion before sonication using a probe sonicator (Vibracell™, VCX 130 PB; Sonics & Materials, Inc, Newtowns, CT, USA) for 30 minutes to reduce the size of the liposomes.

Conventional liposomes (CLs) and ULs were prepared using the same process as UL containing monoterpenes.

Liposomal characterization

Each liposomal formulation was diluted with distilled water prior to the measurement of size, zeta potential, and size distribution using a dynamic light scattering particle size analyzer (Zetasizer Nano-ZS; Malvern Instruments, Malvern, UK) with a 4 mW He-Ne laser at a scattering angle of 173°. All measurements were performed under ambient conditions and in triplicate.

Assessment of liposomal fluidity using ESR

All liposomal formulations were probed with stearic acid spin labels (5- or 16-DSA) using a spin label (5-DSA/16-DSA)-to-lipid ratio of 1:100 M. Each spin label was dissolved in a mixture of chloroform and methanol (2:1 v/v) before being added to a test tube of PC and Chol, followed by thin film formation as described in section Preparation of UL containing monoterpenes. All other ingredients were added except NaFl.

Liposomes probed with each spin label (5- or 16-DSA) were added to a glass capillary tube and sealed with Parafilm® before the ESR experiments. An ESR spectrum was recorded on a model JES-RE2X (JEOL, Tokyo, Japan) equipped with cylindrical cavity resonator and operated in (TE_{101}) mode. The ESR spectrometer was equipped with a microwave unit X band with a frequency of 8.8–9.6 GHz. The operating conditions of the equipment were microwave power of 1 mW, modulation frequency of 100 kHz, modulation amplitude of 2.5×100 mT, magnetic field scan of 1×10 mT, sweep time of 30 seconds, detector time constant of 30 ms, and temperature of 24°C.

For 5-DSA (Figure 2A), the liposomal fluidity was estimated from the outermost separation between the spectral extrema, the maximum hyperfine splitting ($2T_{\parallel}'$). The value of $2T_{\parallel}'$ reflects the motional profiles near the phospholipid polar head group of the lipid bilayer. To determine the motional profiles at the phospholipid acyl chain near the lipophilic region of the phospholipid bilayer, the rotational correlation time (τ_c) obtained from the 16-DSA spectrum (Figure 2B) was used as the liposomal fluidity parameter. The τ_c was calculated from the equation as follows:[27]

$$\tau_c = (6.5\times10^{-10})W_0\left[\left(\frac{h_0}{h_{-1}}\right)^{0.5} - 1\right] \quad (1)$$

where W_0 is the width of the midfield line of the spectrum in Gauss (G), h_0 is the height of the midfield line of the spectrum and h_{-1} is the height of the highfield line (Figure 2B). The $2T_{\parallel}'$ and τ_c increased with a decrease in fluidity.

In vitro skin penetration study

Abdominal neonatal porcine skin (death from natural causes after birth) was obtained from a local slaughter house in Nakhon Pathom province and was used as barrier membrane for this

Table 1 Composition of NaFl-loaded liposomal formulations

Formulation (code)	PC (%w/v)	NaFl (%w/v)	Chol (%w/v)	Tween 20 (%w/v)	Terpenes (%w/v)	PBS (%w/v) (mL)
CL	0.77	0.21	0.07	–	–	ad 100
UL	0.77	0.21	0.07	2	–	ad 100
ULL	0.77	0.21	0.07	2	l	ad 100
ULC	0.77	0.21	0.07	2	l	ad 100
ULG	0.77	0.21	0.07	2	l	ad 100

Abbreviations: Ad, add to; Chol, cholesterol; CL, conventional liposomes; NaFl, sodium fluorescein; PBS, phosphate-buffered saline; PC, phosphatidylcholine; UL, ultradeformable liposomes; ULC, UL with cineole; ULG, UL with geraniol; ULL, UL with d-limonene.

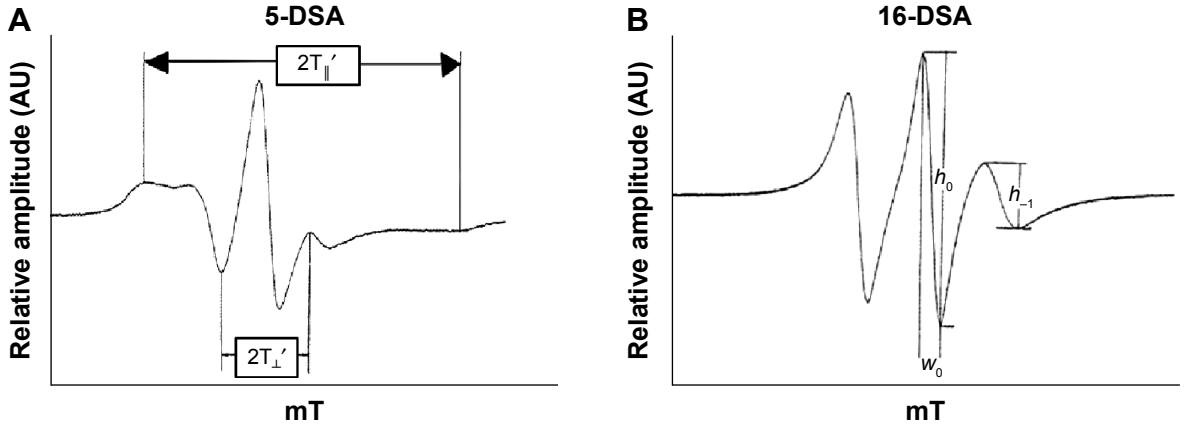

Figure 2 (**A**) ESR spectrum of 5-DSA and (**B**) ESR spectrum of 16-DSA.
Abbreviations: AU, arbitrary unit; 5-DSA, 5-doxyl stearic acid; 16-DSA, 16-doxyl stearic acid; ESR, electron spin resonance.

study. The subcutaneous fat was removed using medical scissors and surgical blades. The thickness of each skin membrane was approximately 0.6–0.7 mm. The skin membranes were frozen at –20°C until use. The membranes were thawed at room temperature using PBS prior to the experiments.

The experiment with NaFl penetration through porcine skin was performed using Franz diffusion cells with a penetration area of 2.31 cm^2. Approximately 6.5 mL PBS was added to the receiver portion and stirred with magnetic bar at 500 rpm. The membrane was mounted between the donor and receiver portion with the stratum corneum facing the donor portion and the dermis facing the receiver medium. The diffusion cells were connected to a water circulating bath to maintain the temperature at 32°C. Two milliliters of NaFl entrapped in the liposome formulation was added into the donor portion. At 1, 2, 4, 6, 8, and 24 hours, 0.5 mL of receiver medium was withdrawn for analysis, and an equal volume of PBS was added to the receiver portion to maintain a constant volume. Each sample was analyzed in triplicate.

The NaFl concentration was analyzed using a fluorescence spectroscopy method. One hundred microliters of the sample was pipetted into a black 96-well plate, and the fluorescence was detected in three replicates using a fluorescence spectrophotometer (Fusion™ Universal Microplate Analyzer; PACKARD Instrument Company, Inc, Downers Grove, IL, USA). The excitation wavelength was 485 nm and the emission wavelength was 535 nm. The calibration curve for NaFl was in the range of 0.5–35 ng/mL.

CLSM study

CLSM was used to evaluate the skin penetration differences between the follicular and nonfollicular regions of three liposomal formulations, CL, UL, and UL with 1% cineole, using a co-localization technique. The differences in the color of the fluorescent compounds were used to observe the vesicle penetration of the treated skin as follows: rhodamine (red)-probed liposomes, NaFl (green)-entrapped drug, and blue from skin autofluorescence.

The fluorescent probe (Rh-PE) was dissolved in a mixture of chloroform and methanol (2:1 v/v) before addition to a test tube of PC and Chol mixture at a ratio of PC:Rh-PE of 100:1 M. The mixture of fluorescent probe and lipid (PC and Chol) was then evaporated using nitrogen gas to form thin film. Non-entrapped NaFl was separated from Rh-PE probed liposomes using a filtration technique with Amicon® Ultra-0.5 centrifugal devices (Millipore Corporation, Billerica, MA, USA). The Rh-PE probed liposomes were added to an ultrafiltration tube with a molecular weight cutoff of 3,000 Da and centrifuged at 4°C at 14,000× *g* for 30 minutes. The non-entrapped NaFl in the filtrate was removed. Then, the retentates device was turned upside down into a new concentrate collection tube and centrifuged at 4°C at 1,000× *g* for 2 minutes to transfer the entrapped NaFl-loaded Rh-PE probed liposomes from the device to the tube. The obtained sample was immediately used for the skin penetration study.

The skin penetration study of the NaFl-loaded Rh-PE probed liposomes was performed using Franz diffusion cells under the same conditions as described in the skin permeation study. The donor compartment was placed with 150 µL of the entrapped NaFl-loaded Rh-PE probed liposomes. At 4 hours, each porcine skin was removed from diffusion cells, washed with PBS at least twice and stored at –20°C prior to the CLSM investigation.

To evaluate the skin penetration of liposomes between the follicular and nonfollicular regions, each treated skin was placed on a 22×50 mm cover slip (MENZEL-GLÄSER®,

Braunschweig, Germany) and then visualized with the 10× objective lens of an inverted Zeiss LSM 510 META microscope (Carl Zeiss Meditec AG, Jena, Germany), equipped with a He-Ne 1 laser (excitation wavelength =543 nm, emission wavelength =580 nm), Ar laser (excitation wavelength =488 nm, emission wavelength =514 nm), and diode laser (excitation wavelength =358 nm, emission wavelength =461 nm) for Rh-PE, NaFl, and skin autofluorescence, respectively. These skin regions were scanned using a 20× objective lens to obtain x–z plane images, by which the laser could scan through the tissue to compare the skin penetration depths and fluorescence intensity of the entrapped drug and liposomes at the follicular and nonfollicular regions.

Data analysis

The cumulative amount of NaFl penetrating the skin per unit area was plotted as a function of time. The skin penetration parameter (flux) was determined from the slope of the linear portion. All data were statistically analyzed using Student's *t*-test and analysis of variance. Differences of $P<0.05$ were considered statistically significant.

Results and discussion

Liposomal characterization

The average size of the liposomes ranged from 39 to 98 nm, with a narrow size distribution (polydispersity index <0.4) as shown in Table 2. The average size of the CLs was significantly larger than that of the ULs and ULs with terpenes. The average size of the ULs was significantly greater than that of the ULs with terpenes. There were no significant differences for the average size of the ULs with terpenes. These results indicate that the addition of Tween 20 and terpenes results in particle size reduction. Tasi et al[28] reported that the surfactants exposed from the outer layer membrane increase the liposome particle curvature, while surfactants exposed to the inner leaflet do the opposite. Thus, we suggested that the decrease of liposomal size by terpenes may occur with the same mechanism as liposomal size reduction by surfactant addition. A reduction in liposomal size could possibly be attributed to a steric repulsion among terpenes molecules, which is exposed from the outer and inner bilayer membranes of liposomes. Addition of terpenes, therefore, reduced the liposomal size because there were more terpenes existing in the outer layer than in the inner bilayer membranes. The zeta potentials of all liposome formulations were negative (−4.7 to −13.2 mV). PC is a zwitterionic compound with an isoelectric point between 6 and 6.7.[29] Under the study conditions (pH 7.4), in which the pH was higher than the isoelectric point, the PC vesicles had an overall negative charge. Several papers reported that non-ionic surfactant-loaded liposomes[30] and invasomes[17] (terpenes-loaded liposomes) exhibit negative zeta potential (−20 to −30 mV and −13 to −14 mV, respectively) similar to our results. These negatively charged liposomal formulations also showed good physical and chemical stability, indicating that these particles had high zeta potential enough for electrostatic stabilization. Polydispersity index of all liposome formulations was less than 0.4 indicating a narrow size distribution of these liposomes.

Table 2 Characterization parameters of different liposomal formulations

Liposomal formulations	Particle size (nm)	Zeta potential (mV)	Polydispersity index
CL	98.41±0.65	−4.70±1.03	0.266±0.002
UL	52.43±0.23	−13.21±0.9	0.384±0.004
ULL	43.82±0.48	−10.30±0.2	0.254±0.010
ULC	43.70±0.61	−8.23±0.31	0.181±0.011
ULG	42.79±0.94	−10.75±3.02	0.280±0.016

Note: Each value represents the mean ± SD (n=3).
Abbreviations: CL, conventional liposomes; SD, standard deviation; UL, ultradeformable liposomes; ULC, UL with cineole; ULG, UL with geraniol; ULL, UL with d-limonene.

Liposomal fluidity

Table 3 shows the ESR parameters ($2T_{\parallel}'$ and τ_c) of the different liposomal formulations. The $2T_{\parallel}'$ obtained from the 5-DSA was used to detect the motional profiles near the polar head group of the phospholipid acyl chain, whereas the τ_c obtained from the 16-DSA was used to detect the motional profiles at the end of the lipophilic chain. The $2T_{\parallel}'$ of the ULs was significantly lower than that of the CLs, whereas the τ_c values were not significantly different between the CLs and the ULs. It is concluded that the addition of Tween 20 to the ULs did not increase the fluidity of the acyl chain near the hydrophobic region of the phospholipid bilayer; however, it increased the fluidity of the acyl chain near

Table 3 ESR parameters (maximum hyperfine splitting and rotational correlation time) and in vitro skin penetration parameter (flux) of each liposomal formulation

Liposomal formulations	$2T_{\parallel}'$ (mT)	τ_c (ns)	Flux (μg/cm²/h)
CL	8.19±0.24	1.76±0.07	0.0137±0.0081
UL	4.70±0.01	1.32±0.01	0.0611±0.0163
ULL	4.71±0.25	0.704±0.001	0.4876±0.0962
ULC	4.68±0.04	0.719±0.071	0.4653±0.1472
ULG	4.89±0.06	0.629±0.022	0.4073±0.1421

Note: Each value represents the mean ± SD (n=3).
Abbreviations: CL, conventional liposomes; ESR, electron spin resonance; SD, standard deviation; UL, ultradeformable liposomes; ULC, UL with cineole; ULG, UL with geraniol; ULL, UL with d-limonene.

the polar head group of the phospholipid bilayer. This result also indicates that Tween 20 molecules are localized near the polar head group of the liposomal bilayer. The τ_c of each ULs with different terpenes, ULL, ULC, and ULG, was significantly decreased compared to that of the ULs, whereas the $2T_{\parallel}'$ values of the ULs and ULs with terpenes were not significantly different. Therefore, terpenes increased the fluidity at the C16 atom of the phospholipid acyl chain of the vesicle bilayer. This result also indicates that terpene molecules are localized in the phospholipid acyl chain near the lipophilic region of the vesicle bilayer. Of the ULs with different terpenes (ULL, ULC, and ULG), the $2T_{\parallel}'$ and τ_c values were not significantly different. We conclude that different types of monoterpenes incorporated in the ULs did not affect vesicle fluidity. Our findings are consistent with those of Dragicevic-Curic et al[25] who showed that the addition of 1% terpene/terpene mixture to invasomes significantly increased the vesicle fluidity around the C16 atom of the phospholipid acyl chain.

In vitro skin penetration study

The flux of different liposomal formulations is shown in Table 3. The flux of NaFl from ULs was significantly higher than that of CLs. The flux of NaFl from ULs with different terpenes (ULL, ULC, and ULG) was significantly higher than that from ULs. The flux among ULL, ULC, and ULG was not significantly different.

Because the $2T_{\parallel}'$ values between ULs and ULs with terpenes were not significantly different, τ_c was selected as a candidate of liposomal fluidity to assess the correlation between fluidity and skin penetration enhancement. From the results of flux and τ_c (Table 3), the flux of NaFl from ULs was significantly higher than that of CLs, whereas the τ_c of ULs was significantly lower than that of CLs. The flux of NaFl from ULs with different terpenes was significantly higher than that of ULs, whereas the τ_c of ULs with different terpenes was significantly lower than that of ULs. There were no significant differences for the flux of ULs with different terpenes, and their τ_c values were also not significantly different. These results indicate that the decrease in τ_c correlated with the increase in NaFl flux. We conclude that the increase in liposomal fluidity results in increased skin penetration of NaFl. According to the invasome fluidity assessment using ESR by Dragicevic-Curic et al[25] there was no direct correlation between invasome fluidity and skin penetration ability.

Molecular structure elucidation

The fluidity assessment using ESR elucidated the molecular structure of ULs with terpenes. From our results, the addition of Tween 20 increased the vesicle fluidity near the polar head group of the phospholipid bilayer. Tween 20 or polyoxyethylene (20) sorbitan monolaurate is a non-ionic surfactant consisting of a polyoxyethylene group as the hydrophilic portion and a hydrocarbon chain of lauric acid as the lipophilic portion. We hypothesize that Tween 20 molecules intercalated between the phospholipid molecules by turning their hydrophilic portion toward the phosphate group, as shown in Figure 3. For terpenes, there was an increase in vesicle fluidity near the C16 atom of the phospholipid acyl chain. Monoterpenes (d-limonene, cineole, and geraniol) added to ULs with different terpenes are small lipophilic molecules. Therefore, terpenes were localized near the end of the phospholipid acyl chain, as shown in Figure 3.

CLSM study

Our previous study[19] found that UL with terpenes increased skin penetration by penetrating through the hair follicle as the primary penetration pathway. Therefore, we tested our hypothesis that ULs with terpenes increase the skin penetration of NaFl by enhancing the follicular penetration to bypass the stratum corneum. Three liposomal formulations were selected to study the follicular penetration enhancement. CLSM was used to visualize the skin penetration of the entrapped drug and liposomes between the near follicular and nonfollicular regions of CLs, ULs, and ULs with 1% cineole (as candidate ULs with terpenes) using a multifluorescence compound technique. Both skin penetration depths and fluorescence intensity were compared to evaluate the follicular penetration enhancement.

CLSM of skin treated with CLs

Top view images of sequential follicular and nonfollicular regions from the same skin tissue at 4 hours are shown in Figure 4A1 and B1, respectively. The marked areas of these images (Figure 4A1 and B1) were scanned to obtain the greatest penetration depths and fluorescence intensity of NaFl and CLs. The x–z plane serial optical images from different skin depths at the follicular and nonfollicular regions are shown in Figure 4A2 and B2. The merge of x–z plane serial optical images from different skin depths at the follicular and nonfollicular regions are shown in Figure 4A3 and B3, respectively. Both NaFl and CLs penetrate through the follicular region and the nonfollicular region with the same distance of only approximately 55 μm.

Figure 4C shows the fluorescence intensity of NaFl (green fluorescence) and CLs (red fluorescence) at different penetration depths from follicular and nonfollicular regions. The fluorescence intensity of NaFl at the follicular region was not different from the nonfollicular region. The fluorescence

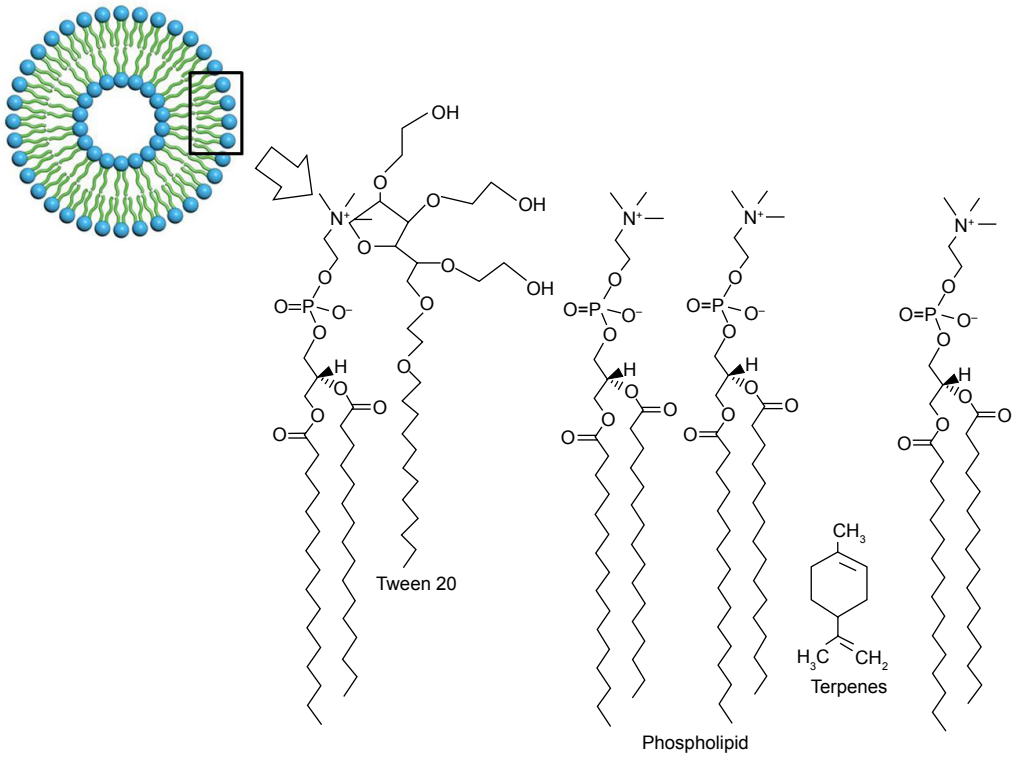

Figure 3 Molecular structure of ultradeformable liposomes with terpenes.

intensity of Rh-PE was also not different between the follicular and nonfollicular regions. These results indicate that CLs penetrated through the follicular region to a similar extent as in the nonfollicular region.

CLSM of skin treated with ULs

Top view images of follicular and nonfollicular regions from the same skin tissue at 4 hours are shown in Figure 5A1 and B1, respectively. The marked areas of these images (Figure 5A1 and B1) were scanned to obtain the greatest penetration depths and fluorescence intensity of NaFl and ULs. The x–z plane serial optical images from different skin depths at the follicular and nonfollicular regions are shown in Figure 5A2 and B2, respectively. The merge of x–z plane serial optical images from different skin depths at the follicular and nonfollicular regions are shown in Figure 5A3 and B3, respectively Both NaFl and ULs penetrated through the follicular region and the nonfollicular region with the same distance of approximately 75 μm.

Figure 5C shows the fluorescence intensity of NaFl (green fluorescence) and ULs (red fluorescence) at different penetration depths from follicular and nonfollicular regions. The fluorescence intensity of NaFl at the nonfollicular region was greater than the follicular region in the beginning distance (0–30 μm). However, for the other distance (30–115 μm), the fluorescence intensity of NaFl was not different between the follicular and nonfollicular regions. The fluorescence intensity of Rh-PE was not different between the follicular and nonfollicular regions. Our results indicate that ULs penetrated through the follicular region to a similar extent as the nonfollicular region.

CLSM of skin treated with ULs with 1% cineole

Top view images of follicular and nonfollicular regions from the same skin tissue are shown in Figure 6A1 and B1, respectively. The marked areas of these images (Figure 6A1 and B1) were scanned to obtain the greatest penetration depths and fluorescence intensity of NaFl-loaded ULs with 1% cineole labeled Rh-PE. The gallery of x–z plane serial optical images from different skin depths at follicular and nonfollicular regions is shown in Figure 6A2 and B2, respectively. The merge of x–z plane serial optical images from different skin depths at the follicular and nonfollicular regions are shown in Figure 6A3 and B3, respectively. NaFl and liposomes penetrated to 90 μm in both follicular and nonfollicular regions.

Figure 6C shows the fluorescence intensity of NaFl (green fluorescence) and liposomes (red fluorescence) at different penetration depths from the follicular and nonfollicular regions. The fluorescence intensity of NaFl between the follicular and nonfollicular regions was not different. However, the fluorescence intensity of Rh-PE at the follicular region

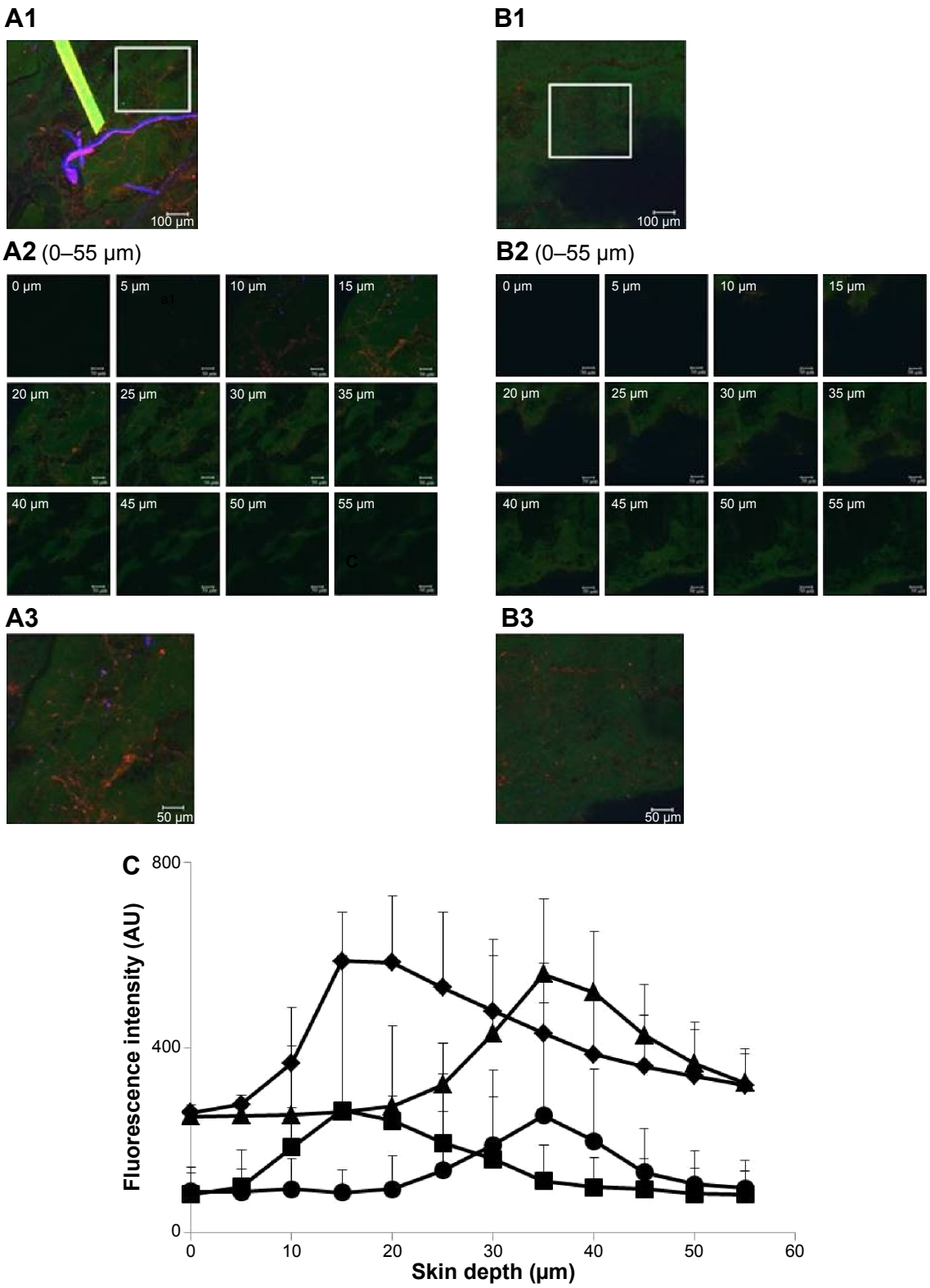

Figure 4 CLSM images of skin treated with CLs.

Notes: (**A1** and **B1**) The x–y plane serial follicular and nonfollicular localization of porcine skin treated with NaFl-loaded Rh-PE-labeled CLs at 4 hours. The scale bar represents 100 µm. (**A2** and **B2**) The serial x–z plane magnification of the marked area from the follicular and nonfollicular regions at different skin depths using a 20× objective lens. The scale bar represents 50 µm. (**A3** and **B3**) The intensity over projection of z–axis images of **A2** and **B2**, respectively. The scale bar represents 50 µm. The blue, green, and red fluorescence are the autofluorescence, NaFl, and Rh-PE, respectively. (**C**) Comparison of fluorescence intensity profiles of NaFl and Rh-PE at different skin depths of **A2** (♦, NaFl; ■, Rh-PE) and **B2** (▲, NaFl; ●, Rh-PE).

Abbreviations: AU, arbitrary unit; CLs, conventional liposomes; CLSM, confocal laser scanning microscopy; NaFl, sodium fluorescein; Rh-PE, rhodamine B 1,2-dihexadecanoyl-sn-glycero-3-phosphoethanolamine triethylammonium salt.

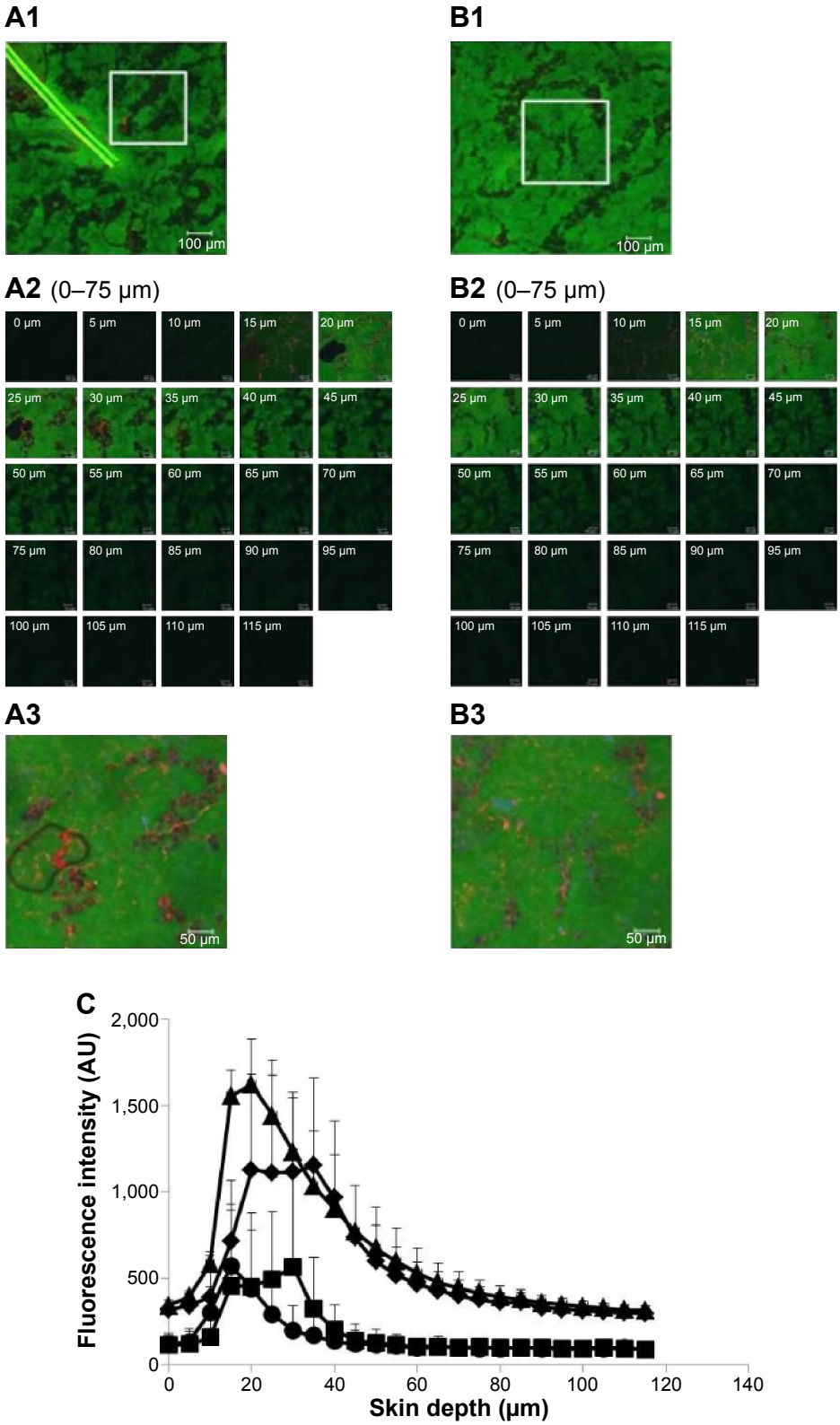

Figure 5 CLSM images of skin treated with ULs.

Notes: (**A1** and **B1**) The x–y plane serial follicular and nonfollicular localization of porcine skin treated with NaFl-loaded Rh-PE-labeled UL at 4 hours. The scale bar represents 100 μm. (**A2** and **B2**) The serial x–z plane magnification of the marked area from the follicular and nonfollicular regions at different skin depths using a 20× objective lens. The scale bar represents 50 μm. (**A3** and **B3**) The intensity over projection of the z-axis images of **A2** and **B2**, respectively. The scale bar represents 50 μm. The blue, green, and red fluorescence are the autofluorescence, NaFl, and Rh-PE, respectively. (**C**) Comparison of the fluorescence intensity profiles of NaFl and Rh-PE at different skin depths of **A2** (♦, NaFl; ■, Rh-PE) and **B2** (▲, NaFl; ●, Rh-PE).

Abbreviations: AU, arbitrary unit; CLSM, confocal laser scanning microscopy; NaFl, sodium fluorescein; Rh-PE, rhodamine B 1,2-dihexadecanoyl-sn-glycero-3-phosphoethanolamine triethylammonium salt; ULs, ultradeformable liposomes.

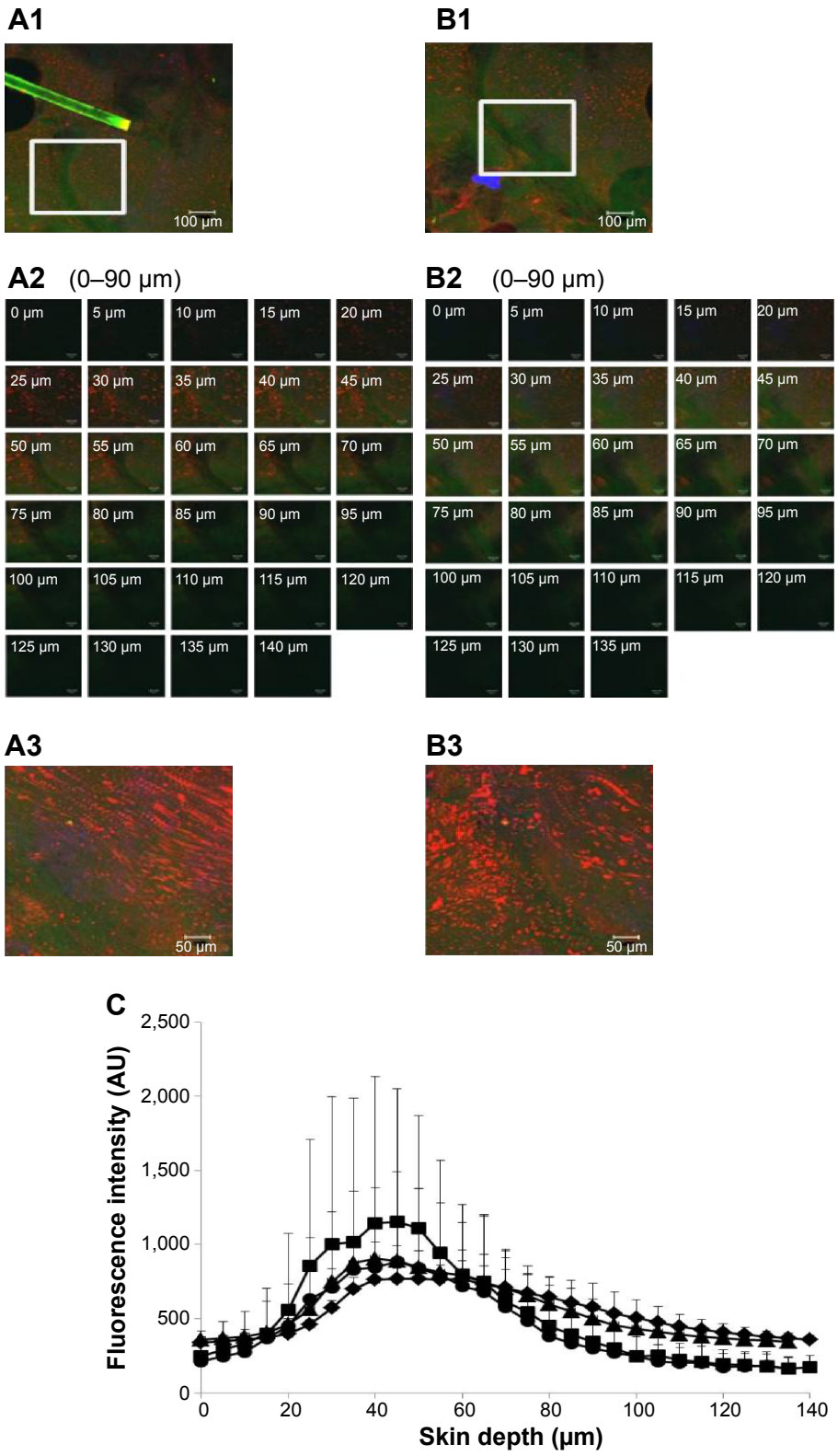

Figure 6 CLSM images of skin treated with ULs with 1% cineole.

Notes: (**A1** and **B1**) The x–y plane serial follicular and nonfollicular localization of porcine skin treated with NaFl-loaded Rh-PE-labeled ULs with 1% cineole at 4 hours. The scale bar represents 100 µm. (**A2** and **B2**) The serial x–z plane magnification of the marked area from the follicular and nonfollicular regions at different skin depths using a 20× objective lens. The scale bar represents 50 µm. (**A3** and **B3**) The intensity over projection of z-axis images of **A2** and **B2**, respectively. The scale bar represents 50 µm. The blue, green, and red fluorescence are the autofluorescence, NaFl, and Rh-PE, respectively. (**C**) Comparison of the fluorescence intensity profiles of NaFl and Rh-PE at different skin depths of **A2** (♦, NaFl; ■, Rh-PE) and **B2** (▲, NaFl; ●, Rh-PE).

Abbreviations: AU, arbitrary unit; CLSM, confocal laser scanning microscopy; NaFl, sodium fluorescein; Rh-PE, rhodamine B 1,2-dihexadecanoyl-sn-glycero-3-phosphoethanolamine triethylammonium salt; ULs, ultradeformable liposomes.

was significantly higher than the nonfollicular region, particularly at penetration depths of 20–60 μm, indicating that ULs with 1% cineole penetrated through the follicular region more than the nonfollicular region. Three skin penetration pathways were proposed, intercellular, transcellular, and the transappendageal or transfollicular pathway.[31] To overcome the stratum corneum barrier, follicular penetration is considered an effective penetration pathway because this pathway can bypass the stratum corneum to the dermis. ULs with 1% cineole increased the skin penetration of NaFl by penetrating via the follicular pathway.

The fluorescence intensity of NaFl in Figure 6A2 and B2 was lower than in Figure 5A2 and B2. This difference may be a result of the different vesicle release rates in the skin tissue. These CLSM studies reveal that the increase in skin penetration of NaFl from ULs with terpenes was caused by the selective follicular penetration of vesicles.

Conclusion

These studies revealed that the liposomal fluidity correlated with the skin penetration enhancement of the entrapped drug. The increase in liposomal fluidity resulted in the skin penetration enhancement of NaFl. Based on the ESR study, the addition of Tween 20 resulted in vesicle fluidity at the C5 atom of the phospholipid acyl chain, indicating that Tween 20 molecules were localized near the hydrophilic portion of the phospholipid bilayer. Terpenes, which were incorporated in ULs, induced liposomal fluidity at the C16 atom of the phospholipid acyl chain, indicating that terpene molecules were localized near the lipophilic region of the phospholipid bilayer. The CLSM study shows that the mechanism of skin penetration enhancement of NaFl from ULs with terpenes occurred because of an increase in the follicular penetration of phospholipid vesicles.

Acknowledgments

The authors gratefully acknowledge the Thailand Research Funds through the Basic Research Grant (Grant No 5680016), and the Faculty of Pharmacy, Silpakorn University, Nakhon Pathom, Thailand for facilities and financial support.

Disclosure

The authors report no conflicts of interest in this work.

References

1. Lee JW, Park JH, Prausnitz MR. Dissolving microneedles for transdermal drug delivery. *Biomaterials*. 2008;29:2113–2124.
2. Djabri A, Guy RH, Delgado-Charro MB. Transdermal iontophoresis of ranitidine: an opportunity in paediatric drug therapy. *Int J Pharm*. 2012; 435:27–32.
3. Herwadkar A, Sachdeva V, Taylor LF, Silver H, Banga AK. Low frequency sonophoresis mediated transdermal and intradermal delivery of ketoprofen. *Int J Pharm*. 2012;423:289–296.
4. Sung KC, Fang JY, Wang JJ, Hu OY. Transdermal delivery of nalbuphine and its prodrugs by electroporation. *Eur J Pharm Sci*. 2003;18:63–70.
5. Andrews SN, Zarnitsin V, Bondy B, Prausnitz MR. Optimization of microdermabrasion for controlled removal of stratum corneum. *Int J Pharm*. 2011;407:95–104.
6. Hathout RM, Nasr M. Transdermal delivery of betahistine hydrochloride using microemulsions: physical characterization, biophysical assessment, confocal imaging and permeation studies. *Colloids Surf B Biointerfaces*. 2013;110:254–260.
7. El-Laithy HM, Shoukry O, Mahran LG. Novel sugar esters proniosomes for transdermal delivery of vinpocetine: preclinical and clinical studies. *Eur J Pharm Biopharm*. 2011;77:43–55.
8. Shen LN, Zhang YT, Wang Q, Xu L, Feng NP. Enhanced *in vitro* and *in vivo* skin deposition of apigenin delivered using ethosomes. *Int J Pharm*. 2014;460:280–288.
9. El-Nabarawi MA, Bendas ER, El Rehem RT, Abary MY. Transdermal drug delivery of paroxetine through lipid-vesicular formulation to augment its bioavailability. *Int J Pharm*. 2013;443:307–317.
10. Cevc G, Blume G. Biological activity and characteristics of triamcinolone–acetonide formulated with the self-regulating drug carriers, Transfersome®. *Biochim Biophys Acta*. 2003;1614:156–164.
11. Cevc G, Blume G. Lipid vesicles penetrate into intact skin owing to the transdermal osmotic gradients and hydration force. *Biochim Biophys Acta*. 1992;1104:226–232.
12. Cevc G, Schätzlein A, Richardsen H. Ultradeformable lipid vesicles can penetrate the skin and other semi-permeable barriers unfragmented: evidence from double label CLSM experiments and direct size measurements. *Biochim Biophys Acta*. 2002;1564:21–30.
13. Rother M, Seidel EJ, Clarkson PM, Mazgareanu S, Vierl U, Rother I. Efficacy of epicutaneous Diractin® (ketoprofen in Transfersome®gel) for the treatment of pain related to eccentric muscle contractions. *Drug Des Devel Ther*. 2009;3:143–149.
14. Cevc G, Mazgareanu S, Rother M. Preclinical characterisation of NSAIDs in ultradeformable carriers or conventional topical gels. *Int J Pharm*. 2008;36:29–39.
15. Kang MJ, Eum JY, Park SH, et al. Pep-1 peptide-conjugated elastic liposomal formulation of taxifolin glycoside for the treatment of atopic dermatitis in NC/Nga mice. *Int J Pharm*. 2010;402:198–204.
16. Dragicevic-Curic N, Scheglmann D, Albrecht V, Fahr A. Development of different temoporfin-loaded invasomes – novel nanocarriers of temoporfin: characterization, stability and *in vitro* skin penetration studies. *Colloid Surf B Biointerfaces*. 2009;70:198–206.
17. Dragicevic-Curic N, Scheglmann D, Albrecht V, Fahr A. Temoporfin-loaded invasomes: development, characterization and *in vitro* skin penetration studies. *J Control Release*. 2008;127:59–69.
18. Subongkot T, Duangjit S, Rojanarata T, Opanasopit P, Ngawhirunpat T. Ultradeformable liposomes with terpenes for delivery of hydrophilic compound. *J Liposome Res*. 2012;22:254–262.
19. Subongkot T, Wonglertnirant N, Songprakhon P, Rojanarata T, Opanasopit P, Ngawhirunpat T. Visualization of ultradeformable liposomes penetration pathways and their skin interaction by confocal laser scanning microscopy. *Int J Pharm*. 2013;441:151–161.
20. Coderch L, Fonollosa J, Pera MD, Estelrich J, Maza ADL, Parra JL. Influence of cholesterol on liposome fluidity by EPR relationship with percutaneous absorption. *J Control Release*. 2000;68:85–95.
21. Man D, Olchawa R, Kubica K. Membrane fluidity and the surface properties of the lipid bilayer: ESR experiment and computer simulation. *J Liposome Res*. 2010;20:211–218.
22. Anjos JLD, Alonso A. Terpenes increase the partitioning and molecular dynamics of an amphipathic spin label in stratum corneum membranes. *Int J Pharm*. 2008;350:103–112.
23. Haag SF, Fleige E, Chen M, et al. Skin penetration enhancement of core–multishell nanotransporters and invasomes measured by electron paramagnetic resonance spectroscopy. *Int J Pharm*. 2011;416:223–228.

24. Lannone A, Rota C, Bergamini S, Tomasi A, Canfield LM. Antioxidant activity of carotenoids: an electron-spin resonance study on beta-carotene and lutein interaction with free radicals generated in a chemical system. *J Biochem Mol Toxicol*. 1998;12:299–304.
25. Dragicevic-Curic N, Friedrich M, Petersen S, et al. Assessment of fluidity of different invasomes by electron spin resonance and differential scanning calorimetry. *Int J Pharm*. 2011;412:85–94.
26. Yeom S, Shin BS, Han S. An electron spin resonance study of non-ionic surfactant vesicles (niosomes). *Chem Phys Lipids*. 2014; 181:83–89.
27. Keith A, Bulfield G, Snipes W. Spin-labeled neurospora mitochondria. *Biophys J*. 1970;10:618–629.
28. Tasi LM, Liu DZ, Chen WY. Microcalorimetric investigation of the interaction of polysorbate surfactants with unilamellar phosphatidylcholines liposomes. *Colloids Surf A*. 2003;213:7–14.
29. Chain E, Kemp I. The isoelectric points of lecithin and sphingomyelin. *Biochem J*. 1934;28:2052–2055.
30. Saesoo S, Sramala I, Soottitantawat A, Charinpanitkul T, Ruktanonchai UR. Enhanced stability and in vitro bioactivity of surfactant-loaded liposomes containing Asiatic Pennywort extract. *J Microencapsul*. 2010; 27:436–446.
31. Maghraby GME, Barry BW, Williams AC. Liposomes and skin: from drug delivery to model membranes. *Eur J Pharm Sci*. 2008;34: 203–222.

Pharmaceutical Development and Technology

http://informahealthcare.com/phd
ISSN: 1083-7450 (print), 1097-9867 (electronic)

Pharm Dev Technol, Early Online: 1–8
 DOI: 10.3109/10837450.2015.1048552

informa healthcare

RESEARCH ARTICLE

Application of Design Expert for the investigation of capsaicin-loaded microemulsions for transdermal delivery

Sureewan Duangjit[1,2], Wisuta Chairat[1], Praneet Opanasopit[1], Theerasak Rojanarata[1], and Tanasait Ngawhirunpat[1]

[1]Faculty of Pharmacy, Silpakorn University, Nakhon Pathom, Thailand and [2]Faculty of Pharmaceutical Sciences, Ubon Ratchathani University, Ubon Ratchathani, Thailand

Abstract

Our previous study reported that the Design Expert® Software showed a beneficial role in the development of microemulsions (ME) for transdermal drug delivery. To fully confirm the reproducibility and the reliability of simultaneous optimal ME formulations, the optimal ME formulations predicted by the Design Expert® Software were experimentally formulated and verified for their skin permeability. Ternary phase diagrams were used to predict the optimal ME area, and the ME formulations selected from outside this area were considered as candidate ME systems. Our ME systems were formulated with isopropyl myristate (IPM) as the oil phase, cocamide diethanolamine (DEA) as the surfactant, ethanol as a co-surfactant and water as the aqueous phase. The droplet size, size distribution, electrical conductivity, pH, drug content and skin permeability of the candidate ME systems were monitored. Our findings indicated that the skin permeability of the optimal ME and all of the candidate ME formulations was significantly greater than that of the commercial capsaicin (CAP) product. Our study succeeded in predicting and developing the ME systems for the transdermal delivery of CAP. The simplex lattice design used in this study is experimentally useful for the development of pharmaceutical formulations.

Keywords

Capsaicin, cocamide diethanolamine, Design Expert, microemulsions, simplex lattice design

History

Received 29 January 2015
Revised 16 April 2015
Accepted 28 April 2015
Published online 21 May 2015

Introduction

In the development of pharmaceutical formulations, a complicated relationship exists between the formulation factors and the pharmaceutical responses. Therefore, design of experiment (DoE) was used to clarify the relationship between the formulation factors or causal factors (X_n) and the pharmaceutical responses or response variables (Y_n). Currently, DoE is an acceptable and well-organized technique for determining the critical attributes that may affect pharmaceutical products and processes[1]. DoE analysis utilizes a response surface method (RSM) to resolve optimization troubles, and several pharmaceutical research studies have successfully utilized RSM[2–4]. Our previous study has also suggested that a simplex lattice design is beneficial for the development of microemulsions (ME) used in transdermal drug delivery[5].

Microemulsions (ME) are transparent colloidal systems composed of two immiscible phases that are stabilized by a surfactant system. ME have long been used in several drug delivery systems, including oral, parenteral, nasal and topical applications[6–10]. ME have also been extensively studied for transdermal delivery because they offer several advantages, such as high-loading capacities for hydrophilic and lipophilic drugs, ease of preparation and thermodynamic stability[11,12]. However, the ME that provides relatively high-skin permeability also contains high concentrations of surfactant systems[13]. Therefore, skin irritation and the safety of the surfactant system used may restrict the utilization of these ME. In the development of suitable ME for transdermal delivery, it is important to prepare optimal ME formulations that have the proper skin permeability without inducing skin irritation. Moreover, ME containing at least three components (oil, water and a surfactant) could simultaneously affect the physicochemical characteristics and the skin permeability of the ME. Therefore, it was appropriate to apply DoE in clarifying the relationships between the causal factors and the response variables to optimize the ME formulation.

Capsaicin (CAP) is a potent, pungent taste compound from chili peppers that is applied for reducing pain associated with various diseases, such as lumbago, sciatica, rheumatism, post-hepatic neuralgia or musculoskeletal inflammation. The hot, pungent taste of CAP reliably relieves pain due to its ability to cause a burning sensation in mammalian tissues[14]. However, high concentrations of CAP (0.75% w/w) may cause local skin irritation[15]. The chemical structure of CAP is shown in Figure 1.

The aims of this study were to develop ME systems based on computer design and to optimize these ME systems for the transdermal delivery of CAP. The challenge in achieving our aims was to discover a potential ME that incorporated a low dose of CAP (0.15% w/w) and a low concentration of the surfactant system. The model ME formulations were obtained from a pseudo-ternary phase diagram. A CAP-loaded ME composed of isopropyl myristate (IPM) as the oil phase, cocamide

Address for correspondence: Tanasait Ngawhirunpat, Faculty of Pharmacy, Silpakorn University, Sanamchan Palace Campus, Nakhon Pathom 73000, Thailand. Tel: +66-34-255800. Fax: +66-34-255801. E-mail: ngawhirunpat_t@su.ac.th

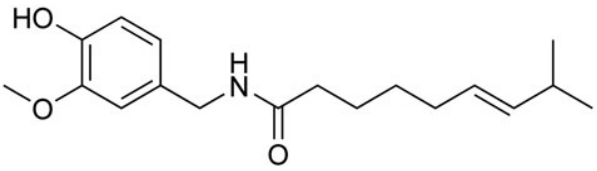

Figure 1. The chemical structure of CAP.

diethanolamine (cocamide DEA) as the surfactant, ethanol as the co-surfactant and reverse osmosis water (RO water) as the aqueous phase was prepared. The physicochemical characteristics of the ME (e.g. droplet size, size distribution, zeta potential, electrical conductivity and pH), the CAP content and the skin permeability were then determined. The response surfaces and optimal ME formulations were estimated using the Design Expert® Software. To fully confirm the reproducibility and to investigate the reliability of the response surface estimated from the computer program, the ME systems outside the optimal ME area were selected as the candidate ME. The optimal ME and the candidate ME selected from outside the optimal area of the ternary phase diagram were experimentally prepared. Finally, the optimal ME and the candidate ME formulations were compared with a commercial CAP product.

Materials and methods

Materials

Isopropyl myristate (IPM) was obtained from Palm-Oleo (Klang) Sdn. Bhd. (KLK Oleo) (Selangor, Malaysia). Cocamide DEA was supplied by BASF (Thai) Co. Ltd. (Bangkok, Thailand). Ethanol was purchased from Commercial Alcohols Inc. (Toronto, ON). CAP was purchased from Hunan Huacheng Biotech, Inc. (Changsha, China). All other chemicals were commercially available and of analytical and high-performance liquid chromatography (HPLC) grade.

Construction of the pseudo-ternary phase diagram

The pseudo-ternary phase diagram of the three components, including the oil phase, the water phase and the surfactant systems, was constructed using the water titration technique[5]. The surfactant system was composed of a mixture of the surfactant (S) and co-surfactant (CoS) at weight ratios of 1:1, 2:1, 3:1 and 4:1. The surfactant system was dissolved in the oil phase at ratios of 9:1, 8:2, 7:3, 6:4, 5:5, 4:6, 3:7, 2:8 and 1:9 (S/CoS:oil) in glass vials at room temperature. Each vial containing the oil phase and the S/CoS mixture was continuously titrated dropwise with RO water using a burette and gentle magnetic stirring until the mixture became turbid. All ME systems were left titrating for at least 10 min before they were defined as turbid in order to prevent metastable systems. The time taken for the ME systems to equilibrate could be significantly increased as the phase boundary was approached. The phase diagrams were time-consuming to construct, particularly when the purpose was to accurately delineate the phase diagram[16]. Thus, the percentage of each component was calculated, and then a pseudo-ternary phase diagram was sketched and constructed from the triangular coordinates[17].

Computer design

A simplex lattice design was utilized to optimize the ME systems. The three components of the ME, including the oil phase (X_1), the water phase (X_2) and the surfactant system (X_3), were defined as causal factors. Based on the ME area under the pseudo-ternary phase diagram (Figure 2A), the upper and lower limits of each component were assigned as follows:

$$20 \leq X_1 \leq 40(\%) \quad (1)$$

$$10 \leq X_2 \leq 30(\%) \quad (2)$$

$$50 \leq X_3 \leq 70(\%) \quad (3)$$

$$X_1 + X_2 + X_3 = 100(\%) \quad (4)$$

The three components of the ME systems were varied simultaneously, and the whole concentration was adjusted to 100%.

Preparation of CAP-loaded ME

The ME were prepared according to the formulations obtained from the ME area under the pseudo-ternary phase diagrams. The ratios of oil phase, water phase and surfactant systems were varied according to the model ME formulation obtained from the computer design, as displayed in Figure 1. The model formulation of the CAP-loaded ME was prepared with IPM as the oil phase, RO water as the water phase, cocamide DEA as the surfactant and ethanol as the co-surfactant (Table 1). All components were accurately weighed and mixed well. CAP was thoroughly weighed, merged with the ME and stirred with a magnetic stirrer. CAP-loaded ME were stored in airtight containers at room temperature prior to further evaluation.

Evaluation of droplet size, size distribution, electrical conductivity and pH

The average droplet size and size distribution of the ME were evaluated by dynamic light scattering (Zetasizer Nano ZS, Malvern Instruments, Worcestershire, UK). The ME samples were measured using a helium-neon laser beam at a wavelength of 632.8 nm. The measurement angles were monitored at 12.8° and 175° at 25 °C. One milliliter of each ME sample was loaded into a disposable zeta cell. The electrical conductivity of the ME formulations was determined using a conductivity meter (S230 SevenCompact™, Mettler Toledo, Switzerland). The pH was measured using a pH meter (S220 SevenCompact™, Mettler Toledo, Switzerland). All measurements were performed in triplicate at 25 °C.

Determination of CAP content

The CAP-loaded ME were extracted with methanol (1:1 v/v), and the ME/methanol mixture was centrifuged at 14 000 rpm at 25 °C for 30 min. The supernatants were collected and filtered through a 0.22 μm nylon filter and then analyzed by ultra-performance liquid chromatography (UPLC).

In vitro skin permeation studies

The protocols utilized to generate the animal experimental data were approved by the ethics committee for the use of laboratory animals, Faculty of Pharmacy, Silpakorn University (Protocol Number: 001/2014). Full-thickness skin from female mice (6–8 weeks old) was used in this study. The subcutaneous fatty tissue was carefully removed from the mice skin using a scalpel and surgical scissors. After the subcutaneous tissue was totally removed, the skin surface was cleaned with phosphate buffer solution pH 7.4. The skin was blotted dry by exposing the ambient air conditions for 20 min and then packed in aluminum foil. All skin samples were stored at −10 °C and thawed

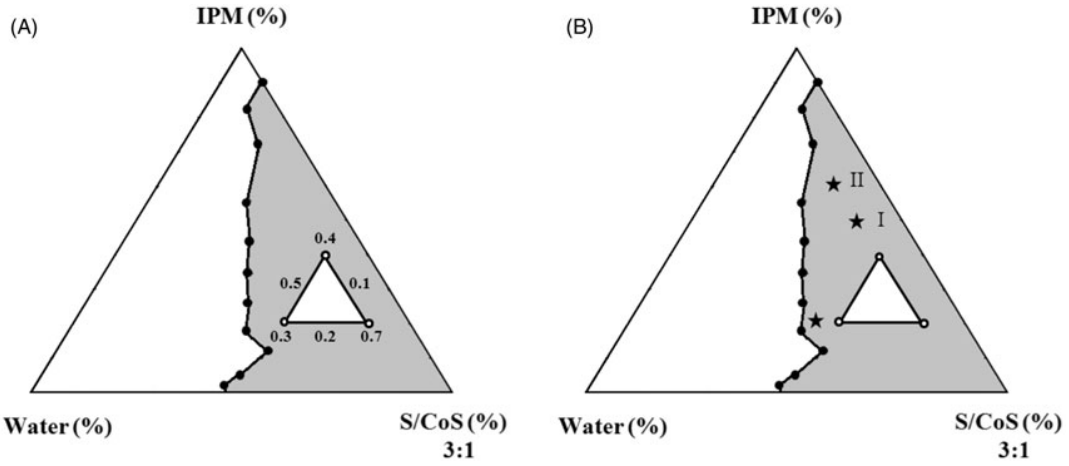

Figure 2. The pseudo-ternary phase diagram. (A) The simplex lattice design for the three formulation factors in the ME area and (B) the exterior optimal ME area of the candidate ME.

Table 1. The model formulations of CAP-loaded microemulsions.

Formulation	IPM (%)	Water (%)	S (%)	CoS (%)
1	40	10	25	25
2	30	20	25	25
3	20	30	25	25
4	20	25	27.5	27.5
5	20	15	32.5	32.5
6	20	10	35	35
7	30	10	30	30

immediately prior to use. After thawing, the skin was cut and immediately mounted between the two chambers of Franz diffusion cells. The stratum corneum side of the mice skin was faced upward into the donor chamber, and the other side was faced downward into the receiver chamber. The diffusion cells had an available diffusion area of 2.3 cm^2 and a water jacket connected to a 32 °C water bath. The donor chamber was filled with 2 g of 0.15% w/v CAP-loaded ME formulations or 0.15% w/v CAP topical solution (a commercial product manufactured in the USA) under occlusive conditions. The receiver chamber was filled with 6.0 ml of an alcohol and phosphate buffer pH 7.4 mixture (1:1 v/v) under sink conditions. At time intervals of 0.5, 1, 2, 3, 4, 5, 6, 7 and 8 h, 0.7 ml of receiver medium was withdrawn and replaced with the same volume of fresh alcohol-phosphate buffer. All samples withdrawn from the receiver medium were stored at 4 °C until UPLC analysis. The cumulative amount of CAP that permeated through the skin was plotted against time. The slope of the linear portion was defined as the skin permeation flux (J).

Determination of CAP concentration

A UPLC system consisting of an ACQUITY UPLC Core system (Waters Corporation, Milford, MA), a binary solvent management system, two switching solvents, a degasser, an ACQUITY TUV Detector and a column heater was used to analyze the CAP in all samples in our study. A Waters® ACQUITY UPLC BEC C18 analytical column (2.1 mm × 100 mm, 1.7 µm) was used (Waters Corporation, Milford, MA). The mobile phase consisted of 1% acetic acid/acetonitrile (60:40 v/v). The flow rate was set at 0.3 ml/min with an injection volume of 2.0 µl. The UV detector was set at 280 nm at 30 °C for all measurements.

Simultaneous optimization of the optimal ME

The optimization of the CAP-loaded ME was studied based on a three-component system consisting of an oil phase (X_1), a water phase (X_2) and a surfactant system (X_3) as the causal factors. The physicochemical characteristics of the ME, such as the droplet size (Y_1), the size distribution (Y_2), the zeta potential (Y_3), the electrical conductivity (Y_4), the pH (Y_5), the CAP content (Y_6) and the skin permeability (Y_7) were defined as response variables. The simplex lattice design was utilized to estimate the relationship between the causal factors and the response variables to statistically predict the optimal ME formulation. The response surfaces of all response variables were evaluated and sketched using the Design Expert® Software (Version 8), Approved No. 009503 (Stat-Ease, Inc., Minneapolis, MN). The best fitting mathematical curves (linear, cubic, special cubic and quadratic) were revealed based on the summary statistics for the model, which were the standard deviation (SD), the multiple correlation coefficient (R^2), the adjusted multiple correlation coefficient (adjusted R^2), the predicted multiple correlation coefficient (predicted R^2) and the predicted residual sum of square (PRESS). These statistics were all verified with the Design Expert® Software. The simultaneous optimal ME formulation was estimated to have the appropriate characteristics prescribed in a previous study[5]. Briefly, the optimal ME formulation was a ME with a small droplet size (nano-sized), a very small charge (or no charge), electrical conductivity (in range), pH (in range), a maximum CAP content, a maximum skin permeation flux and a minimum concentration of the surfactant system.

Evaluation of the optimal ME

After the simultaneous optimal ME formulation was predicted by the Design Expert® Software, the ME systems outside the optimal ME area were selected as the candidate ME (Figure 2B). The optimal ME and the candidate ME systems (candidates I and II) based on ternary phase diagram near the optimal ME formulation were experimentally prepared. The criteria for screening the candidate ME systems were based on the estimation of the response surface. The candidate ME systems were predicted to have a skin permeation flux as high as possible and low S/CoS system level. The ME systems (optimal ME and candidate ME) were characterized and evaluated for their physicochemical characteristics and skin permeability and compared with the commercial CAP product.

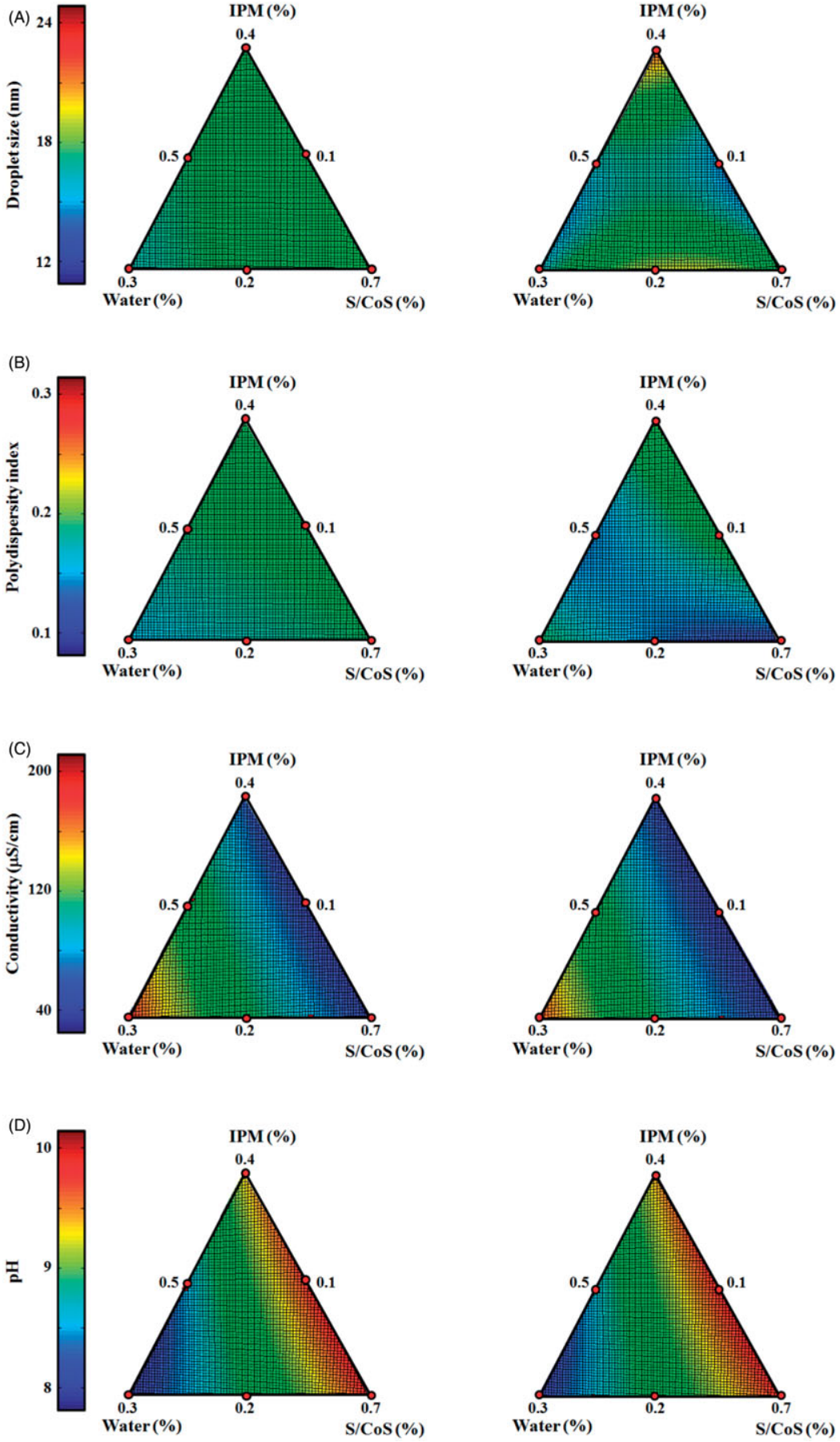

Figure 3. The response surface of (A) droplet size, (B) size distribution, (C) conductivity and (D) pH for both the CAP-free ME (*left column*) and the CAP-loaded ME (*right column*).

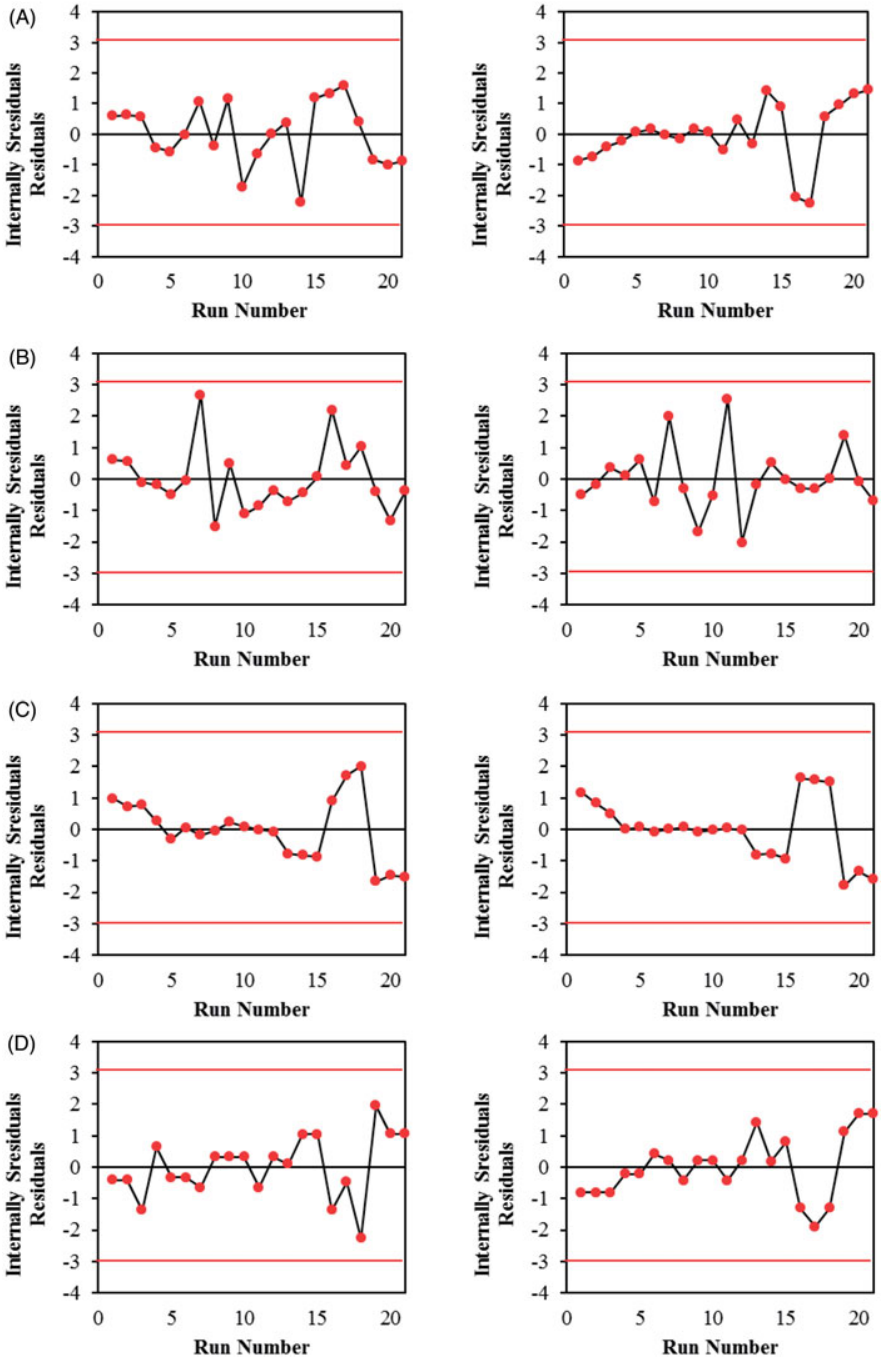

Figure 4. The corresponding residual plot between run number and internally studentized residuals. (A) Droplet size, (B) size distribution, (C) conductivity and (D) pH for both the CAP-free ME (*left column*) and the CAP-loaded ME (*right column*).

Data analysis

All determinations were performed at least in triplicate. The data were exhibited as the mean values ± standard deviation (SD). Statistical analysis of the data was performed using one-way analysis of variance (ANOVA). p Values less than 0.05 were considered to be statistically significant.

Results and discussion

Construction of pseudo-ternary phase diagrams

The pseudo-ternary phase diagrams composed of IPM as the oil phase, cocamide DEA and ethanol as the S/CoS phase and RO water as the water phase were constructed. Based on the visual observation of the phase diagrams of the 1:1, 2:1, 3:1 and 4:1 S/CoS mixtures, the phase diagram with the largest ME area was given by the 3:1 S/CoS mixture. As shown in Figure 2, the shaded area of the phase diagram exhibits the ME area, whereas the non-shaded area defines the turbid area. This phase diagram was used as the primary data source for estimating the response surface and the optimal ME formulation. Thus, it should be noted that each point of the ME system must be accurate in order to construct the phase diagram. Accordingly, none of the ME systems observed in our study were metastable systems[16].

Prediction of response surface and optimal ME using Design Expert®

The appropriate ratio of oil phase, water phase and surfactant systems obtained from the model ME formulation were prepared and investigated experimentally. Based on the experimental results, the response surfaces for each response variable and the

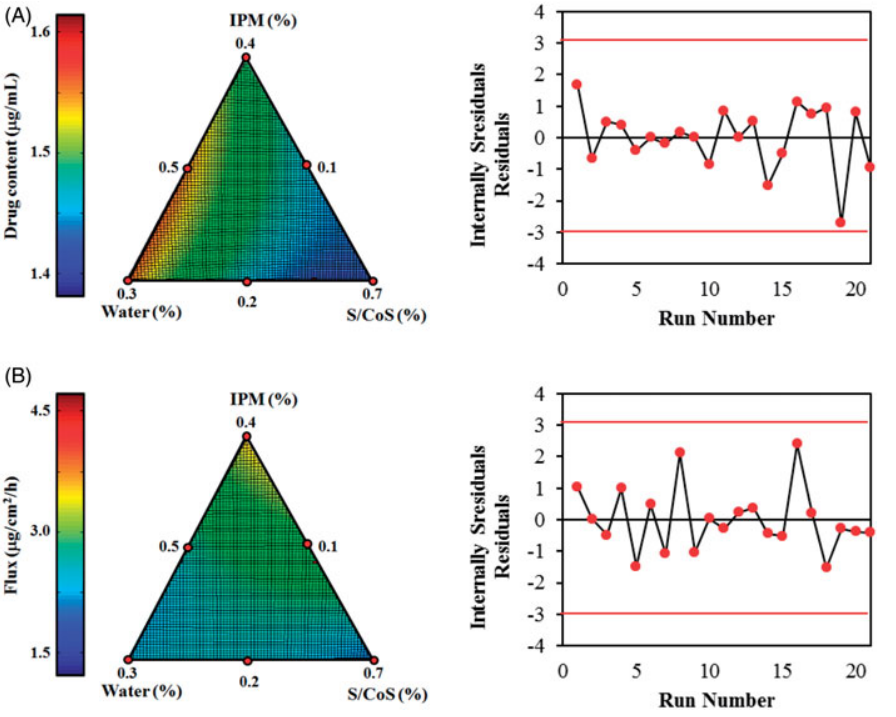

Figure 5. The response surface (*left*) and the corresponding residual plot (*right*) of (A) the drug content and (B) the skin permeation flux of the CAP-loaded ME.

optimal ME formulation were estimated using Design Expert® Software. The ratios of IPM (X_1), RO water (X_2) and S/CoS (X_3) were defined as causal factors, while the physicochemical characteristics of the ME such as droplet size (Y_1), size distribution (Y_2), zeta potential (Y_3), electrical conductivity (Y_4), pH (Y_5), CAP content (Y_6) and skin permeability (Y_7) were defined as response variables. The response surfaces of all the response variables exhibited uncomplicated relationships between the causal factors and the response variables[4,18]. The influences of the formulation factors as causal factors on the physicochemical characteristics of CAP-loaded ME are shown in Figure 3. The response surfaces estimated using the Design Expert® Software could illustrate an obvious relationship between the three components of the ME (IPM, water and S/CoS) and its physicochemical characteristics (droplet size, size distribution, electrical conductivity and pH). Moreover, the role of CAP incorporation in the ME formulation was also represented on these response surfaces.

As shown in Figure 3(A), the response surface indicated that the incorporation of 0.15% w/w CAP into the ME formulation did not significantly affect the droplet size of the ME. The response surface predicted that when the IPM increased (around 0.4), the droplet size of CAP-loaded ME increased. Small droplet sizes of the ME (ranging from 15 to 25 nm) could prevent coalescence and sedimentation, and therefore indicate the ME with good stability[19]. The size distribution of the CAP-loaded ME decreased when the CAP was incorporated, as shown in Figure 3(B). Moreover, the response surface of the size distribution also suggested homogenous size distributions for both the CAP-free ME and the CAP-loaded ME formulations (ranging from 0.1 to 0.2). In the response surface prediction, both the CAP-free ME and the CAP-loaded ME had high-electrical conductivity (>10 μS/cm) and could therefore be classified as water-in-oil ME (Figure 3C). ME with electrical conductivity higher than 10 μS/cm, by contrast, are recognized as oil-in-water ME[20]. The response surface of electrical conductivity generated using the Design Expert® estimation was useful to classify the types of ME,

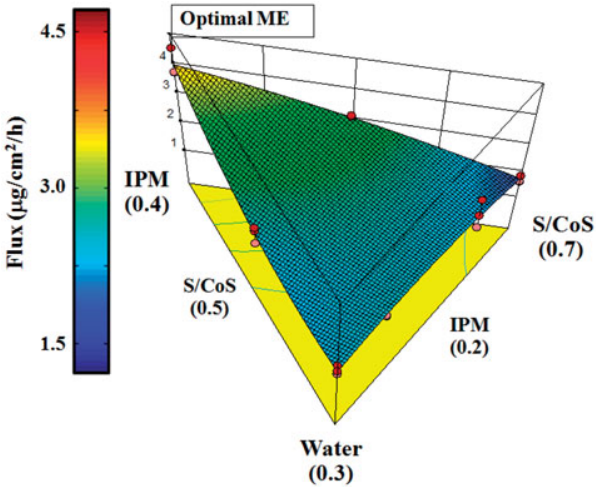

Figure 6. The three-dimensional response surface plot of the desirability of the optimal ME.

revealing that the electrical conductivity of the ME was significantly influenced by the composition of the ME. When the water content was increased, the electrical conductivity significantly increased[21]. The pH of the ME seems to depend on the compositions as represented in the response surface of pH. However, no significant difference was observed between the pH response surfaces of the CAP-free and CAP-loaded ME. Because the pH of the ME formulation depends on the composition of the ME, the incorporation of low concentrations of CAP may not sufficiently affect the pH of the whole ME formulation, as illustrated in Figure 3(D). Baranda et al. reported a significant correlation between skin irritation and pH; however, formulations with pH >11 only resulted in moderate skin irritation[22]. Though none of the ME formulations in our study had pH >11, these ME formulations should be tested for skin irritation *in vivo* in further study.

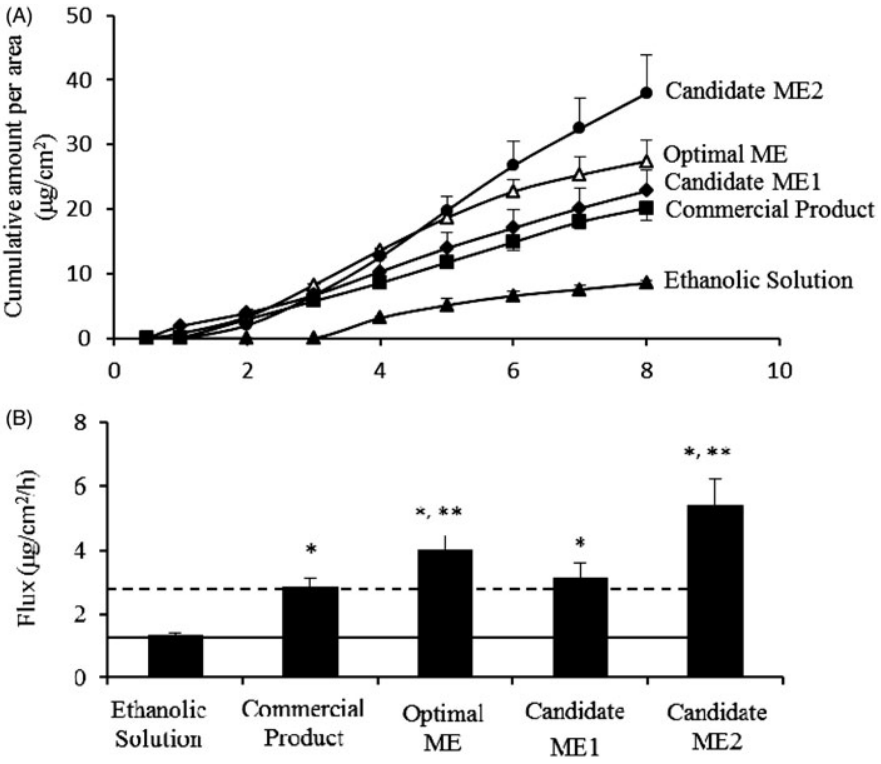

Figure 7. The skin permeation (A) profile and (B) flux of various CAP formulations. * and ** indicate $p < 0.05$ compared with the ethanolic solution and the commercial product, respectively.

The reliability of these response surfaces was confirmed by the corresponding residual plot between the experimental run and the internally studentized residuals for all response variables, as shown in Figure 4. Under the completely randomized run, the vertical distribution of the internally studentized residuals was in line from top-to-bottom. These results revealed that all points fall within the limits of a 95% confidence interval.

Furthermore, the response surfaces for the drug content (as the CAP concentration in the ME formulations) and the skin permeability (as the skin permeation flux values) were also estimated using the Design Expert® Software as shown in Figure 5(A) and (B), respectively. The reliability of the drug content and the skin permeability was also confirmed and is shown in the right column of Figure 5. As shown in Figure 5(A), the response surface of the drug content suggested that although the concentration of S/CoS was low, CAP could be added into the ME systems. Thus, 0.15% (w/w) CAP could be incorporated into our ME systems. The incorporation of S/CoS into ME can result in a high-solubilization capacity, allowing for the incorporation of a large amount of drugs. The incorporation of large amounts of drugs has generated considerable interest in ME systems as alternative pharmaceutical formulations for drug delivery carriers[5]. The response surface of the skin permeation flux of the CAP-loaded ME indicated that a medium-to-high level of IPM and medium-to-low level of S/CoS increased the flux of the ME systems (Figure 5B). Not at all of the penetration enhancers, such as cocamide DEA, increased the skin permeability of the ME[20,23], because several factors including the drug concentration in the formulation or the specific design of formulation can affect the skin permeability. Compared to various vehicles (e.g. Transcutol, Labrafil, Labrasol, glycerine, oleic acid, etc.), IPM has been reported to show the largest *in vitro* skin permeability across the whole intact skin of hairless mice[24]. These results suggested that the Design Expert® Software successfully predicted the response surfaces that exhibited the relationship between the three components of an ME and its physicochemical characteristics.

The optimal CAP-loaded ME was optimized based on the experimental results using Design Expert® Software. The eligible response variables for predicting the optimal ME formulation were used to develop the optimal ME with the highest skin permeability and the lowest amount of surfactant systems employed. The optimal CAP-loaded ME was predicted to have a composition of 40% IPM, 10% water, 25% cocamide DEA and 25% ethanol, with a skin permeation flux of 4.02 μg/cm^2/h. The three-dimensional response surface plot showing the desirability of the optimal ME is shown in Figure 6. The desirability of the prediction was located close to the IPM apex, indicating that the skin permeation flux increased under the ME area when the IPM increased. Several studies have indicated that the experimental value obtained from computer programs, including the Design Expert® Software, all agreed well with the predicted values[2,5,25–27]. In our study, the optimal ME and the ME systems outside the optimal ME area were verified experimentally to fully confirm the reproducibility and reliability of the simultaneous optimal ME formulations.

Comparative study of candidate ME and commercial product

As our previous study suggested that the Design Expert® Software has a beneficial role for the development of ME for transdermal drug delivery, here we fully confirmed and verified the reproducibility and reliability of the Design Expert® Software as well as the predictive ability of the response surfaces. The predictive ability was determined experimentally. Based on the skin permeation flux response surface, the response indicated that the area close to the IPM apex indicated a higher flux value than any other area. Accordingly, the candidate ME systems were selected from the exterior optimal ME area (Figure 2B). The criteria for selecting the candidate ME systems were a high-skin permeation flux and a low amount of surfactant systems in the final mixture. The candidate ME systems were composed of 50%

IPM, 10% water, 20% cocamide DEA and 20% ethanol (as ME candidate I) and 60% IPM, 10% water, 15% cocamide DEA and 15% ethanol (as ME candidate II). The stability of optimal and candidate ME systems was assessed for physical and chemical stability testing at $40 \pm 2\,^{\circ}C/65 \pm 5\%$ RH before the *in vitro* skin permeation study. The result indicated that our ME formulations showed good physical and chemical stability under storage conditions for 2 months.

The skin permeation profiles and the fluxes of the two candidate ME systems (candidates I and II), the optimal ME, the commercial CAP product and the ethanolic CAP solution are illustrated in Figure 7(A) and (B). The results suggested that the skin permeation profiles of CAP in all ME systems were significantly higher ($p < 0.05$) than the ethanolic CAP solution (Figure 7A). The skin permeation fluxes of the experimentally prepared optimal ME and both ME candidates I and II were significantly higher than that of the ethanolic CAP solution (approximately 3, 2 and 4 times, respectively) (Figure 7B). Simultaneously, the skin permeation flux of the experimentally prepared optimal ME and the ME candidate II was significantly higher than that of the commercial CAP product (approximately 1.4 and 1.9 times, respectively). Because a good prediction was obtained from the Design Expert® Software, it could be concluded that the skin permeability of the optimal ME predicted by the Design Expert® Software ($4.02\,\mu g/cm^2/h$) was very close to the actual optimal ME ($4.01 \pm 0.45\,\mu g/cm^2/h$). Furthermore, the skin permeability of the ME candidate II system obtained from the skin permeation flux response surface showed a significantly higher CAP flux ($5.4 \pm 0.81\,\mu g/cm^2/h$) than the other ME, followed by the optimal ME and the ME candidate I. Therefore, the estimation of the simultaneous optimal ME formulation by the Design Expert® Software was verified to be highly predictive. As the experimental results were used as the foremost data source for optimization, it is important that each data value used in estimating the response surface is both precise and accurate.

Conclusion

Using a comparative study, we successfully showed the reliability and reproducibility of the Design Expert® Software for optimization and prediction of a pharmaceutical response. The presented findings indicate that the skin permeability of the optimal ME and the candidate II ME formulations was significantly greater than that of the control and the commercial CAP product. Our study successfully predicted and developed the ME systems for the transdermal delivery of CAP. This is the first study to show that the Design Expert® computer program can be used to obtain candidate ME systems from the exterior optimal ME area that can be established as candidate transdermal delivery carriers.

Declaration of interest

The authors declare no conflicts of interest. The authors gratefully acknowledge the Thailand Research Funds through the Basic Research Grant (Grant No. 5680016), the Silpakorn University Research and Development Institute (Grant No. SURDI 58/01/10), the Faculty of Pharmacy, Silpakorn University, Nakhon Pathom, Thailand, and the Bangkoklab and Cosmetics Co., Ltd, Ratchaburi, Thailand, for the facilities and financial support.

References

1. Hayashi Y, Oshima E, Maeda J, et al. Latent structure analysis of the process variables and pharmaceutical responses of an orally disintegrating tablet. Chem Pharm Bull 2012;60:1419–1425.
2. Obata Y, Ashitaka Y, Kikuchi S, et al. A statistical approach to the development of a transdermal delivery system for ondansetron. Int J Pharm 2010;399:87–93.
3. Norioko T, Hayashi Y, Onuki Y, et al. A novel approach to establishing the design space for the oral formulation manufacturing process. Chem Pharm Bull 2013;61:39–49.
4. Duangjit S, Obata Y, Sano H, et al. Menthosomes, novel ultradeformable vesicles for transdermal drug delivery: optimization and characterization. Biol Pharm Bull 2012;35:1720–1728.
5. Duangjit S, Mehr LM, Kumpugdee-Vollrath M, Ngawhirunpat T. Role of simplex lattice statistical design in the formulation and optimization of microemulsions for transdermal delivery. Biol Pharm Bull 2014;37:1948–1957.
6. Date AA, Nagarsenker MS. Parenteral microemulsions: an overview. Int J Pharm 2008;355:19–30.
7. Li Y, Song J, Tian N, et al. Improving oral bioavailability of metformin hydrochloride using water-in-oil microemulsions and analysis of phase behavior after dilution. Int J Pharm 2014;473:316–325.
8. Butani D, Yewale C, Misra A. Amphotericin B topical microemulsion: formulation, characterization and evaluation. Colloid Surf B 2014;116:351–358.
9. Piaoa HM, Balakrishnana P, Choa HJ, et al. Preparation and evaluation of fexofenadine microemulsions for intranasal delivery. Int J Pharm 2010;395:309–316.
10. Sahoo S, Pani NR, Sahoo SK. Microemulsion based topical hydrogel of sertaconazole: formulation, characterization and evaluation. Colloid Surf B 2014;120:193–199.
11. Bagwe RP, Kanicky JR, Palla BJ, et al. Improved drug delivery using microemulsions: rationale, recent progress, and new horizons. Crit Rev Ther Drug Carrier Syst 2001;18:77–140.
12. Fanun M. Microemulsions as delivery systems. Curr Opin Colloid Interface Sci 2012;17:306–313.
13. Sintov AC, Shapiro L. New microemulsion vehicle facilitates percutaneous penetration in vitro and cutaneous drug bioavailability in vivo. J Control Release 2004;95:173–183.
14. Hayman M, Kam PCA. Capsaicin: a review of its pharmacology and clinical applications. Curr Anaesth Crit Care 2008;19:338–343.
15. Tavano L, Alfano P, Muzzalupo R, de Cindio B. Niosomes vs microemulsions: new carriers for topical delivery of Capsaicin. Colloid Surf B 2011;87:333–339.
16. Lawrence MJ, Rees GD. Microemulsion-based media as novel drug delivery systems. Adv Drug Deliv Rev 2000;45:89–121.
17. Ahmad J, Mir SR, Kohli K, Amin S. Effect of oil and co-surfactant on the formation of Solutol HS 15 based colloidal drug carrier by Box–Behnken statistical design. Colloid Surf A 2014;453:68–77.
18. Duangjit S, Opanasopit P, Rojanarata T, et al. Bootstrap resampling technique to evaluate the reliability of the optimal liposome formulation: skin permeability and stability response variables. Biol Pharm Bull 2014;37:1543–1549.
19. Hathout RM, Woodman TJ, Mansour S, et al. Microemulsion formulations for the transdermal delivery of testosterone. Eur J Pharm Sci 2010;40:188–196.
20. Baroli B, López-Quintela MA, Delgado-Charro MB, et al. Microemulsions for topical delivery of 8-methoxsalen. J Control Release 2000;69:209–218.
21. Zielińska K, Wilk KA, Jezierski A, Jesionowski T. Microstructure and structural transition in microemulsions stabilized by aldonamide-type surfactants. J Colloid Interf Sci 2008;321:408–417.
22. Baranda L, González-Amaro R, Torres-Alvarez B, et al. Correlation between pH and irritant effect of cleansers marketed for dry skin. Int J Dermatol 2002;41:494–499.
23. Peltola S, Saarinen-Savolainen P, Kiesvaara J, et al. Microemulsions for topical delivery of estradiol. Int J Pharm 2003;254:99–107.
24. Cha BJ, Lee ED, Kim WB, et al. Enhanced skin permeation of a new capsaicin derivative (DA-5018) from a binary vehicle system composed of isopropyl myristate and ethoxydiglycol. Arch Pharm Res 2001;24:224–228.
25. Jeirani Z, Mohamed Jan B, Si Ali B, et al. The optimal mixture design of experiments: alternative method in optimizing the aqueous phase composition of a microemulsion. Chemometr Intell Lab 2012;112:1–7.
26. Jeirani Z, Mohamed Jan B, Si Ali B, et al. Prediction of the optimum aqueous phase composition of a triglyceride microemulsion using response surface methodology. J Ind Eng Chem 2013;19:1304–1309.
27. Shi J, Xue SJ, Wang B, et al. Optimization of formulation and influence of environmental stresses on stability of lycopene-microemulsion. LWT Food Sci Technol 2015;60:999–1008.

PHARMACEUTICAL DEVELOPMENT AND TECHNOLOGY, 2016
http://dx.doi.org/10.1080/10837450.2016.1221428

Taylor & Francis
Taylor & Francis Group

RESEARCH ARTICLE

Influence of sonophoresis on transdermal drug delivery of hydrophilic compound-loaded lipid nanocarriers

Worranan Rangsimawong, Praneet Opanasopit, Theerasak Rojanarata, Suwannee Panomsuk and Tanasait Ngawhirunpat

Faculty of Pharmacy, Silpakorn University, Bangkok, Thailand

ABSTRACT

The effect of sonophoresis on the transdermal drug delivery of sodium fluorescein (NaFl)-loaded lipid nanocarriers such as liposomes (LI), niosomes (NI) and solid lipid nanoparticles (SLN) was investigated by confocal laser scanning microscopy (CLSM), Fourier transform infrared spectroscopy (FTIR) and scanning electron microscopy (SEM). The results showed that SN decreased the skin penetration of NaFl-loaded SLN (6.32-fold) and NI (1.79-fold), while it increased the penetration of NaFl-loaded LI (5.36-fold). CLSM images showed the red fluorescence of the LI and NI bilayer on the superficial layer of the stratum corneum. However, the red fluorescent probe of the SLN was not visualized in the skin. FTIR results of the LI and NI with SN showed no effect on lipid stratum corneum ordering, suggesting that the fragment of bilayer vesicles might repair the damaged skin. For SLN, the strengthening of stratum corneum by covering the disrupted skin with solid lipids was shown. SEM images show disrupted carriers of all the formulations adsorbed onto the damaged skin. In conclusion, the SN changed the properties of both the skin surface and lipid nanocarrier, demonstrating that disrupted skin might be repaired by a disrupted nanocarrier.

ARTICLE HISTORY
Received 6 May 2016
Revised 26 June 2016
Accepted 28 June 2016
Published online ▮▮▮

KEYWORDS
Liposomes; niosomes; solid lipid nanoparticles; hydrophilic compound; sonophoresis; skin penetration

Introduction

Sonophoresis (SN) has been proposed as a noninvasive technique for increasing the skin permeability to various drugs by using several mechanisms, such as thermal effects by absorption of ultrasound energy and cavitation effects caused by the collapse and oscillation of cavitation bubbles in an ultrasound field[1,2]. The main effect of cavitation has been found to create aqueous pathways across the stratum corneum by distorting the lipid bilayer, which can lead to enhancement of skin transport of hydrophilic molecules[3].

A simultaneous application of ultrasound to the skin is performed by applying ultrasound energy through a coupling medium containing the drug onto the skin surface, which causes enhancement of drug transport in two ways: (i) by changing the skin structures, leading to increase in skin permeability and (ii) through convection-related mechanisms that occur only when an ultrasound is applied. However, the action of ultrasound on drugs or other active ingredients can cause molecular degradation or other chemical reactions, which can result in a loss of activity or effectiveness of the therapeutic compound and may also cause undesired reactions[1,4,5].

Lipid-based nanocarriers, including liposomes (LI), niosomes (NI), ethosomes, transferosomes, solid lipid nanoparticles (SLN) and nanostructure lipid carriers (NLC), were extensively studied for transdermal delivery of drug by using several permeation mechanisms, such as intact drug-loading vesicle penetration into the different layers of the skin; lipid vesicles acting as penetration enhancers via their skin lipid-fluidizing property; the drug released from carrier and intercalated in the lipid bilayer of the stratum corneum; or lipid vesicle-mediated enhanced transdermal drug delivery via appendageal pathways (e.g. hair follicles and sweat ducts)[6]. A few studies have investigated a combination of SN and a lipid nanocarrier system. Vyas et al. showed that the application of ultrasound and ointment containing LI enhanced diclofenac-entrapped LI permeation across the skin[7], while Dahlan et al. reported that LI application to sonicated skin prior to the application of bovine serum albumin (BSA) solution reduced BSA penetration and transepidermal water loss due to the repair of sonication-induced skin disruption[8]. Moreover, no mechanistic study for the skin penetration of NI and SLN combined with SN has been reported.

Therefore, the aim of this study was to investigate the effect of low frequency SN (20 kHz) on the permeation pathway for the transport of sodium fluorescein (NaFl)-loaded lipid nanocarriers into porcine skin. Lipid nanocarriers, such as LI, NI and SLN, have been used as carriers to enhance the transdermal delivery of NaFl. LI and NI formulations were prepared using a sonication method. SLN was prepared using a *de novo* emulsification method. Particle size, surface charge, entrapment efficiency, loading efficiency and *in vitro* skin penetration were investigated. Confocal laser scanning microscopy (CLSM) was used to visualize the skin penetration pathways of the vesicles. Fourier transform infrared spectroscopy (FTIR) was used to evaluate the stratum corneum change after applying a lipid nanocarrier and SN. Scanning electron microscopy (SEM) was also used to observe the skin surface after applying ultrasound energy.

Materials and methods

Materials

Egg phosphatidylcholine (PC) was a gift from Lipoid GmbH, Ludwigshafen, Germany. Cholesterol (Chol) was obtained from

CONTACT Tanasait Ngawhirunpat ngawhirunpat_t@su.ac.th Department of Pharmaceutical Technology, Silpakorn University, Bangkok 73000, Thailand

Carlo Erba Reagent, Ronado, Italy. Sodium fluorescein ($C_{20}H_{10}Na_2O_5$, MW 376 Da, log $P = -1.52$) was purchased from Sigma-Aldrich, St. Louis, MO. Lissamine™ rhodamine B 1,2-dihexadecanoyl-sn-glycero-3-phosphoethanolamine triethylammonium salt (rhodamine B) was bought from Invitrogen, Carlsbad, CA. Tween 80 was supplied from the NOF Corporation (Osaka, Japan). Cetyl palmitate was purchased from SABO SpA (Levate, Italy).

Nanocarrier formulations

Preparation of LI

A liposomal formulation containing PC and cholesterol (Chol) in the molar ratio 10:2 mM was formulated. Thin film hydration and sonication methods were used to prepare LI[9]. Briefly, PC and Chol were dissolved in chloroform/methanol (2:1, v/v) and then evaporated using nitrogen gas until a thin film formed. The lipid film was placed in a desiccator until completely dry (6 h). NaFl dissolved in phosphate-buffered saline (PBS), pH 7.4 was added to the lipid film to hydrate the LI vesicles. Finally, the dispersion was probe-sonicated under ice-bath for 30 min to reduce the size of the liposomal vesicles. An excess lipid composition was separated from the vesicle formulation by centrifugation at 15,000 rpm at 4 °C for 15 min. A liposomal formulation was collected at 4 °C for 24 h prior to the characterization.

Preparation of NI

A niosomal formulation containing nonionic surfactants (Span 20) and Chol in a 5:5 mM molar ratio was formulated. Thin film hydration and sonication methods were used to prepare NI[9]. Briefly, a mixture of Span20 and Chol dissolved in an ethanol:chloroform mixture (1:1, v/v) were evaporated and placed in desiccator (6 h). NaFl solution was then added to the lipid film to hydrate the NI vesicles. It was then probe-sonicated under an ice-bath for 30 min to reduce their particle size. Excess lipid composition was separated from the vesicle formulation by centrifugation at 15,000 rpm at 4 °C for 15 min. A niosomal formulation was collected at 4 °C for 24 h prior to the characterization.

Preparation of SLN

A SLN formulation was prepared using a *de novo* emulsification method[10]. The composition of an oil phase containing cetyl palmitate and PC was formulated. For an aqueous phase, NaFl and Tween80 were dissolved in PBS. The oil and aqueous phases were heated at 65 ± 5 °C. The aqueous phase was then added to the oil phase with stirring at 14,000 rpm for 5 min using a magnetic stirrer. Emulsions were probe-sonicated for 15 min to reduce the particle size and then filtered through a 0.45-μm membrane filter to remove any precipitate matter.

Characterization of nanocarrier formulations

Particle size and zeta potential analysis

Each formulation was diluted in a 1:20 ratio with water and measured for size distribution and zeta potential, using a Dynamic Light Scattering (DLS) particle size analyzer (Zetasizer Nano-ZS, Malvern Instrument, Worcestershire, UK) with a 4 mW He–Ne laser at a scattering angle of 173°. All measurements were performed in triplicate.

Entrapment efficiency and loading efficiency

Each nanocarrier (0.5 mL) was placed in an ultrafiltration tube with a molecular weight cutoff of 3000 Da (Microcon YM-3; Minipore, Billerica, MA) and centrifuged at 4 °C at 10,000×*g* for 60 min. The filtrate was discarded, and 0.25 mL of PBS was added to the retentate before further centrifugation at 4 °C at 10,000×*g* for 40 min. The collected NaFl-loaded nanocarrier in the retentate was then disrupted with 0.2 mL of 0.1% (w/v) Triton X-100 (for LI and NI) or isopropyl alcohol (for SLNs) and centrifuged at 4 °C at 10,000×*g* for 10 min. The NaFl content of the supernatant was determined by a fluorescence analysis.

The percent of drug entrapment efficiency (%EE) and loading efficiency (%LE) was calculated using the following Equations (1) and (2):

$$\%\mathrm{EE} = \frac{C}{C_i} \times 100 \quad (1)$$

$$\%\mathrm{LE} = \frac{C}{\text{Lipid composition}} \times 100 \quad (2)$$

where C is the concentration of NaFl in the formulation and C_i is the initial concentration of NaFl added.

In vitro *skin permeation study*

Abdominal porcine skin was taken from intrapartum stillborn animals from a farm in Nakhon Pathom. Subcutaneous fat was carefully removed using medical scissors and surgical blades (skin thickness ~0.6–0.7 mm). Samples were frozen at −20 °C until use. The frozen skin was thawed in PBS for 30 min at room temperature.

A skin permeation study was performed using Franz diffusion cells. The receptor compartment of the cell was filled with 6 mL of PBS at 32 °C with stirring at 500 rpm. Approximately 2 mL of NaFl-loaded nanocarrier formulations were applied to the skin in the donor compartment. Samples (0.5 mL) were taken from the receiver compartment at 1, 2, 4, 6, 8 and 24 h for analysis using fluorescence detection. The same volume of PBS was then added to the receiver compartment to maintain a constant volume. Each sample was analyzed in triplicate.

The cumulative amount was plotted against time. The steady-state flux was determined by using the slope of the linear portion of the plot. Lag time was obtained by extrapolating the linear portion of the penetration profile to the abscissa. The skin permeation of each model lipid nanocarrier was analyzed using a mathematical model based on Fick's law of diffusion that included the following Equation (3):

$$K_p = \frac{J}{C_d} \quad (3)$$

where K_p is the permeability coefficients, J is the steady-state flux and C_d is the donor concentration of the formulations.

Sonophoretic treatment

Low frequency SN at 20 kHz was generated using an ultrasonic transducer (Vibra-cell™, VCX130 PB, Sonics and Materials, Inc., Newtown, CT), which has a transducer probe with a radiating diameter of 6 mm. The probe was placed inside the donor compartment with its active horn face located 3 mm above the skin surface. NaFl-loaded lipid nanocarrier formulations (as a coupling medium) were placed in the donor chamber. The skin was then continuously sonicated for 2 min (100% duty cycle, 25% amplitude). The acoustic

intensity applied was 1.90 W/cm^2, which was calculated from the following Equation (4):

$$\text{Intensity}\left(\text{W/cm}^2\right) = \frac{\text{Power (W)}}{\text{Area of skin (cm}^2\text{)}} = \frac{\text{Sound energy (J)}}{\text{Area of skin (cm}^2\text{)} \times \text{Application time (s)}} \quad (4)$$

Fluorescence analysis

Samples (100 μL) were pipetted into a black 96-well plate and analyzed using a fluorescence spectrophotometer (Fusion™ Universal Microplate Analyzer, Packard Instrument Company, Inc., Downers Grove, IL). The excitation wavelength was 485 nm and the emission wavelength was 535 nm. Each sample was determined in triplicate[9].

CLSM study

CLSM was used to visualize the skin penetration pathway of hydrophilic fluorescence-loading in 0.1 mM rhodamine B labeled lipid nanocarriers. After *in vitro* skin permeation experiment at a time of 4 h, whole skin was washed with PBS to remove excess particles on the skin surface. Skin cross sections were made using a cryostat (Leica 1850, Leica Instrument, Wetzlar, Germany). Each skin sample was mounted on a metal sample holder using frozen section medium (Neg50, Microm International, Waldorf, Germany). Frozen skin was sectioned into 10-μm slices and placed on glass microscope slides. Skin tissues were mounted with mounting medium and covered with a cover slip. Confocal images were obtained from ×10 objective lens system of an inverted Zeiss LSM 510 META microscope (Carl Zeiss, Jena, Germany) with a He–Ne laser (excitation wavelength 543 nm; emission wavelength 580 nm), Ar laser (excitation wavelength 488 nm; emission wavelength 514 nm) and diode laser (excitation wavelength 358 nm; emission wavelength 461 nm).

FTIR study

A FTIR spectrophotometer was used to characterize the changes in the stratum corneum on a molecular level. A trypsin digestion method was used to prepare the stratum corneum sheet[11]. The whole skin (stratum corneum side facing upward) was placed on 0.5% w/v trypsin solution in water for 6 h at 37 °C. The stratum corneum sheet was then carefully removed from viable epidermis. Stratum corneum sheets were rinsed with distilled water and dried in a desiccator until they were completely dried. Nanocarrier formulations were applied on stratum corneum sheets for 4 h at 32 °C. The treated sheets were dried and analyzed using a FTIR spectrophotometer (NICOLET4700; Thermo Electron Corporation, Madison, WI) between 4000 and 1000 cm^{-1}. All data were analyzed using version 8 of OMNIC software (Thermo Electron Corporation, Madison, WI).

SEM study

After the *in vitro* skin penetration study at 4 h, the effect of nanocarrier and SN on epidermal structure was observed on the porcine skin. Each skin sample was cut into pieces (1 mm ×2 mm) from the central area. The samples were rapidly frozen in liquid nitrogen and dried using a Freeze-Dry System (FreeZone 2.5; Labconco, Kansas City, MO) for 24 h. The dried specimens were gold-coated using a sputtering device. Specimens were then observed under a scanning electron microscope (Camscan Mx2000, Obducat Camscan Ltd, Cambridge, UK). Photographs were taken from the skin in different penetration regions.

Statistical analysis

All experimental measurements were done in triplicate. Values are expressed as the mean and standard deviation (SD). Statistical significance was analyzed using a one-way analysis of variance (ANOVA) followed by Tukey's *post hoc* test. The significance level was set at $p < .05$.

Results and discussion

Physicochemical characterization of nanocarriers

The average particle sizes of the LI, NI and SLN were 108.07 ± 1.24 nm, 243.73 ± 2.94 nm and 130.23 ± 1.42 nm, respectively. All formulations had a narrow size distribution (polydispersity index; PDI <0.3). The zeta potentials of the LI, NI and SLN were −11.15 ± 2.98 mV, −49.43 ± 1.77 mV and −19.03 ± 1.09 mV, respectively. For the NaFl-loaded lipid nanocarrier, the entrapment efficiencies (%EE) of the LI, NI and SLN were 17.20 ± 1.20%, 40.47 ± 1.08% and 47.31 ± 3.19%, respectively, and the loading efficiency (%LE) of LI, NI and SLN were 4.14 ± 0.05%, 22.13 ± 0.59% and 1.58 ± 0.11%, respectively. In a previous study, the SLN formulations had a high %EE but low %LE because the high lipid composition of the SLNs has more space to entrap NaFl than other formulations. The NI had a higher loading efficiency than the LI or SLN formulations because cholesterol could make the NI bilayer less fluid and increase drug loading efficiency[12].

In vitro *skin penetration study*

As shown in Figure 1, the amount of NaFl delivered from the different lipid nanocarrier formulations through the skin were plotted against time. The skin penetration parameters are shown in Table 1. The rate of absorption or flux (J) of any substance across a barrier is proportional to its concentration difference across that barrier. Thus, the proportionality constant between flux and donor concentration is the permeability coefficient (K_p)[13]. In this study, the lag time of all the formulations were not significantly different. In the result of lipid nanocarrier alone, the flux was in the following order: SLN > NI > LI. This indicated that the SLN has a higher entrapment efficiency and that the more lipophilic solid structure can get into close contact with the skin to form a lipid film on the skin surface. An occlusive effect from lipid wax leads to increased skin hydration. Consequently, the effect of SLN enhances the penetration of the drug from the lipid carrier into the skin[14]. The NI showed a higher NaFl penetration through the skin than the LI because the nonionic surfactant and cholesterol increased penetration of the entrapped substances across the skin[15]. Niosome vesicles can interact with the stratum corneum surface by aggregation and adhesion for the penetration of lipophilic drugs across the stratum corneum[16].

For the application of SN with a lipid nanocarrier, the results of the flux rate were in the following order: NI > LI > SLN. The NI with SN showed a higher NaFl flux than the LI with SN and SLN with SN. The NI alone had a higher NaFl flux than NI with SN (1.79-fold), but the difference was not significant. When applying the SN with NI, the niosomal vesicles might break and release entrapped NaFl before contact with the skin surface[7]. The membrane bilayers were adsorbed and covered the defect skin surface,

COLOR Online / B&W in Print

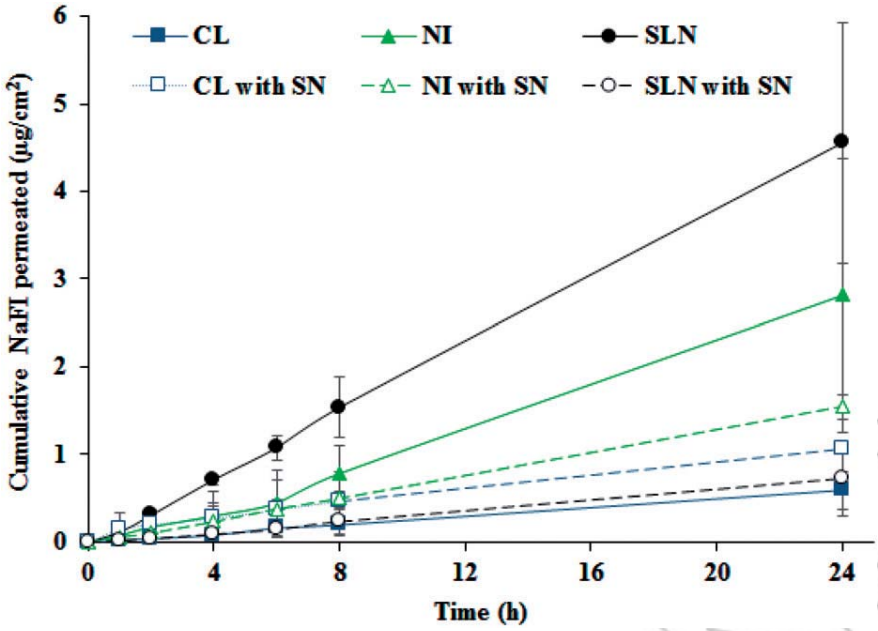

Figure 1. The cumulative amount–time profiles of NaFl in different lipid nanocarrier formulations without and with SN. Symbols: LI with SN (—□—) and without SN (—■—), NI with SN (—Δ—) and without SN (—Δ—), and SLN with SN (—○—) and without SN (—●—). Each value represents the mean ± SD ($n = 3$). *Significant difference between groups ($p < .05$).

Table 1. The penetration parameters of NaFl – lipid nanocarrier formulations. Each value represents the mean ± SD ($n = 3$).

Formulations	Flux (μg/cm²/h)	Lag time (h)	K_p (cm/h) ($\times 10^{-6}$)
LI	0.0078 ± 0.00	1.00 ± 0.35	3.90 ± 2.91
LI with SN	0.0418 ± 0.01[a]	0.20 ± 0.20	20.90 ± 3.49[a]
NI	0.1191 ± 0.06	0.40 ± 0.35	59.60 ± 32.15
NI with SN	0.0666 ± 0.01	0.50 ± 0.35	33.32 ± 3.44
SLN	0.1920 ± 0.06	0.43 ± 0.23	95.98 ± 30.70
SLN with SN	0.0304 ± 0.02[a]	0.50 ± 0.26	15.20 ± 8.89[a]

[a]Significant different from other groups ($p < .05$).

which caused a reduction in transport of the hydrophilic compound through skin.

The flux of the LI with SN was higher than with the LI alone (5.36-fold), but it was not significantly different. From the lag time study, the LI with SN provided rapid NaFl permeation through the skin that was greater than the LI alone, suggesting that the SN can increase penetration rate of the LI. Vyas et al. reported that the sonication energy can break the lamellae of LI[7]. The entrapped drugs were released and transported through the stratum corneum[17]. Moreover, LI made from phospholipids, e.g. fluid-state EPC (L-α-PC from egg yolk), may diffuse into the stratum corneum, enhance drug penetration through the skin and repair ultrasound-induced skin disruption by adsorption onto and fusion with the skin surface defect[8,18].

For the SLN, the SN reduced the NaFl penetration through the skin. Thus, the SLN alone had a significantly higher NaFl flux than the SLN with SN (6.32-fold). Ultrasound energy can produce extreme cavitation transient in the medium, which leads to an increased medium temperature due to the medium expanding and producing energetic shock waves from a bubble implosion. However, maintaining the temperature of the dispersion above the melting point of lipids in SLN is essential to facilitate the breakup of oil droplets[19]. In this study, cetyl palmitate is a solid core of SLN. The melting point of cetyl palmitate is 54 °C. The temperature of the donor solutions in contact with the sonicated skin resulted in temperature increases of ~2 °C from 32 ± 5 °C at the end of a 2-min application[9]. Although the temperature of the SLN dispersion was lower than the melting point of the solid core, the sonication energy could break the solid core of the lipid nanoparticles. Then, the skin surface was covered by a solid lipid fraction, leading to reduced NaFl transport through skin.

CLSM study

As shown in Figure 2, confocal images of the skin cross section obtained at 4 h after deposition of the NaFl-loaded-Rh-PE-labeled lipid nanocarriers were visualized. The LI had both red fluorescence of the membrane vesicle and green fluorescence of NaFl in the skin, while the NI and SLN had little or no red fluorescence labeled in the vesicles in the skin. As the LI are made from phospholipids that have the same properties of stratum corneum lipid, the processes of adhesion onto the skin surface, fusion or mixing with the lipid matrix of stratum corneum, and penetration of intact vesicles associated with entrapped drug have been suggested as the penetration mechanism of LI[20,21]. For the LI with SN-treated skin (Figure 2(B)), a higher fluorescent intensity of NaFl and vesicle in the stratum corneum surface was seen that covered the hair follicle opening compared with the LI alone, indicating that the skin repair by adsorbed LI onto the damage skin might enhance the NaFl permeation into skin[9].

The NI and SLN were not permeated into the skin. Only the drug permeates into the skin surface, suggesting that NaFl might be released from the nanocarriers before permeation through the skin. After applying ultrasound energy onto the skin, the NI with SN had the brightest fluorescence intensity for the Rh-PE-labeled NI membrane covering the stratum corneum surface. However, it did not permeate deeply into the skin layer (Figure 2(C)), suggesting that the ultrasound energy might have disrupted the NI vesicle. The lipid fractions of the NI that were adsorbed onto the damage skin and covered the skin surface might then reduce the hydrophilic compound penetration into skin.

For SLN, Figure 2(E) shows the fluorescence intensity of NaFl deposits along the length of the hair follicles inside the skin more than other formulations, indicating that the transfollicular pathway

COLOR Online / B&W in Print

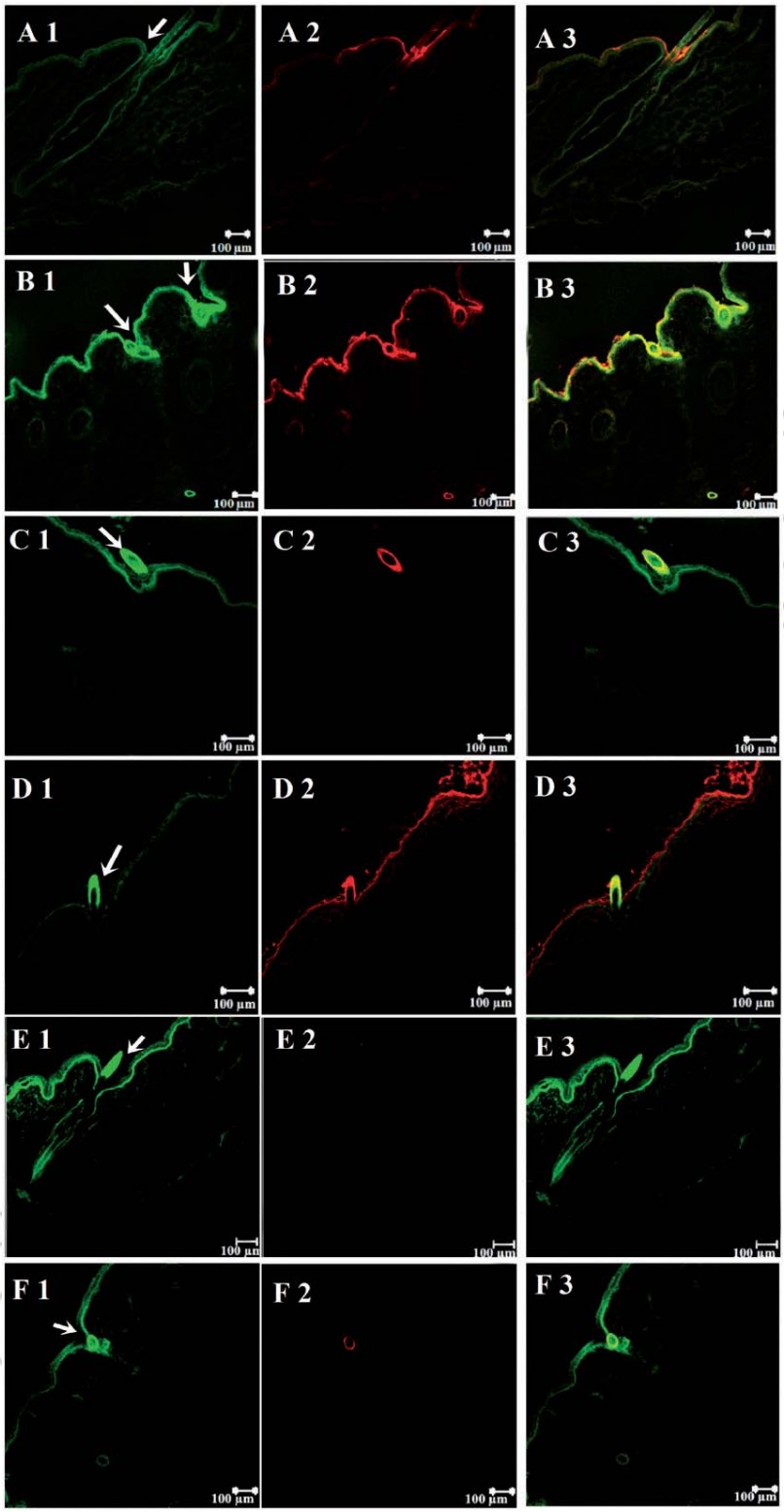

Q3 **Figure 2.** Confocal images of the skin cross-section obtained at 4 h after deposition of the LI alone (A) and with SN (B), NI alone (C) and with SN (D), as well as SLN alone (E) and with SN (F). The image is divided into three parts, with (1) green fluorescence of NaFl, (2) red fluorescence of Rh-PE and (3) an overlay of (1) and (2). The scale bar represents 100 µm. All confocal images were obtained at a magnification of ×10. Symbols: (→, hair follicles).

might be a penetration route of NaFl from the SLN into skin. In the previous study, particulate drug carriers, e.g. lipid nanoparticles, have been shown to penetrate and accumulate preferentially in hair follicles, creating a high local concentration of a drug by using the lipophilicity property of the carriers to improve drug uptake via the hair follicles[22,23]. However, the SLN have a little value of particles in the skin, suggesting that SLN carriers are restricted to permeate into and across deeper skin layers by the barrier function of

the stratum corneum. However, the SLN carriers can be occluded on the top layer of the skin surface that the high concentration of drug on the superficial layer of skin might enhance drug permeation[24,25]. When applying the SN with SLN, the ultrasound energy disrupted the lipid particles at a lower temperature than the melting point of the solid core. Therefore, the fragments of solid lipids might be not covered by surfactant[18,19]. The separation of solid lipid (wax) was irreversible. The CLSM image of the SLN with SN-treated skin showed no value of red fluorescence because the Rh-PE probe may have been released before skin contact by the SLN disruption. Only fragments of solid wax from the disrupted SLN might have covered the top layer of skin leading to reduce the NaFl transport through skin via transdermal and transfollicular pathway.

FTIR study

In this study, the stratum corneum sheets from the porcine abdomen were treated with the lipid nanocarrier and SN. As shown in Figure 3, the phase transition of the lipid was represented by an increase/decrease in the band position of the signals at 2917.6 and 2850.0 of the intact stratum corneum (control). Generally, the prominent peaks obtained near 2920 and 2850 cm^{-1} represent the asymmetric and symmetric stretching modes of the terminal methylene groups of the lipids (ceramides, phospholipids, etc.), respectively, and provide specific information about the interior composition of the lipid bilayer. CH_2 scissoring vibration (1466.2 and 1457.3 cm^{-1}) provides information about the lateral packing of the lipid alkyl chains in the stratum corneum[26–29]. The spilt of the band of the scissoring width was ~10 cm^{-1}, which indicated a high content of the orthorhombic (OR) phase[30]. Additionally, the height intensity of the bands represented the amount of lipid and proteins in the stratum corneum. Any change in the peak intensity suggests the extraction or strengthening of the lipid stratum corneum.

For the results, the LI and NI both without and with the SN showed no or little change in the band position of the CH_2 symmetric and asymmetric stretching and CH_2 scissoring vibration compared with the control. This observation implies a preservation of the conformational order of the SC lipids. However, the band intensity of the LI and NI was lower than the control, indicating that the stratum corneum lipid extraction led to enhanced NaFl permeation through skin. When applying the SN with LI and NI, the result showed lower band intensity than the LI and NI alone, indicating that the ultrasound energy may lead to increased extraction of the membrane lipid from the stratum corneum. These results represent a higher lipid extraction by the SN but no effect on stratum corneum lipid ordering, suggesting that the membrane bilayer of the LI and NI might fuse and repair the skin damage caused by SN.

In the case of SLN, the position of the CH_2 stretching band shifted to a lower wave number with a higher band intensity than the control, suggesting that reorientation of a lipid group by the adsorption of the lipid from the SLN leads to strengthening of the stratum corneum barrier in the presence of orthorhombic phase of chain conformation and preventing evaporation of water from the skin surface by an occlusion effect that provides a high amount of hydrophilic NaFl from the SLN to penetrate into and

COLOR Online / B&W in Print

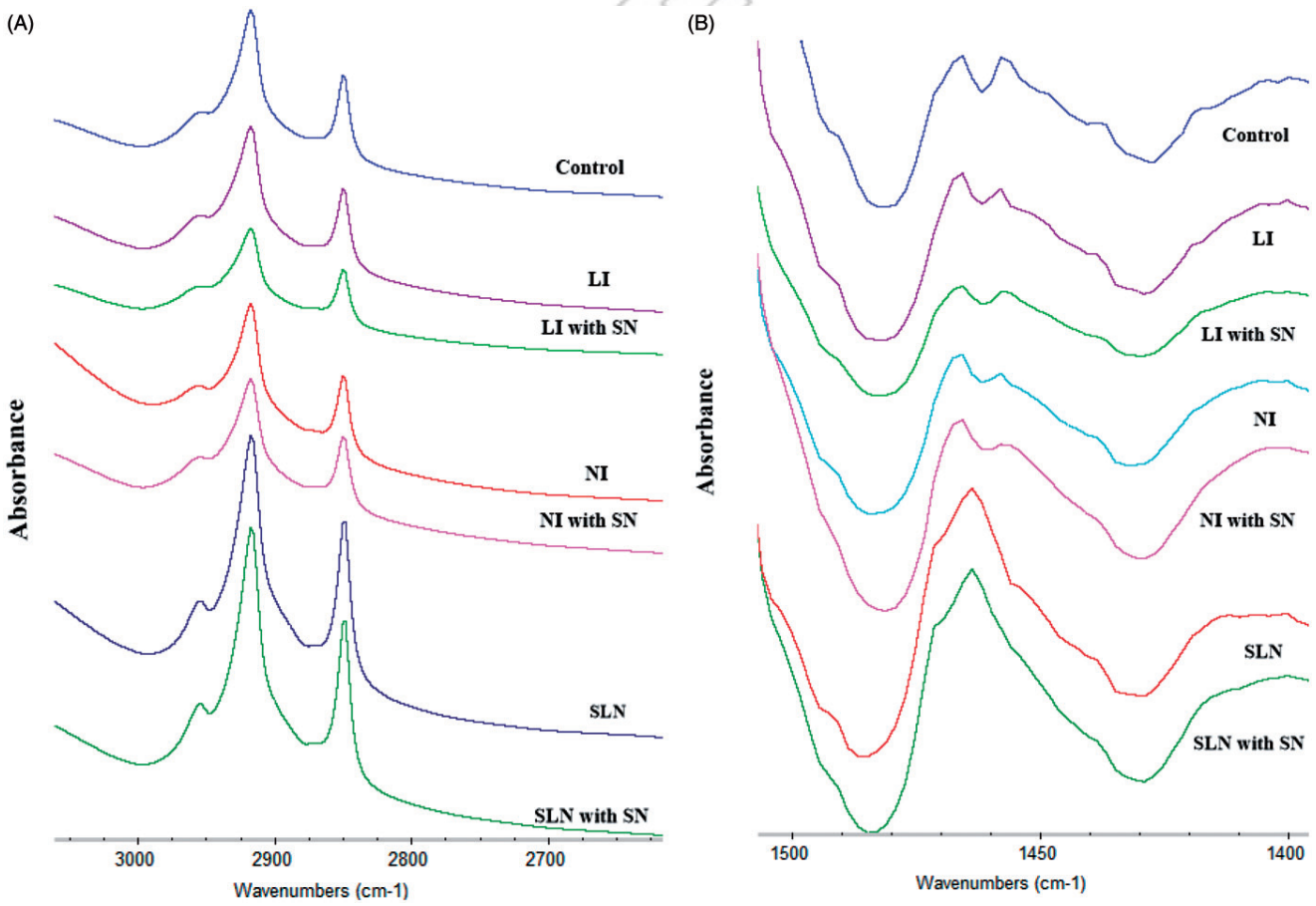

Figure 3. FTIR spectra of the CH_2 asymmetric and symmetric stretching modes (A) and CH_2 scissoring region (B) in the spectra collected from the stratum corneum of the porcine skin after being treated with the different lipid nanocarrier and SN.

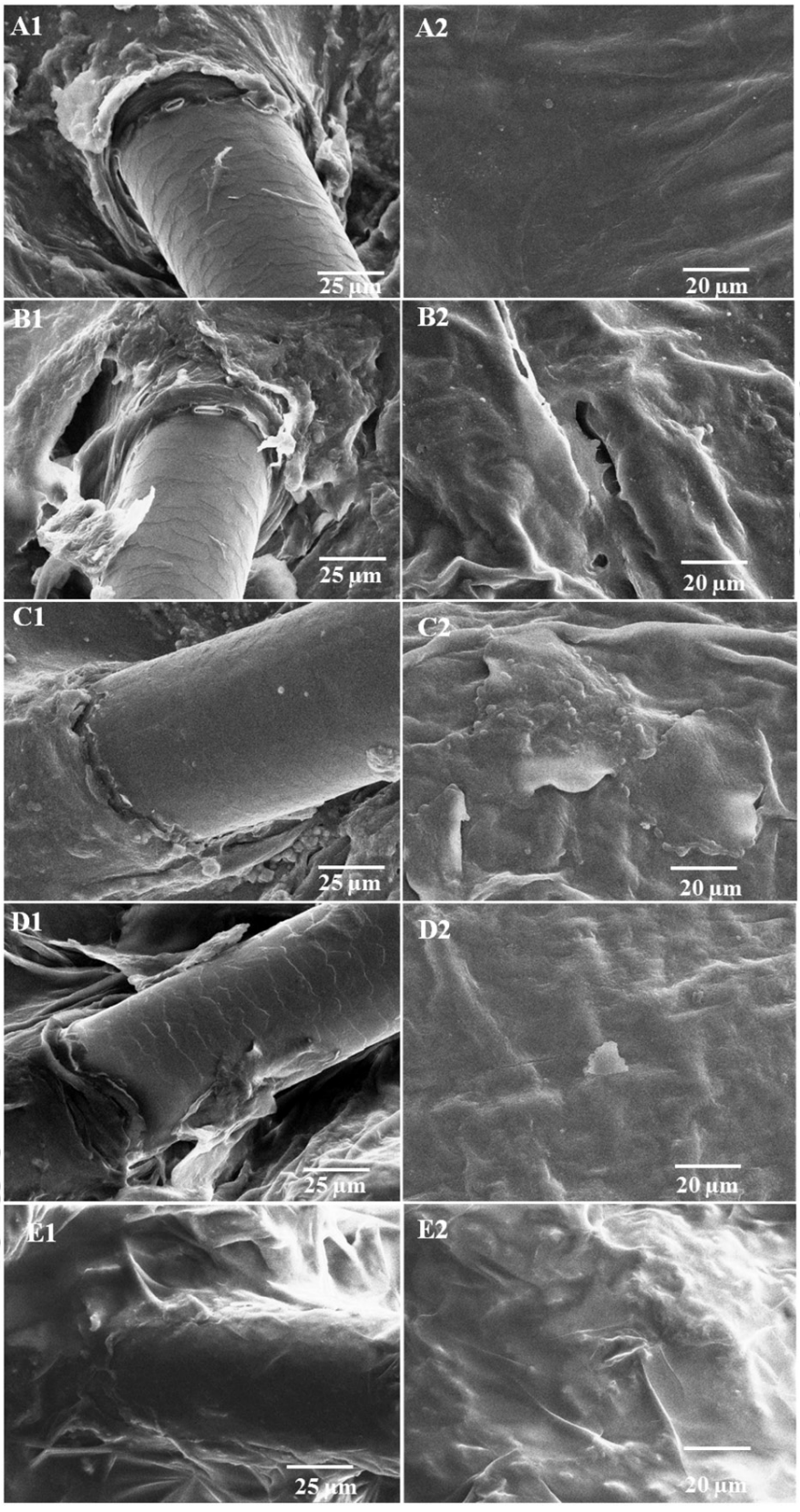

Figure 4. SEM images of the porcine skin surface at (1) the follicular region (original magnification ×400) and (2) nonfollicular region (original magnification ×500): control (PBS) without SN (A) and with SN (B), LI wit SN (C), NI with SN (D) and SLN with SN (E).

through the hydrated skin. However, the SLN-treated skin showed a collapse of the CH_2 scissoring doublet peak (Figure 3(B)), indicating that a disorder of the lipid chain packing might be influenced by the interaction between the lipids from the SLN and the stratum corneum lipids within the orthorhombic lattice and that some fraction of lipid may also be incorporated between stratum corneum lipid tails[31]. After applying the SN, the band intensity was higher than without the SN, suggesting that the fragment of the solid lipid after disruption by the ultrasound energy might adsorb onto the skin stratum corneum and intercalate in the lipid bilayer of the stratum corneum more than the SLN without SN. These results demonstrate that the SLN carrier occluded on the top of the skin surface and released NaFl into the skin, while the SN disrupted the SLN carrier, released NaFl, and provided some solid lipid fragment covering the skin surface and protecting the permeation of NaFl into and through skin.

SEM study

As shown in Figure 4, the SEM images of the porcine skin surface treated with the different lipid nanocarrier compared with the control (PBS) were observed. The stratum corneum surface of the control ultrasound of the treated skin were lifted up and showed crack-like structures (Figure 4(B)). The low-frequency SN induced disruption of the structure of the stratum corneum lipid bilayers and enhanced the skin permeability for hydrophilic molecules in solution into the viable epidermis through an intracellular pathway[32]. The combination of the lipid nanocarriers with SN for the treated skin showed small corneocytes lifting, suggesting that the lipid compositions could cover and repair the damaged skin[9]. In this result, the sonicated skin with the SLN had a thick lipid layer of solid wax (cetyl palmitate). The formation of the lipid film on the skin surface might have decreased the skin permeation of hydrophilic compound.

Conclusion

This work demonstrated that the low frequency SN (20 kHz for 2 min) affected skin penetration of NaFl-loaded lipid nanocarriers. Ultrasound energy breaks lipid nanocarrier and stratum corneum structure. The disrupted skins were repaired by lipid fragment from the nanocarrier. Liposomes made from phospholipids may diffuse with NaFl into the stratum corneum, enhance drug penetrate through skin and repair ultrasound-induced skin disruption. For the NI, the membrane vesicles covered the stratum corneum surface but did not permeate deeply into the skin layer, indicating that the disrupted NI vesicles were on the damaged skin and covered the skin surface, which might decrease the penetration of the hydrophilic compound into the skin. However, the LI and NI might form a bilayer vesicle again after removing the SN, while the change of solid lipid (wax) was irreversible. The solid lipid fraction of the SLN might cover the skin surface. Thus, the penetration of NaFl from the SLN with SN significantly decreased compared with the SLN alone. Therefore, the decrease in skin permeability of hydrophilic compounds could be caused by changing the properties of the lipid nanocarrier on the skin surface, thereby reducing the NaFl permeation into and through the skin.

Acknowledgements

We wish to thank the Division of Medical Molecular Biology (Department of Research and Development, Faculty of Medicine, Siriraj Hospital, Mahidol University) for providing the confocal laser scanning microscope (LSM 510 Meta, Zeiss, Jena, Germany).

Disclosure statement

The authors report no declarations of interest.

Funding

We gratefully thank the Thailand Research Funds through the Royal Golden Jubilee PhD Program [Grant No. PHD/0091/2554] and Basic Research Grant [Grant No. 5680016] for financial support.

References

1. Polat BE, Hart D, Langer R, Blankschtein D. Ultrasound-mediated transdermal drug delivery: mechanisms, scope, and emerging trends. J Control Release 2011;152:330–348.
2. Park D, Park H, Seo J, Lee S. Sonophoresis in transdermal drug deliveries. Ultrasonics 2014;54:56–65.
3. Mitragotri S, Blankschtein D, Langer R. Transdermal drug delivery using low-frequency sonophoresis. Pharm Res 1996;13:411–420.
4. Riesz P, Kondo T. Free radical formation induced by ultrasound and its biological implications. Free Radic Biol Med 1992;13:247–270.
5. Ogura M, Paliwal S, Mitragotri S. Low-frequency sonophoresis: current status and future prospects. Adv Drug Deliv Rev 2008;60:1218–1223.
6. Hua S. Lipid-based nano-delivery systems for skin delivery of drugs and bioactives. Front Pharmacol 2015;6:1–5.
7. Vyas SP, Singh R, Asati RK. Liposomally encapsulated diclofenac for sonophoresis induced systemic delivery. J Microencapsul 1995;12:149–154.
8. Dahlan A, Alpar HO, Murdan S. An investigation into the combination of low frequency ultrasound and liposomes on skin permeability. Int J Pharm 2009;379:139–142.
9. Rangsimawong W, Opanasopit P, Rojanarata T, Ngawhirunpat T. Mechanistic study of decreased skin penetration using a combination of sonophoresis with sodium fluorescein-loaded PEGylated liposomes with d-limonene. Int J Nanomedicine 2015;10:7413–7423.
10. Charoenputtakun P, Pamornpathomkul B, Opanasopit P, et al. Terpene composited lipid nanoparticles for enhanced dermal delivery of all-trans-retinoic acids. Biol Pharm Bull 2014;37:1139–1148.
11. Sakai S, Yasuda R, Sayo T, et al. Hyaluronan exists in the normal stratum corneum. J Invest Dermatol 2000;114:1184–1187.
12. Bin S, Chao F, Yuanying P. Stealth PEG-PHDCA niosomes: effects of chain length of PEG and particle size on noisome surface properties, *in vitro* drug release, phagocytic uptake, in vivo pharmacokinetics and antitumor activity. J Pharm Sci 2005;95:1873–1887.
13. Franz TJ. Kinetics of cutaneous drug penetration. Int J Dermatol 1983;22:499–505.
14. Pardeike J, Hommoss A, Müller RH. Lipid nanoparticles (SLN, NLC) in cosmetic and pharmaceutical dermal products. Int J Pharm 2009;366:170–184.
15. Schneider M, Stracke F, Hansen S, Schaefer UF. Nanoparticles and their interactions with the dermal barrier. Dermatoendocrinology 2009;1:197–206.

16. Ogiso T, Niinaka N, Iwaki M. Mechanism for enhancement effect of lipid disperse system on percutaneous absorption. J Pharm Sci 1996;85:57–64.
17. Subongkot T, Wonglertnirant N, Songprakhon P, et al. Visualization of ultradeformable liposomes penetration pathways and their skin interaction by confocal laser scanning microscopy. Int J Pharm 2013;441:151–161.
18. Kirjavainen M, Mönkkönen J, Saukkosaari M, et al. Phospholipids affect stratum corneum lipid bilayer fluidity and drug partitioning into the bilayers. J Control Release 1999;58:207–214.
19. Siddiqui A, Alayoubi A, El-Malah Y, Nazzal S. Modeling the effect of sonication parameters on size and dispersion temperature of solid lipid nanoparticles (SLNs) by response surface methodology (RSM). Pharm Dev Technol 2014;19:342–346.
20. Kirjavainen M, Urtti A, Jääskeläinen I, et al. Interaction of liposomes with human skin *in vitro* – the influence of lipid composition and structure. Biochim Biophys Acta 1996;1304:179–189.
21. Verma DD, Verma S, Blume G, Fahr A. Liposomes increase skin penetration of entrapped and non-entrapped hydrophilic substances into human skin: a skin penetration and confocal laser scanning microscopy study. Eur J Pharm Biopharm 2003;55:271–277.
22. Lin YK, Al-Suwayeh SA, Leu YL, et al. Squalene-containing nanostructured lipid carriers promote percutaneous absorption and hair follicle targeting of diphencyprone for treating alopecia areata. Pharm Res 2013;30:435–446.
23. Wosicka-Frąckowiak H, Cal K, Stefanowska J, et al. Roxithromycin-loaded lipid nanoparticles for follicular targeting. Int J Pharm 2015;495:807–815.
24. Baroli B. Penetration of nanoparticles and nanomaterials in the skin: fiction or reality? J Pharm Sci 2010;99:21–50.
25. Lauterbach A, Müller-Goymann CC. Applications and limitations of lipid nanoparticles in dermal and transdermal drug delivery via the follicular route. Eur J Pharm Biopharm 2015;97:152–163.
26. Hasanovic A, Winkler R, Resch GP, Valenta C. Modification of the conformational skin structure by treatment with liposomal formulations and its correlation to the penetration depth of aciclovir. Eur J Pharm Biopharm 2011;79:76–81.
27. Mendelsohn R, Chen HC, Rerek ME, Moore DJ. Infrared microspectroscopic imaging maps the spatial distribution of exogenous molecules in skin. J Biomed Opt 2003;8:185–190.
28. Panchagnula R, Salve PS, Thomas NS, et al. Transdermal delivery of naloxone: effect of water, propylene glycol, ethanol and their binary combinations on permeation through rat skin. Int J Pharm 2001;219:95–105.
29. Kaushik D, Michniak-Kohn B. Percutaneous penetration modifiers and formulation effects: thermal and spectral analyses. AAPS PharmSciTech 2010;11:1068–1083.
30. Boncheva M, Damien F, Normand V. Molecular organization of the lipid matrix in intact stratum corneum using ATR-FTIR spectroscopy. Biochim Biophys Acta 2008;1778:1344–1355.
31. Caussin J, Gooris SG, Bouwstra JA. FTIR studies show lipophilic moisturizers to interact with stratum corneum lipids, rendering the more densely packed. Biochim Biophys Acta 2008;1778:1517–1524.
32. Morimoto Y, Mutoh M, Ueda H, et al. Elucidation of the transport pathway in hairless rat skin enhanced by low-frequency sonophoresis based on the solute–water transport relationship and confocal microscopy. J Control Release 2005;103:587–597.

ASIAN JOURNAL OF PHARMACEUTICAL SCIENCES 11 (2016) 52–53

HOSTED BY

ELSEVIER

Available online at www.sciencedirect.com

ScienceDirect

journal homepage: www.elsevier.com/locate/ajps

Design and development of optimal invasomes for transdermal drug delivery using computer program

Sureewan Duangjit [a,c,*], *Tassanan Nimcharoenwan* [b], *Nutcha Chomya* [b], *Natthporn Locharoenrat* [b], *Tanasait Ngawhirunpat* [b,c]

[a] *Division of Pharmaceutical Chemistry and Technology, Faculty of Pharmaceutical sciences, Ubon Ratchathani University, Ubon Ratchathani 34190, Thailand*

[b] *Department of Pharmaceutical Technology, Faculty of Pharmacy, Silpakorn University, Nakhon Pathom 73000, Thailand*

[c] *Pharmaceutical Development of Green Innovations Group (PDGIG), Faculty of Pharmacy, Silpakorn University, Nakhon Pathom 73000, Thailand*

ARTICLE INFO

Article history:
Available online 25 November 2015

Keywords:
Design expert
Invasomes
Liposomes
Capsaicin

Capsaicin (CAP) is a major pungent component that has been widely studied in medical and pharmaceutical fields. CAP was used both orally and topically for pain relief. However, the extreme pungency and the water insolubility of CAP lead to its restriction in the development of CAP as drug delivery system [1]. Our previous study suggested that the computer software exhibited a beneficial role in the development of menthosomes for transdermal drug delivery [2]. To confirm the reliability and reproducibility of simultaneous optimal formulations, the optimal ultraflexible liposomes (invasomes) estimated by the computer software (Design Expert®) were experimentally formulated and investigated. To achieve this purpose, invasomes with Comperlan® KD and *d*-limonene as potential penetration enhancer were developed. Using a two-factor factorial design with centroid replication as a model experimental design, the invasomes were demonstrated. The model invasome formulations containing a constant composition of 10 mM phosphatidylcholine, 1 mM cholesterol and 0.15% capsaicin, and various percentages of *d*-limonene and Comperlan® KD were prepared. The physicochemical characteristics e.g., vesicle size, size distribution, zeta potential, entrapment efficiency and skin permeability of the model invasome formulations were evaluated. The compositions and the physicochemical characteristics of invasomes were defined as formulation factor (X_n) and response variables (Y_n), respectively. The relationship between formulation factor and response variables was predicted, and the optimal invasome formulation was also optimized using Design Expert®. The response surfaces estimated by Design Expert® illustrated obvious relationship between formulation factor and response variables. The formulation factor directly

* *E-mail address:* sureewan.d@ubu.ac.th.

Peer review under responsibility of Shenyang Pharmaceutical University.
http://dx.doi.org/10.1016/j.ajps.2015.10.039

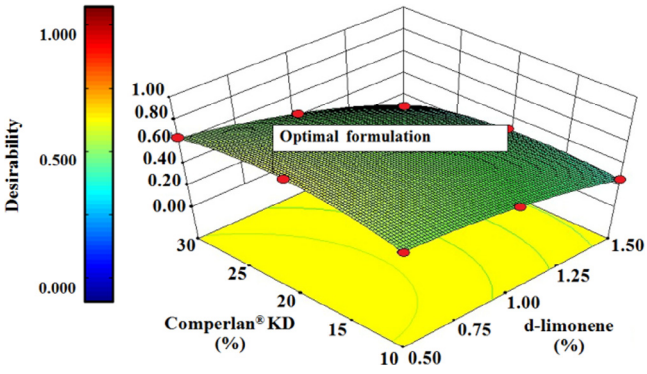

Fig. 1 – The three dimensional response surface plot of the desirability of invasomes.

affected the physicochemical characteristics of invasomes. The 0.15% capsaicin-loaded invasomes were smaller than 100 nm in size, narrow size distribution (0.01–0.30) and had minor negative zeta potential value (less than –20 mV). The skin permeability of the optimal invasomes was significantly higher than conventional liposomes and commercial product (0.15% capsaicin in ethanolic solution). The response surfaces estimated by the computer program were helpful for the development of optimal invasomes for transdermal drug delivery (Fig. 1).

Acknowledgments

The authors gratefully acknowledge the Thailand Research Funds through the Basic Research Grant (Grant No. 5680016), the Silpakorn University Research and Development Institute (Grant No. SURDI 58/01/10), the Faculty of Pharmaceutical Sciences, Ubon Ratchathani University, and the Faculty of Pharmacy, Silpakorn University, Thailand, for facilities and financial support.

REFERENCES

[1] Duangjit S, Chairat W, Opanasopit P, et al. Application of design expert for the investigation of capsaicin-loaded microemulsions for transdermal delivery. Pharm Dev Technol 2015;21:1–8.
[2] Duangjit S, Obata Y, Sano H, et al. Menthosomes, novel ultradeformable vesicles for transdermal drug delivery: optimization and characterization. Biol Pharm Bull 2012;35(10):1720–1728.

Multivariate Statistical Approach to Optimize Menthosomes Incorporating l-menthol as Novel Ultradeformable Vesicles for Transdermal Drug Delivery

Sureewan Duangjit[1,2], Yasuko Obata[2], Hiromu Sano[2], Shingo Kikuchi[2], Yoshinori Onuki[2], Theerasak Rojanarata[1], Praneet Opanasopit[1], Kozo Takayama[2], Yoshie Maitani[3], Tanasait Ngawhirunpat[1]
[1]Faculty of Pharmacy, Silpakorn University, Nakhon Pathom, Thailand.
[2]Department of Pharmaceutics, Hoshi University, Tokyo, Japan
[3]*Department of Drug Delivery Research, Hoshi University, Tokyo, Japan*
E-mail address: tanasait@su.ac.th

Abstract The multivariate statistical techniques were utilized for optimizing novel carrier for transdermal drug delivery of meloxicam, a model water-insoluble drug. Menthosomes (MTS), a novel ultradeformable vesicle composed of phosphatidylcholine (PC), cholesterol (Chol), hexadecyl pyridinium chloride (HPC) and l-menthol (MEN) were formulated. A two-factor spherical and second-order composite experimental design was employed to prepare the model of vesicle formulations. The model formulations were optimized using a nonlinear-response surface method incorporating thin-plate spline interpolation (RSM-S). Moreover, the confidence intervals and the reliability of the optimal MTS formulation predicted by RSM-S were estimated using a bootstrap (BS) resampling method and a Kohonen self-organizing map (SOM), respectively. The various amounts of HPC and Chol were selected as formulation factors. The physicochemical characteristics (e.g. vesicle size, charge, elasticity and drug content) and *in vitro* skin permeability (e.g. flux value) were selected as response variables. The response surface results clearly indicated nonlinear relationships between the formulation factors and the response variables. The experimental values of optimal MTS formulation coincided well with the values predicted by the computer programs. The confocal laser scanning microscopy (CLSM) image displayed the vesicle mechanism for delivery meloxicam across the hairless mice skin. The result indicated that the optimal MTS formulation exhibited higher skin permeability than conventional liposomes. Our study suggested the optimal MTS formulation was successfully optimized using RSM-S and had a potential to use as novel carrier incorporating MEN for transdermal drug delivery of meloxicam. These statistical approaches were helpful in formulating an appropriate transdermal delivery system.

Introduction

Since the first publication reported that the effectiveness of surfactant in deformable liposomes can be used for transdermal delivery of drug into deep skin was distributed, the novel deformable vesicles with various penetration enhancers have been developed (e.g. transfersomes, ethosomes, flexosomes and invasomes).[1] These innovative deformable vesicles mainly were composed of phospholipids and penetration enhancer (e.g. surfactant, ethanol, terpenes etc.) in which only a specially designed vesicle was shown to be able to allow through the deep skin region. Hence, several researchers previously used various penetration enhancers to promote skin delivery of drugs. Menthosomes (MTS), novel ultradeformable liposomes consisting of phospholipids, surfactant and l-menthol were also introduced in this study. L-menthol is well-known as a competent permeation enhancer, and has been reported to improve the skin permeation of various drugs by increasing drug partition and diffusion.[2] In the development of a novel transdermal drug delivery carrier, it is important to determine the optimized vesicle formulations having appropriate skin permeation. A nonlinear response-surface method incorporating thin-plate spline interpolation (RSM-S) was performed in our study. Using RSM-S, the complicated relationships between formulation factors and response variables can be easily understood, and a stable and reproducible simultaneous optimal formulation is obtained. A bootstrap (BS) resampling method and a Kohonen self-organizing map (SOM) were used to evaluate the reliability of the optimal formulation estimated by RSM-S. These statistical approaches are helpful in formulating an appropriate transdermal delivery system. In this study, meloxicam (MX), a nonsteroidal anti-inflammatory drug (NSAID) as a preferential COX-1 inhibitor, was used as the model drug.[3] Because oral and injectable administrations of MX are not appropriate for peptic ulcers and patient compliance, MX is suitable for development as a transdermal delivery candidate. Moreover, MX is a potent drug and safe drug for reducing pain and inflammatory symptoms with low toxicity and low skin irritate less than other NSAID drugs.

Materials and Methods

1) *Materials*: Phosphatidylcholine (PC) was purchased from LIPOID GmbH. Cholesterol (Chol) was purchased from Wako Pure Chemical Industries. Meloxicam (MX) was supplied from Fluka. Hexadecyl pyridinium chloride (HPC) and l-Menthol (MEN) was purchased from Tokyo Chemical Industry. All other chemicals used were of reagent grade and purchased from Wako Pure Chemical Industries (Osaka, Japan).
2) Preparation of menthosomes: The MX-loaded MTS composed of MX, PC, MEN, HPC and Chol were prepared. MTS were prepared by the sonication method.[1] Briefly, all compositions were separately dissolved in chloroform/methanol (2:1 v/v). The lipid mixtures were evaporated under nitrogen gas stream. The lipid film was

placed in a desiccator for 6 h to remove the remaining solvent. The dried lipid film was hydrated with acetate buffer solution (pH 5.5). MTS suspensions were subsequently sonicated for two cycles of 15 min using a sonicator-bath.
3) Experimental design: The various concentration of HPC (X_1) and Chol (X_2) were selected as formulation factors. Based on the turbidity behaviors observed in preliminary experiments, the lower and upper limits of the levels of each factor were sets as follows.

$$10 \leq X_1 \leq 40 \text{ (\%mol)} \quad (1)$$

$$10 \leq X_2 \leq 40 \text{ (\%mol)} \quad (2)$$

Therefore, the feasibly experimental region in the simplex design was spherical shape. The formulation factor assigned according to the ordinary round design, as shown in Figure 1, and 10 formulation, including duplicate of the centroid, were prepared.

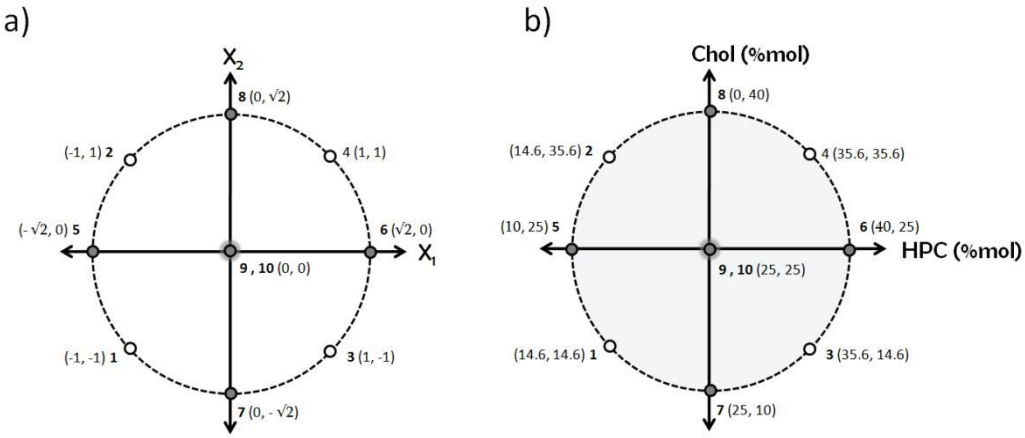

Figure 1 The two-factor spherical and second-order composite experimental design: a) simplex design for two factors, and b) vesicle composition of two components. Ten formulations were assigned to the model formulation loaded menthosomes.

4) Determination and measurement of vesicle size, charge, elasticity and drug content: The vesicle size (nm) and charge (mV) of MTS were measured by photon correlation spectroscopy (PCS) (Zetasizer Nano series, Malvern Instruments, UK). At least three independent samples were taken, and the particle size was measured at least three times. The elasticity value ($mg \cdot sec^{-1} \cdot cm^{-2}$) of the bilayer of MTS was directly proportional to $J_{Flux} \times (r_v/r_p)^2$. Where J_{Flux} is the rate of penetration through a permeable barrier, r_v is the size of the vesicles after extrusion (nm) and r_p is the pore size of the barrier (nm). To measure J_{Flux}, MTS was extruded through a polycarbonate membrane with a pore diameter of 50 nm (r_p), at a pressure of 0.5 MPa. Five minutes, the extrudate was weighed (J_{Flux}), and the average vesicle diameter (r_v) was measured by PCS. The drug content of MX in the MTS formulation was determined by HPLC. The analytical column was YMC-Pack ODS-A (150 mm × 4.6 mm i.d.), and the mobile phase consisted of acetate buffer solution (pH 4.6)/methanol (50:50, v/v). The flow rate was set at 0.8 mL/min, and the wavelength used in this determination was 272 nm.
5) In vitro skin permeability evaluation: The excised skin of hairless mice (Laboskin®, HOS: HR-1 Male, 7 weeks, Sankyo Labo Service Corporation, Inc., Tokyo, Japan) was used as a model membrane. A side-by-side diffusion cell with an available diffusion area of 0.95 cm^2 was employed. The receiver chamber was filled with 3 mL of phosphate buffer solution (pH 7.4, 32 °C) and the donor chamber was filled with 3 mL of MTS formulation. At appropriate times (2-12 h), an aliquot of the receiver fluid (0.5 mL) was withdrawn, and the same volume of fresh buffer solution was placed in the receiver chamber. The concentration of MX in the aliquot was analyzed using HPLC.
6) Measurement of hairless mice skin using confocal laser scanning microscopy (CLSM): The depth of skin permeation of MTS was investigated using CLSM (Radiance 2100, Bio-Rad Laboratories, Inc., Hercules, CA, USA). The Dil-labeled MTS was prepared. The labeled MTS was applied on the hairless mice skin for 12 h. After removed excess amount of MTS formulation, the skin was washed three times and dried with cotton swab. The full skin thickness was sectioned into the pieces of 1 mm^2 size and evaluated for depth of fluorescent probe penetration. Maximum excitation was performed by a 543 nm line of internal He-Neon laser, and fluorescence emission was detected with long pass barrier filter 560 DCLP.
7) Simultaneous optimization and reliability assessment of optimal MTS formulation using RSM-S, BS resampling and Kohonen SOM: The optimal MTS formulation was estimated based on RSM-S, using a data-set obtained from the simplex spherical design. Details of the optimization methods with RSM-S have been fully given previously.[4] The optimal formulation was defined as the sufficient skin permeability of MX-loaded MTS permeated skin at 2-12 h and the flux value. The best vesicle formulation should have the maximum concentration of MX-permeated skin at 2–12 h and flux value. The BS resampling method which has been fully described previously[5], was then applied to evaluate the reliability of the optimal MTS formulation. The number of BS replication was fixed at 2300. BS-

optimal means and their 95% confidence intervals (CI) were calculated from the BS-optimal MTS formulation. The histograms of the BS-optimal MTS formulations were close to a normal distribution. The Kohonen SOM was then applied to the set of BS formulations to separate the global optimal and some local optimal clusters.[6]
8) Computer programs: dataNESIA, Version 3.2 (Yamatake Corp., Fujisawa, Japan) was used for drawing the response surfaces for each variable and predicting the latent variables and response variables (skin permeation) for various formulations. SOM clustering was performed using Viscovery SOMine, (Version 5.0, Eudaptics Software GmbH, Vienna, Austria).
9) Ethics in the animal study: This animal study was performed at Hoshi University and complied with the regulations of the committee on Ethics in the Care and Use of Laboratory Animals.

Results and Discussion
***The prediction of response variables using RSM-S*:** Ten model vesicle formulations including duplicate of the centroid of the simplex spherical design were prepared and investigated. The experimental values obtained from the model formulations were used as the input data for optimization process. The response surfaces of each response variable were estimated by RSM-S based on the original data-set. The physicochemical characteristics of MTS (e.g. vesicle size, charge, elasticity, drug content, and flux value) were selected as response variables. The response surfaces indicated that an increase in HPC resulted in a significant decrease in vesicle size, because the neutralization between the positive charges of vesicle bilayer and negative charges of MX under the experimental pH (5.5) could reduce the repulsive forces between the vesicle bilayers.[7] The composition of HPC in MTS resulted in a significant increase in positive charge, elasticity and MX content in the formulation because of its intrinsic properties of cationic surfactant. HPC has a high radius of curvature that may destabilize lipid bilayers of the MTS and increase deformability of the vesicle bilayers[8] The beneficial role of surfactant within the vesicle bilayer is well recognized to increase MX solubility in MTS bilayer. An increase of Chol resulted in a significant increase in vesicle size, a decrease in elasticity and a slight increase in MX content in the formulation. Because, Chol can increase the net repulsion force and reduce the van der Waals attraction force between the lipid bilayer of vesicle[9] and Chol can increase rigidity and packing density of PC molecules, thus the elasticity of MTS bilayers decreased.[8] The MX content in the formulation slightly increased, as Chol was added because Chol may increase the hydrophobicity of vesicle bilayer as well recognized as the role of "*like dissolves like*" between hydrophobic bilayer and lipophilic drug.[10] The flux response surface of HPC and Chol were inversely correlated. The formulations containing high concentration of HPC but low concentration of Chol showed high flux value. This result indicated that the formulation factor (X_1 and X_2) was the major factor affecting the physicochemical characteristics of MTS vesicles, and also affected the skin permeability of MX-loaded MTS. The accuracy of the response surfaces was determined by leave-one-out-cross-validation. The results indicated that most of the correlation coefficients were sufficiently high (more than 0.9). These results suggested that RSM-S successfully estimated the relationship between the formulation factors and response variables attributed to MTS formulation.[11]
***Formulation optimization using RSM-S*:** The optimal MX-loaded MTS formulation was optimized based on the original data set using RSM-S. The search directions for the response variables were set to produce a high concentration of MX-permeated skin at 2-12 h and also a high flux value. X_1 = 29 (% mole ratio) and X_2 = 10 (% mole ratio) were estimated as the optimal MTS formulation. The flux value = 0.31 μg/cm^2/h was estimated to be the optimal response variables. To confirm the accuracy and reliability of the optimal MTS formulation estimated using RSM-S, the optimal MTS was confirmed by the experiment. The evaluation of physicochemical characteristics and *in vitro* skin permeation study were also performed. The experimental optimal MTS formulation composed of PC:Chol:HPC:MX = 100:10:29:10 mole ratio. The following response variables were obtained from the experimental optimal MTS formulation: vesicle size = 135±40 nm, charge = +57±0.3 mV, elasticity = 166±9 mg·sec^{-1}·cm^{-2} and MX content = 522±3 μg/mL, and the experimental flux value was 0.31±0.06 μg/cm^2/h which were very close to the flux value predicted by RSM-S. The previous study reported that skin permeation flux of the pharmaceutical formulation (ondansetron hydrogels) predicted by RSM-S also coincided well with the experimental value evaluated by *in vitro* skin permeation study.[12] The BS-resampling and Kohonen SOM-clustering methods were applied to determine the set of BS-optimal formulation in the global optimal cluster.[13] The 95% CI for the optimal MTS formulation was calculated using the data in the global optimal cluster. The shape of the histogram constructed from the arithmetic means of the BS samples followed a normal distribution. Most of the histograms were also close to a normal distribution. The estimated lower and upper flux value were 0.28 μg/cm^2/h and 0.33 μg/cm^2/h, respectively. This result revealed that the experimental flux value was also in the 95% CI range. The results were sufficiently high reliability suggesting that RSM-S successfully estimated the optimal MX-loaded MTS formulation, and CI of the formulation factors and the response variables were satisfactorily estimated.
***Skin distribution of fluorescence-labeled MTS vesicles using CLSM*:** According to the CLSM observation, the labeled optimal MTS could penetrate into full-thickness skin. MTS vesicle and conventional liposome (CLP) penetrated into deep layer of the epidermis up to 40 μm and 15 μm, respectively. These results suggested that the rigid or low elasticity vesicles (CLP) had also low permeability, could not penetrate into the deep layer of the

epidermis and only remained to the upper layer of the skin (stratum corneum). On the other hand, the non-rigid or high elasticity vesicles (MTS) showed effective permeability up to deep layer skin, as high fluorescence intensity in the skin between 15-40 μm (viable epidermis layer) was observed. The obtained results indicated that high elasticity MTS penetrated across the skin greater than low elasticity CLP.[14] The incorporation of Chol as membrane stabilizer in the MTS vesicle resulted in an increased packing density of vesicle bilayer and increased stability of vesicle formulation. Whiles, the role of HPC and MEN as penetration enhancer within the vesicle affected the elasticity or deformaiblity of vesicle bilayer. Therefore, HPC and MEN in MTS formulation improved the transdermal delivery of MX. However, the optimal ratio of these compositions in the vesicle formulation was significant to investigate to develop the novel deformable vesicle with sufficient skin permeability and good stability. Our ultradeformable liposomes may promote skin permeation of MX into deep skin by a variety of mechanisms: (a) the free drug mechanism, (b) the penetration-enhancing process of the liposome components, (c) vesicle adsorption to and/or fusion with the stratum corneum and/or (d) intact vesicle penetration into and through the intact skin. It could be concluded that our group were successful in showing the feasibility of transdermal drug delivery of MTS, and we were the first group to achieve in the development of novel carrier incorporating MEN for transdermal drug delivery of meloxicam called "menthosomes".

Acknowledgements
The authors gratefully acknowledge the Thailand Research Funds through the Golden Jubilee Ph.D. Program (Grant No. PHD/0141/2550) and through the Basic Research Grant (BRG 5680016), the Pharmaceutical Development of Green Innovations Group (PDGIG) the Faculty of Pharmacy, Silpakorn University, Nakhon Pathom, Thailand, and Department of Pharmaceutics and Department of *Drug Delivery Research* Hoshi University, Tokyo, Japan for all facilities and support. This study was also supported by MEXT-Supported Program for the Strategic Research Foundation at Private Universities, and a Grant-in-Aid for Scientific Research from the Ministry of Education, Culture, Sports, Science, and Technology of Japan.

References
[1] Duangjit S, Obata Y, Sano H, Kikuchi S, Onuki Y, Opanasopit P, Ngawhirunpat T, Maitani Y & Takayama K (2012) Biol Pharm Bull, 35(10): 1-9.
[2] Okusa T, Obata Y, Takayama K, Higashiyama K & Nagai T (1997) Drug Deliv Syst, 12: 327-333.
[3] Luger P, Daneck K, Engel W, Trummlitz G & Wagner K (1996) Eur J Pharm Sci, 4: 175-187
[4] Takayama K and Nagai T (1991) Int J Pharm, 74(2-3): 115-126.
[5] Dupret G and & Koda M (2001) Eur J Oper Res, 134: 141-156.
[6] Kikuchi S and Takayama K (2010) Int J Pharm, 386: 149-155.
[7] Manosroi A, Khanrin P, Lohcharoenkal W, Werner RG, Götz F, Manosro W & Manosroi J (2010) Int J Pharm, 392: 304-310.
[8] Elsayed MMA, Abdallah OY, Naggar VF & Khalafallah NM (2007) Int J Pharm, 332: 1-16.
[9] Liang X, Mao G & Ng KYS (2004) J Colloid Interface Sci, 278: 53-62.
[10] Tavano L, Muzzalupo R, Cassano R, Trombino S, Ferrarelli T & Picci N (2010) Colloid Surface B, 75: 319-322.
[11] Mohammed AR, Weston N, Coombes AGA, Fitzgerald M & Perrie Y (2004) Int J Pharm, 285: 23-34.
[12] Obata Y, Ashitaka Y, Kikuchi S, Isowa K & Takayama K (2010) Int J Pharm, 399: 87-93.
[13] Higgins JJ (2003). Duxbury Press, Boston.
[14] Duangjit S, Obata Y, Sano H, Onuki Y, Opanasopit P, Ngawhirunpat T, Miyoshi T, Kato S & Takayamaa K (2014) Biol Pharm Bull, 37(2): 239–247.